Identification and characterisation of regulators of nuclear genes encoding mitochondrial proteins

Sophia Ng Jinq Tyan

School of Chemistry and Biochemistry and
the ARC Centre of Excellence in Plant Energy Biology

THE UNIVERSITY OF WESTERN AUSTRALIA

Achieve International Excellence

This thesis is presented for the degree of Doctor of Philosophy of the

University of Western Australia

August 2012

Coordinating supervisor: Winthrop Professor James Whelan

Co-supervisor: Professor Huixia Shou (Zhejiang University, China)

Declaration

The research presented in this thesis is my own work unless otherwise stated. This work was carried out in the Australian Research Council Centre of Excellence in Plant Energy Biology at the University of Western Australia. The material presented in this thesis has not been submitted for any other degree.

_____
Sophia Ng Jinq Tyan

Acknowledgement

This thesis would not have been possible without the help and guidance of several individuals who in one way or the other contributed their valuable assistance in completion of this study.

First and foremost, my deepest gratitude must go to my supervisor Jim Whelan. Thank you for your untiring support and guidance during my study. I would have already given up myself if it were not because of your endless encouragement, especially during the period when I was still mourning for the loss of my brother who passed away due to leukemia.

I would like to thank to: Dr. Aneta Ivanova and Dr. Estelle Giraud, for being my laboratory supervisors and sharing your professional opinions and expertise in carrying out the projects; Chris, Monika, Botao, Reena, Owen and Olivier, for your help on the bench work; Joshua, Yan and Lei, for listening to me whenever I need someone to talk to; and all the members from the Whelan laboratory and everyone else from the ARC centre, thank you for making a great working environment to me and it was my pleasure to work with you over the past few years. In addition, a special thank to Feifei and Wei, for your invaluable friendship. It has been countless evenings that I was invited for having dinners with you after a long day in work.

Lastly, I want to thank to my family and my partner for your unconditional love. I am blessed with having you in my life and I cannot ask for more.

Publications arising from this thesis

Giraud, E.[‡], Ng, S.[‡], Carrie, C., Duncan, O., Low, J., Lee, C.P., Van Aken, O., Millar, A.H., Murcha, M., and Whelan, J. (2010). TCP transcription factors link the regulation of genes encoding mitochondrial proteins with the circadian clock in *Arabidopsis thaliana*. Plant Cell **22,** 3921-3934. (Chapter 2)

Ng, S., Giraud, E., Duncan, O., Law, S.R., Wang, Y., Xu, L., Narsai, R., Carrie, C., Walker, H., Day, D.A., Blanco, N., Strand, A., Whelan, J., and Ivanova, A. (2012). Cyclin-dependent kinase E;1 (CDKE;1) provides a cellular switch in plants between growth and stress responses. J. Biol. Chem. (Chapter 3)

Ng, S.[*], Ivanova, A.[*], Duncan, O., Law, S., de Clerque, I., Wang, Y., Carrie, C., Xu, L., Walker, H., Van Breusegem, F., Whelan, J., and Giraud, E. (2012). A membrane-bound NAC transcription factor controls mitochondrial retrograde and reactive oxygen species signalling in *Arabidopsis thaliana*. (Chapter 4 – to be submitted to *Plant Cell*)

‡ These authors contributed equally to the work in Chapter 2.

* These authors contributed equally to the work in Chapter 4.

Other publications

Narsai, R., Ivanova, A., Ng, S., and Whelan, J. (2010). Defining reference genes in Oryza sativa using organ, development, biotic and abiotic transcriptome datasets. BMC Plant Biol **10,** 56.

Abstract

Mitochondria are semi-autonomous organelles in eukaryotic cells that contain over 1000 proteins. As a result of their endosymbiotic origins, they still retain a small coding capacity of less than 50 proteins in plants. The remainder of mitochondrial proteins is encoded in the nucleus, and under appropriate signals, acting via anterograde or retrograde signalling pathways, to regulate genes encoding mitochondrial proteins. While our knowledge of the mitochondrial proteins, and the various biochemical activities carried out in mitochondria is well advanced, little is known about the molecular components regulating the expression of the nuclear genes encoding mitochondrial proteins. The studies described in this thesis use forward and reverse genetic approaches to identify and characterise components that regulate the expression of genes located in the nucleus that encode mitochondrial proteins.

Using reverse genetic approaches, the role of a sequence motif, called site II (5'-TGGGC(C/T)-3'), in regulation of various genes encoding mitochondrial proteins was investigated. Mutation of the site II element in a variety of promoters regions of genes encoding mitochondrial proteins revealed that they did influence the activity of the promoter, both positively and negatively, that depended on the number and arrangement of these elements and on the time of the day/night period. Binding assays using yeast one-hybrid assays indicated that the site II elements interacts with TEOSINTE BRANCHED1, CYCLOIDEA, PROLIFERATING CELL FACTOR1 (TCP) transcription factors, that can act as positive or negative regulators of gene expression. Furthermore, it was demonstrated that the TCP transcription factors interacted with regulatory components of the circadian clock. Thus, it was

shown that the activities of promoters for nuclear located genes encoding several mitochondrial proteins were regulated in a diurnal manner by TCP transcription factors, and that this diurnal pattern was evident in transcript and protein abundance for these genes.

A forward genetic screen was carried out to identify regulators of the mitochondrial *ALTERNATIVE OXIDASE 1a* (*AOX1a*) gene in *Arabidopsis thaliana*. The 2 kb promoter of *AOX1a* was used to drive the expression of luciferase in transformed Arabidopsis plants. Treatment with antimycin A (AA) led to an induction of the promoter activity. Seeds from this *AOX1a-Luciferease* transformed plant were mutagenised with EMS and screened for inability to induce luciferase under AA treatment. Two mutants were identified;

i) One encoded a cyclic-dependent protein kinase (CDKE;1), that had previously been shown to be a subunit of the plant mediator complex, that relays information from transcription factors to RNA polymerase II to determine the rate of transcript initiation. It was shown that mutations in CDKE;1 have both transcriptional and post-transcriptional affects. Furthermore, CDKE;1 was shown to interact with KIN10, a kinase previously reported to integrate stress and energy signalling in plant cells.

ii) The second mutant identified encoded an endoplasmic reticulum bound NAM, ATAF and CUC (NAC) transcription factor, designated ANAC017. It was demonstrated that this transcription factor bound directly to the *AOX1a* promoter to regulate activity. Analysis of mutants revealed that ANAC017 mediated responses to reactive oxygen species (ROS) in cells as whole genome transcriptional profiling revealed a large

overlap in the genes controlled by ANA017 and that were induced by different treatments that induced oxidative stress.

These studies reveal the molecular components that control the expression of nuclear genes encoding mitochondrial protein under normal growth conditions and under stress. The overall theme that emerged was that the regulators identified also regulated a variety of other genes encoding proteins found in various locations in the cell. Thus, the interconnection between mitochondria and other organelles extends beyond the exchange of metabolites. These organelles also share regulatory networks to coordinate their activities.

Abbreviations

AA	Antimycin A
ABI4	ABSCISIC ACID-INSENSITIVE-4
ANAC017	Arabidopsis NAC-domain containing transcription factor 17
AOX	ALTERNATIVE OXIDASE
AOX1a	ALTERNATIVE OXIDASE1a
Arabidopsis	*Arabidopsis thaliana*
BiFC	Bimolecular fluorescence complementation
CAREs	*Cis*-acting regulatory elements
CCA1	CIRCADIAN CLOCK ASSOCIATED 1
CDKE;1	CYCLIN-DEPENDENT KINASE E;1
CHE	CCA1 HIKING EXPEDITION
CHLM	Mg-ProtoIX methyltransferase
EMS	Ethyl methanesulfonate
EMSA	Electromobility shift assay
ER	Endoplasmic reticulum
Fmt1	Mitochondrial initiation factors (yeast)
GDC	Glycine decarboxylase
GFP	Green fluorescence protein
GUN	GENOME UNCOUPLED
GUS	ß-glucuronidase
H_2O_2	Hydrogen peroxide

HSP90	HEAT SHOCK PROTEIN 90
Lhcb	Nuclear genes encoding light harvesting chlorophyll *a/b*-binding protein
LHON	Leber Heriditary Optic Neuropathy
LSU	Large subunit of ribosome
LUC	Firefly luciferase
MELAS	Mitochondrial Encephalomyopathy, Lactic, Acidosis, Strokelike Episodes
MFA	Monofluoroacetate
Mg-ProtoIX	Mg-protoporphyrin IX
Mrf1	Mitochondrial termination factors (yeast)
MRR	Mitochondrial Retrograde Regulation
mtDNA	Mitochondrial DNA
mTERF1/2/3	Mitochondrial transcription termination factor 1, 2 and 3 (human)
Mtf1p	Mitochondrial transcription factor (yeast)
mtRNAP	Mitochondrial RNA polymerase (yeast)
NAC	NO APICAL MERISTEM (NAM), ARABIDOPSIS TRANSCRIPTION ACTIVATION FACTOR 1/2 (ATAF1/2), CUP SHAPED COTYLEDON2 (CUC2)
Nam1p/Mtf2p	Mitochondrial intron splicing protein (yeast)
NCS	Non-chromosomal stripe mutant
$O_2^{\bullet-}$	Superoxide radical
OXPHOS	Oxidative phosphorylation
PAP	3’-Phosphoadenosine 5’-phosphate

PHD	Plant homeodomain
POLRMT	Mitochondrial RNA polymerase (human)
PPR	Pentatricopeptide repeat
PTM	A PHD type transcription factor with transmembrane domains
RAOs	REGULATORS OF AOX1a
Redox	Reduction-oxidation
ROS	Reactive oxygen species
Rpo41p	Mitochondrial RNA polymerase (yeast)
RpoTmp	Mitochodnrial RNA polymerase (plants)
Rubisco	Ribulase bisphosphate carboxylase/oxygenase
RuBP	Ribuloase-1,5-bisphosphate
SHMT	Serine hydroxymethyltransferase
Sls1p	Mitochondrial translation protein (yeast)
SnRK1	Sucrose non-fermenting1-related protein kinases
SSU	Small subunit of ribosome
TCP	TEOSINTE BRANCHED1, CYCLOIDEA, PROLIFERATING CELL FACTOR1
TEFM	Mitochondrial transcription elongation factor (human)
TFAM	Mitochondrial transcription factor A (human)
TFB1M	Mitochondrial transcription factor B1 (human)
TFB2M	Mitochondrial transcription factor B2 (human)
Tim23-2	Translocase of inner membrane 23-2
TOR	Target of Rapamycin

TORC	TARGET OF RAPAMYCIN (TOR) COMPLEX
Tuf1	Mitochondrial elongation factors (yeast)
XRNs	5’ to 3’ Exoribonucleases
ZmSig2B	A sigma factor that associated with chloroplastic transcription initiation in maize

Table of Contents

Chapter 1 Introduction

1.1. Mitochondria – structure, origin and function

1.1.1. Mitochondrial structure

Mitochondria are double membrane bound organelles found in almost all eukaryotic cells. Meves F. first described the existence of mitochondria in plant cells in 1904, through the observation of the pollen nurse cells in Nymphaeaceae (cited in Millerd and Bonner, 1953). Since the discovery of mitochondria over a century ago, extensive research has been carried out to characterise the structure and function(s) of this organelle that is essential in all eukaryotic cells. The importance of mitochondrial function in biochemistry is evidenced by, but not limited to, the fact that major advances in mitochondrial research have been the recipients of Nobel prizes, from the discovery of the Krebs cycle to the structure of the ATP synthase. Mitochondrial dysfunction is associated with a number of diseases in humans, from Leber Heriditary Optic Neuropathy (LHON) (Wallace et al., 1988), Mitochondrial Encephalomyopathy, Lactic, Acidosis, Strokelike Episodes (MELAS) (Mezghani et al., 2011) to Parkinson's disease and Austism (Sherer et al., 2002; Haas, 2010), and in plants, e.g. cytoplasmic male sterility (Chase, 2007). In plants, correct mitochondrial function is required to support cell growth and development.

Mitochondria are highly dynamic. They undergo fusion, fission and vary in shape and size (Logan and Leaver, 2000; Liu et al., 2009; Wang et al., 2012a). Mitochondria can be static or motile and are able to dynamically move around within the cell in response to cellular signals (Hackenbrock, 1966; Logan and Leaver, 2000). It has been shown that mitochondria move around cytosol through tethering to the F-actin filament and microtubules (Boldogh and Pon, 2006). Mitochondria are on average 0.5 to 2 μm diameter in size and are

typically rod-shaped or sausage-shaped (Logan and Leaver, 2000). The internal compartments within the mitochondrion can essentially be broken down into the outer membrane, the inter-membrane space, the inner membrane and the matrix. The outer membrane has a smooth appearance. It harbours many proteins involved in aspects of cellular signalling, the mitochondrial import components and lipid synthesis machinery (Duncan et al., 2011). The space in between the outer membrane and inner membrane is defined as the intermembrane space. The inner membrane is highly complex in structure and can be divided into several sub-parts: the inner boundary membrane, the cristae membrane, the intracristae space and the cristae junction (Mannella et al., 2001; Mannella, 2006; Neupert, 2012). Cristae are formed through the invagination of the inner membrane. The intracrista space is joined with the intermembrane space through a narrow tubular structure, the cristae junction (Herrmann and Riemer, 2010; Neupert, 2012). It has been postulated that each intracrista space is a specific microenvironment that is related to a mitochondrial function (Herrmann and Riemer, 2010). For instance, the oxidative phosphorylation (OXPHOS) machinery is preferentially located on the cristae membrane. During OXPHOS, protons are pumped into the intracrista space and because the cristae junction is narrow and able to restrict the diffusion of protons throughout the intermembrane space and into the cytosol, therefore maintaining the biochemical gradient of protons that are used to drive the ATP synthase and so improving the efficiency of OXPHOS (Herrmann and Riemer, 2010).

Mitochondria have been shown to exist in two inter-changeable conformational states, defined as a condensed state and an orthodox state, through the visualisation of chemically fixed mitochondria (Hackenbrock, 1966;

Mannella et al., 2001; Mannella, 2006). When mitochondria are in a medium containing ATP, they appeared to be highly motile and have an expanded matrix, this is defined as the orthodox state (Hackenbrock, 1966). Conversely, when mitochondria are treated with ADP, the organelles appear static in motility, with a dilated intracristae space and compacted matrix representing the condensed state (Hackenbrock, 1966). Furthermore, studies have shown that the inner membrane is physically linked to the outer membrane via protein import components that span the two membrane structures, therefore, it is likely that a change in the morphology of the cristae will lead to morphological alterations of the whole mitochondria. With technological advances in electron tomography, it is becoming clear that widely used descriptions of mitochondria as ‘baffle’ structures are inadequate. It has been postulated that the changes within mitochondrial internal structure is linked to the efficiency of ATP production, the elimination of ROS during oxidative stress and other mitochondrial functions; however, the exact mechanism which triggers conformational changes in the mitochondria is unknown (Mannella, 2006).

Mitochondria can also undergo dynamic fusion and fission events. Several models regarding mitochondrial fusion and fission have been proposed (Liu et al., 2009; Wang et al., 2012a). Liu et al. (2009) proposed two types of mitochondrial fusion, transient fusion and a complete fusion. Transient fusion allows the exchange of intermembrane space proteins, while the complete fusion allows the exchange of the protein content and the mitochondrial DNA (mtDNA) located in the intermembrane space and the matrix.

1.1.2. Endosymbiotic origin of mitochondria

It is widely accepted that mitochondria evolved from a single endosymbiotic event, in which an a-protobacterium was engulfed by an archaebacterium (Lang et al., 1999; Gray et al., 2001; van der Giezen and Tovar, 2005). This hypothesis is supported by sequence comparisons between the mitochondrial and ancestral eubacterial genomes (Andersson et al., 1998), and the comparisons of the nuclear-encoded mitochondrial proteins, genome organisation, and gene expression, all of which display many similarities with eubacterial systems (Karlberg et al., 2000; Gabaldon and Huynen, 2004).

Over the course of evolution, it is believed that genes coded for within the mtDNA are transferred to the nuclear genome (Keeling and Palmer, 2008). However, this raises the question: if genes transfer from the mitochondria to the nucleus is an ongoing process, why do mitochondria present in all eukaryotic cells still retain their own genome after 1 billion years of co-evolution? Several hypotheses have been postulated to try to explain this apparent contradiction. Two common explanations are the hydrophobicity theory (von Heijne, 1986) and the co-location for reduction-oxidation (redox) regulation (Allen, 1993). The former proposes that some mitochondrial proteins, due to regions of high hydrophobicity, cannot be imported into mitochondria after synthesis in the cytosol (von Heijne, 1986), and thus need to be synthesised within the mitochondria from mitochondrial genes. Direct experimental evidence exists to support this proposal (Daley and Whelan, 2005). The second proposal states that the expression of mitochondrial genes is linked to the redox state of mitochondria (Allen, 1993). While some plastid encoded genes are under redox regulation, there is no evidence that the expression of mitochondrial genes is under redox regulation (Daley and Whelan, 2005). However, it has to be

pointed out that at least some mitochondrial encoded genes, particularly in plants, encode proteins that are not hydrophobic, e.g. ribosomal proteins. Thus, there is no clear single reason why mitochondria still retain a coding capacity, and it is likely that there are more than one factors involved in the favourable retention of some coding capacity in mitochondria. The theory that mitochondria 'act' as an organism and actively retain their genetic identity, is supported by the fact that mitochondria from different lineages have adapted different strategies, such as non-universal genetic codes or RNA editing (Chateigner-Boutin and Small, 2011; Abascal et al., 2012) to prevent complete transfer of the mitochondrial genome, and should not be overlooked as another possible explanations.

Each mitochondrion can possess multiple copies of its genome, from several to hundreds of copies of the mtDNA (Bendich, 1987). Mitochondrial DNA is maternally inheritable. The factor(s) that regulates the replication and the specific number of mtDNA copies are not known. It has been suggested that mitochondria possess multiple copies of the genome to ensure that an adequate amount of functional proteins can still be produced, even as mtDNA mutations accumulate, as there is no robust DNA repair system in place in mtDNA replication compared to that which takes place in the nucleus. Notably, the mutation rate of plant mitochondria is usually lower in comparison to mammalian counterparts; again the reason for this is unclear (Wolfe et al., 1987). The composition of mtDNA varies in different organisms. Mammalian mtDNA is compact and has little or no intergenic regions while plant mtDNA is relatively large with a high proportion of intergenic regions (Gray et al., 1999).

1.1.3. Mitochondrial function

Mitochondria generate cellular ATP through OXPHOS. The OXPHOS machinery is comprised of four protein complexes, complex I to IV, two electron shuttles, the ubiquinol and cytochrome *c* and the F_0F_1-ATP synthase. Electrons derived from the reducing agents, NAD(P)H and $FADH_2$, are fed into the electron transport chain through complex I and complex II, and eventually passed through to reduce molecular oxygen to form water in complex IV. Mitochondria are also the site of ROS production with the superoxide radical ($O_2^{\bullet -}$) produced at a variety of sites within the mitochondrial electron transport chain, and converted to hydrogen peroxide (H_2O_2) by superoxide dismutase (Liu et al., 2002; Murphy, 2009). Mitochondrial ROS have been implicated in both signalling processes and damage to mitochondrial components (Murphy, 2009; Millar et al., 2011).

In addition to the cytochrome electron transport chain, plant mitochondria also contain a number of molecular by-passes or branches in the electron transport chain, called the alternative NAD(P)H dehydrogenases and the alternative oxidase (AOX) (Vanlerberghe and McIntosh, 1997; Rasmusson et al., 2004). Plant mitochondria are somewhat unusual in that while fungi and some animals also contain these components, components of the alternative respiratory pathway are constitutively expressed in plants and also respond to cellular stress signals (Ho et al., 2007; Millar et al., 2008; McDonald et al., 2009; Millar et al., 2011). The alternative components, discussed in more detail in Section 1.3.2.3, have been extensively studied over the past decades in plant biology in relation to their role in plant stress responses. These components are consistently induced several-fold in stress and have even been suggested to provide some survival role in plants.

In addition to the TCA cycle and electron transport chain, plant mitochondria are the site of several other metabolic processes, from an essential role in the photorespiratory pathway, to being the site of Fe-S clusters synthesis (Bych et al., 2008; Balk and Pilon, 2011), and are also the site for synthesis and catabolism for amino acids, folate and biotin (Millar et al., 2011). The complexity of mitochondrial function can be gauged from the size of the mitochondrial proteome, which is estimated to be over 1,500 proteins in plants (Millar et al., 2011). This proteome is not static, displaying tissue and diurnal variations in the abundance of proteins (Lee et al., 2010; Millar et al., 2011). This complexity of the mitochondrial proteome is underpinned, at least in part, by the regulation of the expression of genes encoding mitochondrial proteins.

1.2. Regulation of mitochondrial located genes

The mitochondrial genome varies greatly in size, form and genomic content across different species. Recently, with full genome sequencing, the size and genetic content of mtDNA from many organisms has been determined. It ranges from ~ 6 kb in *Plalsmodium falciparum* (a parasite that causes malaria in humans) to 1.6 Mb in *Cucumis melo* (muskmelon in plants) (Ward et al., 1981; Gardner et al., 2002). As research model organisms, *Homo sapiens* (human), *Saccharomyces cerevisiae* (yeast) and *Arabidopsis thaliana* (Arabidopsis) contain mitochondrial genomes of 16.5 kb, 85 kb and 366 kb, respectively (Unseld et al., 1997; Foury et al., 1998; Rackham et al., 2012). Mitochondrial DNA exists in circular or linear forms (Bendich, 1993; Valach et al., 2012) and with different sizes. For examples, in *Cucumis sativus* (cucumber), mtDNA consists of a master circular form which is, 1.5 Mb in size, and two smaller circular mtDNA copies with ~ 84 kb and ~ 45 kb of DNA

(Alverson et al., 2011) while *Chlamydomonas reinhardtii* (a green alga) has linear mtDNA 15.8 kb in size (Fan and Lee, 2002).

Even though mitochondria still retain the ability to transcribe and translate proteins within the organelle, more than 95 % of mitochondrial proteins are nuclear encoded, translated in the cytosol and imported into mitochondria. The number of proteins that are mitochondrial encoded are between three proteins in *P. falciparum* to 83 proteins in some plants (Mower et al., 2012). In Arabidopsis, there are ~ 1,500 mitochondrial proteins yet only 32 proteins are encoded by mtDNA (Unseld et al., 1997; Klodmann et al., 2011). Most of the mtDNA encodes for limited types of RNAs, including the small subunit (SSU) and large subunit (LSU) of ribosomal RNAs and either the full or partial complement of mitochondrial tRNA species (Gray et al., 1999), as well as protein components of the mitochondrial electron transport chain, e.g. components of complex I, III and IV and ATP synthase (Lipinski et al., 2010; Herrmann et al., 2012b; Herrmann et al., 2012a). Notably, all proteins encoded in the mtDNA are found in a protein complex with nuclear encoded subunits.

While mammalian mtDNA has a compact genomic structure, with no intron or intergenic regions (Rackham et al., 2012), plants have a relatively large and more varied mtDNA structure, due to the presence of repetitive non-coding DNA in the genome (Knoop, 2004). With the differences in the genomic structures, different organisms also display differences in the processes of transcription and translation of the mitochondrial genome. In humans, several mitochondrial RNAs are transcribed through a single promoter, either from the heavy strand or the light strand promoter (Temperley et al., 2010). The polycistronic system used in mammalian mitochondria is similar to the transcriptional control of bacterial genomic DNA. Furthermore, in mammals the

transcription of mtDNA requires additional accessory proteins other than RNA polymerase and transcription factors, e.g. the transcription termination factors 1, 2 and 3 (mTERF1, mTERF2 and mTERF3) that act on mitochondrial promoters to modulate gene expression (Wenz et al., 2009). Due to larger mtDNA present in yeast and plants, genes are transcribed through the use of several promoters (Binder and Brennicke, 2003; Lipinski et al., 2010). In Arabidopsis, it is expected to utilise around 29 promoters in mtDNA expression (Binder and Brennicke, 2003). However, despite extensive studies, the exact nature of the plant mtDNA promoter remains elusive (Kuhn et al., 2009).

Mitochondria are semi-autonomous organelles because the transcription and translation of the mitochondrial genes are partly controlled by nuclear encoded proteins. In humans, nuclear encoded mitochondrial transcriptional machinery includes mitochondrial RNA polymerase (POLRMT), mitochondrial transcription factor A (TFAM), mitochondrial transcription factor B1 and B2 (TFB1M and TFB2M) and a transcription elongation factor for mitochondria (TEFM) (Asin-Cayuela and Gustafsson, 2007). In yeast, the nuclear encoded proteins implicated in mitochondrial gene expression include the mitochondrial RNA polymerase (mtRNAP/Rpo41p) (Greenleaf et al., 1986), and transcription factor Mtf1p (Biswas and Getz, 2002), proteins involved in intron splicing Nam1p (also known as Mtf2p) (Rodeheffer et al., 2001) and translation Sls1p (Bryan et al., 2002)**.** There are six nuclear encoded plastid sigma factors, SIG1-SIG6, which are involved in light-dependent activation of chloroplastic promoters in Arabidopsis (Tanaka et al., 1997; Fujiwara et al., 2000). In plants, no transcription factor for mitochondrial transcription has been identified to date. However, several proteins that are dual-targeted to chloroplasts and mitochondria have been identified in organellar gene expression systems, these

include the nuclear encoded phage-type RNA polymerase, RpoTmp (Kobayashi et al., 2001), and a plastid sigma factor in maize, ZmSig2B (Beardslee et al., 2002). As these proteins are involved in organellar gene expression, they could play a role in coordinating the gene expression in the three independent genomes present in plant cells; the mitochondrial, chloroplast and nuclear genomes.

In yeast, nuclear encoded translational activators control the initiation of mitochondrial translation. Translational activators control the mitochondrial translation by binding to the 5'UTR of the mitochondrial mRNA and interacting with the ribosomes and the inner membrane (Herrmann et al., 2012a). Similar to the transcriptional control provided by transcription factors, the translation of each particular mitochondrial mRNA is controlled by one or more specific translational activator(s) (Herrmann et al., 2012a). Besides the translational activators, nuclear encoded proteins necessary for mitochondrial protein synthesis include the initiation factors (e.g. Fmt1), elongation factors (e.g. Tuf1) and termination factors (e.g. Mrf1) in *Sachromyces cerevisiae* (Herrmann et al., 2012a).

While much of the knowledge of the regulation of mitochondrial located gene expression in mammals and yeasts has been characterised in details, relatively little is known about the regulation of expression of plant mtDNA. Most plant mitochondrial transcripts contain introns that need to be spliced and processed, and undergo various events of RNA editing. RNA editing usually occurs in the exons with C-to-U conversions. However, RNA editing was also found to occur inside introns to affect intron splicing (Castandet et al., 2010). With a larger mtDNA size compared to other organisms and with distinct metabolic activities of mitochondria intimately linked with that of chloroplasts in

plant cells, the factors that regulate the expression of the mitochondrial genome are likely to be complex and largely unknown. Studies of Arabidopsis suspension cells under sugar starvation and re-feeding treatment revealed that coordination of nuclear and mitochondrial gene expression occurred at the post-translational level, where the expression of mtDNA encoded genes was not affected by the sugar starvation and. Furthermore, the biogenesis of the mitochondrial protein complexes was regulated through the changes in nuclear gene expression and protein assembly process (Giege et al., 2005).

1.3. Regulation of nuclear located genes encoding mitochondrial proteins

The expression of nuclear located genes is controlled at different levels, from the organisation of the chromatin structure to the activation of the promoters through the binding of transcription factors. Chromatin organisation is determined by the genomic sequence, the nucleosomes and the chromosomal arrangement (Fransz and de Jong, 2011). Chromatin structure determines gene activity through the binding or release of histone proteins to the DNA. The binding of histone proteins to the DNA obscures the accessibility of the transcription machinery to promoter regions, and so affects the expression of genes. The recruitment and release of histones from chromatin DNA is controlled by several factors, including epigenetic regulation, e.g. DNA methylation often leads to the repression of gene expression (Fuks, 2005). The initiation of transcription by the binding of transcription factors and the transcription machinery is affected by the signals generated inside the cell (i.e. retrograde signals emitted from organelles) and signals outside the immediate cellular environment (i.e. developmental and environmental cues). These

signals in turn recruit specific sets of transcription factors to the nuclear gene promoters.

1.3.1. Anterograde signalling

It is important for cells to adjust the protein contents to suit specific functional states required for efficient growth and development. Gene expression is constantly and dynamically regulated to meet the energetic demands of the cell. This transcriptional control is regulated by the combinatorial control of transcription factor networks, in which the activation or repression of particular sets of genes are controlled by a set of transcription factors initiated in response to a particular signal. Therefore different combinations of transcription factors yield a differential response in gene expression.

Anterograde signalling is often referred to as a “top-down” signalling pathway where changes in the expression of organellar proteins are controlled by environmental (e.g. light) and developmental (e.g. hormone) signals perceived directly by the nucleus. Anterograde regulation modulates organellar protein expression by (i) changing the expression of nuclear located genes encoding mitochondrial proteins or by (ii) changing the expression of nuclear encoded protein components of the mitochondrial transcription and translation machinery.

Classic examples of the anterograde regulation of nuclear encoded organellar proteins are the light dependent regulation of glycine decarboxylase (GDC) subunits and the serine hydroxymethyltransferase (SHMT) in mitochondria and the expression of photosynthetic associated nuclear genes in

chloroplasts (Turner et al., 1993; Walters and Horton, 1994). In plants, mitochondrial GDC and SHMT proteins are involved in photorespiration, a reaction involved in the oxygenation of ribuloase-1,5-bisphosphate (RuBP, a carbon compound) by ribulase bisphosphate carboxylase/oxygenase (Rubisco) (Andrews et al., 1973). Photorespiration involves reactions in chloroplasts, peroxisomes and mitochondria. There are four nuclear encoded GDC subunits, the L, H, T and P subunits (Walker and Oliver, 1986). The light-dependent expression of GDC subunits was examined in pea. Turner et al. (1993) measured the mRNA level of GDC subunits and SHMT in peas and found that the mRNA level of GDC and SHMT declined to almost undetectable level after pea seedlings were placed in the dark for 48 hours and the mRNA expression increase rapidly after re-exposure of light (Turner et al., 1993).

1.3.2. Retrograde regulation

Mitochondrial retrograde regulation (MRR) refers to the regulation of nuclear gene expression by the signals generated in mitochondria. Identification of MRR signalling molecules is largely dependent on the study of mutants that have aberrant gene expression of nuclear located genes encoding mitochondrial proteins during mitochondrial dysfunction. These studies have predominantly been performed in mitochondrial mutants, or in studies utilising chemical treatments that transiently disrupt mitochondrial function. Several retrograde signalling components have been proposed, including transcription factors that act to influence the expression of genes in response to organelle signals, specific metabolites that are generated in the organelle, organelle gene expression, ROS and the redox state of organelles (Kobayashi et al., 2001;

Mochizuki et al., 2001; Fey et al., 2005; Pogson et al., 2008; Giraud et al., 2009).

1.3.2.1. Mitochondrial retrograde regulation in yeast

Yeast retrograde signalling has been well defined in the literature. There are at least three retrograde signalling pathways that exist in yeast. The earliest studied pathway is the RTG pathway, with the second and third retrograde pathways involving AFO1/MRPL25 and the mitochondrial translation complex, respectively (Liu and Butow, 2006; Heeren et al., 2009; Caballero et al., 2011). It has been observed that the activation of yeast retrograde signalling often leads to an extended yeast replicative lifespan (Jazwinski, 2005a). The best-studied retrograde regulation pathway in yeast is the RTG pathway, involving the molecular components Rtg2p, Rtg1p and Rtg3p (Liu and Butow, 2006). Rtg2p is a positive regulator for the activation of the RTG pathway (Jazwinski, 2005b). Mechanistically, it is unknown exactly how Rtg2 perceive signals during mitochondrial dysfunction, however, it has been shown that decreased membrane potential activates this retrograde regulation pathway through Rtg2p function and in turn increases lifespan of the yeast (Jazwinski, 2012; Miceli et al., 2012). Rtg1p and Rtg3p function downstream of Rtg2p in the signal cascade and upon activation, Rtg1p and Rtg3p form heterodimers and translocate into the nucleus and activate transcription of retrograde responsive genes. Additionally, target of rapamycin (TOR) complex 1 (TORC1), Bmh1/2p, Mks1p and Lst8p are negative regulators of the RTG pathway (van Heusden and Steensma, 2001; Ferreira Junior et al., 2005; Liu and Butow, 2006).

1.3.2.2. Chloroplast retrograde regulation

In plants, retrograde signalling molecules and signal transduction cascades are generated from both mitochondria and chloroplasts. Similar to mitochondria, chloroplasts originated from an endosymbiotic event and most of the coding capacity of the original genome of the bacterium has been transferred to the nucleus over time. Therefore, like mitochondria, most chloroplastic proteins are nuclear encoded and regulated by nuclear transcription factors. Several signalling components have been identified in chloroplast retrograde regulation. Studies of *genome uncoupled* (*gun*) mutants have identified Mg-protoporphyrin IX (Mg-ProtoIX), a tetrapyrrole molecule, as an important signalling molecule (Mochizuki et al., 2001; Larkin et al., 2003; Strand et al., 2003). In *gun* mutants, the expression of nuclear genes encoding chloroplastic proteins was uncoupled from chloroplast development under conditions where chloroplast function was compromised by norflurazon treatment, a chemical that causes aberrant chlorophyll metabolism and bleaches the organelle. Early studies of the *gun* mutants suggested that the accumulation of the intermediate Mg-ProtoIX, which was caused by the disruption of the tetrapyrrole biosynthesis pathway, was the retrograde signal that triggered the expression of photosynthetic genes in the nucleus (Strand et al., 2003). However, these studies did not provide any direct evidence of the translocation of the Mg-ProtoIX or any of its binding partners from the chloroplasts to the nucleus (Strand et al., 2003). In fact, follow-up studies carried out by two independent groups have showed a contradicting result to those presented by Strand et al. (2003). Moulin et al. (2008) and Mochizuki et al. (2008) used different methods in measuring tetrapyrrole intermediates and found that plants treated with norflurazon fail to accumulate MgProtoIX.

Moreover, Mochizuki group (2008) generated a double mutant that accumulated Mg-ProtoIX in *gun*s background by crossing it with the *chlm* knockout mutant (*CHLM* encodes for Mg-ProtoIX methyltransferase) to test if accumulation of Mg-ProtoIX to a wild-type level under norflurazon treatment could suppress the *gun* phenotype, i.e. the inhibition of *Lhcb* (nuclear genes encoding light harvesting chlorophyll *a/b*-binding protein) expression in these double mutants. However, despite a high accumulation of Mg-ProtoIX, *gun5 chlm* or *gun4 chlm* double mutants still accumulated similar amount of *Lhcb* mRNA as in the single *gun5* or *gun4* mutant (Mochizuki et al., 2008). On the other hand, the Moulin group (2008) also conducted a microarray analysis on norflurazon-treated plants and found that the expression of genes of tetrapyrrole synthesis related pathways were down regulated (Moulin et al., 2008). Taken together, both groups came to similar conclusions that the expression of *Lhcb* (and other photosynthetic associated nuclear genes) did not correlate with the steady state of the Mg-ProtoIX. A subsequent explanation was proposed for the previous observation made by Strand et al. (2003), in that the signaling molecules responsible for the induction of *Lhcb* were possibly by-products derived from the Mg-ProtoIX (e.g. ROS) or its synthesis pathway (Mochizuki et al., 2008; Moulin et al., 2008).

Recently, several other chloroplast retrograde signalling components have been identified, i.e. heme molecules (Woodson et al., 2011), a heat shock protein (HSP90) (Kindgren et al., 2011; Kindgren et al., 2012), a plant homeodomain (PHD)-type transcription factor with a transmembrane domain (PTM) (Sun et al., 2011), and 3'-phosphoadenosine 5'-phosphate (PAP) (Estavillo et al., 2011). Heme, HSP90 and PTM are all tetrapyrrole-mediated plastid retrograde regulation-related, however, the proposed models for each of

these molecules is different. It has been demonstrated that the increase of flux into the heme branch of tetrapyrrole synthesis would increase the expression of nuclear encoded chloroplastic proteins. However, whether heme itself is translocated directly from chloroplasts to the nucleus or is involved in a retrograde relay signal via second messengers is yet to be determined (Woodson et al., 2011). Secondly, HSP90 was found to interact with Mg-ProtoIX and control the expression of nuclear encoded photosynthetic genes during oxidative stress (Kindgren et al., 2011; Kindgren et al., 2012). On the other hand, the transcription factor PTM has been demonstrated to function downstream of GUN1 and affect the nuclear gene expression of plastid components regulated through the activity of the transcription factor ABA-insensitive-4 (ABI4). Instead of interacting with tetrapyrroles, PTM receives signals upstream from GUN1, which has been shown to be the convergent point for retrograde signals inside the chloroplast (Koussevitzky et al., 2007). PTM is activated through a cleavage event where it is released from the chloroplast membrane and then translocated into the nucleus to activate ABI4 under chloroplast dysfunction (Sun et al., 2011). Lastly, Gonzaloz et al (2011) recently showed that during high light and drought stress, another metabolite, PAP, was able to move from the chloroplast to the nucleus to inhibit the activity of 5' to 3' exoribonucleases (XRNs, enzymes that are involved in RNA metabolism). This in turn regulates the expression of stress responsive genes encoded in the nucleus (Estavillo et al., 2011). Interestingly, the catabolism of PAP was SAL1 enzyme dependent, and SAL1 was co-localised to chloroplasts and mitochondria (Estavillo et al., 2011). Whether PAP also functions as a mitochondrial retrograde signalling molecule is yet to be confirmed. To-date, no retrograde signalling molecules have been identified in plant mitochondria.

Even though the ROS and redox state of organelles have been implicated in mitochondria retrograde signalling pathway, the mechanistic details of how the signalling molecules are transferred, whether there is any secondary messengers involved and the exact identities of signalling molecules remain unknown.

1.3.2.3. Mitochondrial retrograde regulation in plants

An early example of the existence of plant MRR responses on the scale of plant development is shown in the identification of variegated non-chromosomal stripe (NCS) mutants in maize (Newton and Coe, 1986). These mutants contained an abnormal mtDNA rearrangement that resulted in altered chloroplast development and function, and, ultimately caused yellow sectors within the leaves of these mutants. This provides direct evidence that mitochondrial dysfunction would not only cause alterations in nuclear gene expression of mitochondrial proteins, but on a cellular-wide scale cause changes that affect the function and development of other organelles. A recent meta-analysis of MRR concluded that during mitochondrial dysfunction, nuclear located genes encoding chloroplastic proteins, pentatricopeptide repeat (PPR) proteins and translational machinery were significantly altered (Schwarzlander et al., 2012).

The most studied MRR system in plants is the nuclear encoded *ALTERNATIVE OXIDASE1a* (*AOX1a*). In plants, AOX is encoded by a small multigene family. In Arabidopsis, there are five members of the AOX gene family, AOX1a, 1b, 1c, 1d and AOX2. The expression of each AOX isoform is regulated by developmental and tissues specific signals (Saisho et al., 1997;

Clifton et al., 2006). For example, *AOX1a* is expressed throughout the plant developmental stages and in almost all tissue types, while *AOX1b* expression is limited to stages related to flower development (Clifton et al., 2006). Moreover, only *AOX1a* and *AOX1d* are highly stress responsive upon treatment with a number of different forms of environmental stress and chemical inhibition (Clifton et al., 2006). It has been long been known that AOX plays a major role in modulating ROS production in plant mitochondria. However, studies carried out in tobacco leaves only recently provide a direct observation that AOX modulates the concentration of ROS and reactive nitrogen species (Cvetkovska and Vanlerberghe, 2012b). It was proposed that AOX controls ROS production by consuming reducing equivalents, preventing the mitochondrial electron transport chain from becoming over-reduced, therefore, reducing the probability of single electron leaks to O_2 to form $O_2^{\bullet}-$, which can be used as substrate to generate other ROS species (Cvetkovska and Vanlerberghe, 2012b). The factors that make *AOX1a* a suitable model for MRR studies are (i) its expression is highly stress responsive to a wide range of mitochondrial stresses and, (ii) the molecular defect caused by knocking out *AOX1a* cannot be compensated by other AOX gene members, as shown in the increased sensitivity of *aox1a* mutants to combined light and drought stress where this stress sensitive phenotype could not be shielded by the expression of other AOX members (Giraud et al., 2008). *AOX1a* is up-regulated when mitochondrial complex III is inhibited by AA treatment in several species, including tobacco, maize, soybean and Arabidopsis (Vanlerberghe and McLntosh, 1996; Djajanegara et al., 2002; Karpova et al., 2002; Clifton et al., 2005). Inhibition of aconitase activity in the TCA cycle by monofluoroacetate (MFA) or by nitric oxide also induced *AOX1a* expression (Dojcinovic et al., 2005; Gupta et al.,

2012). Other common stresses that induce *AOX1a* include cold, high light, drought, oxidative stress and pathogen infection (Calegario et al., 2003; Giraud et al., 2009; Wang et al., 2011; Cvetkovska and Vanlerberghe, 2012a). Only under stress conditions, phenotypic differences were observed in plants with altered *AOX1a* expression compared to wild-type plants, therefore suggesting that AOX also plays a role in plant growth during stress conditions (Fiorani et al., 2005; Giraud et al., 2008). For instance, when grown under low temperatures, there was up to a 33 % decrease or increase in rosette size in plants with reduced or over-expressed of *AOX1a,* respectively (Fiorani et al., 2005).

To-date, the only molecular component identified as a regulator of MRR in plants is the ABI4 transcription factor (Giraud et al., 2009). Through yeast 1-hybrid assays, it has shown that ABI4 binds to the *AOX1a* promoter and functions as a transcriptional repressor during mitochondrial dysfunction (Giraud et al., 2009). Moreover, ABI4 was also able to bind to the promoter of chloroplast retrograde responsive gene, *Lhcb* (Koussevitzky et al., 2007). ABI4 has been shown to act downstream of GUN1 and repress *Lhcb* during chloroplast dysfunction (Koussevitzky et al., 2007). Therefore, it was postulated that ABI4 might coordinate the expression of both mitochondrial and chloroplastic proteins and integrate the organellar retrograde signalling into regulatory pathways involving the important hormone abscisic acid during stress conditions.

1.4. Research proposal

Mitochondria are one of the main sites of cellular ATP synthesis and sites for many other crucial aspects of cellular metabolism, including stress sensing and programmed cell death in plant cells (Giege et al., 2005; Millar et al., 2008; Bolouri-Moghaddam et al., 2010; Biasutto et al., 2011). Mitochondrial biogenesis involves the expression of both nuclear and mitochondrial located genes and has been shown to be under the tight and complex control of both anterograde and retrograde signalling pathways, many of which intersect with signals from other compartments in the cell. While numerous studies on mitochondria have focused on the metabolic function and architecture of the organelle, the mechanisms of how organelles communicate with the nucleus and other organelles, and how mitochondrial gene expression is coordinated with the function of the whole cell are largely unknown. This regulation of mitochondrial function is undoubtedly linked with cross talk with other energy organelles and these signalling pathways might in fact intersect or overlap with each other, however, no distinct and complete pathway has been characterised in plants. One of the aims of this project was to identify and characterise novel signalling components involved in MRR in Arabidopsis. This project consisted of two main components. Firstly, a reverse genetic approach was carried out to identify *cis*-acting regulatory elements (CAREs) involved in the co-regulation of groups of nuclear genes involved in organelle biogenesis. Secondly, a forward genetic approach was utilised to identify and characterise regulatory components that control the expression of *AOX1a* in response to cellular stresses that initiate mitochondrial retrograde signalling.

1.4.1. Reverse genetic approach

Through genome-wide transcript analyses, hundreds if not thousands of genes are co-expressed during organellar biogenesis. While genes can be co-expressed, the magnitude of expression of each gene is different. However, genes that are co-expressed might not be co-regulated. Co-regulated genes are genes that share at least one common transcription factor that binds to specific CAREs in the promoter regions of genes contributing to the initiation of transcription. It is postulated that genes involved in organellar biogenesis and cell division are co-regulated at the transcriptional level through a CARE termed site II elements. Site II elements have a DNA sequence of 5'-TGGGC(C/T)-3' or the reverse complement, and are overrepresented in the promoter regions of nuclear located genes encoding mitochondrial OXPHOS proteins and ribosomal proteins (Li et al., 2005; Welchen and Gonzalez, 2005, 2006). It has been found that plant specific transcription factors, TCP proteins, were able to bind to site II elements and contributed to the transcription initiation (Li et al., 2005; Welchen and Gonzalez, 2005). Li et al. (2005) showed that site II elements are essential for a high expression of cyclin *CYCB1;1* and ribosomal proteins L24 and S2. Additionally, it was shown that TCP20 binds directly to site II elements in these promoters, therefore suggesting that TCP20 is involved in coordinating plant growth and cell division (Li et al., 2005). Circadian regulation is conserved in almost all organisms. Although many metabolic pathways and circadian regulatory proteins have been identified in plants, there has been very little work dissecting the control and mechanisms of organellar biogenesis under circadian control reported in the literature (Harmer et al., 2000; Sanchez et al., 2011; Farre and Weise, 2012).

This work presents evidence for a direct mechanistic link between organellar biogenesis and circadian control. Site II elements were found to be overrepresented in the nuclear genes encoding mitochondrial, chloroplastic and peroxisomal proteins. The functionality of the site II elements was examined using biolistic transient transformation combined with GUS reporter gene assays in selected genes. The ability of TCP proteins to bind to the site II element was examined through yeast-1 hybrid assays. The expression profiles of TCP transcripts were also examined over a 24-hour period and the interactions of TCP proteins with circadian regulatory proteins were examined through yeast-2 hybrid assays. This work is presented in Chapter 2.

1.4.2. Forward genetic approach

A reporter gene system was utilised in a forward genetic approach to define unknown components of mitochondrial retrograde signalling. Arabidopsis plants, ecotype Columbio-0, were transformed with a construct harbouring the *AOX1a* promoter region driving the expression of the firefly luciferase gene (*AOX1a-LUC*). This transgenic plant was named Col:*LUC*. Seeds collected from Col:*LUC* were then chemically mutagenised using ethyl methanesulfonate (EMS). Screening was then carried out to select for mutants that have altered LUC expression and therefore an aberrant regulation of *AOX1a* gene expression in response to mitochondrial stress. These mutants were referred to as *REGULATORS OF AOX1a* (*RAO*s). In this genetic screen, AA was used as the mitochondrial stress to identify for mitochondrial retrograde mutants. It has been reported that AA affects both the functions of the mitochondrial respiratory chain (Rieske et al., 1967) and the chloroplastic photosystem I (Ivanov et al., 1998). Additionally, *AOX1a* has been reported to response to a variety of

oxidative stresses and not restricted to mitochondria stresses (Yoshida et al., 2007), therefore, its expression possibly also affected by the functional states of chloroplasts, therefore, one can argue that by using AA as the screening reagent and *AOX1a* as the reporter gene for retrograde signalling pathway to look for mitochondrial retrograde mutants could result in obtaining mutants encoding general regulators of mitochondrial and/or chloroplastic proteins and these mutants cannot be deem to be genuine mitochondrial retrograde mutants. However, how chloroplastic dysfunction causes changes in mitochondrial protein expression is not known. These changes in gene expression could be triggered through a chloroplastic retrograde signalling pathway that changes the nuclear gene expression for mitochondrial proteins or by signalling molecules (generated in chloroplasts due to stress) that translocate from chloroplasts to the mitochondria and in turn trigger a mitochondrial retrograde signalling pathway. Even though the latter assumption has not been reported before, it should not be ruled out. As the controls to the specificity of mitochondrial stresses, another complex III inhibitor (myxothiazol) and TCA cycle inhibitor (MFA) were also been used in our screening process to act as controls of mitochondrial stress specificity (von Jagow et al., 1984; Vanlerberghe and McLntosh, 1996). Identified and characterised *rao* mutants were categorised into three groups according to the LUC expression upon AA treatment. There are (1) mutants that have reduced or no *AOX1a-LUC* expression under AA treatment, (2) mutants that over-express *AOX1a-LUC* under AA treatment and (3) mutants that constitutively express *AOX1a-LUC* even without AA treatment.

Two novel mitochondrial retrograde regulators, named *rao1* and *rao2*, were identified in this project. In both mutants, the application of AA failed to induce *AOX1a-LUC*, i.e. mitochondrial retrograde signalling pathway was

disrupted therefore expression of *AOX1a* was not induced under conditions of mitochondrial dysfunction, indicating that *rao1* and *rao2* are positive regulators of *AOX1a*. The *rao1* mutant encodes for a cyclin-dependent kinase (CDKE;1) while the *rao2* mutant encodes for a NAC-domain containing transcription factor (ANAC017). The expression of *AOX1a* of *rao1* and *rao2* was examined using quantitative RT-PCR and in immunodetection assays under different abiotic stress treatments. RAO1 was found to associate with KIN10, a protein subunit of the Snf1-related protein kinases (SnRK1) complexes. KIN10 links and integrates the cellular transcriptional responses to molecular signals from stress, sugar and developmental pathways (Baena-Gonzalez et al., 2007). In this work, RAO1 was shown to interact with KIN10 through bimolecular fluorescence complementation (BiFC) assays, thus providing a link between mitochondrial retrograde signalling and developmental pathways. ANAC017 is a transcription factor that directly regulates the expression of *AOX1a* by binding to the *AOX1a* promoter. ANAC017 contains a transmembrane domain at the C-terminus of the protein and is targeted to the endoplasmic reticulum (ER) as shown by green fluorescence protein (GFP)-targeting assay. It is postulated that ANAC017 is cleaved and translocated to the nucleus upon activation by a mitochondrial-derived signal. Three NAC-binding sites were found in *AOX1a* promoter and the functionality of these regulatory elements was examined. We have also shown that ANAC017 binds to the *AOX1a* promoter through electromobility shift assay (EMSA) and yeast 1-hybrid assay. Detailed characterisation of *rao1* and *rao2* mutants is presented in Chapter 3 and Chapter 4, respectively.

Chapter 2

TCP Transcription Factors Link the Regulation of Genes Encoding Mitochondrial Proteins with the Circadian Clock in *Arabidopsis thaliana*

The Plant Cell, Vol. 22: 3921–3934, December 2010, www.plantcell.org © 2010 American Society of Plant Biologists

TCP Transcription Factors Link the Regulation of Genes Encoding Mitochondrial Proteins with the Circadian Clock in *Arabidopsis thaliana* [W][OA]

Estelle Giraud,[1] Sophia Ng,[1] Chris Carrie, Owen Duncan, Jasmine Low, Chun Pong Lee, Olivier Van Aken, A. Harvey Millar, Monika Murcha, and James Whelan[2]

Australian Research Council Centre of Excellence in Plant Energy Biology, University of Western Australia, Crawley, Western Australia 6009, Australia

Diurnal regulation of transcripts encoding proteins located in mitochondria, plastids, and peroxisomes is important for adaptation of organelle biogenesis and metabolism to meet cellular requirements. We show this regulation is related to diurnal changes in promoter activities and the presence of specific *cis*-acting regulatory elements in the proximal promoter region [TGGGC(C/T)], previously defined as site II elements, and leads to diurnal changes in organelle protein abundances. These site II elements can act both as activators or repressors of transcription, depending on the night/day period and on the number and arrangement of site II elements in the promoter tested. These elements bind to the TCP family of transcriptions factors in *Arabidopsis thaliana*, which nearly all display distinct diurnal patterns of cycling transcript abundance. TCP2, TCP3, TCP11, and TCP15 were found to interact with different components of the core circadian clock in both yeast two-hybrid and direct protein–protein interaction assays, and *tcp11* and *tcp15* mutant plants showed altered transcript profiles for a number of core clock components, including *LATE ELONGATED HYPOCOTYL1* and *PSEUDO RESPONSE REGULATOR5*. Thus, site II elements in the promoter regions of genes encoding mitochondrial, plastid, and peroxisomal proteins provide a direct mechanism for the coordination of expression for genes involved in a variety of organellar functions, including energy metabolism, with the time-of-day specific needs of the organism.

INTRODUCTION

All eukaryotes studied to date and even some prokaryotes have evolved an internal timekeeper in the form of a circadian clock. The central oscillator in this clock is made up of a series of interlocking, autoregulatory, negative feedback loops of gene expression thath produce self-sustained rhythms with a period length of ~24 h (Harmer, 2009). In its simplest form, the clock consists of (1) input sites that entrain the clock, including light, temperature, and nutrient availability (Harmer, 2009), (2) the core oscillator itself, and (3) a myriad of output sites to temporally coordinate biological processes (Harmer, 2009). In *Arabidopsis thaliana*, the core clock involves the reciprocal evening phase expression of TIMING OF CAB EXPRESSION1 (TOC1) with the morning phase expression of two MYB family transcription factors, CIRCADIAN CLOCK ASSOCIATED1 (CCA1) and LATE ELONGATED HYPOCOTYL (LHY) (Harmer, 2009). A recent study has found that the transcription factor TCP21, termed CHE (for CCA1 Hiking Expedition), binds to TOC1, providing an important missing link to explain how TOC1 can regulate expression of CCA1, as TOC1 lacks a DNA binding domain (Pruneda-Paz et al., 2009). CHE acts as a repressor of *CCA1* expression, as shown in CHE deficient plants, where *CCA1* expression was increased (Pruneda-Paz et al., 2009).

TCPs are a plant-specific family of transcription factors, named after the transcription factors TEOSINTE BRANCHED1 in *Zea mays*, CYCLOIDEA in *Anthirrinum majus*, and PCF (proliferating cell nuclear antigen factor) in *Oryza sativa* (Navaud et al., 2007; Busch and Zachgo, 2009). As suggested by their name, the founding members of this family have been characterized to be involved in growth, cell proliferation, and organ identity in plants (Doebley et al., 1995; Luo et al., 1996, 1999; Nath et al., 2003; Takeda et al., 2003). They are basic-helix-loop-helix type transcription factors that can be divided into two main groups as a result of an ancient duplication event, TCP-P and TCP-C. TCP-P genes encode proteins that act to positively regulate gene expression, while TCP-C genes encode negative regulators (Kosugi and Ohashi, 2002; Li et al., 2005). TCP transcription factors bind *cis*-acting regulatory elements (CAREs), known as site II, with the core binding sequence TGGGC(C/T) in the promoter regions of various genes, the proliferating cell nuclear antigen from *Arabidopsis* and rice (Kosugi et al., 1995; Kosugi and Ohashi, 2002; Trémousaygue et al., 2003), as well as cyclin B and ribosomal protein genes in *Arabidopsis* (Li et al., 2005). Site II elements have been shown to be involved in the regulation of nuclear-located genes encoding mitochondrial proteins, specifically *cytochrome oxidase 6b-2* (*Cyt6b-2*), *Cyt5b-2*, *cytochrome*

[1] These authors contributed equally to this work.
[2] Address correspondence to seamus@cyllene.uwa.edu.au.
The author responsible for distribution of materials integral to the findings presented in this article in accordance with the policy described in the Instructions for Authors (www.plantcell.org) is: James Whelan (seamus@cyllene.uwa.edu.au).
[W]Online version contains Web-only data.
[OA]Open Access articles can be viewed online without a subscription.
www.plantcell.org/cgi/doi/10.1105/tpc.110.074518

c1, and *cytochrome c2* in *Arabidopsis* (Welchen and Gonzalez, 2005; Gonzalez et al., 2007; Comelli and Gonzalez, 2009; Mufarrege et al., 2009; Welchen et al., 2009). Site II elements have also been shown to be involved in the regulation of *Alternative oxidase1c* in *Arabidopsis*, a non-stress-inducible alternative oxidase gene in *Arabidopsis* (Ho et al., 2007).

Although site II elements appear to be involved in the regulation of nuclear genes encoding mitochondrial proteins, the mechanism of their action is unclear as well as the nature of the link between circadian regulation of gene expression and the expression of nuclear genes encoding organellar proteins. Thus, we investigated the activity of a variety of gene promoters containing site II elements from genes encoding organelle proteins and found their activity was dependent on the phase of the day/light cycle. This dependency correlated to the diurnal variation in transcript abundance of both the genes regulated by these promoters and a range of TCP transcription factors. In a number of cases, we could show that the mitochondrial proteins encoded by the transcripts regulated by these promoters also varied in abundance in the day/light cycle. We determined which TCP transcription factors can interact with the site II element TGGGC (C/T) using yeast one-hybrid analysis and studied the interaction of TCP transcription factors with known components of the circadian clock in *Arabidopsis*, using yeast two-hybrid analysis and protein–protein interaction assays. Finally, we show how mutants of *TCP* transcription factors influence the expression of clock components in *Arabidopsis*. In this way, we established the mechanistic link of TCP transcription factors with both clock function and the expression of nuclear genes encoding organelle proteins in *Arabidopsis*.

RESULTS

Function of Site II Elements in Nuclear Genes Encoding Organelle Proteins Depends on the Phase of the Diurnal Cycle

To analyze the function of site II elements in the regulation of transcription for nuclear-encoded organellar proteins, the promoter regions of 15 nuclear genes encoding mitochondrial, plastid, peroxisomal, and ribosomal proteins were cloned. Initial characterization of the role of these site II elements in driving reporter activity indicated that there was no consistent significant effect of site II element deletions. The effect of site II promoter deletions varied on a day by day basis for a number of promoters tested, and an example of these data, obtained for the *RIP* promoter, is shown in Supplemental Figure 1A online. This technique has been used extensively to define promoter activity in our laboratory (Thirkettle-Watts et al., 2003; Ho et al., 2008; Giraud et al., 2009) and in other studies (Schmidt et al., 2004; Omidvar et al., 2008), so the variation cannot be ascribed to the method of transformation. The only variation in the above experimental design that we were aware of was the time of transformation during the light cycle. Quantitative RT-PCR (qRT-PCR) of *RIP* was performed to determine if and when transcript abundances for this gene varied. Supplemental Figure 1B online shows that the level of *RIP* transcript varied considerably and was lowest in the night period.

qRT-PCR was then performed to identify any patterns of transcript cycling abundance over the diurnal period for the other genes being studied with site II promoter elements. The transcripts of eight genes encoding mitochondrial proteins involved in a number of different functional processes from import to energy were evaluated. Specifically, these were *MITOCHONDRIAL CARRIER PROTEIN3* (*MCP3*), *MCP4*, *RISKE IRON SULFUR COMPLEX III SUBUNIT* (*RIP*), *ATP50 COMPLEX V SUBUNIT* (*ATP50*), *SCO1 COMPLEX IV SUBUNIT* (*SCO1*), *TRANSLOCASE OF THE OUTER MEMBRANE 20.2* (*TOM20.2*), *TOM20.3*, and *TOM20.4*. Two genes encoding plastid proteins were also tested, *TRANSLOCASE OF THE OUTER CHLOROPLAST MEMBRANE120* (*TOC120*) and *60S RIBOSOMAL PROTEIN L34* (*60SRPL34*). Transcript abundances were also determined for two genes encoding peroxisomal proteins, *PEROXISOME BIOGENESIS FACTOR11* (*PEX11*) and *ALTERNATIVE NADH DEHYDROGENASE A1* (*NDA1*), which is dual targeted to the mitochondrion and the peroxisome (Carrie et al., 2008), along with four genes encoding known circadian-regulated transcripts, including the two morning associated transcripts, *LHY1* and *CCA1*, and two evening phased transcripts, *PSEUDO RESPONSE REGULATOR1* (*PRR1*/*TOC1*) and *PRR5*. Finally, one gene encoding a cytosolic ribosomal protein (*60S ACIDIC RIBOSOMAL PROTEIN 0A* [*RPP0A*]) was also tested (Li et al., 2005). The transcript abundances for all 24 genes encoding TCP proteins were also determined as these transcription factors are reported to be the binding partners for site II elements (Kosugi and Ohashi, 2002; Welchen and Gonzalez, 2005). However, for a number of TCPs, including TCP1, TCP6, TCP12, TCP16, TCP18, and TCP23, transcript abundances were too low to be accurately detected and were therefore omitted from further analysis.

Six distinct expression patterns were observed. First, *LHY1* and *CCA1*, which were analyzed as positive controls, along with the mitochondrial/peroxisomal *NDA1*, displayed classic morning phased expression that peaked as previously characterized (Elhafez et al., 2006) (Figure 1A, cluster 1; see Supplemental Figure 1C online). The second pattern represented the evening phased peak in expression levels for clock components PRR1 (TOC1) and PRR5 (Figure 1A, cluster 2). Another cluster was characterized by transcript abundances that rose during the light period and peaked at midday before decreasing to minimum levels at midnight. This pattern was evident for *TOM20-2*, *TOM20-3*, *TOM20-4*, *SCO1*, and *PEX11* along with six *TCP* genes (Figure 1A, cluster 4; see Supplemental Figure 1C online). Transcripts in a fifth cluster group (*MCP3*, *MCP4*, *RIP*, *60SRPL34*, *RPP0B*, *ATP50*, and *TCO120*, along with nine transcripts encoding TCPs) decreased throughout the day period to a minimum of roughly 3 h into the dark period and then increased throughout the night (Figure 1A, cluster 5; see Supplemental Figure 1C online). The sixth pattern (comprising *TCP24* and *TCP8*) was opposite to that of the other clusters in that their transcript abundances were highest during the night period and there was a distinct plateau of transcript abundance during that period (Figure 1A, cluster 6). TCP11 showed relatively constitutive expression levels over the time series and no consistent diurnal pattern (Figure 1A, cluster 3).

To further investigate the links between cycling abundances for mitochondrial located proteins and transcriptional regulation

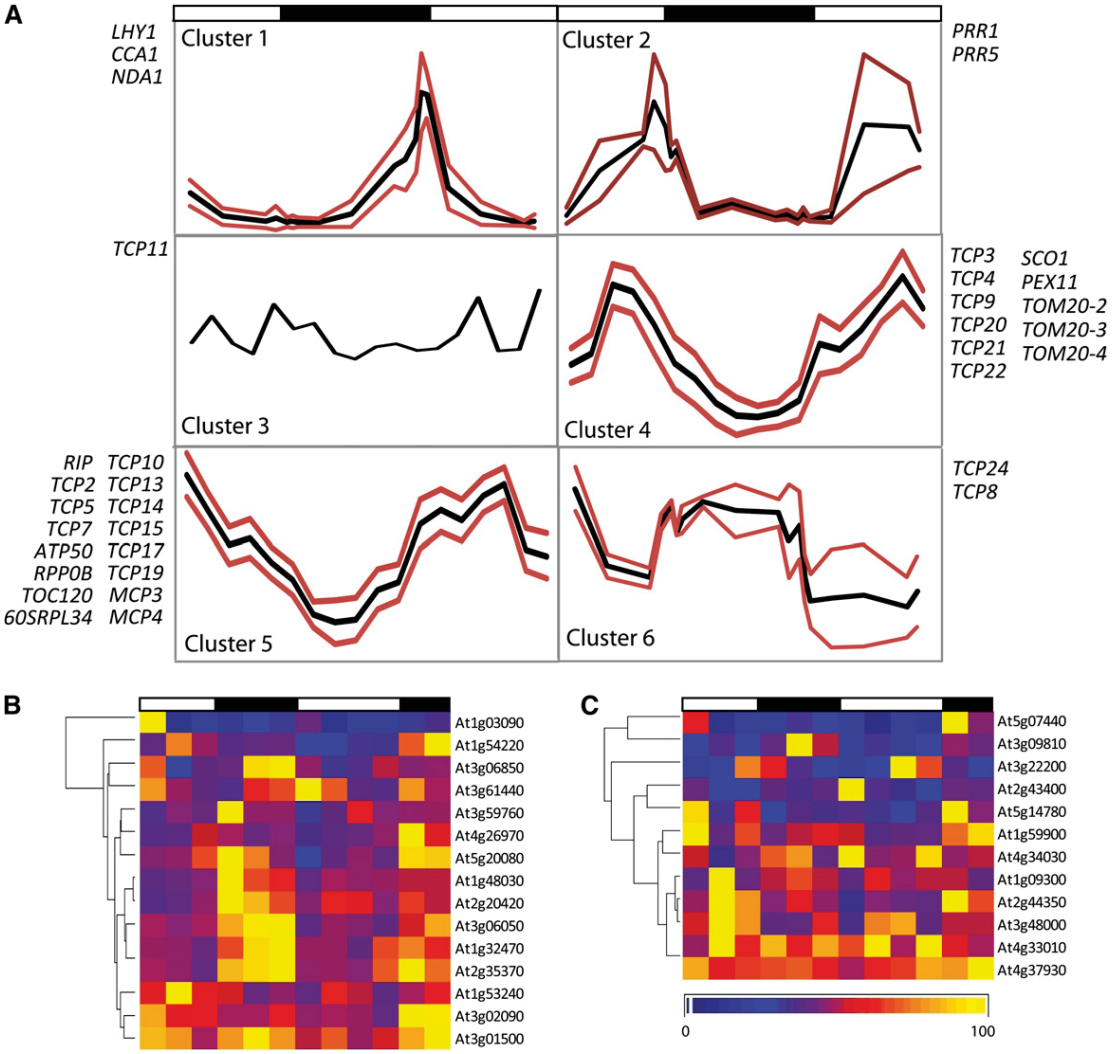

Figure 1. Diurnal Regulation of Transcript Abundance for *Arabidopsis* Genes Encoding Organelle Proteins, Core Clock Components, and TCP Transcription Factors.

(A) Transcript abundances were measured over a day/night time course for a range of transcripts encoding clock components, TCP factors, and organellar proteins with site II elements in their promoter regions. Fifteen-day-old *Arabidopsis* seedlings grown in a 12-h/12-h light-dark period were sampled at the times indicated. The maximum transcript abundance for each gene across the time series was set to 1, and all other values were expressed in a relative manner. Specific primer information is outlined in Supplemental Table 1B online. Transcript profiles were hierarchically clustered (shown in Supplemental Figure 1C online), and subclusters were defined as described in Methods. The trend for each subcluster (average of the cluster) is shown in black, and positive/negative limits (SD) are shown in red.

(B) and **(C)** Transcript abundance profiles over a 48-h day/night period for the 27 unique mitochondrial proteins that were defined as being diurnally regulated at a protein level in Lee et al. (2010). Public microarray data were taken from Smith et al. (2004) (first 24 h) and Bläsing et al. (2005) (second 24-h period). For each transcript, the maximum level across the time series was set to 1 with measurements for other time points being expressed in a relative manner. Expression levels are indicated by the scale bar below the profile in **(C)**.

(B) Transcripts with site II elements in their promoter regions.

(C) Transcripts that lack site II elements in their promoter regions.

via site II CAREs in diurnal conditions, a transcriptional analysis of previously defined diurnally regulated mitochondrial proteins was undertaken. Lee et al. (2010) performed an in-depth analysis of the cycling patterns in protein abundances over day/night periods for mitochondrial located proteins. They identified 27 unique mitochondrial proteins with cycling abundances from differential two-dimensional gel electrophoresis isoelectric focusing/SDS-PAGE analysis (see Supplemental Data Set 1A online). From this list of 27 genes, we identified genes with site II elements within their 1000-bp promoter regions (Figures 1B and 1C). Over 50% of these diurnally regulated mitochondrial proteins had site II CAREs within their promoter region (15 out of

27), which is significantly more than would be expected by chance for a 6-mer in the genome. Changes in transcript abundance for these 15 genes with site II elements versus the remaining 12 genes without site II elements were visualized in diurnal microarray time series (Figures 1B and 1C, respectively). Genes with site II CAREs present in their promoter regions showed a significant cycling (one-way analysis of variance [ANOVA], $P < 0.001$) in transcript abundance over the day/night period (Figure 1B; see Supplemental Data Set 1B online), with generally higher levels of transcript abundance observed during the night period. By contrast, those genes without site II CAREs did not show clear cycling transcript abundance patterns (one-way ANOVA, $P > 0.5$) (Figure 1C; see Supplemental Data Set 1B online). A Tukey range test of the transcript patterns for the site II element-containing genes shows the variation between groups was all between dark and light periods (see Supplemental Data Set 1C online). This indicates that, while there are obviously other posttranscriptional mechanisms that also contribute to the diurnal changes observed in these mitochondrial proteins, the presence of site II elements in the promoter regions of those proteins diurnally regulated at the transcriptional level could play an important role in defining the variation observed. To analyze diurnal fluctuations in abundance of a mitochondrial protein encoded by one of the transcripts directly analyzed here, we performed immunoblots with the diurnal mitochondrial samples reported in Lee et al. (2010) using antibodies raised to TOM20-4. This also showed a significant diurnal pattern (one-way ANOVA, $P < 0.001$) with highest abundance early in the light period and lowest abundance early in the night (see Supplemental Data Set 1D online).

Taking into account these expression data, plants were transformed with wild-type or mutant promoter-reporter constructs lacking one or more site II elements either 2 h into the day or 2 h before the end of night conditions and harvested exactly 24 h later (in the same day/night conditions) to determine promoter activity. For the *RIP* promoter, it was observed that the site II element functioned as a strong repressor during the day (Figure 2, *RIP*), but it was not functional during the night period. Similarly for the *ATP50* promoter, a 5-fold increase in promoter activity was observed under day conditions when the site II element was deleted, indicating that this element functions as a repressor during the day, and in contrast with this, during the night it acts as an activator of transcription (Figure 2, *ATP50*). *ATP50* wild-type promoter activity was also reduced in light conditions to roughly half that of wild-type activity in the dark, consistent with these observations that site II elements present in the promoter activate expression of the gene during the night and strongly repress it during the day. In the case of the *SCO1* and *TOM20-2* promoters, the opposite was observed, with the site II element acting as a repressor at night and an activator during the day (Figure 2, *SCO1* and *TOM20-2*). Altered wild-type promoter activity was also observed for *TOM20-2* between day/night conditions with double the wild-type promoter activity observed during the day (also correlating with the activator activity of the site II element during the day) (Figure 2). In the *MCP3* promoter, the site II element functioned as an activator both in the day and at night (Figure 2, *MCP3*). The *MCP4* promoter was more complex due to the presence of multiple site II elements. A 5-fold increase in promoter activity was observed between night and day with the wild-type promoter, consistent with several site II elements acting as activators of transcription during the day (Figure 2, *MCP4*). Another site II element, which was not active during the day, acts as a repressor during the night, indicated by the slight increase in reporter gene activity when the element is mutated (Figure 2, *MCP4*, dark-blue bars). Therefore, in *MCP4*, a different set of site II promoter elements is used in dark versus light conditions rather than the same element having altered functionality at different points in the day/night cycle.

To determine whether site II elements also played a role in regulating other organellar and energy-related components in a diurnal manner, a number of other gene promoters were cloned and mutagenized for analysis in biolistic transformation assays as outlined above. Again, different site II functionality was observed under day and night conditions (Figure 3). *TOC120* (chloroplastic) and *RPP0A* (ribosomal) promoters both showed a 2- to 4-fold decrease in wild-type promoter activity in the day compared with the night, and both promoters contain several site II elements that acted as strong activators in the dark (Figure 3, *TOC120* and *RPP0A*). In the case of *RPP0A*, several of these elements also acted as repressors in the day, as indicated by increased reporter gene activity when they were mutated (Figure 3, *RPP0A*). The wild-type *PEX11* promoter showed decreased activity during the day and contained a site II element that was not active at night but acted as a repressor during the day (Figure 3, *PEX11*). Similarly, in the *NDA1* promoter, a number of site II elements present in the promoter were not functional during the night but acted as strong repressors during the day (Figure 3, *NDA1*).

Comparison of these data sets showed that transcripts that clustered together in Figure 1A had similar functionality of the site II elements in their promoters. For example, *SCO1* and *TOM20-2* grouped together in cluster 3, which was characterized by decreased transcript abundances during the night (Figure 1A), and both these promoters contained site II elements that functioned as strong repressors during the night. While *RIP*, *ATP50*, *MCP4*, *TOC132*, and *RPP0B4* all showed transcript abundances that generally increased throughout the night, all clustered together in cluster 4 (Figure 1A), and all have site II elements that were either not functional at night and were strong repressors during the day or acted as activators of transcription during the night (Figures 2 and 3). A number of additional promoters from genes encoding organelle proteins also showed altered functionality of the site II elements present depending on whether the elements were tested in day or night conditions (see Supplemental Figure 2 online).

TCP Proteins Are Able to Interact with Site II Elements in Yeast One-Hybrid Assays

To test the DNA binding ability and specificity of the 24 *Arabidopsis* TCP proteins with the characteristic site II C (TGGGCC) or site II T (TGGGCT) promoter sequences, yeast one-hybrid assays were performed (see Supplemental Figure 3 online; Table 1). Almost all of the TCPs tested were able to bind site II T or site II C sequences, with the exception of TCP8 and TCP22, which showed no interaction with the DNA sequences tested in this study. However, these factors may bind other sequences similar

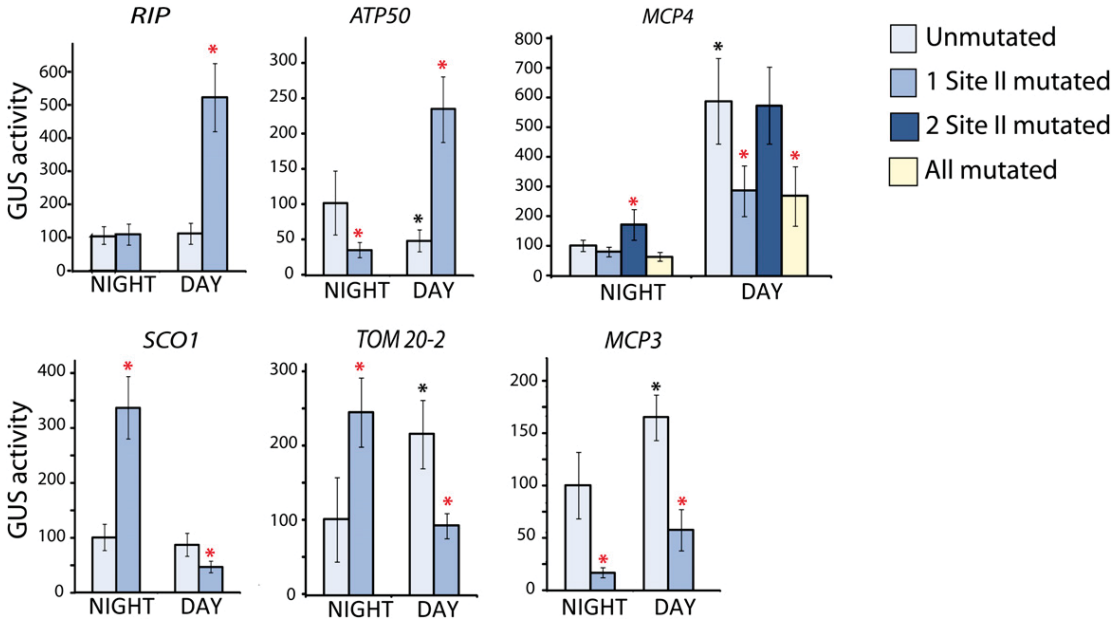

Figure 2. Activity of the Promoter Regions of Mitochondria Gene Promoters with Site II Elements at Defined Points in the Diurnal Cycle.

GUS reporter activity of six mitochondrial promoters measured 2 h before the end of the night period and 2 h after the start of the day period are shown. The nighttime activity of the wild-type promoter was set to 100%, and other values were expressed in a relative manner for each promoter. Independent transformations using ~50 *Arabidopsis* seedlings were repeated at least nine times for each construct under day or night conditions, and the standard errors are indicated by error bars. Black asterisks indicate a significant difference ($P < 0.05$, Student's *t* test) between day and night reporter activity of the wild-type promoter. Red asterisks indicate a significant difference ($P < 0.05$, Student's *t* test) between the wild type and the promoter that contained one or more mutated site II elements.

to site II or may bind the class II like sequences described by Kosugi and Ohashi (2002). TCP12, TCP4, TCP17, and TCP21 showed the strongest interaction with both forms of site II elements, while TCP3 and TCP11 seemed to show specificity for site II C elements, and TCP13 showed a strong interaction with site II T elements but was not able to bind site II C DNA sequences.

TCP Proteins Interact with a Number of Central Clock Components in Yeast Two-Hybrid Assays

All 24 *Arabidopsis* TCP transcription factors were cloned for analysis in yeast two-hybrid assays to test their ability to interact with known components of the plant circadian clock. Interactions were tested with PhyA, two MYB factors that are central regulators in the circadian clock (CCA1 and LHY), PIF3, and all five PRR proteins with proposed functions in the circadian clock (PRR1, 3, 5, 7, and 9). The ability of TCP proteins to autoactivate in yeast hybrid screens has been described previously (Kosugi and Ohashi, 2002; Koyama et al., 2007); thus, the ability of all these factors to autoactivate was tested in every mating (Figures 4A and 4B; see Supplemental Figure 4 online). TCP1, 4, 10, 12, 18, 20, and 24 consistently autoactivated when cloned into both prey and bait vectors; thus, interactions with these components could not be determined (Table 1; see Supplemental Figure 4 online). TCP2 was found to interact very strongly with CCA1 (Figure 4A, Table 1). Interactions may also take place between TCP2 and LHY, PIF3, PRR1, PRR3, and PRR5; however, this cannot be fully determined as TCP2 was able to autoactivate when it was cloned into the bait vector for yeast two-hybrid assays. When cloned into the prey vector for a reversed assay, some interactions with these components were observed (Table 1). TCP3 was found to interact very strongly with PRR1 (also known as TOC1) (Figure 4A, Table 1). TCP15 was found to interact with PRR5 and to a lesser extent with PRR1/TOC1 (Figure 4B). Finally, TCP11 interacted very strongly with PRR1 (TOC1), LHY, CCA1, and PRR3 and to a lesser extent with PRR5 (Figure 4A, Table 1). Additionally, TCP11 was observed to interact with PHYA; however, this interaction could not be confirmed in matings when the yeast two-ybrid prey and bait vectors were reversed due to autoactivation (Table 1; see Supplemental Figure 4 online). No interactions were observed for TCP21, even though this factor was previously described by Pruneda-Paz et al. (2009) to interact with PRR1 (TOC1) in the central circadian clock (see Supplemental Figure 4 online).

To confirm the interactions observed in the yeast two-hybrid analyses, direct protein–protein interactions were also undertaken. This was achieved by expressing His-tagged versions of the target proteins, binding them to a nickel affinity column under native conditions, and testing their ability to bind other proteins. His-tagged versions of LYH1, CCA1, TCP2, and TCP11 were expressed in a wheat germ translation system and bound to a nickel affinity column as target genes. As a control, a similar procedure was performed for β-glucuronidase (GUS). To test for protein–protein interactions, radiolabeled proteins were

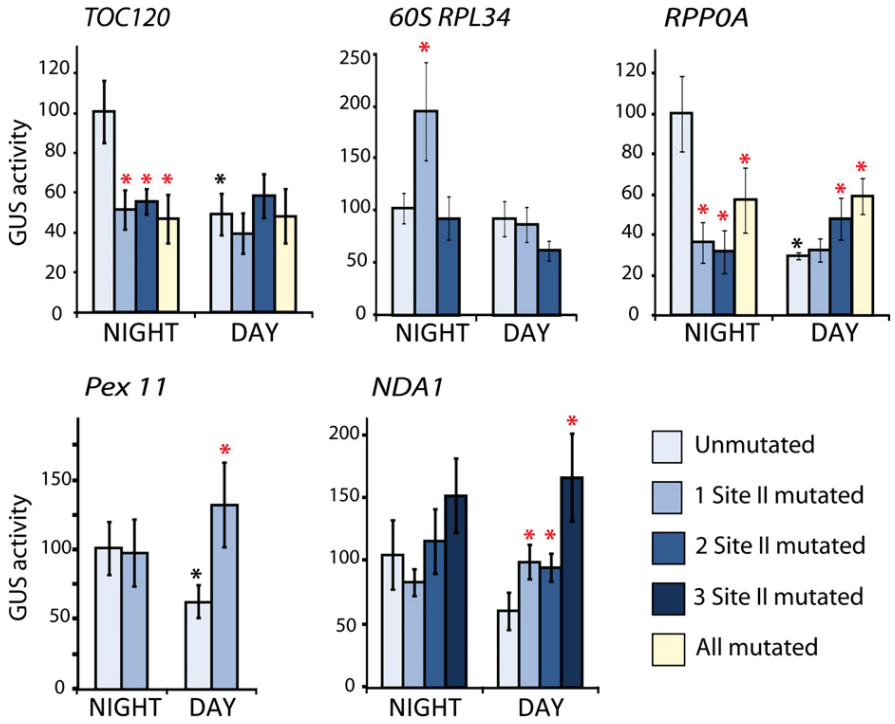

Figure 3. Activity of the Promoter Regions and Site II Elements for Genes Encoding Proteins Targeted to Peroxisomes, Plastids, or Ribosomal Proteins.

GUS reporter activity was assayed 2 h before the end of the night period and 2 h after the start of the day period. The night time activity of the wild-type promoter was set to 100%, and other values are expressed in a relative manner for each promoter. Independent transformations using ~50 *Arabidopsis* seedlings were repeated at least nine times for each construct under day or night conditions, and the standard errors are indicated by error bars. Black asterisks indicate a significant difference ($P < 0.05$, Student's *t* test) between day and night reporter activity of the wild-type promoter. Red asterisks indicate a significant difference ($P < 0.05$, Student's *t* test) between the wild-type and the promoter containing one or more mutated site II elements.

synthesized and applied to columns containing the putative binding partners. The ability of the protein to interact with circadian regulators was determined by the retention of the protein on the column, which could then only be eluted under conditions that eluted the His-tagged proteins (Figure 4C, Elution 2). When TCP2, TCP11, and PRR1 were applied to the columns containing the bound GUS-HIS control protein, no radiolabeled protein was retained on the column, but instead it appeared in the flow-through and in small amounts after elution with 10 mM imidazole (Figure 4C, bottom three blot panels). By contrast, when TCP2, TCP11, CCA1, or LHY1 were bound on the column, the radiolabeled proteins were retained on the column and were absent in the flow-through, indicating protein–protein interactions. Different binding affinities were suggested by elution under different imidazole concentrations. For [^{35}S]Met-TCP2, strong binding was evident with both LHY1-His and CCA1-His, as protein was only eluted under conditions that eluted the tag from the column (Figure 4C). In yeast two-hybrid assays, interactions between TCP2 and LHY1 could not be determined due to autoactivation (Figure 4A, Table 1). The binding of TCP2 to LHY1 was evident in the affinity purification assays as the radiolabeled TCP2 protein was only eluted from the column under conditions that eluted the HIS-tagged LHY1 protein (Figure 4C).

A strong protein–protein interaction was evident between PRR1 and both TCP2-His and TCP11-His, as the correct full-length PRR1 protein product (top band shown by arrow in gel panels 5 and 6, Figure 4C) was only eluted under conditions that elute TCP2-HIS and TCP11-HIS. Interestingly, two translation products were evident for PRR1, a full-length product (indicated with an arrow) and a second shorter translation product initiated from an internal Met codon that was 75 amino acids into the protein (indicated by an asterisk) (Figure 4C). The shorter PRR1 translation product was evident in the flow-through and the first elution wash with 10 mM imidazole; therefore, efficient binding of TCP factors requires the first 75 amino acids of PRR1. Binding of TCP11 to CCA1 and LHY1 was suggested by retention on the column and low abundance in the flow-through fraction. Some protein from these interaction assays was eluted at 10 mM imidazole and all at 250 mM imidazole, suggesting under these assay conditions that binding was weaker than the interactions outlined above. The interaction of PRR1 with TCP2 and TCP11 provides a molecular mechanism for these regulators to bind and act as transcriptional activators and further supports the hypothesis that TCP transcription factors function as DNA binding partners of PRR proteins in the circadian clock.

Table 1. Summary of Results from Yeast One-Hybrid and Yeast Two-Hybrid Assays Showing Binding Specificity and Binding Partner Interactions for the TCP Family of Plant Transcription Factors

				Yeast One-Hybrid		Yeast Two-Hybrid								
Probe	AT No.	TCP Name	Type	Site II C (TGGGCC)	Site II T (TGGGCT)	PhyA	LHY	CCA1	PIF3	PRR1	PRR3	PRR5	PRR7	PRR9
	At1g67260	AtTCP1	CYC/TB1	±	–	*	*	*	*	*	*	*	*	*
254670_at	At4g18390	AtTCP2	CIN	+	±	–	o	++	o	o	o	o	–	–
260618_at	At1g53230	AtTCP3	CIN	++	±	–	–	–	–	++	–	–	–	–
257267_at	At3g15030	AtTCP4	CIN	++	++	*	*	*	*	*	*	*	*	*
247605_at	At5g60970	AtTCP5	CIN	–	±	–	–	–	–	–	–	–	–	–
	At5g41030	AtTCP6	PCF	+	+	–	–	–	–	–	–	–	–	–
	At5g23280	AtTCP7	PCF	+	+	–	–	–	–	–	–	–	–	–
246398_at	At1g58100	AtTCP8	PCF	–	–	–	–	–	–	–	–	–	–	–
267515_at	At2g45680	AtTCP9	PCF	+	+	–	–	–	–	–	–	–	–	–
266481_at	At2g31070	AtTCP10	CIN	±	±	*	*	*	*	*	*	*	*	*
263888_at	At2g37000	AtTCP11	PCF	++	+	o	++	++	–	++	++	+	–	–
	At1g68800	AtTCP12	CYC/TB1	++	++	–	–	–	–	–	–	–	–	–
259129_at	At3g02150	AtTCP13	CIN	–	++	–	–	–	–	–	–	–	–	–
252425_at	At3g47620	AtTCP14	PCF	±	±	–	–	–	–	–	–	–	–	–
260371_at	At1g69690	AtTCP15	PCF	+	–	–	–	–	–	+	–	++	–	–
	At3g45150	AtTCP16	PCF			–	–	–	–	–	–	–	–	–
250566_at	At5g08070	AtTCP17	CIN	++	++	–	–	–	–	–	–	–	–	–
	At3g18550	AtTCP18	CYC/TB1	+	+	*	*	*	*	*	*	*	*	*
248385_at	At5g51910	AtTCP19	PCF	+	+	–	–	–	–	–	–	–	–	–
257788_at	At3g27010	AtTCP20	PCF	±	+	*	*	*	*	*	*	*	*	*
246011_at	At5g08330	AtTCP21	PCF	++	++	–	–	–	–	–	–	–	–	–
	At1g72010	AtTCP22	PCF	–	–	–	–	–	–	–	–	–	–	–
262028_at	At1g35560	AtTCP23	PCF	+	+	–	–	–	–	–	–	–	–	–
245774_at	At1g30210	AtTCP24	CIN	+	±	*	*	*	*	*	*	*	*	*

The 24 *Arabidopsis* TCPs were tested, and Affymetrix probe IDs are shown where available. Type refers to the class of TCP protein and is based on the founding members of the TCP family. Yeast one-hybrid assays were carried out with DNA sequences containing three copies of the classic site II sequence in tandem with either a C or a T in the last position (TGGGCC or TGGGCT). Yeast two-hybrid assays were performed to test for interactions with known components of the plant circadian clock as prey. All interactions were repeated a minimum of four times, and the strength of the interactions was graded as very strong (++), strong (+), very weak (±), or no interaction (–). For some TCP factors, consistently strong autoactivation was observed; thus, true interactions could not be determined (indicated by an asterisk). For TCP2, some autoactivation was observed when cloned into the bait vector for yeast two-hybrid assays; however, this was variable, and in some matings, interactions could be observed with LHY, PIF3, PRR1, PRR3, and PRR5 (indicated by o).

Transcript Abundance Profiles for Clock Components Are Altered in TCP Mutants

To address whether the TCP factors are necessary to correctly regulate clock function in vivo, transcript abundance profiles for several marker genes for clock function were monitored in TCP mutants grown in normal diurnal growth conditions. T-DNA insertional lines were obtained for TCP11 and TCP15 to determine if the central oscillator loop was affected in the absence of these factors (*tcp11* and *tcp15* plants) (see Supplemental Figure 5 online). In *tcp11* (the knockout of a TCP that showed direct protein interactions with LHY1, CCA1, PRR1, PRR3, and PRR5 in Figure 4), the expected peak in LHY1 expression during the early morning was increased by 30%, indicating that TCP11 plays some role in repressing LHY1 expression levels (Figure 5A). There were no differences in phase or period of the LHY1 expression profile in *tcp11* plants compared with the wild type. Transcript profiles for CCA1 and TOC1 were not significantly altered in *tcp11* lines (Figure 5A). The expression profile of PRR5 was also measured, as TCP11 interacts with this PRR factor in yeast two-hybrid analyses (Figure 4). The expected peak in PRR5 expression in the late afternoon was significantly decreased by over 30% in the *tcp11* lines, indicating that TCP11 also appears to have a role in the transcriptional activation of this PRR factor in a time-of-day specific manner (Figure 5A). The same four marker genes were measured in *tcp15* plants, with no significant differences seen between the mutant and wild type in amplitude, phase, or period of the transcript profiles for CCA1, LHY1, or TOC1. However, a >30% decrease in the amplitude of peak expression for PRR5 was observed in *tcp15* plant profiles (Figure 5A). This is in agreement with protein interaction studies, as TCP15 was only observed to interact with PRR5 (Figure 4B); thus, PRR5 regulation also appears to require the presence of TCP15.

Additionally, a list of 365 nuclear genes encoding mitochondrial proteins with site II elements in their proximal promoter regions was generated. Transcript abundance profiles for these genes were investigated for 10 mutant backgrounds, namely, *phyB9*, *lhy1*, *cca1*, *tcp14*, *tcp13*, *pif1-2*, *cry*, *hy5*, *phyA*, and a *tcp13 tcp14* double mutant (McCormac and Terry, 2002; Kleine et al., 2007;

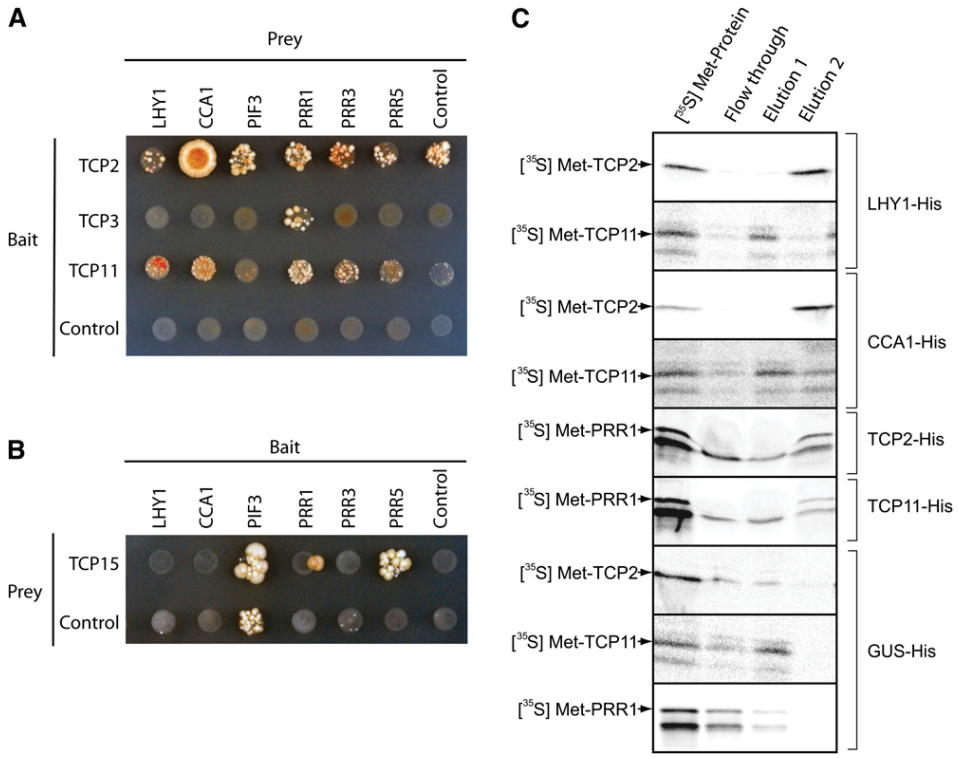

Figure 4. Protein Interactions between TCP Factors and Circadian Regulators.

(A) and **(B)** Yeast two-hybrid assays. Positive interactions were determined through auxotrophic selection media, SD-Trp/-Leu/-Ade/-His. TCP2, TCP3, and TCP11 were cloned into the bait vector and were able to activate the transcription of reporter genes.

(A) TCP proteins were cloned into the bait vector and circadian regulators were cloned into the prey vector. TCP2 interacts with CCA1. TCP3 interacts with PRR1. TCP11 interacts with LHY1, CCA1, PRR1, PRR3, and PRR5.

(B) TCP15 was cloned into the prey vector, while circadian regulators were cloned into the bait vector. TCP15 interacts with PRR1 and PRR5. Controls are bait empty vector or prey empty vector.

(C) Protein–protein interaction determined using affinity purification and His-tagged proteins. Tagged versions of LHY1, CCA1, TCP2, and TCP 11 were expressed and bound to a nickel affinity resin under native conditions. The ability to bind other proteins was determined by applying translation lysates programmed with TCP2, TCP11, and PRR1. The first lane represents 2.5% of the radiolabeled protein applied to the column, flow-through represents unbound protein, Elution 1 represents washing with 10 mM imidazole, which will not disrupt binding of His-tag protein to resin, and Elution 2 represents washing with 250 mM imidazole, which will elute the tagged protein and any protein bound. The presence of radiolabeled protein in Elution 2 represents strong binding, seen with TCP2 to LYH1, CCA1, and PRR1. TCP11 was able to bind to PRR1 and weakly to CCA1. Note that radiolabeled TCP2, TCP11, and PRR1 present in the flow-through fraction indicate no binding to the GUS-His (control). Arrows indicate the correct size, full-length translation product. Note that for PRR1, the second product in the translation mixture marked with an asterisk was also present in the flow-through fraction, but the full-length product was only evident in Elution 2 (see text).

Nozue et al., 2007; Michael et al., 2008; Moon et al., 2008) (see Methods). Transcript profiles were hierarchically clustered, revealing both up- and downregulation of transcripts across the mutants (see Supplemental Figure 6 online). From this list, 293 genes were significantly upregulated or downregulated >1.5-fold in at least one of these mutant backgrounds. This represents just over 80% of the total set of 365 genes with site II elements encoding mitochondrial-located proteins. Many of the remaining 72 transcripts were very low in abundance and could not be accurately detected on the microarray chips. Additionally, 117 of the genes on this list had significantly altered expression levels in more than five clock-related mutant microarray experiments. As further confirmation that the nuclear-encoded mitochondrial transcription networks regulated by site II elements are directly affected in mutants of clock function, differences in transcript profiles for genes of the promoters that were characterized in Figure 2 were further examined in these 10 mutant backgrounds (Figure 5B). For each of these transcripts, transcript abundances different to those observed in wild-type plants were evident in at least two and up to nine of the mutant backgrounds (Figure 5B).

DISCUSSION

This study aimed to define the role of site II *cis*-acting regulatory elements in the promoters of nuclear genes encoding organellar proteins and to investigate whether these genes display diurnal cycling patterns of expression due to the presence of site II elements. It was important to determine if they were explicitly

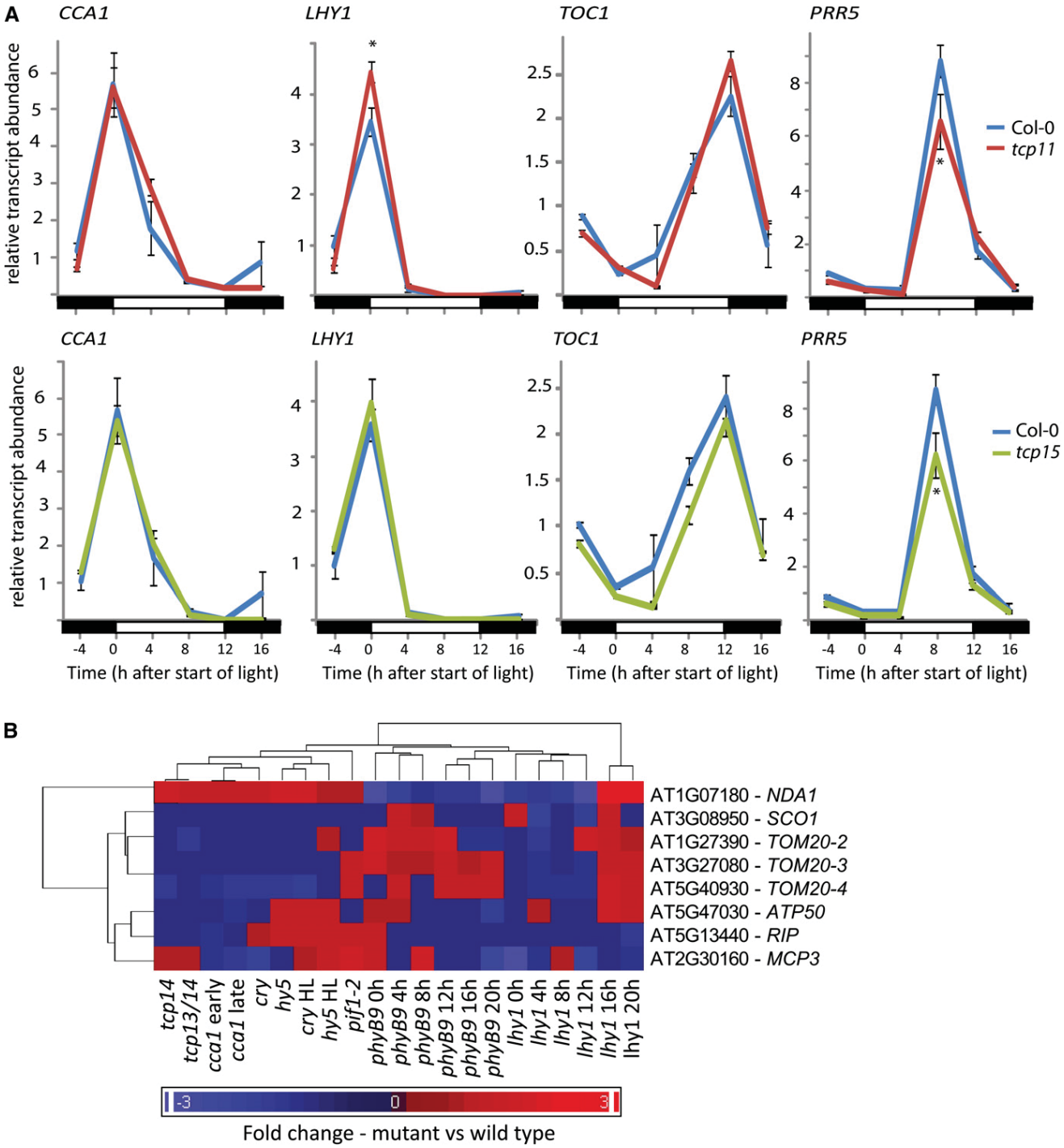

Figure 5. Analysis of Transcript Abundance Profiles for Core Clock Marker Genes in TCP Transgenic Plant Backgrounds.

(A) Transcript abundance profiles for *CCA1*, *LHY1*, *PRR1*, and *PRR5* were measured via qRT-PCR over a 24-h period in 16-d-old, wild-type *Arabidopsis* plants (blue), plants lacking a functional TCP11 protein (*tcp11*- red), or plants lacking a functional TCP15 factor (*tcp15*, green). Plants were grown in 12-h/12-h day-night conditions, and samples were taken every 4 h over a diurnal time course (−4, 0, 4, 8, 12, and 16 h after the start of light conditions). Transcripts were measured in technical duplicate for each of the three biological replicates, consisting of pooled tissue collected from approximately five seedlings at each time point. Average relative transcript abundances are shown with standard errors for each time point. Asterisks indicate a significant difference between the abundance observed between mutant and wild-type plants (Student's *t* test, $P < 0.001$). Black bar, night; white bar, day.

linked to the clock input and core feedback loops of gene expression or whether they just regulated the cycling expression of organellar proteins temporally as one of the multitude of clock-regulated output sites in plants. TCP2, TCP3, TCP11, and TCP15 were all found to interact with different components of the core circadian clock in both yeast two-hybrid assays and protein–protein interaction assays, indicating that the TCP family of transcription factors is intricately linked with circadian regulation of gene expression in *Arabidopsis*. TCP3 only interacts with PRR1 in the core feedback loop, and TCP2 and TCP11 interact with a variety of components, including PRR1. Notably, a second translation product for PRR1 (minus the N-terminal 75 amino acids) was observed for the column affinity purification interaction assays, and only the full-length translational product was able to interact with the TCP11 and TCP 2 factors. The CCT domain at the C-terminal of the PRR proteins is believed to mediate protein–protein interactions; however, our data indicate the N-terminal 75 amino acids of PPR1 are necessary to mediate binding to the TCP factors either directly or by providing conformational or structural support for the interaction.

TCP11 is the only *Arabidopsis* TCP that is not diurnally regulated at a transcript abundance level in the qRT-PCR assays performed in this study, and it was the only *Arabidopsis* TCP that was not defined as diurnally regulated ($r > 0.8$) in any public microarray data set using the DIURNAL database (Mockler et al., 2007) (http://diurnal.cgrb.oregonstate.edu/). TCP11 interacts with the greatest number of clock components in this study, including three different PRR factors. A recent study illustrated that PRR factors (TOC1 and PRR5) interact with each other in vitro and in vivo to enhance nuclear accumulation of TOC1 over 2-fold, in a time-of-day specific manner (Wang et al., 2010). PRR5 also recruits TOC1 to large subnuclear foci and promotes phosphorylation of the N-terminal region of TOC1 (the region that was found to be necessary for the TCP interactions shown in Figure 4C). Notably, these are the two PRR factors that showed the greatest ability to interact with TCP factors in this study, at least in terms of the number of TCP partners and the strength of the interactions. It is possible that TCP11 is recruited by TOC1 or PRR5 in a similar fashion and, thus, its activity would be regulated in a location-dependent manner rather than at the transcriptional level. Another possible explanation for the lack of cycling transcript abundance observed for *TCP11* is that it is constitutively expressed as a transcriptional repressor of LHY1, mediated via interactions with the various PRR factors during the day time period. Traditionally, the circadian clock has been assumed to consist of a single core negative loop (CCA1, LHY1, and TOC1) (Alabadí et al., 2001) and a number of additional feedback loops and other factors associated with many oscillators integrated outside the central loop (PRR3, PRR5, PRR7, PRR9, and GI) that generally have less well known molecular functions within the clock, as reviewed by Harmer (2009). However, studies have now shown that the other PRR factors are able to act as transcriptional repressors of *CCA1* and *LHY1* promoter activity along with TOC1/PRR1 (Nakamichi et al., 2005b, 2010). *PRR9*, *7*, *5*, and *1* all display sequential peaks in expression throughout the day period and have been characterized as direct repressors of CCA1 and LHY1 in vitro and in vivo (Matsushika et al., 2000; Nakamichi et al., 2005a, 2005b, 2010). Binding of the constitutively expressed TCP11 to the *LHY1* promoter provides a mechanism through which each of these PRR factors could associate with TCP11 to repress *LHY1* throughout the day period (consistent with the timing of decreased *LHY1* expression; Figure 5). This is also in agreement with the observed increase in *LHY1* expression levels in plants lacking TCP11 in this study (Figure 5). Pruneda-Paz et al. (2009) similarly identified CHE as a transcriptional repressor of CCA1 in association with TOC1, but CHE does not appear to regulate *LHY1* transcriptionally. Thus, the results presented in this work would represent a similar mechanism by which *LHY1* is also transcriptionally repressed during the day through TCP factors associated with TOC1. Interestingly, the proposed role of TCP11 within the central clock in *Arabidopsis* as outlined in this study represents the involvement of a factor that does not cycle in transcript abundance itself.

TCP15 was shown to interact with PRR5, whose role in the circadian clock is not fully elucidated, but is likely to involve subsequent feedback loops to repress the expression of *CCA1* and *LHY* (Nakamichi et al., 2005a, 2005b; Locke et al., 2006). As shown by the transcript profiles of marker clock genes analyzed in *tcp15* plants, *PRR5* was the only transcript that was significantly altered compared with wild-type expression peaks, again confirming interactions between PRR5 and TCP15 and the related regulation of these factors in vivo. Interestingly, the factors that exhibited the strongest interactions in the yeast two-hybrid analysis also displayed the strongest interactions in the direct protein–protein interactions tested in the affinity purification column assays (e.g., CCA1 with TCP2), reinforcing the combined use of these assays to confirm TCP binding partners for the clock components and PRR factors that lack DNA binding domains.

A number of recent metabolomic and transcriptomic studies have revealed a central role for PRR5, 7, and 9 in regulating metabolic homeostasis in the tricarboxylic acid (TCA) cycle within plant mitochondria (Fukushima et al., 2009; Nakamichi et al., 2009). In these previous studies, *prr5 prr7 prr9* triple knockout mutants displayed dramatic increases in intermediates of the TCA cycle in the metabolomic analysis. In the study by Lee et al. (2010), which characterized a small but significant set of mitochondrial proteins that are diurnally regulated at the protein level, a significant number of TCA cycle components and components of energy and amino acid metabolism were also identified. An examination of these protein changes at the transcriptional level

Figure 5. (continued).

(B) Hierarchical cluster of expression profiles for the genes shown in Figure 2 in a range of mutant backgrounds at different time points after exposure to light. Fold changes are presented as values compared with the corresponding transcript abundance observed for wild-type plants. Blue indicates genes that are downregulated compared with the wild type in particular mutants, and red represents an upregulation compared with the wild type. For detailed methods on experimental data sets used and cluster generation see Supplemental Figure 6 online.

in this study indicates that site II elements may play a significant role in the diurnal transcriptional regulation of these genes. This can be observed in the diurnal cycling patterns in the transcripts with site II in contrast with a relative lack of cycling pattern in genes lacking site II promoter elements from this set of diurnal mitochondrial proteins identified by Lee et al. (2010). This also suggests the presence of additional mechanisms, separate from transcriptional control, by which mitochondrial protein abundances are altered diurnally. However, site II elements and the TCP factors that bind to them appear to link the diurnal changes in mitochondrial function, particularly TCA cycle function and core energy metabolism/amino acid metabolism, with transcriptional changes that are regulated and integrated with the central clock and PRR family function (Fukushima et al., 2009; Nakamichi et al., 2009). Many studies have identified a link between sucrose or organellar metabolism and diurnal regulation of gene expression (Smith et al., 2004; Bläsing et al., 2005; Usadel et al., 2008). From the results here, we propose that the missing molecular link between cellular and organelle metabolic activity and the circadian clock in plants is provided by the TCP family of transcription factors and the site II CAREs to which they bind.

Overall, our data show that *Arabidopsis* TCP transcription factors appear to be central regulators in circadian clock input sites, the clock oscillator itself, and a myriad of clock output sites, directing and regulating the expression of genes encoding cellular energy metabolism components, particularly in the plant energy organelles. The involvement of TCP transcription factors in various growth and developmental processes and the regulation of genes encoding ribosomal proteins provides a molecular link to finely coordinate metabolism, growth, and development.

METHODS

Plant Materials and Growth Conditions

Arabidopsis thaliana plants, ecotype Columbia (Col-0) were grown at 22°C under medium day conditions, 12 h at 100 μE m^{-2} s^{-1} light conditions and 12 h of dark, for 16 d. Plants were grown on Murashige and Skoog (MS) agar plates for transient transformation assays and all transcript analysis. Homozygous transgenic T-DNA insertion lines were obtained and confirmed for TCP 11 (SALK_003042 and SALK_020124.38.95.x) and TCP15 (SALK_011491) (see Supplemental Figure 5 online). The two independent T-DNA insertional lines for TCP11 were combined for qRT-PCR analysis so that an average response of the lines was determined compared with wild-type plants. Screening primers are shown in see Supplemental Tables 1A and 1B online.

Transient Transformation Assays

Transformation was performed using the PDS-1000 system with the Hepta adaptor according to the manufacturer's instructions (Bio-Rad), as previously described (Thirkettle-Watts et al., 2003; Ho et al., 2008). For each of the 15 promoters analyzed, transient transformations were repeated independently over several different days a minimum of nine times. For each transformation, ~50 16-d-old *Arabidopsis* seedlings grown on MS plates (as described above) were transformed. Thus, for each promoter construct to be tested, ~500 plants were transformed independently. Dark transformations were performed in the dark 2 h prior to the start of light conditions, and light transformations were performed 2 h after the initiation of light conditions. Transformed seedling leaf tissue was harvested from the plates 24 h later under the same conditions as used for the transformation, for analysis of GUS and LUC reporter gene activity. Reporter gene activities for transformations performed 12 h apart could not be directly compared. Determination of GUS and Luc activities and all data processing steps were performed as described previously (Ho et al., 2008). The inclusion of a second, constitutively driven, reporter gene, LUC, in the transient transformation vector enabled the transformation efficiency for each transformation to be calculated and corrected for, thus providing a far more accurate analysis of variations in promoter activity (outlined in Ho et al., 2008).

Transcript Abundance Analysis

qRT-PCR analysis was performed on green tissue excised from approximately five 2-week-old *Arabidopsis* seedlings, per sample, grown on MS plates, and sampled at various time points throughout the 12-h/12-h light/dark day conditions in which the seedlings had been grown. For profiles shown in Figure 1, samples were taken at 3, 6, 10, 11, and 12 h after illumination, 0.5, 1, 3, 6, 10, 11, and 12 h after the start of dark conditions, and finally 0.5, 1, 3, 6, 10, and 11 h after illumination, resulting in an 18-point time course over 36 h. For transcript profiles of core clock components in the TCP mutant backgrounds (Figure 5), samples were taken every 4 h over a 20 h, period resulting in a six-point time series (−4, 0, 4, 8, 12, and 16 h ZT time) for wild-type and each of the mutant backgrounds. Samples collected for each time point for the two confirmed *tcp15* insertional lines were combined for qRT-PCR analysis. Samples for each time point were taken in biological triplicate (from seedlings grown on separate MS plates) and snap frozen under liquid nitrogen. Total RNA isolation and cDNA synthesis was performed as described previously (Lister et al., 2004). Transcript levels were assayed using the LightCycler 480 and the LightCycler 480 SYBR Green I Master (Roche). From each independent cDNA preparation, each transcript was analyzed twice. Absolute transcript abundance measurements, determined by standard curves for each gene, were normalized to that of *UBC*, which was analyzed as a constitutive control. To normalize for differences in the basal level of expression between the different genes measured in qRT-PCR assays, the values of absolute transcript abundance for each gene were expressed relative to the maximum value recorded for the gene (i.e., transcript abundance values ranged from 0 to 1 for each gene measured). Hierarchically, clusters were generated using Euclidian distance and average linkage measures. The trend (average) of each subcluster was graphed (in black) along with the positive and negative standard deviation limits (in red). qRT-PCR primer sequences used for all transcripts measured are listed in Supplemental Table 1B online. Summary statistics and quality measure for each of the assays performed are shown in Supplemental Data Set 2A online. Normalized absolute transcript abundance data used to generate the cluster images in Figure 1 and Supplemental Figure 1 online are also supplied in Supplemental Data Set 2B online.

Analysis of Public Microarray Data Sets

Raw CEL file microarray data sets were downloaded from the NASC-arrays repository (http://affy.Arabidopsis.info/narrays/experimentbrowse.pl), ArrayExpress (Smith et al., 2004), and from the Gene Expression Omnibus (http://www.ncbi.nlm.nih.gov/geo) (Bläsing et al., 2005). The two data sets, each with a 24-h diurnal time course of plants grown under 12-h/12-h light-dark conditions, were combined to form a 48-h time series with 0-, 4-, 8-, 12-, 16-, and 20-h time points taken from Smith et al. (2004), followed by 0-, 4-, 8-, 12-, 16-, and 20-h time points taken from Bläsing et al. (2005). These two experimental data sets were taken as they most closely resemble the sampling, age of plants, and growth conditions used in Lee et al. (2010). CEL files were subjected to GC-robust multi-array average normalization in Partek Genomics Suite software version 6.4. The linear transcript abundance profiles for the 27 mitochondrial

proteins defined as diurnally regulated by Lee et al. (2010) were isolated. To normalize for differences in the basal level of expression between the different genes, the fluorescence intensity profile for each gene was expressed relative to the maximum value recorded for the gene (i.e., transcript abundance values ranged from 0 to 100 for each gene measured), with 100 being the maximum expression level and all other time points expressed relative to this. The presence of site II elements or site II–like elements was searched in these 27 gene promoters using The Arabidopsis Information Resource PATMATCH function (http://www.Arabidopsis.org/cgi-bin/patmatch/nph-patmatch.pl), resulting in 15 genes out of 27. Transcript profiles over the diurnal time series for both gene sets, with or without site II elements, were hierarchically clustered using Euclidean distance and average linkage measures in Partek Genomics Suite software version 6.4.

Yeast One-Hybrid Screen

For construction of the pHIS2 bait vectors, forward and reverse oligonucleotides (see Supplemental Table 1A online) were annealed and ligated into *Eco*RI-*Sac*I–linearized pHIS2 vector. Three tandem repeats of the site II C (TGGGCC) or site II T (TGGGCT) were cloned into the pHIS2 reporter vector upstream of the minimal *HIS3* promoter region and *HIS3* nutritional reporter gene. For transformation, competent yeast cells were prepared according to the Clontech Yeast Protocols Handbook using the Y187 yeast strain (Clontech). Yeast one-hybrid transformation screens were performed using the Clontech Matchmaker one hybrid library construction and screening kit. For each yeast one-hybrid transformation screen, 100 μL of competent yeast cells were incubated with 100 ng of pHIS2 bait vector and 100 ng of pGADT7-Rec2 prey vector, 100 μg herring testes carrier DNA (Clontech), and 0.6 mL PEG/LiAc solution. Cells were transformed according to the manufacturer's instructions. Transformations were plated onto SD media -Leu-Trp to select for cotransformed cells and incubated at 28°C for 4 d. The pGADT7-rec2-p53 prey vector in combination with p53HIS2 was used as a positive control and pGADT7-rec2-p53 in combination with pHIS2 as negative control. Transformed yeast cells were subsequently grown overnight in YPD liquid media to an OD_{600} of 0.1 and diluted in a 10× dilution series. From each dilution, 5 μL was spotted on SD-Trp-Leu (DDO) and on SD-Trp-Leu-His (TDO) media plates supplemented with 90 mM 3-amino-1,2,4-triazole (Sigma-Aldrich). The plates were then incubated for 3 d at 28°C.

Yeast Two-Hybrid Assay

Protein–protein interactions were analyzed using a GAL-4–based yeast hybrid system (Matchmaker two-hybrid system; Clontech). Full-length cDNAs of all *Arabidopsis* TCP proteins were cloned into pGBKT7 (bait vector; Clontech) and pGADT7-Rec (prey vector; Clontech) and transformed into the Y187 yeast strain. Transformants were selected on synthetic dropout (SD)-Trp media. *PHYA*, *LHY1*, *CCA1*, *PIF3*, *PRR1*, *PRR3*, *PRR5*, *PRR7*, and *PRR9* full-length cDNAs were cloned into the prey vector pGADT7-Rec (Clontech) and transformed into the AH109 yeast strain. Transformants were selected on SD-Leu medium. All cloning primers are listed in Supplemental Table 1A online. *TCP16* and *PRR5* cDNAs were obtained from the ABRC (clone PYAt3g45150) and Takeshi Mizuno (Laboratory of Molecular Microbiology, Nagoya University), respectively. Bait and prey strains were inoculated in YPDA and combined in a 96-well plate (NUNC) for mating, and yeast culture was then incubated at 28°C with shaking for 16 to 19 h. Successful yeast matings were confirmed on SD-Trp/-Leu, and positive interactions were selected on SD-Trp/-Leu/-His/-Ade. pGBKT7-53 and pGBKT7-Lam (Clonetech) were used as a positive and a negative bait control, while pGADT7-RecT (Clontech) was used as a prey control. Nonmated yeast cultures were also spotted on SD media as negative controls. pGBKT7 and pGADT7-Rec were used as negative controls for autoactivation. To discover interactions that might be masked from autoactivation when expressing TCP proteins as baits, TCP proteins were also cloned as preys, while potential interactors were cloned as baits for yeast matings. Each mating was performed a minimum of four times.

Protein Pull-Down Assays

For protein pull-down assays, LHY1, CCA1, TCP2, TCP11, and GUS were expressed in a cell-free wheat germ lysate with 6X HIS tags (Roche). After expression, the lysates were made up to 5 mL with native immobilized metal-ion affinity chromatography (IMAC) wash buffer 1 (300 mM KCl, 50 mM KH_2PO_4, and 5 mM imidazole, pH 8.0). These proteins were then bound to an IMAC purification column (Bio-Rad) using the Profinia purification system (Bio-Rad). The proteins were loaded on the column and washed once with native IMAC wash buffer 1 and once with native IMAC wash buffer 2 (300 mM KCl, 50 mM KH_2PO_4, and 10 mM imidazole, pH 8.0). To perform the pull-down assay, [^{35}S]-Met radiolabeled proteins (TCP2, TCP11, and PRR1) expressed via the Promega T_nT transcription/translation kit (Promega) were made up to 5 mL in native IMAC wash buffer 1 supplemented with 0.5% BSA and 2 mM $MgCl_2$. Radiolabeled proteins were washed over the columns containing the already bound 6X HIS–containing proteins. Columns were washed once in native IMAC wash buffer 1 (termed the flow through) and then eluted first with elution buffer 1 (300 mM KCl, 50 mM KH_2PO_4, and 10 mM imidazole, pH 8.0) and subsequently with elution buffer 2 (300 mM KCl, 50 mM KH_2PO_4, and 250 mM imidazole, pH 8.0) to determine the strength of the interaction. The GUS protein was used as a control for nonspecific binding of radiolabeled proteins to the column. After each elution and wash step was performed, fractions were analyzed by SDS-PAGE and then subjected to radioautography to detect the presence of radiolabeled proteins in the various fractions.

Supplemental Data

The following materials are available in the online version of this article.

Supplemental Figure 1. Results for Initial Promoter Transformations and qRT-PCR Analysis for *Arabidopsis* Genes Encoding Organelle Proteins, Core Clock Components, and TCP Transcription Factors over a 38-h Period under Diurnal Conditions.

Supplemental Figure 2. Additional Promoter Elements Tested.

Supplemental Figure 3. Yeast One-Hybrid Assays.

Supplemental Figure 4. Yeast Two-Hybrid Analysis for Interactions between *Arabidopsis* TCP Family Proteins and Components of the Circadian Clock.

Supplemental Figure 5. Characterization of the T-DNA Insertional Lines Inactivating TCP11 and TCP15.

Supplemental Figure 6. Transcript Abundances for Genes Encoding Mitochondrial Proteins with Site II in a Range of Mutant Backgrounds.

Supplemental Table 1A. Primer Sequences for Cloning of All TCP Factors and Clock Components for Yeast Hybrid and Protein Interaction Studies.

Supplemental Table 1B. Primer Sequences for All Quantitative RT-PCR Assays along with Primers Used for Screening T-DNA Insertional Lines.

Supplemental Data Set 1A. Summary of the Mitochondrial Proteins That Were Found to Cycle in Protein Abundance in a Diurnal Manner, as Characterized by Lee et al. (2010).

Supplemental Data Set 1B. One-Way ANOVA Statistical Analysis for Transcript Abundance Profiles for Genes with and without Site II Elements Shown in Figures 1B and 1C, Respectively.

Supplemental Data Set 1C. Tukey Range Analysis of Diurnal Transcript Abundance Profiles for Genes with and without Site II Elements Shown in Cluster Images in Figures 1B and 1C, Respectively.

Supplemental Data Set 1D. One-Way ANOVA Statistical Analysis for Protein Abundance Profiles Shown in Figure 4 for TOM20-4 and TOM40-1.

Supplemental Data Set 2A. qRT-PCR Assay Summaries for Cluster Generation.

Supplemental Data Set 2B. Normalized Absolute Transcript Abundance Values as Determined by qRT-PCR Analysis Used for the Generation of Cluster Images in Figure 1 and Supplemental Figure 1.

ACKNOWLEDGMENTS

This work was supported by the Australian Research Council Centre of Excellence Program CEO561495.

Received February 4, 2010; revised November 12, 2010; accepted December 2, 2010; published December 23, 2010.

REFERENCES

Alabadí, D., Oyama, T., Yanovsky, M.J., Harmon, F.G., Más, P., and Kay, S.A. (2001). Reciprocal regulation between TOC1 and LHY/CCA1 within the Arabidopsis circadian clock. Science **293:** 880–883.

Bläsing, O.E., Gibon, Y., Günther, M., Höhne, M., Morcuende, R., Osuna, D., Thimm, O., Usadel, B., Scheible, W.R., and Stitt, M. (2005). Sugars and circadian regulation make major contributions to the global regulation of diurnal gene expression in *Arabidopsis*. Plant Cell **17:** 3257–3281.

Busch, A., and Zachgo, S. (2009). Flower symmetry evolution: Towards understanding the abominable mystery of angiosperm radiation. Bioessays **31:** 1181–1190.

Carrie, C., Murcha, M.W., Kuehn, K., Duncan, O., Barthet, M., Smith, P.M., Eubel, H., Meyer, E., Day, D.A., Millar, A.H., and Whelan, J. (2008). Type II NAD(P)H dehydrogenases are targeted to mitochondria and chloroplasts or peroxisomes in *Arabidopsis thaliana*. FEBS Lett. **582:** 3073–3079.

Comelli, R.N., and Gonzalez, D.H. (2009). Identification of regulatory elements involved in expression and induction by sucrose and UV-B light of the *Arabidopsis thaliana* COX5b-2 gene, encoding an isoform of cytochrome c oxidase subunit 5b. Physiol. Plant. **137:** 213–224.

Doebley, J., Stec, A., and Gustus, C. (1995). teosinte branched1 and the origin of maize: evidence for epistasis and the evolution of dominance. Genetics **141:** 333–346.

Elhafez, D., Murcha, M.W., Clifton, R., Soole, K.L., Day, D.A., and Whelan, J. (2006). Characterization of mitochondrial alternative NAD(P)H dehydrogenases in Arabidopsis: Intraorganelle location and expression. Plant Cell Physiol. **47:** 43–54.

Fukushima, A., Kusano, M., Nakamichi, N., Kobayashi, M., Hayashi, N., Sakakibara, H., Mizuno, T., and Saito, K. (2009). Impact of clock-associated Arabidopsis pseudo-response regulators in metabolic coordination. Proc. Natl. Acad. Sci. USA **106:** 7251–7256.

Giraud, E., Van Aken, O., Ho, L.H., and Whelan, J. (2009). The transcription factor ABI4 is a regulator of mitochondrial retrograde expression of ALTERNATIVE OXIDASE1a. Plant Physiol. **150:** 1286–1296.

Gonzalez, D.H., Welchen, E., Attallah, C.V., Comelli, R.N., and Mufarrege, E.F. (2007). Transcriptional coordination of the biogenesis of the oxidative phosphorylation machinery in plants. Plant J. **51:** 105–116.

Harmer, S.L. (2009). The circadian system in higher plants. Annu. Rev. Plant Biol. **60:** 357–377.

Ho, L.H., Giraud, E., Lister, R., Thirkettle-Watts, D., Low, J., Clifton, R., Howell, K.A., Carrie, C., Donald, T., and Whelan, J. (2007). Characterization of the regulatory and expression context of an alternative oxidase gene provides insights into cyanide-insensitive respiration during growth and development. Plant Physiol. **143:** 1519–1533.

Ho, L.H., Giraud, E., Uggalla, V., Lister, R., Clifton, R., Glen, A., Thirkettle-Watts, D., Van Aken, O., and Whelan, J. (2008). Identification of regulatory pathways controlling gene expression of stress-responsive mitochondrial proteins in Arabidopsis. Plant Physiol. **147:** 1858–1873.

Kleine, T., Kindgren, P., Benedict, C., Hendrickson, L., and Strand, A. (2007). Genome-wide gene expression analysis reveals a critical role for CRYPTOCHROME1 in the response of Arabidopsis to high irradiance. Plant Physiol. **144:** 1391–1406.

Kosugi, S., and Ohashi, Y. (2002). DNA binding and dimerization specificity and potential targets for the TCP protein family. Plant J. **30:** 337–348.

Kosugi, S., Suzuka, I., and Ohashi, Y. (1995). Two of three promoter elements identified in a rice gene for proliferating cell nuclear antigen are essential for meristematic tissue-specific expression. Plant J. **7:** 877–886.

Koyama, T., Furutani, M., Tasaka, M., and Ohme-Takagi, M. (2007). TCP transcription factors control the morphology of shoot lateral organs via negative regulation of the expression of boundary-specific genes in *Arabidopsis*. Plant Cell **19:** 473–484.

Lee, C.P., Eubel, H., and Millar, A.H. (2010) Diurnal changes in mitochondrial function reveal daily optimization of light and dark respiratory metabolism in Arabidopsis. Mol. Cell Proteomics **9:** 2125–2139.

Li, C., Potuschak, T., Colón-Carmona, A., Gutiérrez, R.A., and Doerner, P. (2005). Arabidopsis TCP20 links regulation of growth and cell division control pathways. Proc. Natl. Acad. Sci. USA **102:** 12978–12983.

Lister, R., Chew, O., Lee, M.N., Heazlewood, J.L., Clifton, R., Parker, K.L., Millar, A.H., and Whelan, J. (2004). A transcriptomic and proteomic characterization of the Arabidopsis mitochondrial protein import apparatus and its response to mitochondrial dysfunction. Plant Physiol. **134:** 777–789.

Locke, J.C., Kozma-Bognár, L., Gould, P.D., Fehér, B., Kevei, E., Nagy, F., Turner, M.S., Hall, A., and Millar, A.J. (2006). Experimental validation of a predicted feedback loop in the multi-oscillator clock of *Arabidopsis thaliana*. Mol. Syst. Biol. **2:** 59.

Luo, D., Carpenter, R., Copsey, L., Vincent, C., Clark, J., and Coen, E. (1999). Control of organ asymmetry in flowers of Antirrhinum. Cell **99:** 367–376.

Luo, D., Carpenter, R., Vincent, C., Copsey, L., and Coen, E. (1996). Origin of floral asymmetry in Antirrhinum. Nature **383:** 794–799.

Matsushika, A., Makino, S., Kojima, M., and Mizuno, T. (2000). Circadian waves of expression of the APRR1/TOC1 family of pseudo-response regulators in *Arabidopsis thaliana*: Insight into the plant circadian clock. Plant Cell Physiol. **41:** 1002–1012.

McCormac, A.C., and Terry, M.J. (2002). Loss of nuclear gene expression during the phytochrome A-mediated far-red block of greening response. Plant Physiol. **130:** 402–414.

Michael, T.P., et al. (2008). Network discovery pipeline elucidates conserved time-of-day-specific cis-regulatory modules. PLoS Genet. **4:** e14.

Mockler, T.C., Michael, T.P., Priest, H.D., Shen, R., Sullivan, C.M., Givan, S.A., McEntee, C., Kay, S.A., and Chory, J. (2007). The DIURNAL project: DIURNAL and circadian expression profiling, model-based pattern matching, and promoter analysis. Cold Spring Harb. Symp. Quant. Biol. **72:** 353–363.

Moon, J., Zhu, L., Shen, H., and Huq, E. (2008). PIF1 directly and indirectly regulates chlorophyll biosynthesis to optimize the greening process in Arabidopsis. Proc. Natl. Acad. Sci. USA **105:** 9433–9438.

Mufarrege, E.F., Curi, G.C., and Gonzalez, D.H. (2009). Common sets of promoter elements determine the expression characteristics of three Arabidopsis genes encoding isoforms of mitochondrial cytochrome c oxidase subunit 6b. Plant Cell Physiol. **50:** 1393–1399.

Nakamichi, N., Fukushima, A., Kusano, M., Sakakibara, H., Mizuno, T., and Saito, K. (2009). Linkage between circadian clock and tricarboxylic acid cycle in Arabidopsis. Plant Signal. Behav. **4:** 660–662.

Nakamichi, N., Kiba, T., Henriques, R., Mizuno, T., Chua, N.-H., and Sakakibara, H. (2010). PSEUDO-RESPONSE REGULATORS 9, 7, and 5 are transcriptional repressors in the *Arabidopsis* circadian clock. Plant Cell **22:** 594–605.

Nakamichi, N., Kita, M., Ito, S., Sato, E., Yamashino, T., and Mizuno, T. (2005a). The *Arabidopsis* pseudo-response regulators, PRR5 and PRR7, coordinately play essential roles for circadian clock function. Plant Cell Physiol. **46:** 609–619.

Nakamichi, N., Kita, M., Ito, S., Yamashino, T., and Mizuno, T. (2005b). PSEUDO-RESPONSE REGULATORS, PRR9, PRR7 and PRR5, together play essential roles close to the circadian clock of *Arabidopsis thaliana*. Plant Cell Physiol. **46:** 686–698.

Nath, U., Crawford, B.C., Carpenter, R., and Coen, E. (2003). Genetic control of surface curvature. Science **299:** 1404–1407.

Navaud, O., Dabos, P., Carnus, E., Tremousaygue, D., and Hervé, C. (2007). TCP transcription factors predate the emergence of land plants. J. Mol. Evol. **65:** 23–33.

Nozue, K., Covington, M.F., Duek, P.D., Lorrain, S., Fankhauser, C., Harmer, S.L., and Maloof, J.N. (2007). Rhythmic growth explained by coincidence between internal and external cues. Nature **448:** 358–361.

Omidvar, V., Siti Nor Akmar, A., Marziah, M., and Maheran, A.A. (2008). A transient assay to evaluate the expression of polyhydroxybutyrate genes regulated by oil palm mesocarp-specific promoter. Plant Cell Rep. **27:** 1451–1459.

Pruneda-Paz, J.L., Breton, G., Para, A., and Kay, S.A. (2009). A functional genomics approach reveals CHE as a component of the Arabidopsis circadian clock. Science **323:** 1481–1485.

Schmidt, K., Heberle, B., Kurrasch, J., Nehls, R., and Stahl, D.J. (2004). Suppression of phenylalanine ammonia lyase expression in sugar beet by the fungal pathogen *Cercospora beticola* is mediated at the core promoter of the gene. Plant Mol. Biol. **55:** 835–852.

Smith, S.M., Fulton, D.C., Chia, T., Thorneycroft, D., Chapple, A., Dunstan, H., Hylton, C., Zeeman, S.C., and Smith, A.M. (2004). Diurnal changes in the transcriptome encoding enzymes of starch metabolism provide evidence for both transcriptional and posttranscriptional regulation of starch metabolism in Arabidopsis leaves. Plant Physiol. **136:** 2687–2699.

Takeda, T., Suwa, Y., Suzuki, M., Kitano, H., Ueguchi-Tanaka, M., Ashikari, M., Matsuoka, M., and Ueguchi, C. (2003). The OsTB1 gene negatively regulates lateral branching in rice. Plant J. **33:** 513–520.

Thirkettle-Watts, D., McCabe, T.C., Clifton, R., Moore, C., Finnegan, P.M., Day, D.A., and Whelan, J. (2003). Analysis of the alternative oxidase promoters from soybean. Plant Physiol. **133:** 1158–1169.

Trémousaygue, D., Garnier, L., Bardet, C., Dabos, P., Hervé, C., and Lescure, B. (2003). Internal telomeric repeats and 'TCP domain' protein-binding sites co-operate to regulate gene expression in *Arabidopsis thaliana* cycling cells. Plant J. **33:** 957–966.

Usadel, B., Bläsing, O.E., Gibon, Y., Retzlaff, K., Höhne, M., Günther, M., and Stitt, M. (2008). Global transcript levels respond to small changes of the carbon status during progressive exhaustion of carbohydrates in Arabidopsis rosettes. Plant Physiol. **146:** 1834–1861.

Wang, L., Fujiwara, S., and Somers, D.E. (2010). PRR5 regulates phosphorylation, nuclear import and subnuclear localization of TOC1 in the Arabidopsis circadian clock. EMBO J. **29:** 1903–1915.

Welchen, E., and Gonzalez, D.H. (2005). Differential expression of the Arabidopsis cytochrome c genes Cytc-1 and Cytc-2. Evidence for the involvement of TCP-domain protein-binding elements in anther- and meristem-specific expression of the Cytc-1 gene. Plant Physiol. **139:** 88–100.

Welchen, E., Viola, I.L., Kim, H.J., Prendes, L.P., Comelli, R.N., Hong, J.C., and Gonzalez, D.H. (2009). A segment containing a G-box and an ACGT motif confers differential expression characteristics and responses to the Arabidopsis Cytc-2 gene, encoding an isoform of cytochrome c. J. Exp. Bot. **60:** 829–845.

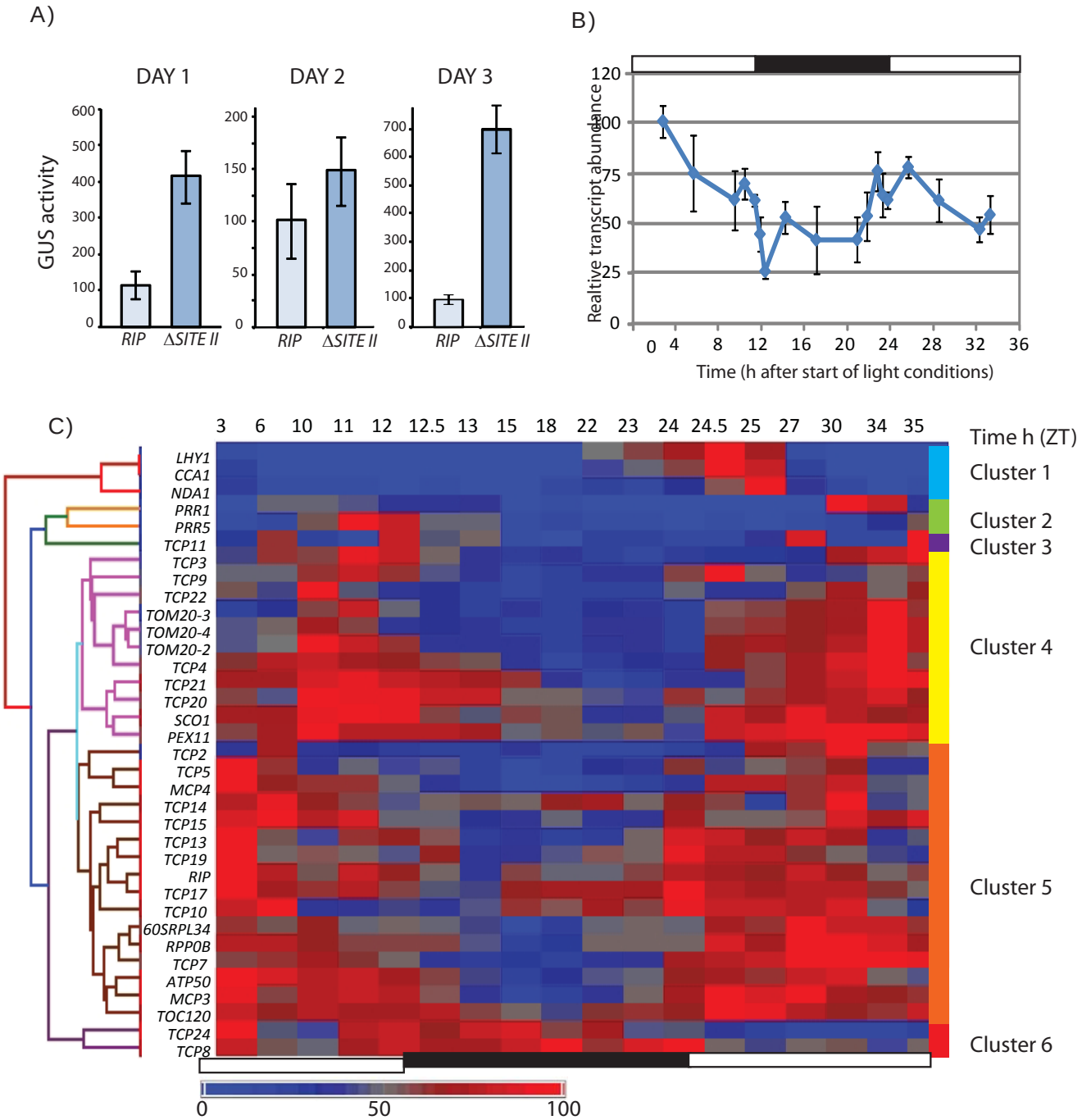

Supplemental Figure 1. Quantitative RT-PCR analysis of transcript abundance for *Arabidopsis* genes encoding organelle proteins, core clock components and TCP transcription factors over a 38 h period under diurnal conditions. A) The GUS reporter activity of the RIP promoter was analysed in transient transformations of pooled groups of ~50 Arabidopsis seedlings for wild-type and mutant promoter constructs, in triplicate on three different days. Although a trend of an increase in reporter activity was observed when the site II element within the promoter was mutated (ΔSITE II) there was a large variation in the extent by which reporter activity increased. Standard errors are shown. **B)** and **C)** Transcript abundances were measured over a day/night time course for **B)** RIP and **C**) a range of transcripts encoding clock components, TCP factors and organellar proteins with site II elements in their promoter regions. Fifteen-day-old *Arabidopsis* seedlings grown in a 12 h/12 h light dark period were sampled in triplicate at the times indicated. The maximum transcript abundance for each gene was set to 100 and all other values were expressed in a relative manner. The scale shows relative transcript abundance. Standard deviation error bars are shown in (B). Normalised transcript abundances were hierarchically clustered using Euclidean distance measures and average linkage. ZT - Zeitgeber time defined as ZT=1 at 1 hour after the start of the light. Light and dark periods are represented graphically above the graph in (B) and below the heat map in (C) by white and black boxes, respectively. Full gene names are listed in Methods. Representative cluster profiles are shown in Figure 1 from the six sub-clusters shown here.

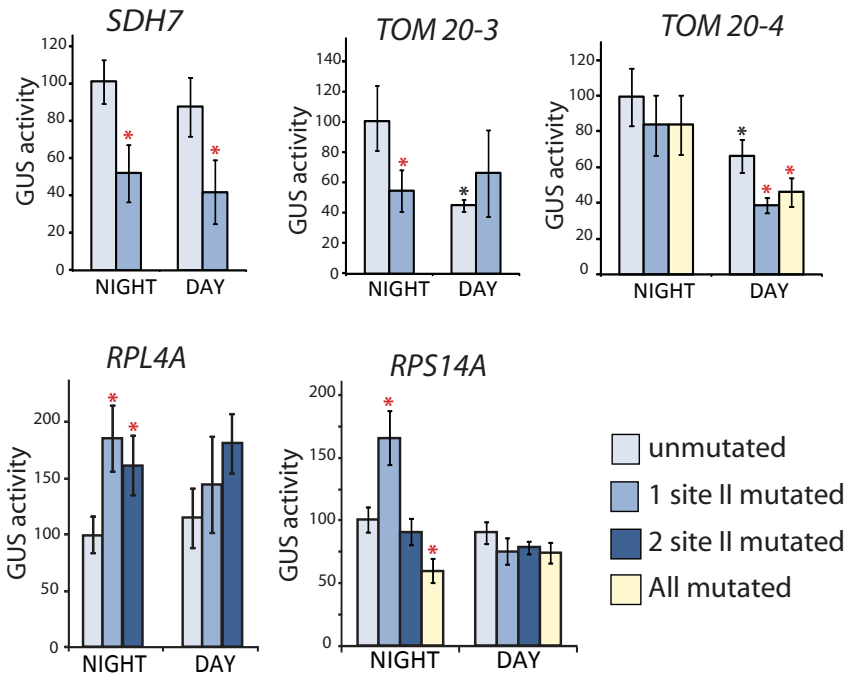

Supplemental Figure 2. Additional promoter elements tested. Promoter activities for a number of additional genes encoding mitochondrial proteins and genes encoding proteins located in other locations. Reporter activity was assayed 2 h before the end of the dark conditions (NIGHT) and 2 h after the start of the light conditions (DAY). The night time activity of the wild-type promoter was set to 100% and other values are expressed in a relative manner for each promoter. Independent transformations using ~50 *Arabidopsis* seedlings were repeated at least nine times for each construct under day or night conditions and the standard errors are indicated by error bars. Black asterisks * = a significant difference ($P<0.05$) between day and night reporter activity of the wild-type promoter. Red asterisks * = a significant difference ($P<0.05$) between the wild-type and mutated promoter.

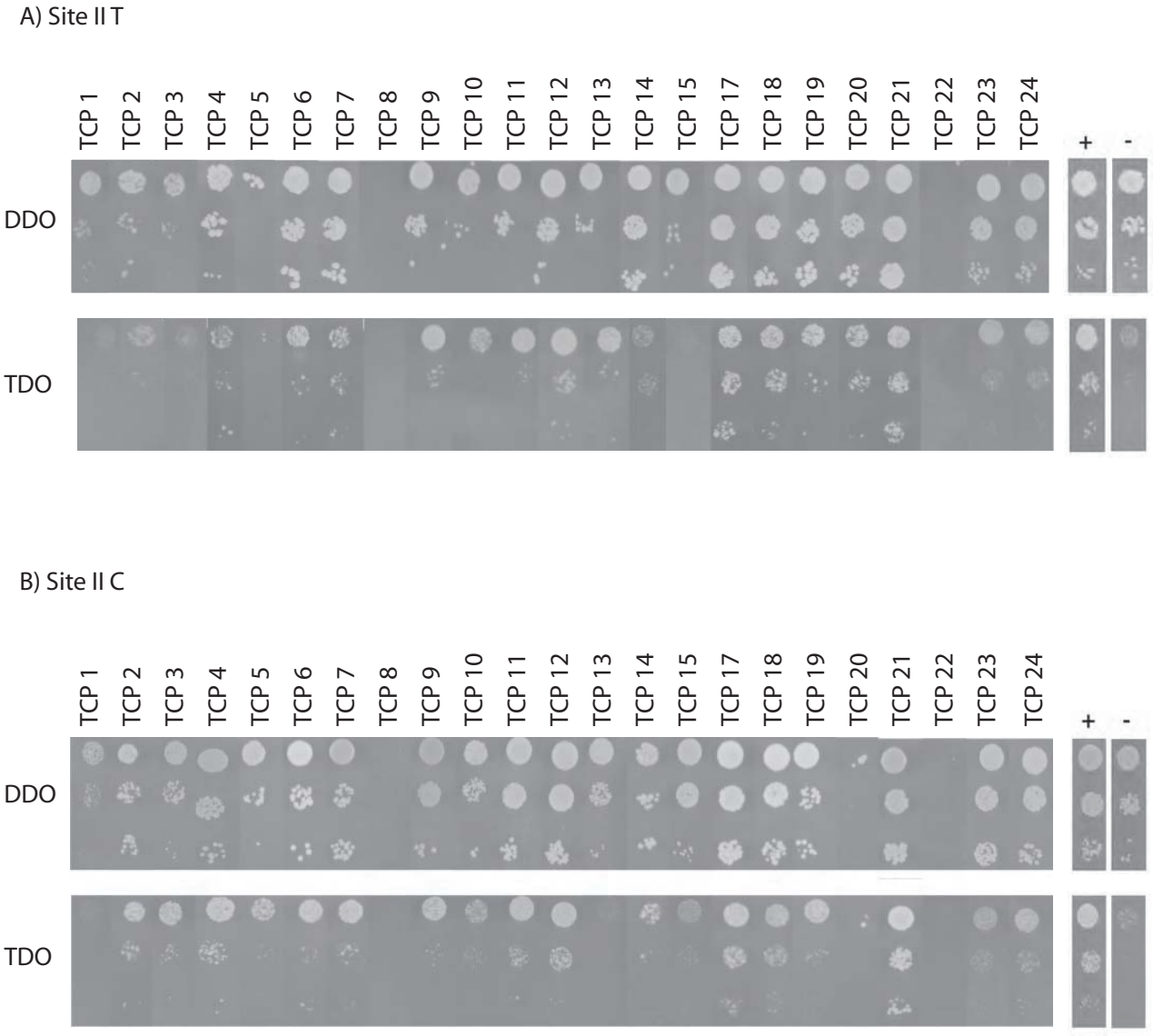

Supplemental Figure 3. Yeast one-hybrid assays. Representative yeast colony growth from yeast one-hybrid assays for binding of the 24 *Arabidopsis* TCP transcription factors with DNA sequences containing site II elements with either a T in the last position (TGGGCT - shown in **A**) or a C in the last position (TGGGCC - shown in **B**) in tandem triplicate. Serial dilutions of yeast culture were spotted below to test the strength of the binding. Positive and negative controls supplied with the Clontech kit (see Methods) are shown on the right (+ and -). DDO = double drop out media to test for transformation. TDO = triple drop out media to test for binding ability.

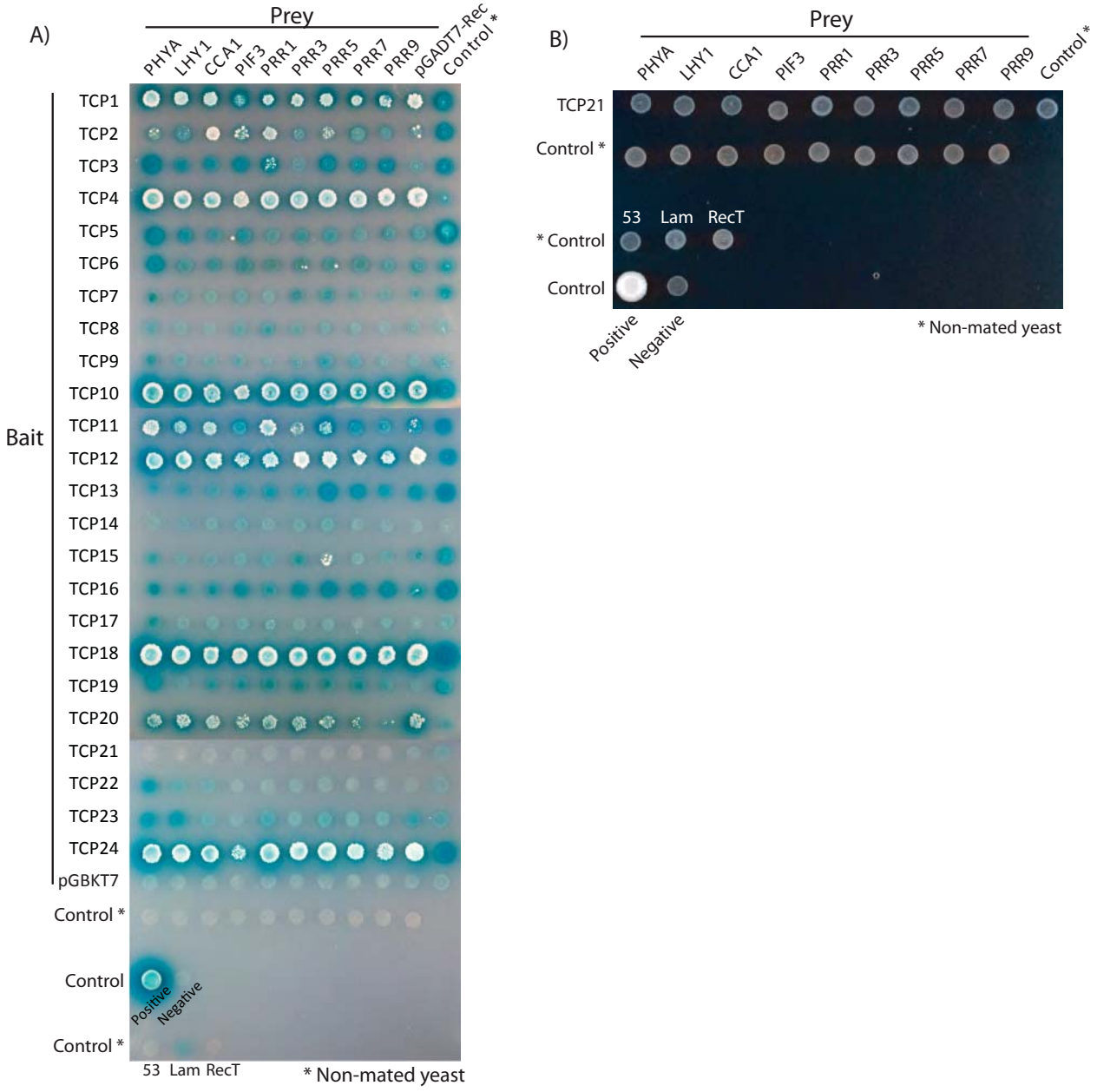

Supplemental Figure 4. Yeast two-hybrid analysis for interactions between *Arabidopsis* TCP family proteins and components of the circadian clock. A) All 24 *Arabidopsis* TCP proteins were cloned into pGBKT7 vector (Bait) and components of the plant circadian clock, PhyA, LHY1, CCA1, PIF3 and PRRs 1, 3, 5, 7 and 9 were cloned into the pGADT7-rec vector (prey) as shown. Additionally, all the TCPs and clock components were also cloned into the opposite vectors for yeast-two-hybrid assays with bait and prey vectors reversed to further confirm the interactions. Both prey and bait empty vectors were grown on the appropriate media to check for the ability of any of the components to auto-activate in the yeast hybrid system utilised. Unmated yeast plated out as controls are indicated by asterisks (*) in the appropriate rows or columns. Additional controls include 53 – pGBKT7-53, Lam – pGBKT7-Lam and RecT – pGADT7-RecT along with positive and negative interactions provided as part of the Clontech kit (positive and negative). All matings were carried out a minimum of four times (representative matings are shown) TCPs 1, 4, 10, 12, 18, 20 and 24 showed a consistently high level of autoactivation when cloned into both bait and prey vectors and thus true interactions could not be determined for these factors. A summary of the interactions from all yeast hybrid assays is shown in Table 1. B) To further confirm the absence of interactions for TCP21, mated yeast were plated out on TDO (triple drop out medium). Asterisks (*) indicate non-mated yeast as controls, 53 – pGBKT7-53, Lam – pGBKT7-Lam and RecT – pGADT7-RecT. Positive and negative interacting controls supplied with the Clontech kit (see methods) are also shown.

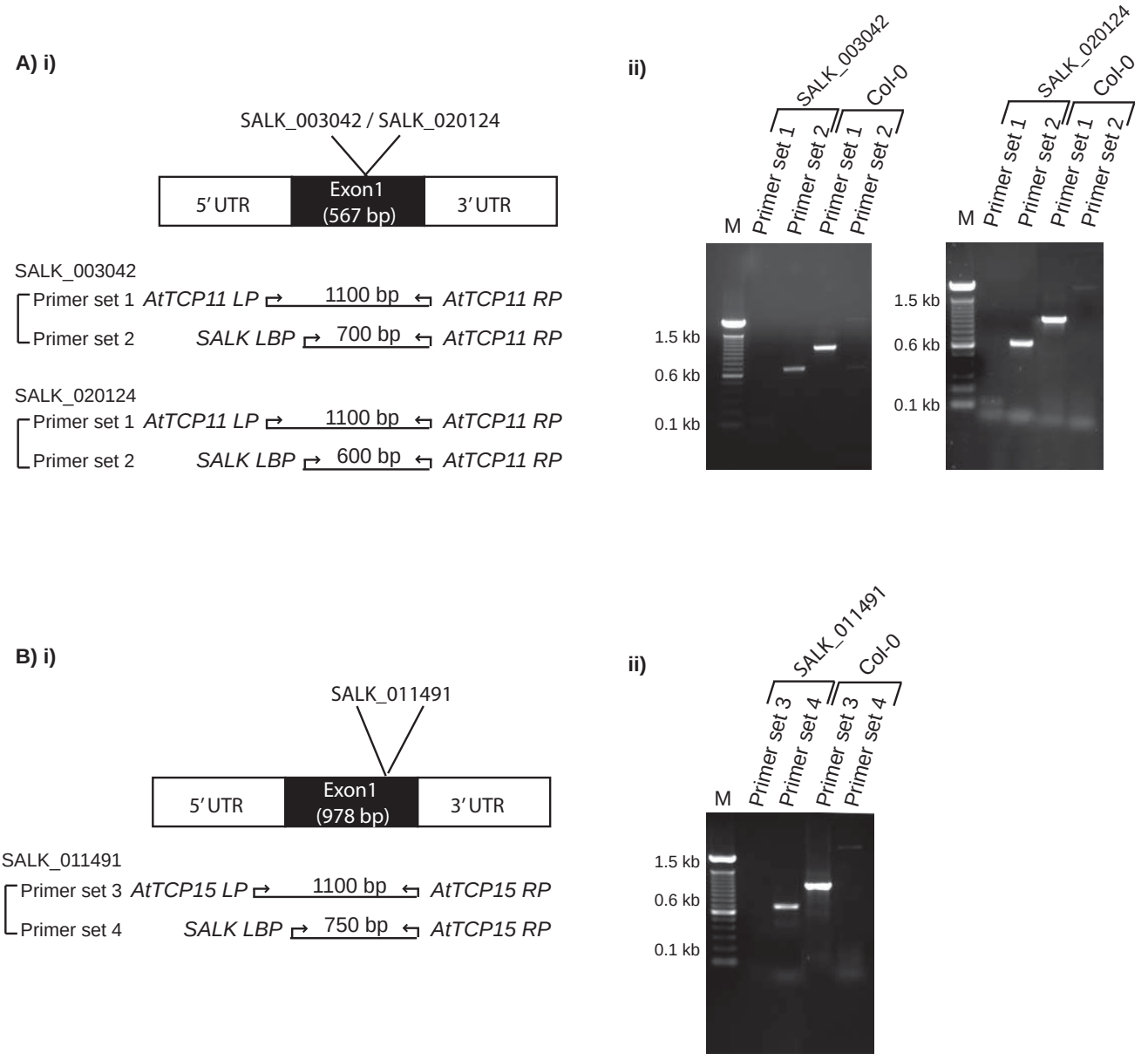

Supplemental Figure 5. Characterisation of the T-DNA insertional lines inactivating *TCP11* and *TCP15*. A) Lines for inactivation of *TCP11* i) A diagrammatic representation of the *TCP11* gene structure and the primer sets 1 and 2 used to determine if each of the T-DNA inserts for SALK_003042 and SALK_020124 were present. ii) RT-PCR werer performed in technical duplicate with different primer sets, which were designed to amplify a fragment if the gene is uninterrupted, to determine if a T-DNA insert was present in the gene; the failure to produce a fragment using primer set 1 in both insertional lines, and the production of a fragment using primers to the left border of the T-DNA (primer set 2) indicates that both lines are homozygous knock-out lines. B) Line for inactivation of *TCP15* i) A diagrammatic representation of the *TCP15* gene structure and the primers sets 3 and 4 used. ii) RT-PCR with different primer sets to determine if a T-DNA insert was present in the gene; the failure to produce a fragment using primer set 3, which was designed to amplify a fragment if the gene was uninterrupted, and the production of a fragment using primers to the left border of the T-DNA (primer set 4) indicates a homozygous knock-out line. M =100-bp molecular weight marker. Primer sequences are shown in Supplemental Table 1B.

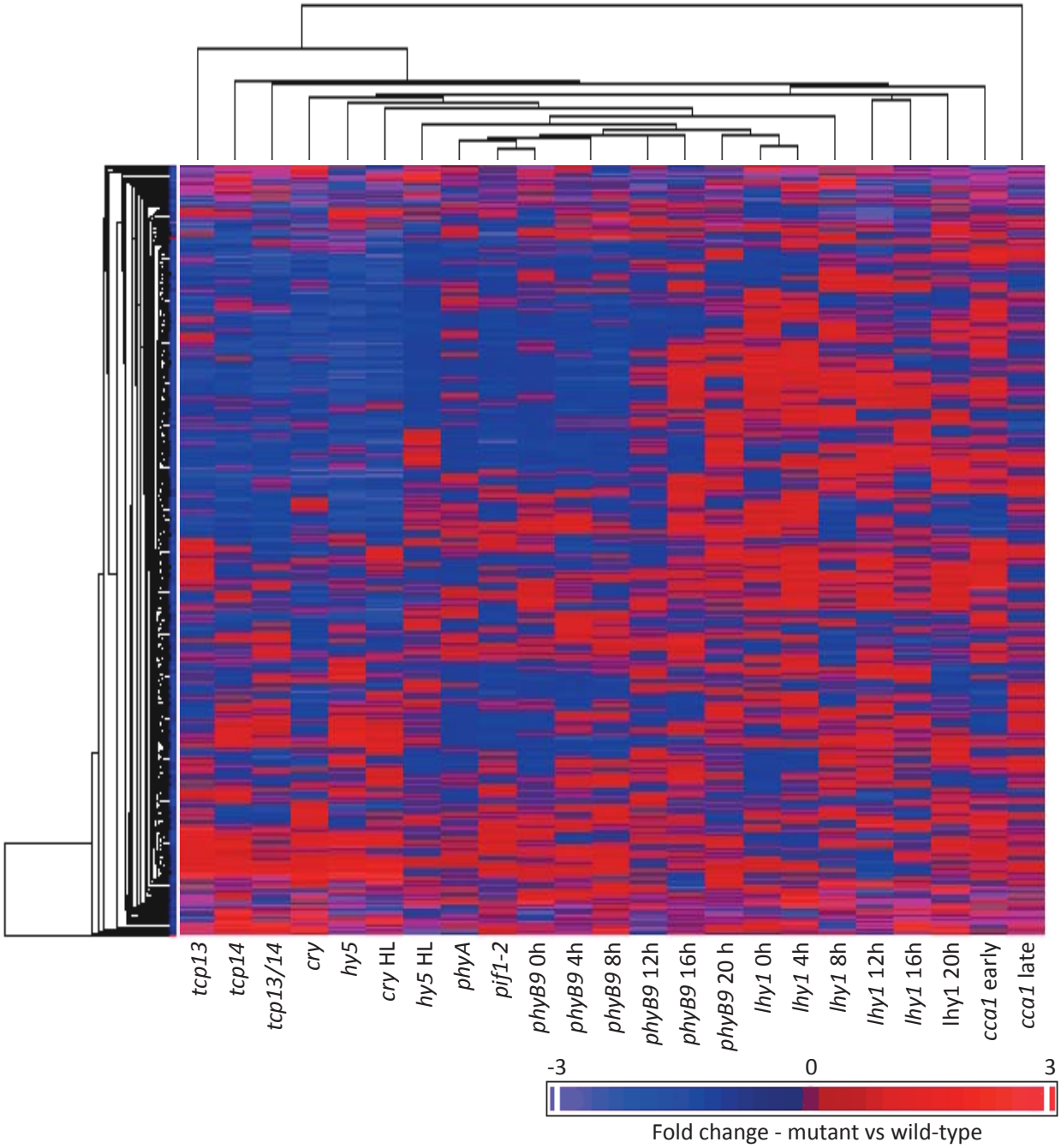

Supplemental Figure 6 Transcript abundances for genes encoding mitochondrial proteins with site II in a range of mutant backgrounds. Data for transcript abundances for *Arabidopsis* genes encoding mitochondrial proteins with site II in a range of mutant backgrounds was obtained from GENEVESTIGATOR (https://www.genevestigator.com/gv/index.jsp). A list of nuclear genes encoding mitochondrial proteins (Van Aken et al., 2009) was cross-referenced with a list of genes with site II elements in their 5' 500-bp promoter regions to obtain a complete list of nuclear-encoded mitochondrial proteins with site II elements in their promoter regions. The expression patterns of these 365 genes were investigated in microarray datasets for a range of light/circadian related mutants. Mutants were: *phyB9, lhy1, cca1, tcp14, tcp13, pif1-2, cry, hy5, phyA* and a *tcp13 tcp14* double mutant. Genevestigator experiment reference numbers for these datasets are as follows, AT-00240, AT-00083, AT-00100, AT-00246, AT-00008 and AT-00300. Information regarding specific experimental details can be found in the original references (McCormac and Terry, 2002; Kleine et al., 2007; Nozue et al., 2007; Michael et al., 2008; Moon et al., 2008). Normalised data were downloaded and fold changes between mutant and the appropriate wild type was calculated. Transcript profiles were clustered using Euclidian distance and average linkage measures in Partek Genomics Suite software version 6.4. Clustering dendrogram trees were drawn under defult settings. Fold changes in transcript abundances between the mutant and the corresponding wild-type control background are shown by the colour scale. h represents time (hours) into the day cycle.

Supplemental Table 1A. Primer sequences for cloning of all TCP factors and clock components for yeast hybrid and protein interaction studies

AT number	Name	Forward Cloning Primer seq	Reverse Cloning Primer seq
At1g30210	TCP24	catatggccatggaggttgacgaagacattg	ctcgaggatcccgggtctcctttcctttgccttgtca
At1g35560	TCP23	catatggccatggagtcccacaacaacaacc	ctcgaggatcccgggaggagaaccatctatagtaggatt
At1g53230	TCP3	catatggccatggcaccagataacgaccatt	ctcgaggatcccgggatggcgagaatcggatgaagc
At1g58100	TCP8	catatggccatggatctctccgacatccg	ctcgaggatcccgggctcagagctatttgagttctcc
At1g67260	TCP1	catatggccatggcgtcttccaccaatgact	ctcgaggatcccggggtttacaaaagagtcttgaatccaaac
At1g68800	TCP12	catatggccatggttccttctctagataccaatg	ctcgaggatcccggggtagcagagataatcatatagagag
At1g69690	TCP15	catatggccatggatccggatccggatca	ctcgaggatcccgggggaatgatgactggtgcttcc
At1g72010	TCP22	catatggccatggatcagaattcctctgttgcg	ctcgaggatcccgggctttttgtcatcaccaccattttc
At2g31070	TCP10	catatggccatgggacttaaaggatatagcgtc	ctcgaggatcccggggaggtgtgagtttggaggag
At2g37000	TCP11	catatggccatggtttttcagaatgtgtgcagaaat	ctcgaggatcccgggatggtgacggcgtctacgtt
At2g45680	TCP9	catatggccatggcgacaattcagaagcttg	ctcgaggatcccggggtggttcgatgaccgtgctg
At3g02150	TCP13	catatggccatggatatcgtctcttggaaagatg	ctcgaggatcccgggcatatggtgatcacttcctctac
At3g15030	TCP4	catatggccatggctgacgaccaattccatc	ctcgaggatcccgggatggcgagaaatagaggaagca
At3g18550	TCP18	catatggccatggacaacaacattttcagtactact	ctcgaggatcccgggatacatgttttgatagttgtgcatgag
At3g27010	TCP20	catatggccatggatcccaagaacctaaatcg	ctcgaggatcccgggacgacctgagccttgagaatc
At3g47620	TCP14	catatggccatggaaaagccaacatcaagtatc	ctcgaggatcccgggatcttgctgatcctcctcatca
At4g18390	TCP2	catatggccatggttggagatctaatgaagaataac	ctcgaggatcccggggttcttgcctttacccttatgttc
At5g08070	TCP17	catatggccatgggaataaaaaaagaagatcagaaaag	ctcgaggatcccgggctcgatatggtctggttgtgag
At5g08330	TCP21	catatggccatggccgacaacgacggag	ctcgaggatcccgggacgtggttcgtggtcgtctt
At5g23280	TCP7	catatggccatggctattaacaacaacaacaacaac	ctcgaggatcccgggacgtggatcttcctctcttcg
At5g41030	TCP6	catatggccatggtcatggagcccaagaag	ctcgaggatcccgggtgaaccattttcctctgcactc
At5g51910	TCP19	catatggccatggaatcgaatcacgaaggca	ctcgaggatcccgggagtctcatgacatgaagacgga
At5g60970	TCP5	catatggccatgggatcaggagaatgtgatgaa	ctcgaggatcccgggagaatctgattcattatcgctactatg
At1g09570	phy A	catatggccatggctctgtttgagcttttcag	ctcgaggatcccgggcgacgatccacaaaactgatca
At2g18790	phy B	catatggccatggcaggctctaggccgac	ctcgaggatcccgggcttgtttgctgcagcgagttc
At1g09530	PIF3	catatggccatggtttccggagtcgggg	ctcgaggatcccgggatatggcatcatcagcatcatgtc
At2g46830	CCA1	catatggccatggagacaaattcgtctggag	ctcgaggatcccgggtgtggaagcttgagtttccaaccgc
At1g01060	LHY	catatggccatggatactaatacatctggag	ctcgaggatcccgggtgtagaagcttctccttccaatcg
At5g61380	TOC1 (PRR1)	catatggccatggatttgaacggtgagtg	ctcgaggatcccgggagttcccaaagcatcatcctgagg
At5g60100	PRR 3	catatggccatgggttttaataacattgaaactggtg	ctcgaggatcccgggattgtcttcacttcctga
At5g02810	PRR7	catatggccatggatgctaatgaggaggggaggg	ctcgaggatcccggggctatcctcaatgtttttttatgtcg
At2g46790	PRR9	catatggccatgggggagattgtggttttaag	ctcgaggatcccgggtgattttgtagacgcgtctg

Supplemental Table 1B. Primer sequences for all Quantitative RT-PCR assays along with primers used for screening T-DNA insertional lines

Quantitative RT-PCR primers

AGI	Forward Primer Sequence	Reverse Primer Sequence
AT1G53230	tagcttcaacgcaacagagc	ggttctgtgtattgcctcgtg
AT1G58100	ggtttagttttccgatggatca	gctgcggctgagctaaaa
AT2G37000	gagctcggtcacaaaactga	atcgacggttcagcttgact
AT5G60970	tattcccgacataccttcg	ctccatcgacgacatgatga
AT1G35560	accactgctccaaactccac	gtcgttttgcgggtgtttta
AT1G67260	ttggaggcgatgtagaacaa	aagctcttatcgccattgtca
AT3G47620	ttcaacaagctgaaccatctgt	aattcgccgggattgttc
AT3G15030	cacgacggtctcactcacaa	aatctaagtcaagcttcaatgtgc
AT1G30210	gctcatgacaagaatctgaagaaa	tgttgcagtgataaacttttgaattt
AT3G02150	tcacaacctggaacatcatca	tgatgactatgataatctgcctgtaa
AT4G18390	cgtcacctactactactaactccaagc	ctgaaatgatttttaaccacaagc
AT1G68800	agaagtttcttggactaaccagtga	attcctcggagtcaccaaaa
AT1G69690	ttgcagctcctattgctttg	cacctcctcctcctccataa
AT1G72010	acgcttctttacgcagtggt	aagaagatttcgacgcctga
AT2G31070	ccacggagaagaagctactca	tcatcatgaatttgaacctcca
AT2G45680	cgtcgaatcagcctcagtta	cgtaagacgacggcgaag
AT3G18550	atcgcgacaaccctttctc	gaagatgtgtccatggatcctaa
AT3G27010	cttattgaaacctctgcaaaaaca	aaatctctggctgtgtgtattcaa
AT3G45150	cgaaaaatggaattaacaacagc	aattttcaaatggcggtcttt
AT5G08070	tggctcttagaagttgccaaa	tgaaaaccaggtgggaattg
AT5G08330	ccgtctaaagatcgacacagc	tgattggcatacgaatccttc
AT5G23280	cgacatagcaaagtcgatgg	cacgagcagcacatataatcg
AT5G41030	gggttcttcatcatcattcaca	atgaaccattttcctctgcac
AT5G51910	cccgaatccgaaaaccaaac	caccggctgcaaatacccg
AT5G62575	gctttatcaatatcgcgtcgtgg	gcagaatcttcagccaagaga
AT5G13440	caccggagcgttataagagg	ggtgttttgacagcttcgact
AT3G08950	cattgtcccgatatctgtcctg	ctggcaccacgtctactcccg
AT5G47030	gagaaagcagaggcacagattgg	ccttcttttagcccgagagagc
AT2G30160	ggatgaggaaggttggttga	cggtcacaaccacacacac
AT2G46320	atcagtacaagggaactcttgatg	ccaaagcctagaaaacccttcc
AT2G46830	ggatcagaaaaagtgtcgcatcc	caatctgaacagttgtcttcctgc
AT1G01060	cagaagtcatgcacaaaagttc	tttctatgtccaaagcttggc
AT5G61380	agtcaccaggaaaatgagtgg	catcagcaccaagaccaccatc
AT5G24470	gtgcctcagctttcacacg	tcttgacttgctgcaacattct
AT3G16620	tcattgctcgtgctaatctga	tgtttacgcggatgcttactt
AT3G61070	gtgcagtcgagattggtgag	tgatttctgaagcttagcacga
AT1G26880	ccagcaccgtatcgtcaag	ggcctcaagtgagggattc
AT3G09200	gcttatcgatgagtacacccaga	aaaccaacgtttccctgaag
AT3G27080	cgataatctgactagatgggg	gcttcagtctcgtcaggagtc
AT1G27390	ccaagttggaagaggccttg	gtgtcattacctggatcctc
AT5G40930	ccagagagcgaactctatcgg	gacaccggcgtctgagaattg
AT1G07180	gtccgtgagagcaaggaagg	ggcgaagtggaggggatatg
AT5G25760	ctgcgactcagggaatcttcta	ttgtgccattgaattgaattgaaccc

Screening primers

SALK line	LP Sequence	RP Sequence
SALK_020124	gtgtccaacaaacatcaaccc	tgaaggagaaaccatcgaatg
SALK_003042	gtgtccaacaaacatcaaccc	tgaaggagaaaccatcgaatg
SALK_011491	agaaccacgtaagcccatctc	tcaaatgaactccactaccgc

TCP Transcription Factors Link the Regulation of Genes Encoding Mitochondrial Proteins with the Circadian Clock in *Arabidopsis thaliana*

Estelle Giraud, Sophia Ng, Chris Carrie, Owen Duncan, Jasmine Low, Chun Pong Lee, Olivier Van Aken, A. Harvey Millar, Monika Murcha and James Whelan

Plant Cell 2010;22;3921-3934; originally published online December 23, 2010;
DOI 10.1105/tpc.110.074518

Chapter 3

Cyclin-Dependent Kinase E;1 (CDKE;1) Provides a Cellular Switch in Plants Between Growth and Stress Responses

Cyclin-dependent kinase E;1 (CDKE;1) provides a cellular switch in plants between growth and stress responses*

Sophia Ng[1], Estelle Giraud[1], Owen Duncan[1], Simon R. Law[1], Yan Wang[1], Lin Xu[1], Reena Narsai[1], Chris Carrie[1], Hayden Walker[1], David A. Day[2], Nicolás Blanco[3], Åsa Strand[3], James Whelan[1], Aneta Ivanova[1]

[1] Australian Research Council Centre of Excellence in Plant Energy Biology. University of Western Australia, 35 Stirling Highway, Crawley, Western Australia, 6009. Australia. [2]School of Biological Sciences, Flinders University, Adelaide 5001, South Australia, Australia. [3] Umeå Plant Science Centre, Department of Plant Physiology, Umeå University, SE-901 87 Umeå, Sweden.

***Running title:** *Mitochondrial retrograde regulation*

To whom correspondences should be addressed: Aneta Ivanova ARC Centre of Excellence in Plant Energy Biology. University of Western Australia, 35 Stirling Highway, Crawley 6009 WA, Australia, Tel: +61 8 6488 1749; Fax: +61 8 6488 4401. Email: aneta.ivanova@uwa.edu.au

Keywords: *Arabidopsis thaliana*, mitochondria, anterograde regulation, retrograde regulation, kinase, stress, growth

Background: Mitochondria send signals to the nucleus to modulate gene expression when mitochondrial function is perturbed.
Results: CDKE;1 was identified as an essential component in regulation of responses to perturbation of mitochondrial electron transport.
Conclusion: Mitochondrial regulation is integrated with growth, energy and other cellular stress signalling pathways.
Significance: Identified a molecular link between mitochondrial retrograde regulation and growth and stress signalling pathways.

SUMMARY

Plants must deal effectively with unfavourable growth conditions that necessitate a coordinated response to integrate cellular signals with mitochondrial retrograde signals. A genetic screen was carried out to identify *regulators of alternative oxidase* (*rao* mutants), using *AOX1*a expression as a model system to study retrograde signalling in plants. Two independent *rao1* mutant alleles identified *CDKE;1* as a central nuclear component integrating mitochondrial retrograde signals with energy signals under stress. CDKE;1 is also necessary for responses to general cellular stresses, such as H_2O_2 and cold that act, at least in part, via anterograde pathways, and integrates signals from central energy/stress sensing kinase signal transduction pathways within the nucleus. Together, these results place CDKE;1 as a central kinase integrating diverse cellular signals and shed light on a mechanism by which plants can effectively switch between growth and stress responses.

Mitochondria and plastids are semi-autonomous organelles found in all plant cells. While they contain a limited genetic coding capacity, encoding 57 and 128

proteins, respectively in *Arabidopsis thaliana* (Arabidopsis) (1), greater than 95 % of the 1500 and 2500 proteins estimated to be present in mitochondria and chloroplasts are encoded by genes located in the nucleus. The expression of nuclear located genes encoding mitochondrial and chloroplast proteins is controlled by either anterograde or retrograde pathways, depending on the source of the signal(s) regulating these sets of genes (2). Anterograde regulation refers to top-down regulatory pathways, where endogenous (e.g. hormones) or exogenous (e.g. light) signals directly impact nuclear gene expression. Retrograde regulation refers to signals (e.g. reactive oxygen species, (ROS)) that originate in mitochondria or plastids and modify or alter nuclear gene expression networks.

The concept of retrograde regulation for mitochondria and plastids is over 30 years old (3,4). For plastid retrograde regulation, signals have been classified into five different groups, plastidial gene expression, pigment biosynthesis, ROS, redox effectors and metabolites. Plastidial retrograde regulation has been investigated with forward genetic approaches, and *genome uncoupled* (*gun*) mutants were identified. Five of the six GUN genes, *GUN2-6*, encode components closely associated with tetrapyrrole biosynthesis. GUN1 on the other hand, is a chloroplast localized pentatricopeptide-repeat (PPR) (2,5). The report of a gain-of-function *gun* mutant, *gun6*, (5) strongly supports the role for heme as a signalling molecule and a mechanistic model for the Mg-ProtoIX mediated plastid signal was recently presented (6). Additional factors or signals associated with plastid retrograde signalling include a plastid bound homeodomain transcription factor (9), the transcription factor ABI4 (7), 3'-phosphoadenosine 5'-phosphate (PAP) (8) and β-cyclocitral (9).

The characterisation of mitochondrial retrograde signalling has been extensively carried out in *Saccharomyces cerevisiae* (yeast), where several retrograde pathways and the components involved have been identified and characterised (10). The most extensively characterised system is associated with inhibition or dysfunction of the TCA cycle, and three factors, called Rtg1, 2 and 3, have been characterised to mediate this response, in addition to a number of positive and negative regulators (10). Whereas Rtg1 and 3 are basic helix-loop-helix leucine transcription factors (10), Rtg2 contains a kinase domain that shares similarties with a variety of proteins, including cell cycle proteins (11). Furthermore, it has been demonstrated that the Rtg regulated pathway interacts with the target of rapamycin (TOR) pathway, involved in nitrogen metabolism in yeast, via Lst8p as a negative regulator of the Rtg pathway (12). In mammalian cells the master regulator NF_kB links mitochondrial retrograde regulation with other regulatory pathways (13).

The induction of the alternative oxidase (AOX) at a transcript and protein level has been widely used as a model system to study mitochondrial retrograde signalling in plants (14), and a genetic system designed to identify components in these signal transduction pathways has been reported (15); but to date no components have been identified. Studies on mitochondrial retrograde signalling suggest converging or synergistic pathways with plastidial retrograde pathways. A study investigating the role of Arabidopsis prolyl-tRNA synthetase, a dual targeted protein required for both mitochondria and plastid translation, has shown that disruption of both mitochondrial and plastidial translation is required to elicit retrograde signals (16). At the receiver end, the transcription factor ABI4, has been shown to regulate targets of both plastidial and mitochondrial retrograde signalling pathways (17,18).

Here, we describe the identification of the *regulator of AOX1a 1 (rao1)* mutant, encoding a nuclear localised Cyclin-Dependent Kinase E1 (CDKE;1), as an essential molecular component of mitochondrial retrograde signalling in

Arabidopsis. Furthermore, we show that the induction of AOX in response to retrograde signals is likely under the control of both transcriptional and post-transcriptional regulation.

EXPERIMENTAL PROCEDURES

Col:LUC construction and line selection The -2000 bp *AOX1a* promoter region upstream of the translation start site, previously shown to be responsive to a variety of treatments that perturb mitochondrial function (17,19), was cloned in front of the reporter gene *LUCIFERASE* (*LUC*). A *Col:LUC* line with a single T-DNA insertion was isolated by Southern blot analysis and hybridised with a 500 bp probe amplified from the inserted *LUC* gene (Supplementary Fig S1).

Mutagenesis and mutant screen Approximately 30000 homozygous Col:*LUC* seeds were mutagenised for 16 h in 100 ml of 0.25 % (*v/v*) ethyl methane sulfonate (EMS), then washed in several volumes of water over a period of 6 h. Seeds were sown on soil and grown in growth chambers at 22°C, 16 h 120 µmol $m^{-2}s^{-1}$ light /8 h dark. ~20 000 M2 plants, representing 20 pooled family populations were screened for altered *LUC* reporter gene expression under mitochondrial stress. Plants were grown for 14 days on Gamborg's B5 growth media (PhytoTechnology) with 3 % (*w/v*) sucrose and 0.8 % agar (*w/v*). Stress treatments were applied 3 h into the light cycle by spraying plants with either 50 µM antimycin A (AA), 50 µM myxothiazol, 25 mM Monofluoracetate (MFA) or 20 mM H_2O_2, as described previously (17,20). Plants were returned to normal growth conditions for 6 h. Cold treatment was applied to 14 day old plants by placing them at 4°C for 16 h. Ultraviolet light (UV) was applied for 30 min and then plants were placed in normal growth conditions for 6 h. After 6 h (or 16 h for cold treatment), 2.5 mM luciferin (GoldBio) was applied to plants and luminescence was measured using a NightOWL bioluminescence imaging system (Berthold).

Genetic mapping and gene identification Transgenic Arabidopsis lines carrying the *LUCIFERASE* reporter gene system, linked to the 2000 bp *AOX1a* promoter region upstream of the translational start site (referred to as Col:*LUC*) were generated. A single insert homozygous line for the T-DNA insertion in the Columbia-0 (Col-0) background was mutagenized by ethane methyl sulfonate (EMS) (Supplementary Fig 1, ColTL3). A similar line carrying a single, homozygous copy of the T-DNA construct was generated in *Landsberg erecta* ecotype (L.*er*:*LUC*) for mapping purposes. *rao1-1* and *rao1-2* mutants were crossed with L.*er*:*LUC*. Homozygous F2 *rao1-1* and *rao1-2* plants were selected and DNA extracted. Linkage between Small Sequence Length Polymorphism (SSLP) markers (i.e. a set of insertion/deletion (Indel) polymorphism sites between Col-0 and Landsberg *erecta* (L.*er*) Arabidopsis ecotypes) (21) and a mutation was established based on a low recombination frequency. Markers were selected from Cereon database - www.arabidopsis.org/Cereon/index.jsp (Supplementary Table 1 and Supplementary Fig 2). Initial mapping of a population of 50 homozygous F2 *rao1-1* and *rao1-2* plants all mapped at 25.478Mb (MBK5 - SSPL marker, Supplementary Fig 2). A second mapping was carried out with expanded SSPL markers in 50 homozygous F2 *rao1-1* plants and 138 homozygous F2 *rao1-2* plants and 50 homozygous F2 *rao1-1* plants, recombinants were identified and genotyped. Both *rao1-1* and *rao1-2* mutations mapped to a 2.48 Mb region on chromosome 5 between marker CER457391 and the end of the chromosome.

Allelism between *rao1-1* and *rao1-2* was confirmed by the lack of phenotype complementation in F1 seeds resulting from cross between the 2 lines. *rao1-1* and *rao1-2* mutant plants were complemented with the full length coding sequence of *CDKE;1* that

was PCR amplified from Col-0 cDNA and cloned into pDONR201 (Invitrogen), and subsequently transferred to a binary vector pK7WG2 under the control of the constitutive *Cauliflower Mosaic Virus 35S (CaMV 35S)* promoter. This binary vector was then transformed into *A. tumefaciens* GV3130 strain. Floral dipping was performed with an inoculum medium containing 10 % (*w/v*) sucrose and 0.05 % (*v/v*) Silwet-77, as previously described (22). T1 transformants were screened on kanamycin antibiotic as described (23). The presence of the transgene in the complemented plants was confirmed by PCR analysis. The progeny of the primary transformants segregated for wild-type and *rao1* mutant phenotypes; plants with wild-type induction responses all contained the transgene, whereas plants showing the *rao1* phenotype did not.

Next Generation Sequencing and data analysis 50 ng of genomic DNA isolated from pooled Arabidopsis seedlings for each line (Col:*LUC* (wild-type), *rao1-1* backcrossed line 1, *rao1-1* backcrossed line 2, *rao1-1* backcrossed line 3 and *rao1-2*) using DNeasy Plant Maxi kit (QIAGEN), according to manufacturer's instructions. Genomic DNA was used as input in library generation using Nextera DNA sample prep kits (EpiCentre) according to manufacturer's instructions. Library quality was checked using an Agilent bioanalyser and quantified using a Nanodrop (Thermo Scientific) and Qubit (Invitrogen) before Next-Generation Sequencing with 2x50 bp paired-end read lengths on an Illumina HiSeq1000. Primary data processing was performed by RTA, .BCL conversion and de-multiplexing was performed by CASAVA V1.8.2. Alignments for Col*:LUC* read sequences were performed against TAIR9 reference sequences (www.arabidopsis.org) and a fasta reference genome sequence (Col*:LUC* reference) was generated for Col*:LUC* to ensure SNP calls present in the wild-type parental lineage could be excluded from *rao1* sequence data analysis. Read sequences for *rao1-1* and *rao1-2* re-sequencing were aligned to the Col*:LUC* reference genome sequence using CASAVA V1.8.2 and SNP calls generated using GATK software pipelines (www.broadinstitute.org/gsa/wiki/index.php/The_Genome_Analysis_Toolkit) and best practices (www.broadinstitute.org/gsa/wiki/index.php/Best_Practice_Variant_Detection_with_the_GATK_v3). Only homozygous SNP calls were used and SNPs were also filtered on base call quality, mapping quality scores, mutations occurring in annotated coding regions only and base changes generated by EMS mutagenesis. Furthermore, mutations were shortlisted only if all back-crossed lines contained the mutation, and there was a candidate mutation in the same gene in the allelic line. Sorted .bam and .gvf files were visualised in IGV (http://www.broadinstitute.org/igv/) and Tablet (http://bioinf.scri.ac.uk/tablet/) viewers to identify candidate SNPs in the pre-defined genomic region of interest at the base of chromosome 5.

Protein sequence alignment and phylogenetic tree generation The protein coding sequence for CDKE;1 (AT5G63610) was downloaded from TAIR website (www.arabidopsis.org). Using the CDKE;1 sequence to perform a blast serach of selected plant species was carried out using the Phytozome website (www.phytozome.net). The most related sequences were then aligned using the sequence alignment program MAFFT (24). Multiple sequence alignments were visualised using the program Multiple Align Show. Phylogeneitic trees were drawn using the Phylip (V3.68) software package and visualised using A tree Viewer (ATV) (25).

QRT-PCR Leaf tissue from Col*:LUC*, *rao1-1* and *rao1-2* 14-day-old seedlings treated with 50 µM AA, UV or mock control treatments, as described above, were harvested in biological triplicate at 30 min, 1 h and 3 h after treatment. RNA isolation, cDNA generation and QRT-PCR were

performed as described previously (26). Primers and assay details for AOX1a have been described previously (26). *LUC* primers are listed (Supplementary Table 1).

Global transcript analyses Analysis of global changes in transcript abundance in response to AA treatment in the *rao1* mutants and in the KIN10 RNAi lines were carried out using Affymetrix ATH1 microarray genechips. For the *rao1* mutant analysis, arrays were performed using RNA isolated in biological triplicate from Col:*LUC*, *rao1-1* and *rao1-2* 14-day-old seedlings treated with either mock treatment or 3 h of 50 µM AA treatments. Similarly, for the KIN10 RNAi expression analysis, arrays were performed using RNA isolated in biological triplicate from Ler, KIN10 RNAi#1 and KIN10 RNAi#7 14-day-old seedlings with either mock treatment or 3 h of 50 µM AA treatments. aRNA generation, hybridisation, washing and scanning the gene chips and all primary data analysis was performed according to manufacturer's instructions. CEL files were MAS5 normalised to obtain present/absent calls across all Genechips. Probesets were defined as absent and removed from further analysis if they returned absent or marginal calls in 2 or more of the 3 biological replicates in all geneotypes/conditions tested. Probesets relating to organelle transcripts and Affymetrix bacterial controls were also removed, leaving a present set of 16, 607 probesets for the rao1 arrays and 16, 423 for the KIN10 arrays. GC-RMA normalised gene expression values from the defined present set were analyzed to identify differentially expressed genes by a regularized t test based on a Bayesian statistical framework using the software program Cyber-T (27) (http://cybert.microarray.ics.uci.edu/) as in (28). Microarray data for the two independent mutant lines (*rao1-1* and *rao1-2*) were analysed independently at first to ensure no probes displayed differential expression between the genotypes. Changes were considered significant at an FDR correction level of PPDE (>P) >0.95 and a fold change greater than 1.5 fold (positive or negative). Protein-protein interaction networks were drawn using online tools BAR Arabidopsis Interaction Viewer (29) and PAIR (30). Gene lists of stress responsive transcripts controlled via *RAO1* activity were defined as shown in Fig S8. Gene lists of KIN10 associated transcripts were utilised from (31) and hierarchical clusters of Log_2 fold-changes were generated in Partek Genomics Suite V6.5 (Partek) using average linkage and Euclidean distance parameters. The stress responsive network affected by mutation in CDKE;1 is shown in Supplementary Table 2 to 7.

Western blots Mitochondria were isolated from 14-day-old plants treated with 50 µM AA or exposed with 30 min UV light, as described above. Western blot immunodetections were carried out as described previously (32) using antibodies to AOX (33) and TOM40 (32). Serial dilutions of total mitochondrial protein were used to ensure that the signal obtained was in the linear range related to protein levels.

GFP localisation GFP localisation of CDKE;1 was performed as described previously, with mitochondrial mCherry utilised as a mitochondrial marker and DAPI staining (Invitrogen) to confirm nuclear localisation (34).

Biomolecular Flourescence Complementation Biomolecular Fluorescence Complementation was carried out as outlined previously (35) in onion epithelial cells. DAPI staining (Invitrogen) was utilised as per the manufacturer's instructions, to confirm nuclear localisation.

Phenotypic characterisation of rao1 and T-DNA insert lines A full phenotypic characterisation of wild-type (Col:*LUC*) and mutant lines (*rao1-1, rao1-2* and GABI_564F11) analysed in this study is shown in Supplementary Fig 10 and carried

out as described (36). At least 15 plants per genotype were used for analysis. For plate-based phenotypic analysis, seedlings were grown on Gamborg's B5 agar medium supplemented with 30 % (*w/v*) sucrose. For the quantification of maximum root length and maximum rosette leave area, photos were first taken of the plants and the root length and leave area were then measured using Image Processing and Analysis tool in the software ImageJ64.

T-DNA insertion line Four T-DNA insertion lines for *cdke;1* (SALK_072781, SALK_117306, SALK_138675 and GABI_564F11) were obtained from the NASC (European Arabidopsis Stock Centre). However, homozygous lines were only obtained from Gabi564F11 through PCR analyses. T-DNA insertion homozygous lines were confirmed by PCR using the gene-specific primers (LP and RP) and T-DNA-specific primer (LB). The precise location of the T-DNA insertion was determined by sequencing.

RESULTS

Identification of regulators of alternative oxidase1a (rao) mutants

A genetic screen to identify the molecular components of mitochondrial retrograde signalling was developed using a transgenic Arabidopsis line carrying the *LUCIFERASE* reporter gene system, linked to the 2000 bp *AOX1a* promoter region upstream of the translational start site (*AOX1a:LUC*, Fig 1A, Supplementary Fig 1, plants referred to as Col:*LUC* plants). Transgenic *Col:LUC* plants in the wild type background showed low *LUC* expression under normal growth conditions (Fig 1B, -AA) but this increased substantially after 6 h treatment with 50 µM AA, an inhibitor of Complex III of the mitochondrial electron transport chain (Fig 1B, +AA 50 µM). Mutagenised M2 progeny were screened for the inability to induce LUC in response to retrograde signals after treatment with AA. Two mutant lines, *rao1-1* and *rao1-2,* were identified (Fig 1C), both mapped to a 2.48 Mb region at the bottom of chromosome 5 (Supplementary Fig 2), and therefore, were crossed to test for allelism. *rao1-1* and *rao1-2* are recessive mutations and the first filial generation (F1) progeny from the cross all F1 plants showed a *rao1* mutant phenotype, confirming that *rao1-1* and *rao1-2* are allelic mutations in the same gene (Fig 1D).

Next generation sequencing was used to catalogue candidate mutations in common genes in these lines. Short sequence reads were aligned to a reference sequence generated from the re-sequencing of the Col:*LUC* line, and homozygous SNPs were called. *rao1-1* and *rao1-2* alignment coverage and details are shown in Fig 2A. A candidate mutation was identified in AT5G63610, that encodes a Cyclin-Dependent Kinase E;1 (CDKE;1) (Fig 2A – SNPs visualised in Tablet (http://bioinf.scri.ac.uk/tablet/) Supplementary Fig 3). Both *rao1-1* and *rao1-2* contain non-synonymous mutations in the *CDKE;1* coding sequence as confirmed by Sanger sequence analysis (Fig 2B). *rao1-1* contains an amino acid change from an arginine (R) to a lysine (K) at position 153 within the serine/threonine protein kinase active site (Fig 2B and C). *rao1-2* contains an amino acid change from an alanine (A) to a threonine (T) at position 53 in the protein kinase ATP binding site (Fig 2B and C). Both these mutations occur in highly conserved regions of the coding sequence (Fig 2C). In both *rao1-1* and *rao1-2* lines, the mutant phenotype could be rescued by complementation with constructs containing the wild-type *CDKE;1* coding sequence; as shown by fully restored, wild-type induction of LUC in response to AA treatment in the primary transformants (Fig 2D). These results confirm that the *rao1* phenotype is the result of a mutation in CDKE;1.

Diverse cellular stress signalling pathways are regulated through RAO1 While AA is a well defined inhibitor of Complex III, it also acts as an inhibitor to one pathway of cyclic electron transport (37). Therefore plants were screened for a retrograde response to

50 µM myxothiazol (which, like AA, inhibits Complex III in the mitochondrial respiratory chain but at a different site: AA inhibits at the N site and myxothiazol inhibits at the P site (38)). Neither *rao1-1* nor *rao1-2* could induce LUC expression in response to myxothiazol (Fig 3A, B and G). *rao1* plants were treated with monofluoracetate (MFA), an inhibitor of the TCA cycle at the site of aconitase (15). While MFA induced LUC in Col:*LUC* plants, this induction was abolished in both *rao1-1* and *rao1-2* (Fig 3C and G). Therefore, the *rao1* mutant plants failed to induce *AOX1a* in response to three different inhibitors affecting mitochondrial function. *rao1* plants were also treated with 20 mM H_2O_2, an important ROS signalling molecule (39,40), to investigate RAO1 function in a wider stress signalling context. The induction of LUC observed in Col:*LUC* plants in response to H_2O_2 was abolished in the *rao1* mutant background (Fig 3D and G). Thus, RAO1 is also involved in mediating the response of *AOX1a* to more general cellular oxidative stress signals. To investigate the extent of RAO1 regulation in general abiotic stress responses we also subjected plants to 16 h cold treatment, which also failed to induce reporter gene expression in the mutant background compared to Col:*LUC* plants (Fig 3E and G). Finally, *rao1* mutants were also exposed to ultraviolet (UV) light, to primarily target chloroplast function and, possibly generate alternative cellular ROS species (41). *rao1-1* and *rao1-2* lines showed no impairment of the observed wild-type induction of LUC in response to UV treatment, indicating that cellular responses to UV stress are signalled via pathway(s) independent of RAO1 function (Fig 3F and G). Previously studies also have shown that there are distinct pathways for induction of *AOX1a*, where mutants were identified that do not induce LUC expression with AA treatment, yet induce LUC with MFA treatment (13). Together, these screens demonstrate that *rao1* mutants provide a powerful tool to investigate and dissect the stress signalling pathways operating in plants and are involved in both anterograde and retrograde signalling pathways.

RAO1 is responsible for gating the extent of AOX1a induction in response to retrograde signals. *AOX1a* transcript and protein abundances were measured over a 5 h time course during AA and UV treatment (Fig 4). At 3 h of exposure to AA, the ~ 28-fold significant induction ($p<0.001$, Student's t-test) of *AOX1a* transcript that was observed in Col:*LUC* plants was significantly reduced (~ 18-fold, $p<0.01$, Student's t-test) in both *rao1-1* and *rao1-2* lines (Fig 4). As expected, AOX protein abundance in Col:*LUC* plants increased substantially, but this was essentially absent in *rao1* mutants (Fig 4B). As *rao1-1* and *rao1-2* represented EMS mutants that resulted in a single amino acid change (Fig 2B and C), T-DNA insertions for this gene were analysed. Of four T-DNA mutants annotated as containing an insertion in *CDKE:1* (At5g63610), only one (GABI_564F11) was found to be truly located in this gene. Analysis of the transcript and protein abundance for AOX in this T-DNA line revealed a similar pattern to that observed in *rao1-1* and *rao1-2*, in that induction of transcript abundance by AA treatment is reduced by ~ 50 % and induction of protein abundance is reduced (Supplementary Fig 5 A and B).

The results presented in Fig 4A and B suggest that RAO1 can act at two levels to regulate the expression of *AOX1a*, at a transcript level, where transcript abundance was significantly reduced by between 30% and 50% (Fig 4A, Supplementary Fig 5A), depending on the mutant examined, and at a post-transcriptional level, as a greater reduction in AOX1a protein was observed (Fig 4B, Supplementary Fig 5B). In order to study this further we investigated conditions where induction of *LUC* was normal, and subsequently examined AOX1a transcript and protein levels in this situation. From the analysis of the LUC screening assay (Fig 3), treatment with UV led to induction of luminescence in both Col-*LUC* and *rao-1*

mutant lines. Thus transcript and protein abundance for AOX1a was examined under UV treatment (Fig 4C and D). Induction of *AOX1a* transcript was not significantly reduced in the *rao-1* mutant lines compared to Col-LUC (Fig 4C), however the induction of protein was reduced by ~40% (Fig 4D). This was consistently observed in both *rao-1* lines. QRT-PCR assays confirmed that the differences observed between the *AOX1a* transcript and protein responses to AA treatment are not due to a splicing defect or incomplete transcript processing in the *rao1* background (Supplementary Fig 6).

Genome-wide transcriptome responses in rao-1 mutant plants To investigate the extent to which RAO1 is necessary to regulate genome wide responses to mitochondrial dysfunction, Affymetrix microarray analyses were performed on Col:*LUC*, *rao1-1* and *rao1-2* plants under untreated conditions and under 3 h stress treatment with AA (GEO accession GSE36011). Gene transcripts were classified into one of four gene lists: (1) Not significantly changed under any condition comparison tested; (2) transcripts with altered expression in response to AA treatment, that are controlled independently of RAO1 function or activity; (3) gene targets positively regulated through RAO1 and (4) gene targets negatively regulated through RAO1 activity (Supplementary Fig 7, Supplementary Datasets 1-6).

To identify early target genes regulated synergistically with *AOX1a* through RAO1, gene expression profiles for Gene set 3 were further filtered for positive wild-type responses greater than 3-fold (Log_2 Fold-change, untreated vs AA treated), that were significantly impaired by greater than 30 % in both *rao1-1* and *rao1-2* under stress. This produced a list of 337 transcripts encoding proteins with diverse functions and cellular localisations (Fig 5A). In this list, there is a significant over-representation of transcripts involved in stress responses to biotic and abiotic stimuli (22.68 % vs 7.25 % genome wide) and a significant under-representation of transcripts involved in protein metabolism and synthesis (4.99 % vs 9.51 % genome wide) (Fig 5B). Within this list of core stress responsive transcripts regulated through RAO1 are numerous transcription factors, including AP2 domain factors (Supplementary Dataset 5). Within this core list of 337 transcripts are those associated with energy status (*Dark-induced 6 (DIN6)* (31), numerous protein kinases, MAPK kinases, a predicted mitochondrial PPR protein (AT2G20720) and transmembrane receptor proteins, including one predicted to be localised to the chloroplast (AT2G32140) (Supplementary Dataset 5). Nine mitochondrial components were identified, all of which have been previously defined as part of the mitochondrial stress response (42) (Fig 5C). This indicates that the primary mitochondrial response to diverse stress conditions is mediated via RAO1 activity. Binding sites for a number of transcription factor families with proposed roles mediating plant abiotic stress responses and controlling mitochondrial energy metabolism were over-represented in this 337 gene set. These included AP2/EREBP (ABI4 binding sequences (17)), MYB and bZIP (31), MADS, Homeodomain (HD factors), and C2C2 DOF, TCP factors (28) (Fig 5D). Indeed, a predicted binding site for several of these classes of transcription factors were found in the upstream regions of all 337 transcripts in this stress responsive sub-network (Fig 5D, asterisks).

RAO1 interacts with the energy sensing SnRK1 kinase KIN10 As the core stress response mediated through RAO1 activity appears to include diverse functions in stress responses and energy state perception, the predicted protein-protein interactome for CDKE;1 was defined (Supplementary Fig 8A). A protein kinase, KIN10, which has been shown previously to integrate stress, darkness and energy signalling with growth was identified as having putative interactions with CDKE;1 (Interlog confidence value 21, (31) (Supplementary Fig 8A). Expression profiles for the *KIN10* gene targets show dramatic

overlap with the expression profiles observed for *rao1* mutant plants under AA treatment (Supplementary Fig 8B).

We sought to confirm the interaction between RAO1 and KIN10 using biomolecular fluorescence complementation assays (BiFC) (Fig 6). RAO1 and KIN10 show a clear interaction within the nucleus, evidenced by yellow fluorescent protein (YFP) signal distinct from auto fluorescence (Fig 6A). Interactions between RAO1 and KIN11 were also tested as a control but no YFP signal that was independent of auto fluorescence could be detected (Fig 6B). Analysis of the KIN10 coding sequence revealed a nuclear localisation sequence and GFP localisation shows clear nuclear targeting, as well as cytosolic targeting (Supplementary Fig 4). Here, we confirm that KIN10 can be transported to the nucleus where it interacts with the exclusively nuclear localised RAO1 (Fig 6, Supplementary Fig 4). To further explore the functional significance of RAO1:KIN10 interaction, it was reasoned that the 337 genes that were identified as regulated by RAO1 (Fig 5Aii), should change in a similar manner in *kin10* mutants under AA treatment. While none of the T-DNA insertions annotated represent a knock-out, two RNAi lines, previously used to characterise KIN10 (31), were obtained and it was confirmed that transcript abundance for *KIN10* was reduced to between 40% (*kin10#1*) and 20% (*kin10#7*) of wild-type levels, in a Landsberg (Ler) background (Supplementary Fig 5C). Of the 337 genes identified in the direct regulatory context of *AOX1a* by RAO1 (Fig 5Aii), 279 were expressed in the Ler ecotype. Of these, 244 genes were induced in response to AA treatment in Ler plants, and 217 of these were also induced in response to AA in one or both *kin10* RNAi lines (Fig 6C). Notably, as was seen for the *rao* lines (Figure 5Aii), the magnitude of expression induction seen in the *kin10* RNAi plants was smaller than the inductions seen in Ler plants (for 191 out of the 217 genes) (Fig 6C compare to Fig 5Aii; Supplementary Dataset 5).

DISCUSSION

While the induction of AOX in a variety of plant species has been used as a model system to study mitochondrial to nuclear communication for almost two decades (14), the molecular components that mediate this signalling are largely unknown. As so called end-points of retrograde signalling, ABI4 and WRKY transcription factors have been previously shown to co-ordinate both mitochondrial and plastid retrograde signalling within the nucleus (17,18,43), but it is unclear how diverse hormone, energy, stress and developmental signals concurrently influence transcription factor activity and transcription rates. The identification of CDKE;1/RAO1 in this study provides a far greater understanding of how the induction of AOX is integrated into the general regulatory context of the cell. As the name indicates, cell cycle-dependent kinases are associated with cell division, and CDKE;1/RAO1 is proposed to play a role in integrating environmental signals with plant development, but CDKE;1/RAO1 does not directly interact with any other cyclin components (44). CDKE;1/RAO1 is a component of the kinase module of the plant mediator complex that relays regulatory signals between specific transcription factors bound to the promoter and RNA polymerase II (45). Importantly, *rao1* mutant plants do not show the transcriptional reprogramming of stress responsive components (such as ABI4) under normal conditions that is observed with complete *aox1a* knock–out plants (26). Indeed, only 119 transcripts genome wide are significantly altered under normal conditions in both *rao1-1* and *rao1-2* by greater than 2.5 fold compared to Col:*LUC*. Thus, the genome wide transcriptional response shown here represents the integrated network controlled through direct phosphorylation events associated with the mediator complex of RNA polymerase and not any secondary

affect of mis-regulated central stress responsive transcription factors.

This particular kinase appears to have a dual role(s) central to the mediator complex of RNA polymerase II. Firstly, CDKE;1/RAO1 has a demonstrated role as a CDK, integrating cellular responses to environmental signals with cell division or elongation. Mutation in CDKE;1/RAO1 has been identified previously in genetic screens for flowering abnormalities (*hen3* - HUA enhancer mutants) with a mild early flowering phenotype when mutated alone, and abnormalities in cell fate determination in a *hua1-1/hua2-1* background (Supplementary Fig 9) (46). Secondly, from the results presented here CDKE;1/RAO1 has a central role as a sensitive relay between specific stress induced transcription factors actively bound to the promoter and RNA polymerase II, thereby directly affecting transcription under stress. Together, this suggests that CDKE;1/RAO1 provides a mechanism by which plant cells can switch between growth and stress responses to changing environmental conditions. This is further supported by the results of the global transcriptional analyses, as transcripts relating to both growth and stress are affected in the *rao1* mutant background, albeit in opposite ways (Fig 4B, Supplementary Fig 9). Cell wide stress responses are initiated by CDKE;1, while protein metabolism and protein synthesis (essentially the building blocks for cell division and growth) and photosynthetic components are switched off (Fig 4B).

It is apparent from the results obtained that CDKE;1/RAO1 acts both at a transcriptional and post-transcriptional level to regulate *AOX1a* expression. The phenomena of additional means of post-transcriptional control of AOX in response to stress has been observed or suggested independently in a number of different stress conditions in previous studies (19,47,48), however without any likely explanation of the molecular mechanisms involved. In particular induction of AOX1a transcript and protein takes place under phosphate starvation in plants, along with the synthesis of galactoglycerolipid, that occurs via three different pathways (47). A suppressor of one of these pathways identified a mitochondrial outer membrane protein that has an identical affect on the induction of AOX1a as *rao-1*, namely *digalactosyldiacylglycerol1* (*dgd1*) SUPPRESSOR1 (DGS1) (47). Under AA stimulation in this mutant while induction of transcript abundance for *AOX1a* appeared normal as determined by Northern blotting, induction of AOX1a protein was essentially abolished. Furthermore this mutant had the same root growth delayed phenotype as was observed with *rao-1* mutants (Supplementary Fig 9B). Thus there appears to be a specific regulatory pathway that regulates the accumulation of *AOX1a* protein. It is interesting to note that the yeast orthologues of DGS1 on the mitochondrial outer membrane, called with the nuclear control of ATPase 2 (NCA2) are involved in regulating mitochondrial gene expression in yeast (49,50). While it is not possible to determine if the accumulation of AOX1a protein is due to a translational or post-translation affect it is notable that there are a number of post-transcriptional control mechanisms that govern mRNA fate both prior to nuclear export and within the cytoplasm, which we know very little about in plants. A number of these processes are regulated by phosphorylation events. For example, in mammals, the 5' capping events and cap binding proteins that occur co-transcriptionally on the nascent pre-mRNA as it emerges from RNA polymerase II, are regulated in part through the activity of mTOR kinases, with central roles in cell proliferation, growth and energy sensing (51). The 5' cap is postulated to have roles in mRNA protection, promoting downstream processing and, via TOR signaling, interacting with cap-binding proteins and other RNA binding complexes to preferentially stimulate synthesis of proteins from new transcripts (allowing quick responses under stress conditions with limited translational machinery) (51,52). This function of TOR in Arabidopsis

appears to be conserved and may be a downstream acceptor for KIN10 signaling in plants (53), perhaps also mediated through CDKE;1 in the nucleus in a post-transcriptional manner.

Previously it has been shown that the SnRK1 protein kinase KIN10 in Arabidopsis acts as a central regulator or integrator of signals for growth, energy metabolism and stress (31). Here we have shown that KIN10 can be targeted to the nucleus that is consistent with previous reports of nuclear targeting of KIN10 (54), with this report noting that KIN10 nuclear localization depending on tissue and developmental stage, which suggests that its location in the nucleus may be regulated. The interaction with CDKE;1/RAO1 in the nucleus, provide evidence that CDKE;1/RAO1 is the acceptor site for KIN10 signals. Consistent with the interaction demonstrated in this study between KIN10 and CDKE;1/RAO1, it has been shown that yeast Snf1 interacts physically with proteins of the yeast mediator complex (55). Furthermore, analysis of changes in transcript abundance in *kin10* RNAi lines shows a large overlap with the genes identified as regulated by RAO1.

Consistent with this proposal of a switch between growth and stress response, genetic manipulation of AOX results in altered growth of plants. Tobacco suspension cells unable to induce AOX continue to grow under severe nutrient limiting conditions in contrast to cells that can induce AOX and essentially stop growing (56). Furthermore in tobacco cells and *Chlamydomonas reinhardtii,* a lack of AOX results in a larger cells (57,58). Thus the KIN10 and CDKE;1/RAO1 interplay represents an efficient protein kinase signal cascade that essentially provides a mechanism by which plants can detect and integrate signals from multiple input sources, and switch between growth and stress responses. The results presented here suggest that anterograde and retrograde pathway interact at an early stage in the signaling process, i.e. KIN10, and that both transcriptional and post-transcriptional pathway operate, but the extent of each may differ under different treatments, as observed with the differences between UV and the other treatments used in this study. Combined these responses reveal how fine-tuned the signalling system is an how responses to different treatments can differ, even if some of the components used in the response to different treatments are the same.

REFERENCES

1. Pfannschmidt, T. (2010) Plastidial retrograde signalling--a true "plastid factor" or just metabolite signatures? *Trends Plant Sci* **15**, 427-435
2. Woodson, J. D., and Chory, J. (2008) Coordination of gene expression between organellar and nuclear genomes. *NatureRrev Genetics* **9**, 383-395
3. Bradbeer, J. W., Atkinson, Y. E., Borner, T., and Hagemann, R. (1979) Cytoplasmic synthesis of plastid polypeptides may be controlled by plastid-synthesised RNA. *Nature* **279**, 816-817
4. Liao, X. S., Small, W. C., Srere, P. A., and Butow, R. A. (1991) Intramitochondrial functions regulate nonmitochondrial citrate synthase (CIT2) expression in Saccharomyces cerevisiae. *Mol Cellular Biol* **11**, 38-46
5. Woodson, J. D., Perez-Ruiz, J. M., and Chory, J. (2011) Heme synthesis by plastid ferrochelatase I regulates nuclear gene expression in plants. *Curr Biol* **21**, 897-903
6. Kindgren, P., Noren, L., Barajas Lopez, J. D., Shaikhali, J., and Strand, A. (2011) Interplay between HEAT SHOCK PROTEIN 90 and HY5 Controls PhANG Expression in Response to the GUN5 Plastid Signal. *Mol Plant* **5,** 901-913
7. Sun, X., Feng, P., Xu, X., Guo, H., Ma, J., Chi, W., Lin, R., Lu, C., and Zhang, L. (2011) A chloroplast envelope-bound PHD transcription factor mediates chloroplast signals to the nucleus. *Nat Commun* **2**, 477 doi: 10.1038/ncomms1486
8. Estavillo, G. M., Crisp, P. A., Pornsiriwong, W., Wirtz, M., Collinge, D., Carrie, C., Giraud, E., Whelan, J., David, P., Javot, H., Brearley, C., Hell, R., Marin, E., and Pogson, B. J. (2011) Evidence for a SAL1-PAP chloroplast retrograde pathway that functions in drought and high light signaling in Arabidopsis. *Plant Cell* **23**, 3992-4012
9. Ramel, F., Birtic, S., Ginies, C., Soubigou-Taconnat, L., Triantaphylides, C., and Havaux, M. (2012) Carotenoid oxidation products are stress signals that mediate gene responses to singlet oxygen in plants. *Proc Natl Acad Sci U S A* **109**, 5535-5540
10. Liu, Z., and Butow, R. A. (2006) Mitochondrial retrograde signaling. *Annu Rev Genet* **40**, 159-185
11. Bork, P., Sander, C., and Valencia, A. (1992) An ATPase domain common to prokaryotic cell cycle proteins, sugar kinases, actin, and hsp70 heat shock proteins. *Proc Natl Acad Sci U S A* **89**, 7290-7294
12. Giannattasio, S., Liu, Z., Thornton, J., and Butow, R. A. (2005) Retrograde response to mitochondrial dysfunction is separable from TOR1/2 regulation of retrograde gene expression. *J Biol Chem* **280**, 42528-42535
13. Jazwinski, S. M., and Kriete, A. (2012) The yeast retrograde response as a model of intracellular signaling of mitochondrial dysfunction. *Front Physiol* **3**, 139
14. Millar, A. H., Whelan, J., Soole, K. L., and Day, D. A. (2011) Organization and regulation of mitochondrial respiration in plants. *Annu Rev Plant Biol* **62**, 79-104
15. Zarkovic, J., Anderson, S. L., and Rhoads, D. M. (2005) A reporter gene system used to study developmental expression of alternative oxidase and isolate mitochondrial retrograde regulation mutants in Arabidopsis. *Plant Mol Biol* **57**, 871-888
16. Kleine, T., Voigt, C., and Leister, D. (2009) Plastid signalling to the nucleus: messengers still lost in the mists? *Trends Genet* **25**, 185-192
17. Giraud, E., Van Aken, O., Ho, L. H., and Whelan, J. (2009) The transcription factor ABI4 is a regulator of mitochondrial retrograde expression of ALTERNATIVE OXIDASE1a. *Plant Physiol* **150**, 1286-1296
18. Koussevitzky, S., Nott, A., Mockler, T. C., Hong, F., Sachetto-Martins, G., Surpin, M., Lim, J., Mittler, R., and Chory, J. (2007) Signals from chloroplasts converge to regulate nuclear gene expression. *Science* **316**, 715-719

19. Ho, L. H., Giraud, E., Uggalla, V., Lister, R., Clifton, R., Glen, A., Thirkettle-Watts, D., Van Aken, O., and Whelan, J. (2008) Identification of regulatory pathways controlling gene expression of stress-responsive mitochondrial proteins in Arabidopsis. *Plant Physiol* **147**, 1858-1873
20. Clifton, R., Lister, R., Parker, K. L., Sappl, P. G., Elhafez, D., Millar, A. H., Day, D. A., and Whelan, J. (2005) Stress-induced co-expression of alternative respiratory chain components in Arabidopsis thaliana. *Plant Mol Biol* **58**, 193-212
21. Bell, C. J., and Ecker, J. R. (1994) Assignment of 30 microsatellite loci to the linkage map of Arabidopsis. *Genomics* **19**, 137-144
22. Clough, S. J., and Bent, A. F. (1998) Floral dip: a simplified method for Agrobacterium-mediated transformation of Arabidopsis thaliana. *Plant J* **16**, 735-743
23. Harrison, S. J., Mott, E. K., Parsley, K., Aspinall, S., Gray, J. C., and Cottage, A. (2006) A rapid and robust method of identifying transformed Arabidopsis thaliana seedlings following floral dip transformation. *Plant Methods* **2**, 19
24. Katoh, K., Misawa, K., Kuma, K., and Miyata, T. (2002) MAFFT: a novel method for rapid multiple sequence alignment based on fast Fourier transform. *Nucleic Acids Res* **30**, 3059-3066
25. Zmasek, C. M., and Eddy, S. R. (2001) ATV: display and manipulation of annotated phylogenetic trees. *Bioinformatics* **17**, 383-384
26. Giraud, E., Ho, L. H., Clifton, R., Carroll, A., Estavillo, G., Tan, Y. F., Howell, K. A., Ivanova, A., Pogson, B. J., Millar, A. H., and Whelan, J. (2008) The absence of ALTERNATIVE OXIDASE1a in Arabidopsis results in acute sensitivity to combined light and drought stress. *Plant Physiol* **147**, 595-610
27. Baldi, P., and Long, A. D. (2001) A Bayesian framework for the analysis of microarray expression data: regularized t -test and statistical inferences of gene changes. *Bioinformatics* **17**, 509-519
28. Giraud, E., Ng, S., Carrie, C., Duncan, O., Low, J., Lee, C. P., Van Aken, O., Millar, A. H., Murcha, M., and Whelan, J. (2010) TCP transcription factors link the regulation of genes encoding mitochondrial proteins with the circadian clock in Arabidopsis thaliana. *Plant Cell* **22**, 3921-3934
29. Geisler-Lee, J., O'Toole, N., Ammar, R., Provart, N. J., Millar, A. H., and Geisler, M. (2007) A predicted interactome for Arabidopsis. *Plant Physiol* **145**, 317-329
30. Lin, M., Shen, X., and Chen, X. (2011) PAIR: the predicted Arabidopsis interactome resource. *Nucleic Acids Res* **39**, D1134-1140
31. Baena-Gonzalez, E., Rolland, F., Thevelein, J. M., and Sheen, J. (2007) A central integrator of transcription networks in plant stress and energy signalling. *Nature* **448**, 938-942
32. Lister, R., Carrie, C., Duncan, O., Ho, L. H., Howell, K. A., Murcha, M. W., and Whelan, J. (2007) Functional definition of outer membrane proteins involved in preprotein import into mitochondria. *Plant Cell* **19**, 3739-3759
33. Elthon, T. E., Nickels, R. L., and McIntosh, L. (1989) Monoclonal Antibodies to the Alternative Oxidase of Higher Plant Mitochondria. *Plant Physiol* **89**, 1311-1217
34. Carrie, C., Kuhn, K., Murcha, M. W., Duncan, O., Small, I. D., O'Toole, N., and Whelan, J. (2009) Approaches to defining dual-targeted proteins in Arabidopsis. *Plant J* **57**, 1128-1139
35. Citovsky, V., Gafni, Y., and Tzfira, T. (2008) Localizing protein-protein interactions by bimolecular fluorescence complementation in planta. *Methods* **45**, 196-206
36. Boyes, D. C., Zayed, A. M., Ascenzi, R., McCaskill, A. J., Hoffman, N. E., Davis, K. R., and Gorlach, J. (2001) Growth stage-based phenotypic analysis of Arabidopsis: a model for high throughput functional genomics in plants. *Plant Cell* **13**, 1499-1510

37. Zhang, R., and Sharkey, T. D. (2009) Photosynthetic electron transport and proton flux under moderate heat stress. *Photosynthesis Reserach* **100**, 29-43
38. Busso, C., Tahara, E. B., Ogusucu, R., Augusto, O., Ferreira-Junior, J. R., Tzagoloff, A., Kowaltowski, A. J., and Barros, M. H. (2010) Saccharomyces cerevisiae coq10 null mutants are responsive to antimycin A. *FEBS J* **277**, 4530-4538
39. Mittler, R., Vanderauwera, S., Suzuki, N., Miller, G., Tognetti, V. B., Vandepoele, K., Gollery, M., Shulaev, V., and Van Breusegem, F. (2011) ROS signaling: the new wave? *Trends Plant Sci* **16**, 300-309
40. Suzuki, N., Koussevitzky, S., Mittler, R., and Miller, G. (2012) ROS and redox signalling in the response of plants to abiotic stress. *Plant, Cell & Environ* **35**, 259-270
41. Jenkins, G. I. (2009) Signal transduction in responses to UV-B radiation. *Ann Rev Plant Biol* **60**, 407-431
42. Van Aken, O., Zhang, B., Carrie, C., Uggalla, V., Paynter, E., Giraud, E., and Whelan, J. (2009) Defining the mitochondrial stress response in Arabidopsis thaliana. *Mol Plant* **2**, 1310-1324
43. Shang, Y., Yan, L., Liu, Z. Q., Cao, Z., Mei, C., Xin, Q., Wu, F. Q., Wang, X. F., Du, S. Y., Jiang, T., Zhang, X. F., Zhao, R., Sun, H. L., Liu, R., Yu, Y. T., and Zhang, D. P. (2010) The Mg-chelatase H subunit of Arabidopsis antagonizes a group of WRKY transcription repressors to relieve ABA-responsive genes of inhibition. *Plant Cell* **22**, 1909-1935
44. Boruc, J., Van den Daele, H., Hollunder, J., Rombauts, S., Mylle, E., Hilson, P., Inze, D., De Veylder, L., and Russinova, E. (2010) Functional modules in the Arabidopsis core cell cycle binary protein-protein interaction network. *Plant Cell* **22**, 1264-1280
45. Mathur, S., Vyas, S., Kapoor, S., and Tyagi, A. K. (2011) The mediator complex in plants: structure, phylogeny and expression profiling of representative genes in a dicot (Arabidopsis thaliana) and a monocot (Oryza sativa) during reproduction and abiotic stress. *Plant Physiol* **157,** 1609-1627
46. Wang, W., and Chen, X. (2004) HUA ENHANCER3 reveals a role for a cyclin-dependent protein kinase in the specification of floral organ identity in Arabidopsis. *Development* **131**, 3147-3156
47. Moellering, E. R., and Benning, C. (2010) Phosphate regulation of lipid biosynthesis in Arabidopsis is independent of the mitochondrial outer membrane DGS1 complex. *Plant Physiol* **152**, 1951-1959
48. Rhoads, D. M., and McIntosh, L. (1992) Salicylic Acid Regulation of Respiration in Higher Plants: Alternative Oxidase Expression. *Plant Cell* **4**, 1131-1139
49. Camougrand, N., Pelissier, P., Velours, G., and Guerin, M. (1995) NCA2, a second nuclear gene required for the control of mitochondrial synthesis of subunits 6 and 8 of ATP synthase in Saccharomyces cerevisiae. *J Mol Biol* **247**, 588-596
50. Pelissier, P., Camougrand, N., Velours, G., and Guerin, M. (1995) NCA3, a nuclear gene involved in the mitochondrial expression of subunits 6 and 8 of the Fo-F1 ATP synthase of S. cerevisiae. *Curr Genet* **27**, 409-416
51. Topisirovic, I., Svitkin, Y. V., Sonenberg, N., and Shatkin, A. J. (2011) Cap and cap-binding proteins in the control of gene expression. *RNA* **2**, 277-298
52. Le Hir, H., and Seraphin, B. (2008) EJCs at the heart of translational control. *Cell* **133**, 213-216
53. Baena-Gonzalez, E., and Sheen, J. (2008) Convergent energy and stress signaling. *Trends Plant Sci* **13**, 474-482

54. Bitrian, M., Roodbarkelari, F., Horvath, M., and Koncz, C. (2011) BAC-recombineering for studying plant gene regulation: developmental control and cellular localization of SnRK1 kinase subunits. *Plant J* **65**, 829-842
55. Kuchin, S., Treich, I., and Carlson, M. (2000) A regulatory shortcut between the Snf1 protein kinase and RNA polymerase II holoenzyme. *Proc Natl Acad Sci U S A* **97**, 7916-7920
56. Sieger, S. M., Kristensen, B. K., Robson, C. A., Amirsadeghi, S., Eng, E. W., Abdel-Mesih, A., Moller, I. M., and Vanlerberghe, G. C. (2005) The role of alternative oxidase in modulating carbon use efficiency and growth during macronutrient stress in tobacco cells. *J Exp Bot* **56**, 1499-1515
57. Gerin, S., Mathy, G., Blomme, A., Franck, F., and Sluse, F. E. (2010) Plasticity of the mitoproteome to nitrogen sources (nitrate and ammonium) in Chlamydomonas reinhardtii: the logic of Aox1 gene localization. *Biochim Biophys Acta* **1797**, 994-1003
58. Parsons, H. L., Yip, J. Y., and Vanlerberghe, G. C. (1999) Increased respiratory restriction during phosphate-limited growth in transgenic tobacco cells lacking alternative oxidase. *Plant Physiol* **121**, 1309-1320

Figure Legends

Figure 1 Identification of two allelic mutants *rao1-1* and *rao1-2* as upstream retrograde regulators of AOX1a. (A) A schematic diagram of the T-DNA insert containing *ALTERNATIVE OXIDASE1a* promoter driving a luciferase reporter gene (*AOX1a*:*LUC*). The *AOX1a* promoter consists of the region 2000 bp upstream of the translational start site of *AOX1a,* including the 99 bp *AOX1a* 5' UTR. LB, T-DNA left border sequences; *HPTII*, *Hygromycin phosphotransferase II*; *35S CaMV*, *35S Cauliflower mosaic virus promoter*; RB, T-DNA right border sequences. (B) Col*:LUC* plants sprayed with deionised water (-AA) or with 50 μM antimycin A (AA) to elicit a mitochondrial retrograde signal. Luciferin was applied and LUC reporter activity was visualised in a NightOwl bioluminescence imager after 6 h treatment. (C) *rao1-1* and *rao1-2* do not express *AOX1a:LUC* under AA treatment. (D) Allelism of *rao1-1* and *rao1-2*. F1, the first filial generation from *rao1-1* and *rao1-2* crosses.

Figure 2 *rao1-1* and *rao1-2* encode a C*yclin-Dependent Kinase E;1* (*CDKE;1*, AT5G63610). (A) Next generation sequencing analysis identified 2 candidate mutations in CDKE;1 including a summary of alignment and .bam alignments for region of interest visualised in Tablet (http://bioinf.scri.ac.uk/tablet/)) (B) Sanger sequence chromatographs confirming nucleotide changes within the *RAO1* coding sequence. (C) A schematic model of AT5G63610 gene structure with the relative position of amino changes shown in red for *rao1-1* and *rao1-2*. Alignments of CDKE;1 proteins from a range of plant species are shown. Asterisks indicate mutated amino acid in *rao1-1* (left panel) and *rao1-2* (right panel). At, *Arabidopsis thaliana* (Arabidopsis); Gm, *Glycine max* (soybean); Pp, *Physcomitrella patens* (moss); Pt, *Populus trichocarpa* (poplar); Os, *Oryza sativa* (rice); Vv, *Vitis Vinifera* (grape); Zm, *Zea mays* (maize); Cr, *Chlamydomonas reinhardtii* (green algae). (D) Complementation of *rao1-1* and *rao1-2* with wild-type *RAO1* results in restored wild-type induction of *AOX1a:LUC* under antimycin A (AA) treatment.

Figure 3 Characterisation and quantification of *AOX1a* promoter inductions in *rao1-1* and *rao1-2* following different stress treatments. *Col:LUC*, *rao1-1* and *rao1-2* seedlings were treated with (A) 50 μM antimycin A (AA), (B) 50 μM myxothiazol, (C) 25 mM Monofluoracetate (MFA), (D) 20 mM H_2O_2, (E) 16 h cold treatment (4°C) (F) 30 min ultraviolet (UV) light. *Luciferase (LUC*) reporter gene activity was visualised in a NightOwl bioluminescence imager after 6 h treatment unless otherwise stated. Scale bars indicate 1cm. (G) Processed images were analysed for quantification of *LUC* expression using the Integrated Light Intensity from 8-bit images calculated in the Java software ImageJ. Error bars denote standard errors (n>8 measurements).

Figure 4. Characterisation of AOX1a transcript and protein inductions in *rao1-1* and *rao1-2*. (A) *AOX1a* transcript abundance in Col:LUC, *rao1-1* and *rao1-2* lines after 30 min, 1 h and 3 h AA treatment. Seventeen-day-old plants were sprayed with deionised water (-AA) or 50 μM AA. Relative transcript abundance fold-changes between mock treated and AA treated plants for the respective genotypes are shown. (B) Immunodetection of AOX1a in isolated mitochondria after 5 h AA treatment. Plants were sprayed with deionised water (-AA) or 50 μM AA. Relative protein abundance (quantification values indicated below each blot) was determined by quantitative densitometry. TOM40-1 protein abundance is also shown as a loading control. (C) *AOX1a* transcript abundance in Col:LUC, rao1-1 and rao1-2 lines at 30 min, 1 h, and 3 h recovery after 30 min treatment with UV. Relative transcript abundance fold-changes between untreated and UV treated plants are shown. (D) Immunodetection of

AOX1a in isolated mitochondria from plants treated with UV for 30 min followed by 5 h recovery. TOM40-1 protein abundance is also shown as a loading control.

Figure 5 Global identification of target genes regulated through *RAO1* activity in response to mitochondrial retrograde stress signals. Affymetrix microarray analysis of global gene expression responses to antimycin A (AA) treatment in Col*:LUC, rao1-1* and *rao1-2* plants was conducted as shown in Fig S8 - See SI Appendix. A Gene set was identified that contains transcripts that are positively regulated through RAO1 function in response to mitochondrial retrograde signals (Gene set 3). (A) Hierarchical cluster of fold change responses to AA treatment for those transcripts in Gene set 3. This set was further filtered for positive responses > 3 fold to give 337 genes. Scale bar shows the Log_2 magnitude of Fold-changes. (B) Functional categorisation (GO Biological process, http://www.arabidopsis.org/tools/bulk/go/) for the 337 genes defined as the direct regulatory context for *AOX1a*. Annotations in red are significantly over-represented and those in blue are significantly under-represented (p<0.0001, Chi-squared test). (C) List of the genes from the 337 genes that are localised in the mitochondria. (D) Occurrence of known transcription factor binding site sequences over-represented within the 1000 bp upstream regions for these genes. Binding sites are coloured according to transcription factor family groups, specific family members with characterised binding sites are shown in the x-axis. Asterisks represent binding sites that are present in all 337 upstream regions.

Figure 6 Bimolecular fluorescence complementation of CDKE;1 with KIN10 and KIN11. (A) CDKE;1, KIN10 and KIN11 were incorporated into a split-YFP system, with C and N terminal fusions to either the 1-174 amino acids (AA) or 175-end AA of YFP. These constructs were biolistically transformed into onion epidermal cells in a variety of construct combinations, to identify protein-protein interactions (see Methods). To control for auto-fluorescence, the RFP channel was observed in addition to the YFP channel. (A) For KIN10 and CDKE;1, an interaction was observed, with a clear YFP signal in the nucleus and a diffused signal in the cytoplasm. (B) For KIN11 and CDKE;1, no independent YFP signal (differentiated from auto-fluorescence) could be observed. (C) Affymetrix microarray analysis of the 337 genes defines as positively regulated by RAO1 were analysed in response to antimycin A (AA) treatment in Ler, *kin10 #1* and *Kin10 #2* plants. The genes are ordered in the same order as in Figure 4Aii, showing that the induction in transcript abundance of genes is reduced in the kin10 RNAi lines compared to wild-type (Ler) (Fold-changes are shown in Supplementary Dataset 5). Scale bar shows the Log_2 magnitude of Fold-changes.

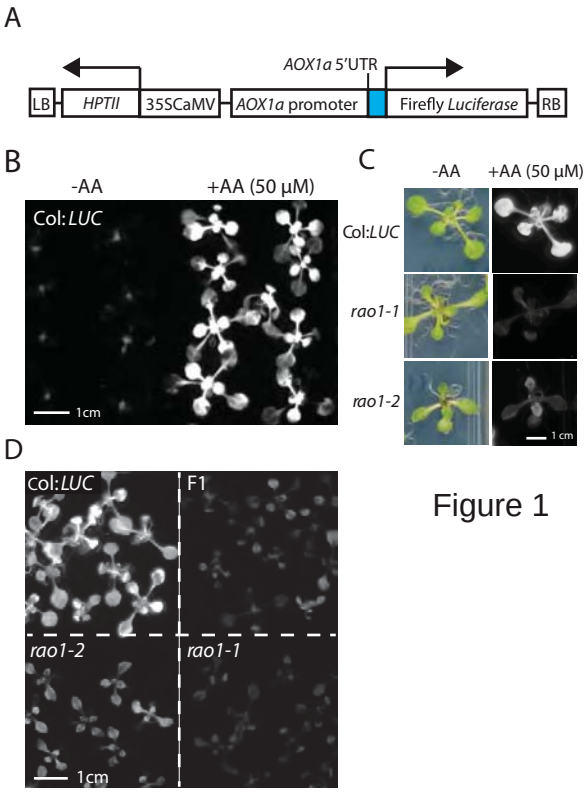
A
AOX1a 5'UTR
LB
HPTII
35SCaMV
AOX1a promoter
Firefly Luciferase
RB
B
-AA
+AA (50 µM)
Col:LUC
1cm
C
-AA
+AA (50 µM)
Col:LUC
rao1-1
rao1-2
1 cm
D
Col:LUC
F1
rao1-2
rao1-1
1cm

Figure 1

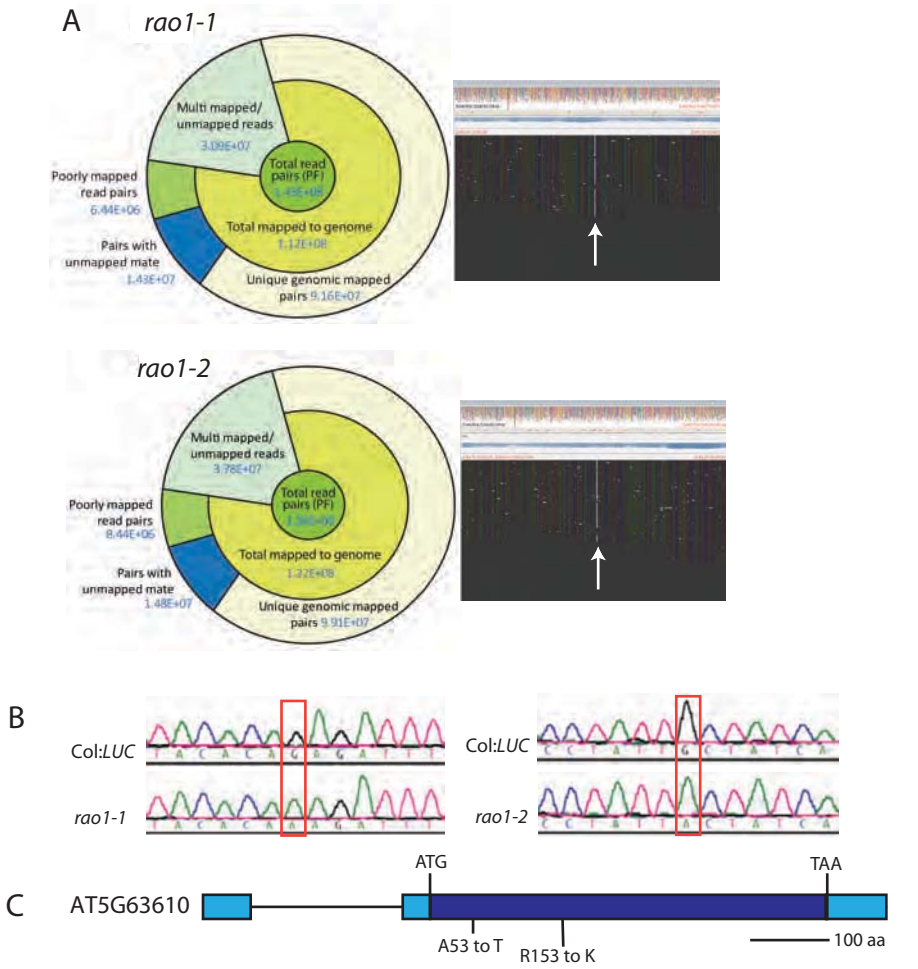
A
rao1-1
Multi mapped/
unmapped reads
3.09E+07
Total read
pairs (PF)
Poorly mapped
read pairs
6.44E+06
Total mapped to genome
Pairs with
unmapped mate
1.43E+07
Unique genomic mapped
pairs 9.16E+07
rao1-2
Multi mapped/
unmapped reads
3.78E+07
Total read
pairs (PF)
Poorly mapped
read pairs
8.44E+06
Total mapped to genome
Pairs with
unmapped mate
1.48E+07
Unique genomic mapped
pairs 9.91E+07

B
Col:LUC
rao1-1
Col:LUC
rao1-2

C
AT5G63610
ATG
TAA
A53 to T
R153 to K
100 aa

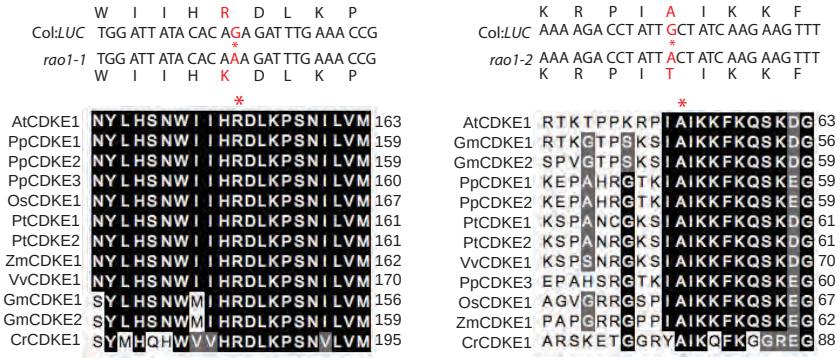
W I I H R D L K P
Col:LUC TGG ATT ATA CAC AGA GAT TTG AAA CCG
rao1-1 TGG ATT ATA CAC AAA GAT TTG AAA CCG
W I I H K D L K P
AtCDKE1 NYLHSNWIIHRDLKPSNILVM 163
PpCDKE1 NYLHSNWIIHRDLKPSNILVM 159
PpCDKE2 NYLHSNWIIHRDLKPSNILVM 159
PpCDKE3 NYLHSNWIIHRDLKPSNILVM 160
OsCDKE1 NYLHSNWIIHRDLKPSNILVM 167
PtCDKE1 NYLHSNWIIHRDLKPSNILVM 161
PtCDKE2 NYLHSNWIIHRDLKPSNILVM 161
ZmCDKE1 NYLHSNWIIHRDLKPSNILVM 162
VvCDKE1 NYLHSNWIIHRDLKPSNILVM 170
GmCDKE1 SYLHSNWMIHRDLKPSNILVM 156
GmCDKE2 SYLHSNWMIHRDLKPSNILVM 159
CrCDKE1 SYMHQHWVVHRDLKPSNVLVM 195
K R P I A I K K F
Col:LUC AAA AGA CCT ATT GCT ATC AAG AAG TTT
rao1-2 AAA AGA CCT ATT ACT ATC AAG AAG TTT
K R P I T I K K F
AtCDKE1 RTKTPPKRPIAIKKFKQSKDG 63
GmCDKE1 RTKGTPSKSIAIKKFKQSKDG 56
GmCDKE2 SPVGTPSKSIAIKKFKQSKDG 59
PpCDKE1 KEPAHRGTKIAIKKFKQSKEG 59
PpCDKE2 KEPAHRGTKIAIKKFKQSKEG 59
PtCDKE1 KSPANCGKSIAIKKFKQSKDG 61
PtCDKE2 KSPANRGKSIAIKKFKQSKDG 61
VvCDKE1 KSPSNRGKSIAIKKFKQSKDG 70
PpCDKE3 EPAHSRGTKIAIKKFKQSKEG 60
OsCDKE1 AGVGRRGSPIAIKKFKQSKEG 67
ZmCDKE1 PAPGRRGPPIAIKKFKQSKEG 62
CrCDKE1 ARSKETGGRYAIKQFKGGREG 88

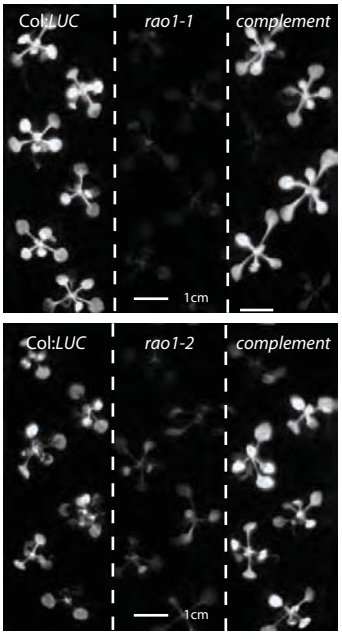
D
Col:LUC
rao1-1
complement
1cm
Col:LUC
rao1-2
complement
1cm

Figure 2

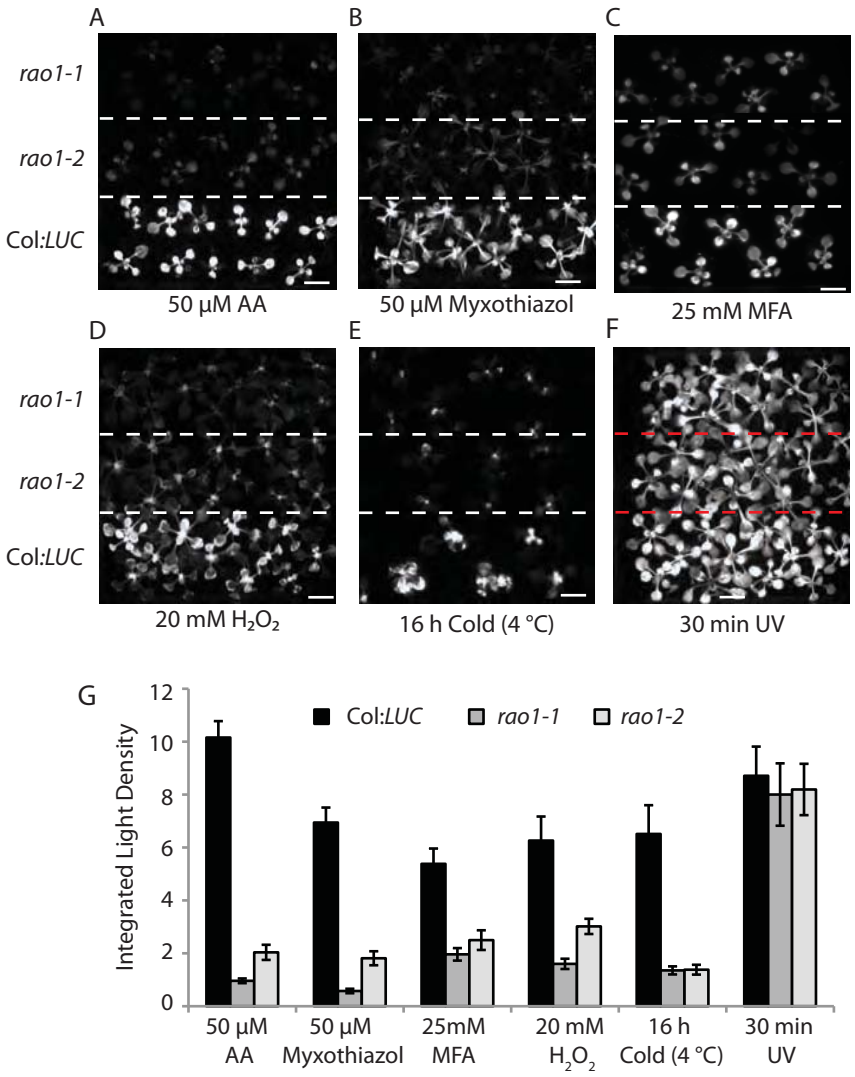
A
B
C
rao1-1
rao1-2
Col:LUC
50 µM AA
50 µM Myxothiazol
25 mM MFA
D
E
F
rao1-1
rao1-2
Col:LUC
20 mM H2O2
16 h Cold (4 °C)
30 min UV
G
Integrated Light Density
12
10
8
6
4
2
0
Col:LUC
rao1-1
rao1-2
50 µM AA
50 µM Myxothiazol
25mM MFA
20 mM H2O2
16 h Cold (4 °C)
30 min UV

Figure 3

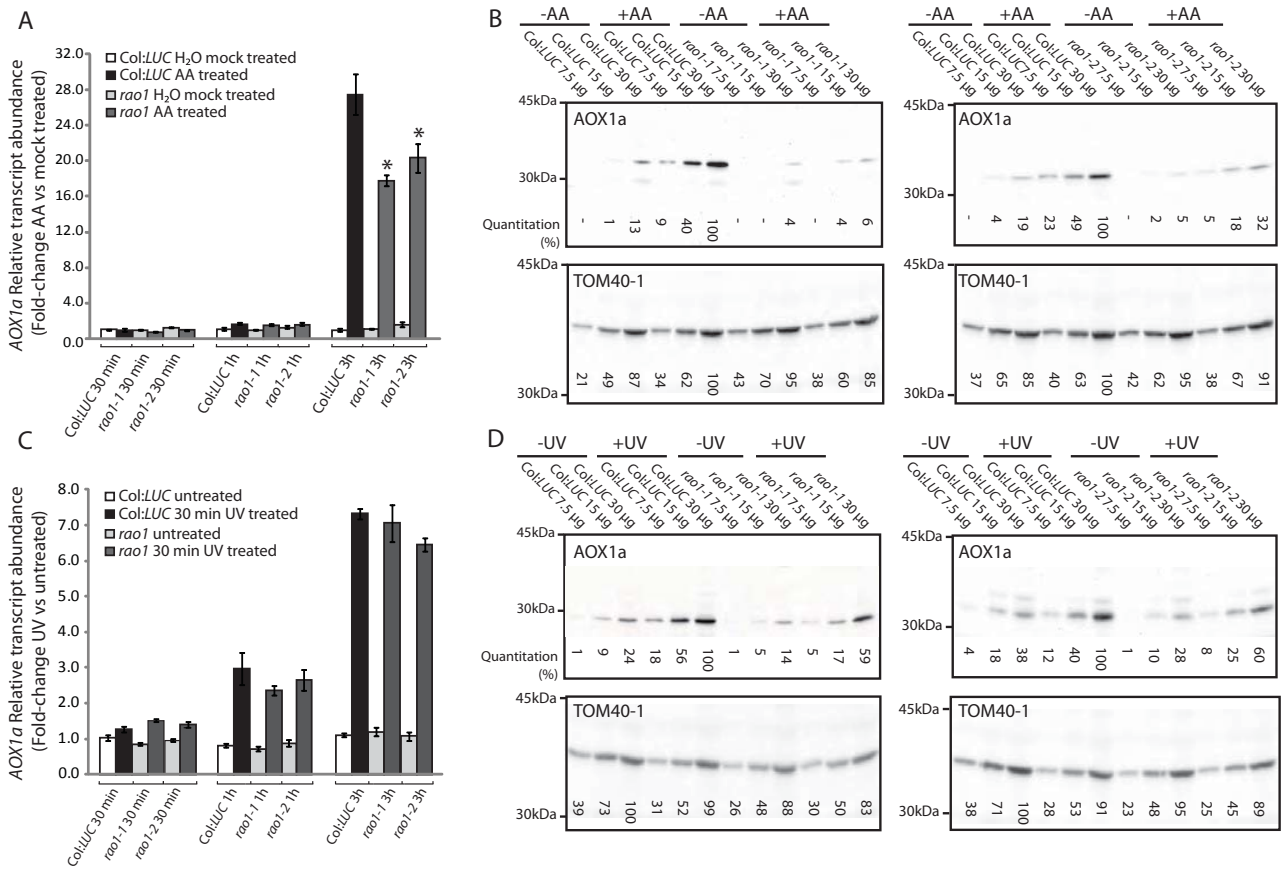
A
AOX1a Relative transcript abundance (Fold-change AA vs mock treated)
Col:LUC H2O mock treated
Col:LUC AA treated
rao1 H2O mock treated
rao1 AA treated
Col:LUC 30 min
rao1-1 30 min
rao1-2 30 min
Col:LUC 1h
rao1-1 1h
rao1-2 1h
Col:LUC 3h
rao1-1 3h
rao1-2 3h
B
-AA
+AA
AOX1a
TOM40-1
45kDa
30kDa
Quantitation (%)
C
AOX1a Relative transcript abundance (Fold-change UV vs untreated)
Col:LUC untreated
Col:LUC 30 min UV treated
rao1 untreated
rao1 30 min UV treated
D
-UV
+UV

Figure 4

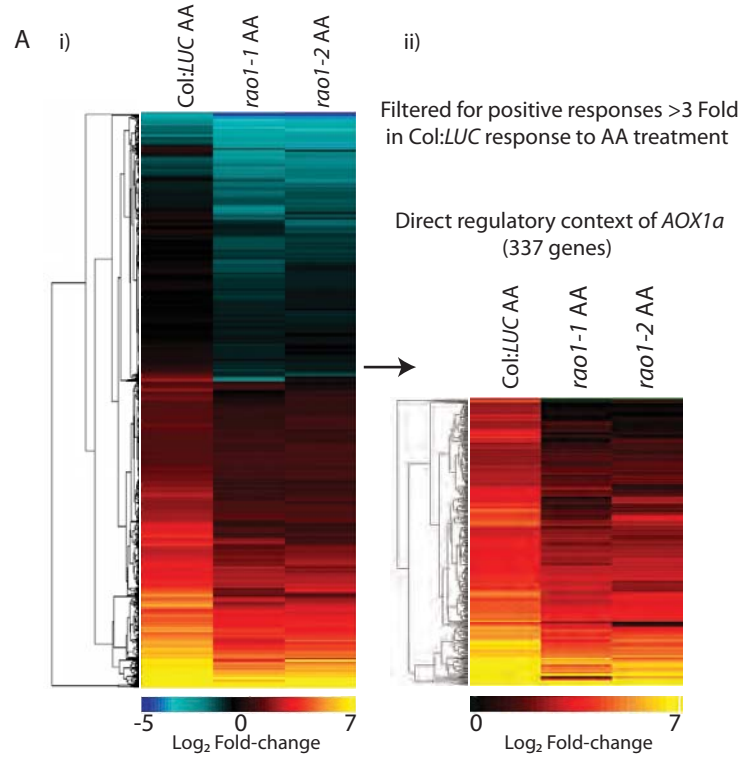

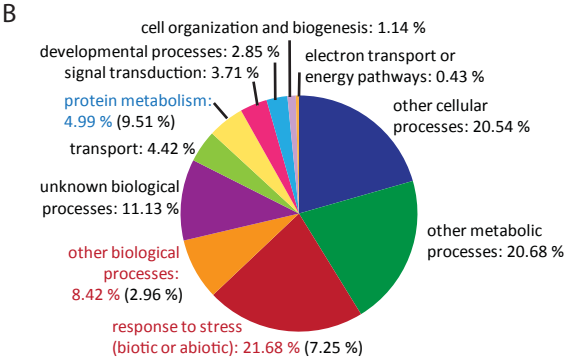

C Mitochondrial regulatory context of *AOX1a*

AGI	Name	Annotation
AT1G20350	TIM17-1	mitochondrial inner membrane translocase
AT1G32350	AOX1D	alternative oxidase 1D (AOX1D)
AT2G20800	NDB4	NAD(P)H dehydrogenase B4 (NDB4)
AT2G21640	UPOX	unknown function, marker for oxidative stress
AT3G10930		unknown protein
AT3G22370	AOX1A	ALTERNATIVE OXIDASE 1A
AT3G50930	BCS1	cytochrome BC1 synthesis (BCS1)
AT5G09470	DIC3	A mitochondrial dicarboxylate carrier (DIC)
AT4G05020	NDB2	NAD(P)H dehydrogenase B2 (NDB2)

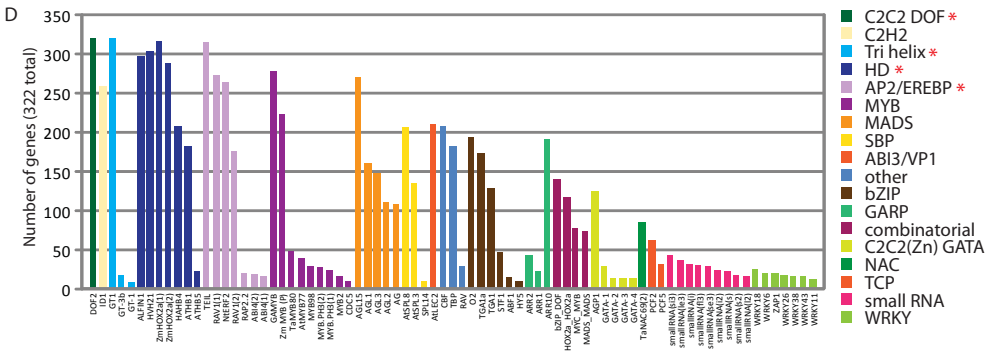

Figure 5

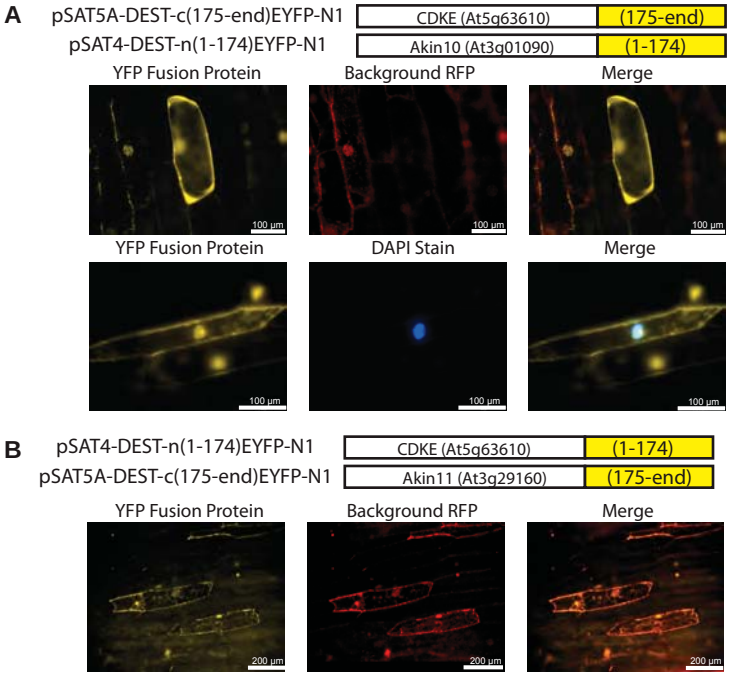
A
pSAT5A-DEST-c(175-end)EYFP-N1
CDKE (At5g63610)
(175-end)
pSAT4-DEST-n(1-174)EYFP-N1
Akin10 (At3g01090)
(1-174)
YFP Fusion Protein
Background RFP
Merge
YFP Fusion Protein
DAPI Stain
Merge
100 µm
B
pSAT4-DEST-n(1-174)EYFP-N1
CDKE (At5g63610)
(1-174)
pSAT5A-DEST-c(175-end)EYFP-N1
Akin11 (At3g29160)
(175-end)
YFP Fusion Protein
Background RFP
Merge
200 µm

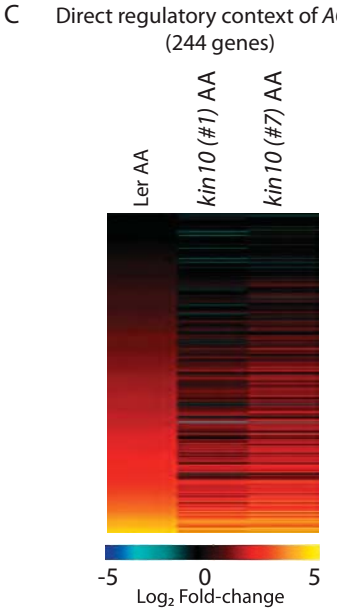
C
Direct regulatory context of AOX1a
(244 genes)
Ler AA
kin10 (#1) AA
kin10 (#7) AA
-5
0
5
Log2 Fold-change

Figure 6

Supplementary Table 1 Col -0/L.er insertion/deletion (Indel) Small Sequence Length Polymorphism(SSLP) primers and primers for Southern blot. Indel SSLP information was downloaded from Monsanto Arabidopsis Polymorphism and L.er Sequence Collections (https://www.arabidopsis.org/browse/Cereon/index.jsp). Primers were designed to flank the Indels as such that the Indel sequences were approximately 1/10 of the the amplicon length. Location is shown in mega base pairs (Mb) from the top of each chromosome. Asterisk indicates the fine mapping marker for *rao1* where last recombinant was found in L.er mapping population.

Indel name	Chromosome	Location (Mb)	Forward primer (5' - 3')	Reverse primer (5' - 3')
NGA63	1	3.224	ACCCAAGTGATCACCACC	AACCAAGGCACAGAAGCGC
CER449719	1	11.016	GCTGGCGGGCAGTAGAAAAGC	GCAGCCAAAAGATTAATGGAAAC
CER458022	1	16.37	GAATCACAATAACCTTCTAGAGC	CCAGATCTAGCTCATTCTGTTG
CER451253	1	23.072	CGTGCGATTCCCTATAATAC	GGCTCCAATCAATAAATGC
CER449372	2	4.322	GTCTGCTTACAGGGGTTATCG	GTATTTGGGAAAGGTGAGG
CER460085	2	10.152	GGAAACAGAACCAATGTGGTG	CAAATATATCATAGTACCTAGC
NGA168	2	16.291	GAGGACATGTATAGGAGCCTCG	TCGTCTACTGCACTGCCG
CER455387	3	4.608	GAGGGAGTGGCCTCGTGTAGAG	GTCACTCTTTTCCTCTGGTTTG
CER454776	3	8.931	CAATGTGAGGACAAAAGCAGAGAAG	CCTATAGGTGGCAGAAAAACCACC
CER458675	3	17.69	CATGTTGTCATATCTTTGTG	GTGTAATTGATTTTACGTC
CER451787	3	20.342	GAATTGAATAAACCATGTTGCC	CCGAAATACTAATACGATCC
CER460827	4	1.82	CCAGCTGAATGATATTCGC	GTAGTAAGATTGATTTATAGTG
CER451764	4	6.342	CCTCCATTCCAATTCTCGTGAAC	CCCGTTCCACCAAACTAGTCC
CER466354	4	11.015	CGAGAGCCACTTTAGCTTTC	GCAAGCAGGTGGGTAACACAGTG
NGA1107	4	18.096	CGACGAATCGACAGAATTAGG	GCGAAAAAACAAAAAAATCCA
ATHCTR1	5	0.979	CCACTTGTTTCTCTCTCTAG	TATCAACAGAAACGCACCGAG
CER456650	5	5.464	GCAAGTGTCGATGGAAAACATAAG	CAGCCTTATAGTTCATTAGCTC
ATHPHYC	5	14.007	CTCAGAGAATTCCCAGAAAAATCT	AAACTCGAGAGTTTTGTCTAGATC
CER451137	5	22.104	GGTTTAGAAGCGTCTCCGAGAACACC	CCTTGGACGAGAATAATCCTTTATCC
*CER457391	5	24.421	CCAGCATCTCTCGTAACATCC	GGTATTATAGGTGTCCAATC
MBK-5	5	25.477	GAGCATTTCACAGAGACG	ATCACTGTTGTTTACCATTA

Name	Primer (5'-3')
Southern primer 1	CGCTTAGACAACTTAATAACAC
Southern primer 2	CCAATACGAGGTCGCCAACATC

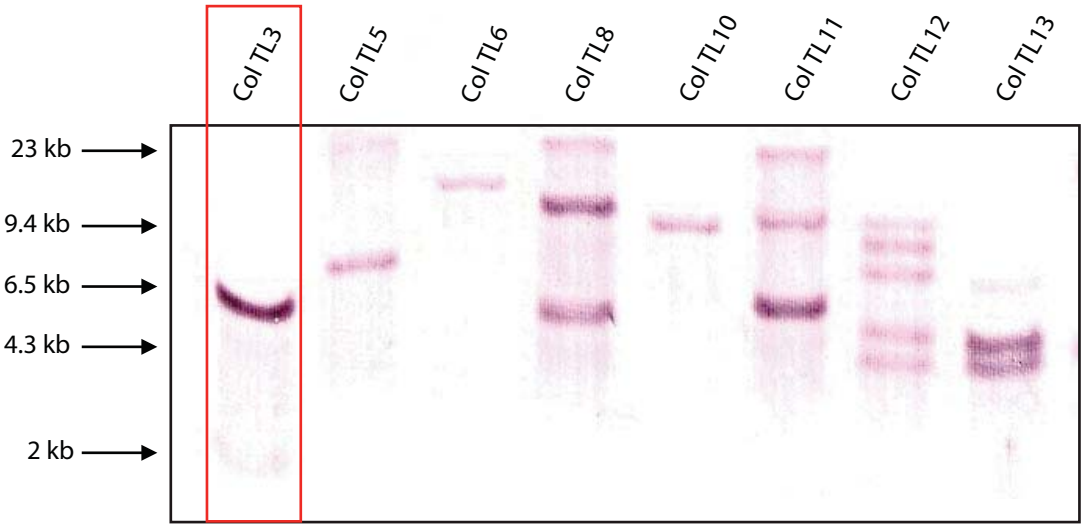

Supplementary Figure 1 Southern blot confirmation of single T-DNA insert and selection of Col:*LUC* line. DNA from 8 transgenic Arabidopsis Columbia-0 lines, containing *AOX1a:LUC* construct were blotted after digestion with BamHI and hybridised with a *LUC* gene specific probe. Line Col TL3 re-named as Col:*LUC* was selected for further study.

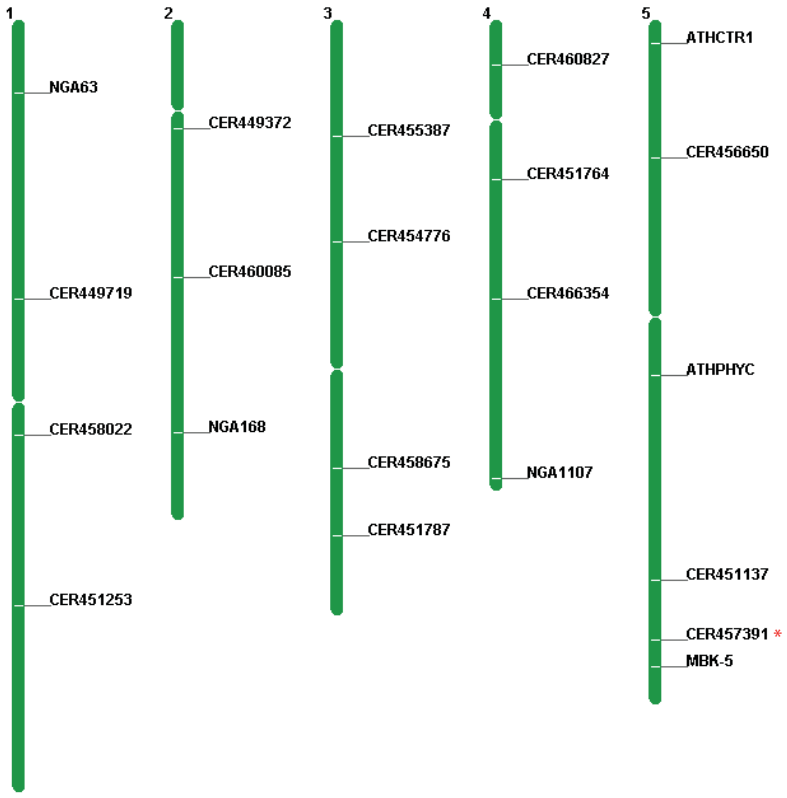

Supplementary Figure 2 Col-0/L. *er* insertion/deletion (Indel) polymorphism map. Indel polymorphism markers were used in map-based cloning to locate mutations of interest in *rao1-1*and *rao1-2*. The number 1-5 refers to chromosome 1 to chromosome 5 of the Arabidopsis genome. Markers were not more than 6 million base pairs apart from the next marker or the centromere. Indel schematic map was drawn using Chromosome Map Tool (https://www.arabidopsis.org/jsp/ChromosomeMap/tool.jsp). See Supplementary Methods for specific mapping details. Asterisk indicates the fine mapping marker for *rao1* where last recombinant was found in L.*er* mapping population.

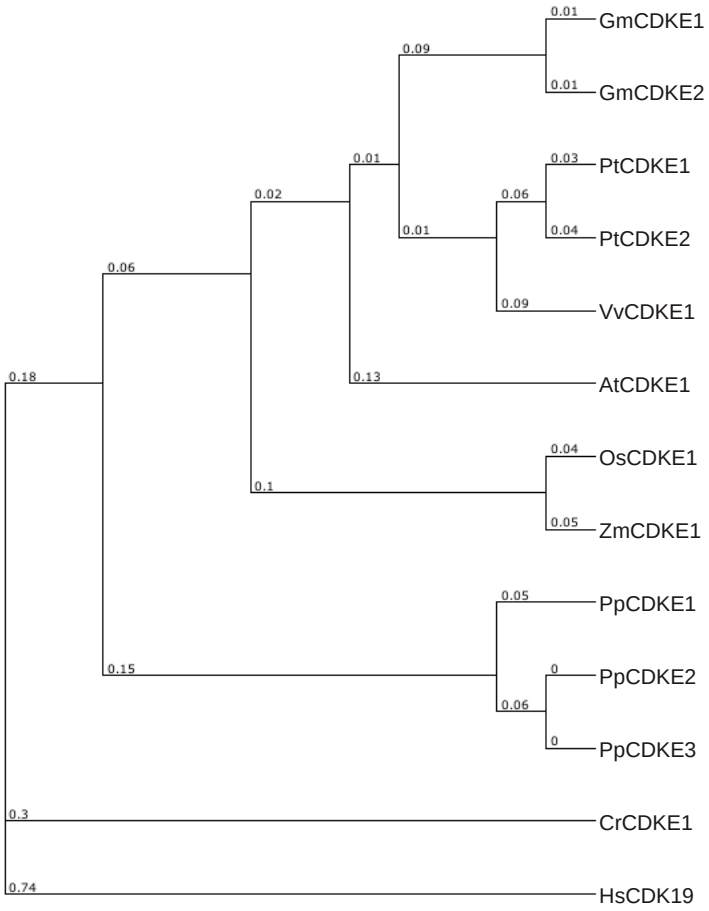

Supplementary Figure 3 Phylo genetic tree of *CDKE;1* across different plant species and human. Numbers indicate the branch length values. Gm, *Glycine max* (soybean); Pt, *Populus trichocarpa* (poplar); Vv, *Vitis vinifera (*grape); At, *Arabidopsis thaliana* (Arabidopsis); Os, *Oryza sativa* (rice); Zm, *Zea mays* (maize); Pp, *Physcomitrella patens* (moss); Cr, *Chlamydomonas reinhardtii* (green alga); Hs, *Homo sapiens* (Human).

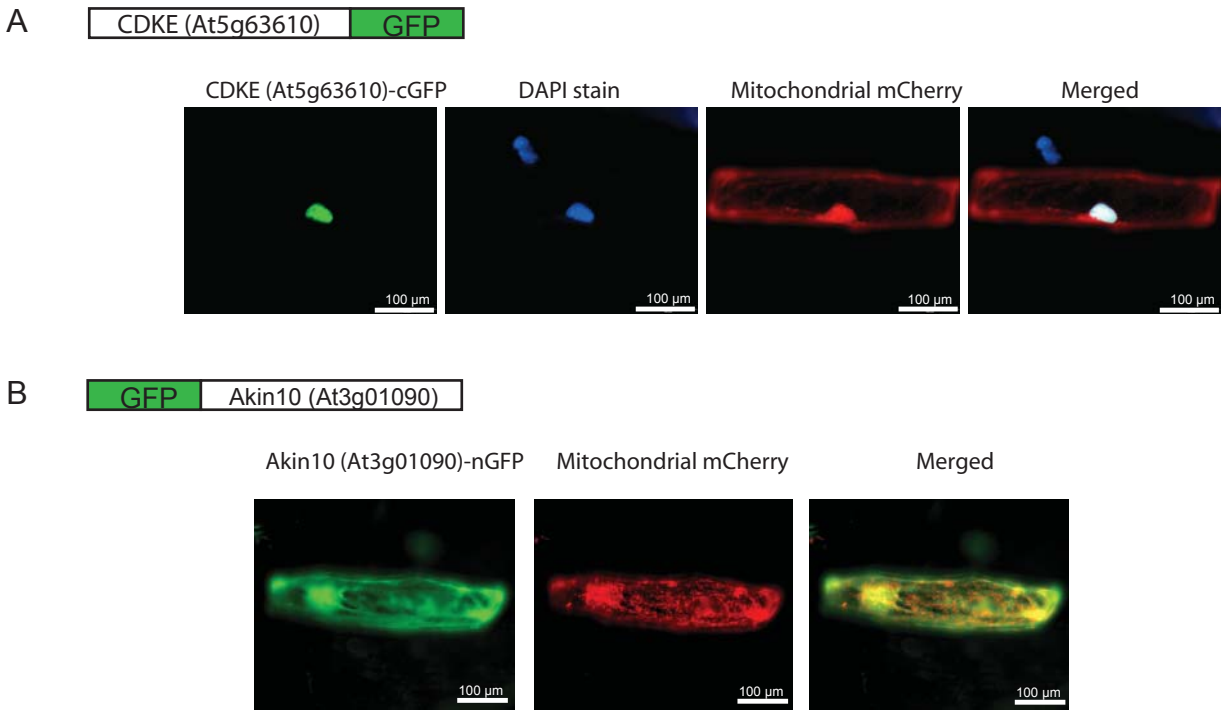

Supplementary Figure S4 Cellular localisation of CDKE;1 and AKIN10 in onion epidermal cells. The subcellular localisation of CDKE;1 (CDKE;1-GFP) and AKIN10 (GFP-AKIN10) were determined through transient biolistic transformation into onion epidermal cells alongside a mitochondrial RFP marker (Mitochondrial mCherry) and in the case of CDKE;1 a DAPI stain, to identify the nucleus. GFP, green fluorescent protein. Scale bars are shown. (A) CDKE;1-GFP was observed to localise to the nucleus. (B) AKIN10 was observed to have both nuclear and cytosolic localisation.

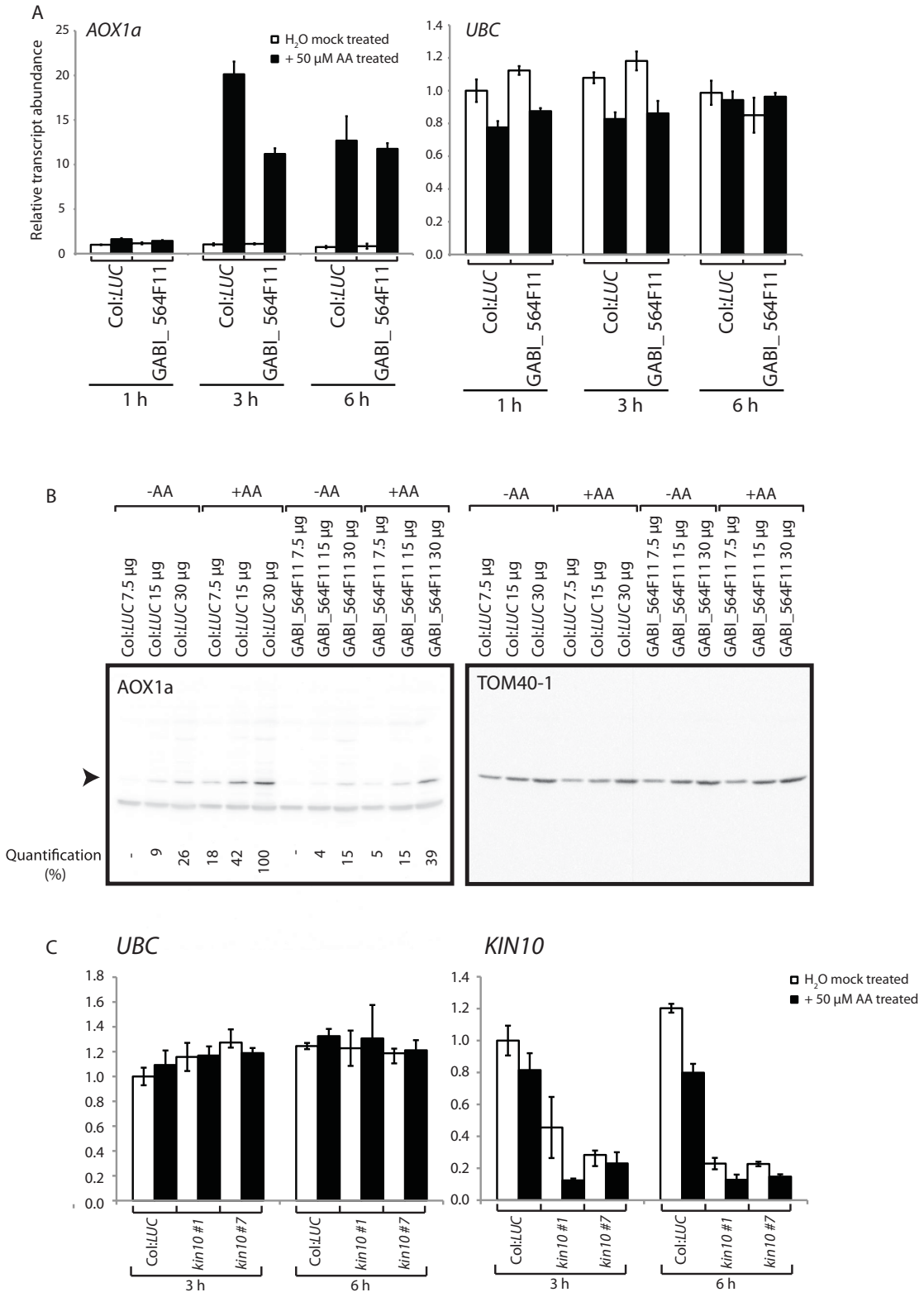

Supplementary Figure 5 Characterisation of transcript and protein induction in T-DNA insertion line, GABI_564F11, and transcript abundance for kin10 RNAi lines, under antimycin A treatment. (A) *AOX1a* relative transcript abundance under AA treatment. Seedlings were treated with 50 µM antimycin A (+50 µM AA) or with deionised water (H2O mock) for 1 h, 3 h and 6 h. Ubiquitin C (*UBC*) transcript abundance was checked in each collected sample. (B) Immunodetection of AOX1a protein under 5 h AA treatment. Mitochondria were isolated from seedlings treated with AA (+AA) or with deinonised water (-AA). Relative protein abundance (quantification values are indicated under each blot) was quantified by densitometry. TOM40-1 protein abundance is shown as aloading control. (C) *KIN10* transcript abundance was determined after 3 h and 6 h AA treatment. Seventeen-day-old plants were sprayed with deionised water (-AA) or 50 µM AA. Relative transcript abundance fold-changes between mock treated and AA treated plants for the respective genotypes are shown. Ubiquitin C (*UBC*) transcript abundance was measured as a control.

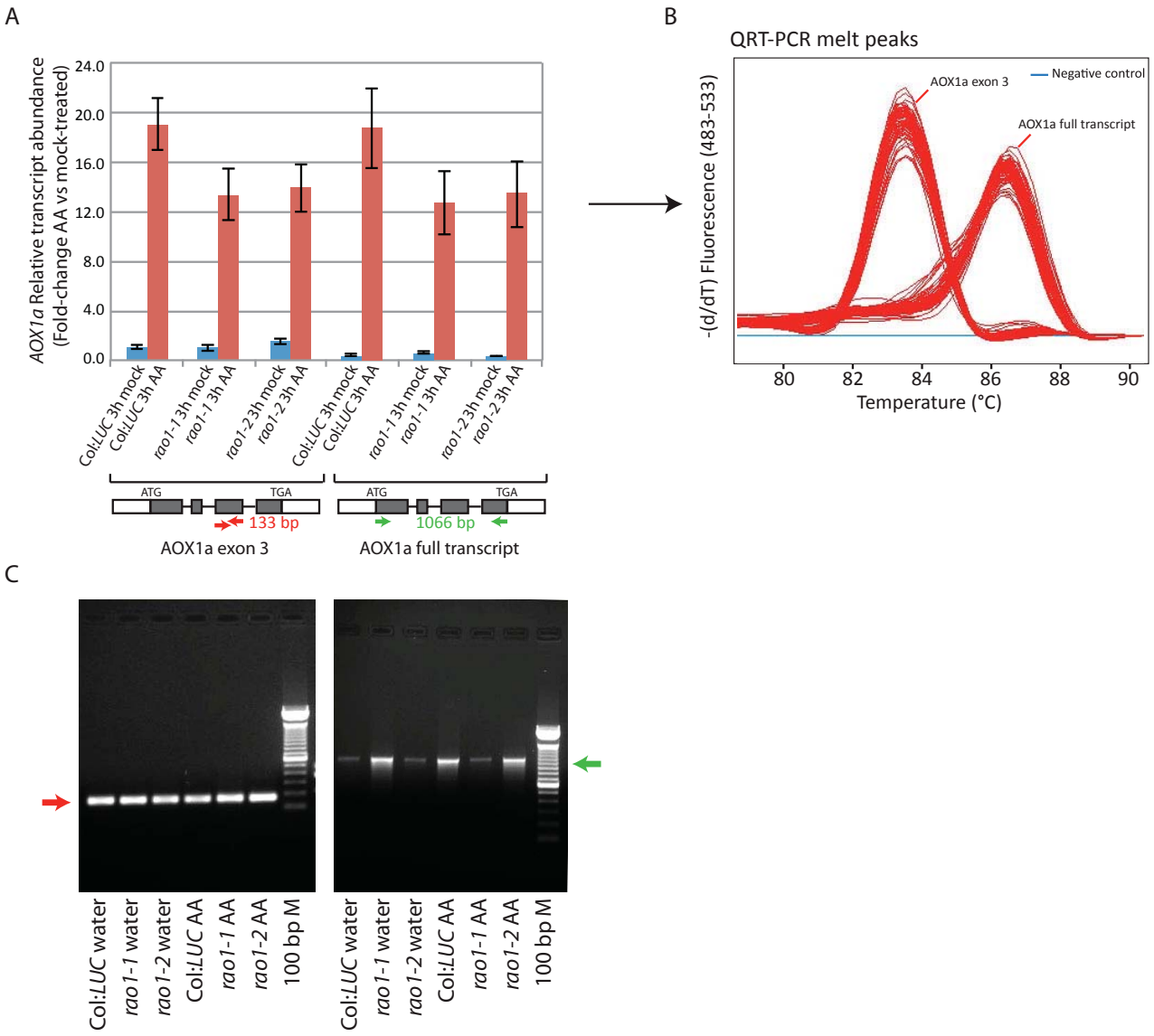

Supplementary Figure 6 Confirmation of correct transcript processing of *AOX1a* in *rao1-1* and *rao1-2* lines. (A) *AOX1a* relative transcript abundance measured by Quantitative RT-PCR (QRT-PCR) assays designed to amplify the complete, processed *AOX1a* full transcript along with an assay using internal primer sets that bind within exon 3. A schematic of the *AOX1a* transcript with primer binding sites and expected amplicon length is shown. Transcript abundance was measured in Col:*LUC*, *rao1-1* and *rao1-2* lines after 3 hours treatment with deionised water (mock) or antimycin A (AA). (B) Melt peak analysis was performed on QRT-PCR end point products, showing 2 distinct melt peaks for the products of each assay, and a single uniform peak for *AOX1a* full length primers. (C) PCR products visualised by agarose gel electrophoresis to indicate correct amplicon sizes and no splicing defect in *rao1-1* and *rao1-2* lines under AA treatment.

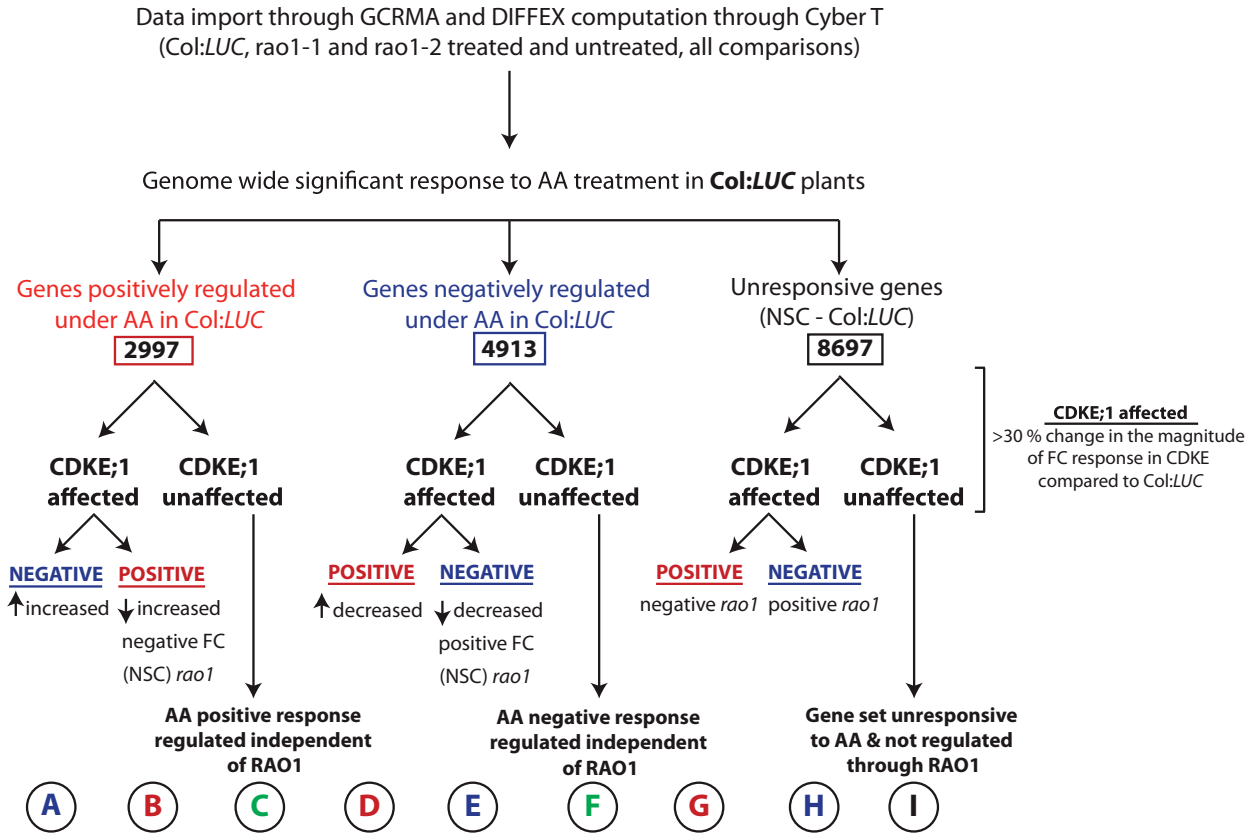

Gene lists defined

1) No significant changes = I
2) Response to AA regulated **independant of RAO1** = C + F
3) Gene targets **positively** regulated through RAO1via retrograde signals = B + D + G
4) Gene targets **negatively** regulated through RAO1via retrograde signals = A + E + H

Analysis performed independently for *rao1-1* and *rao1-2*
Final gene lists contain only genes classified identically in both lines

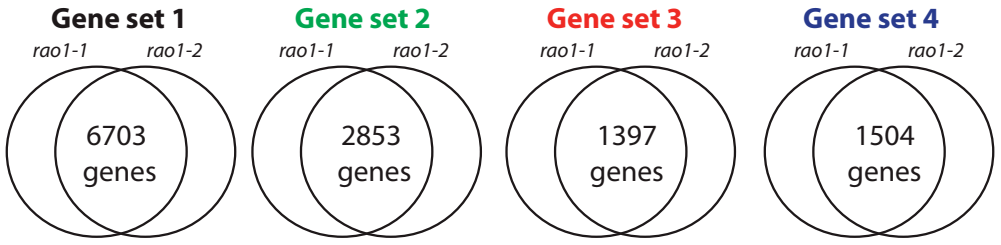

** 12, 457 out of 16, 607 (>75 % genes, genome wide) showed identical classification in Gene set lists in both *rao1-1* and *rao1-2* microarray analysis.

Changes were considered significant if
Fold-change >1.5 fold in magnitude
PPDE *p*-value corection >0.95
Not mitochondrial, plastid, absent or Affy control

Supplementary Figure 7 Overview of the logic and criteria for global transcript classification into one of 4 lists of genes depending of stress response and regulation through RAO1 function.

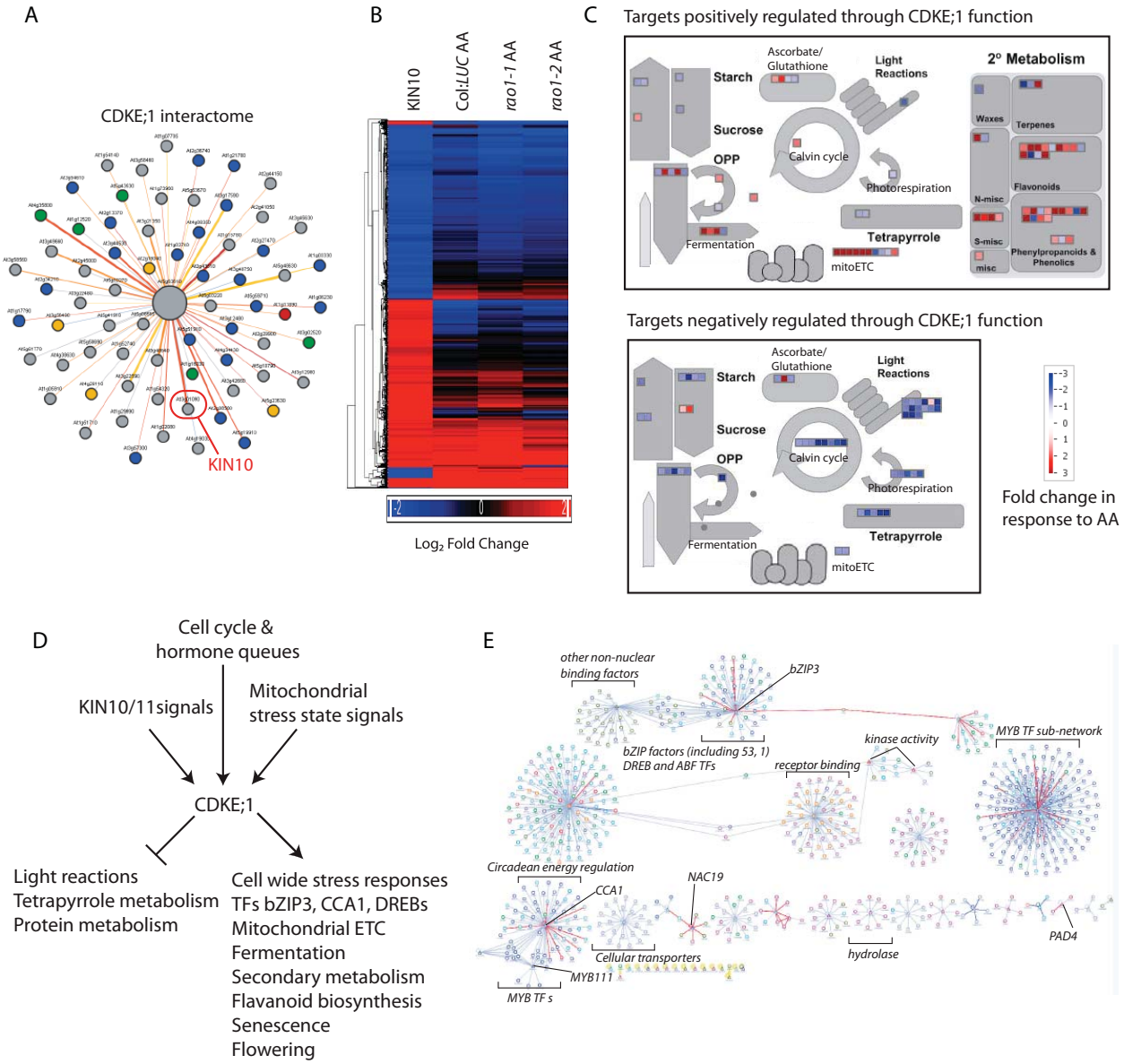

Supplementary Figure 8 Analysis of transcriptional output networks regulated through CDKE;1 function. (A) Predicted interactome for CDKE;1 (http://www.cls.zju.edu.cn/pair/) (B) Hierarchical cluster of fold change responses for transcripts associated with KIN10 signaling in Col:*LUC*, *rao1-1* and *rao1-2* plants under mitochondrial stress. Red colour indicates transcripts that are up-regulated and blue colour indicates transcripts that are down-regulated according to the scale. (C) Stress responses for CDKE;1 targets visualised in MapMan software (http://mapman.gabipd.org/). Scale bar shows the magnitude of fold change in response to stress. (D) Schematic model for integration of cellular stress, energy status and growth signals through CDKE;1 activity to directly influence transcription factor (TF) activity and fine tune diverse transcriptional processes within the nucleus. The transcriptional gene networks affected by CDKE;1 function show massive reprogramming under stress with output sites beyond mitochondrial metabolism such as flowering, growth, secondary metabolism and photosynthesis. The network influenced by CDKE;1 appears to be overlapping but distinct from KIN10 affected regulatory networks, and may be involved in fine-tunning sugar, ABA and stress signals through KIN10 with the direct organelle feedback provided in retrograde signals to initiate protective cascades against cellular ROS damage due to organelle misfunction under these conditions. (E) Protein-Protein interaction network, laid out with force directed algorithm for the 119 transcripts significantly up or down regulated in *rao1-1* and *rao1-2* plants under normal conditions prior to stress treatment (http://www.cls.zju.edu.cn/pair/).

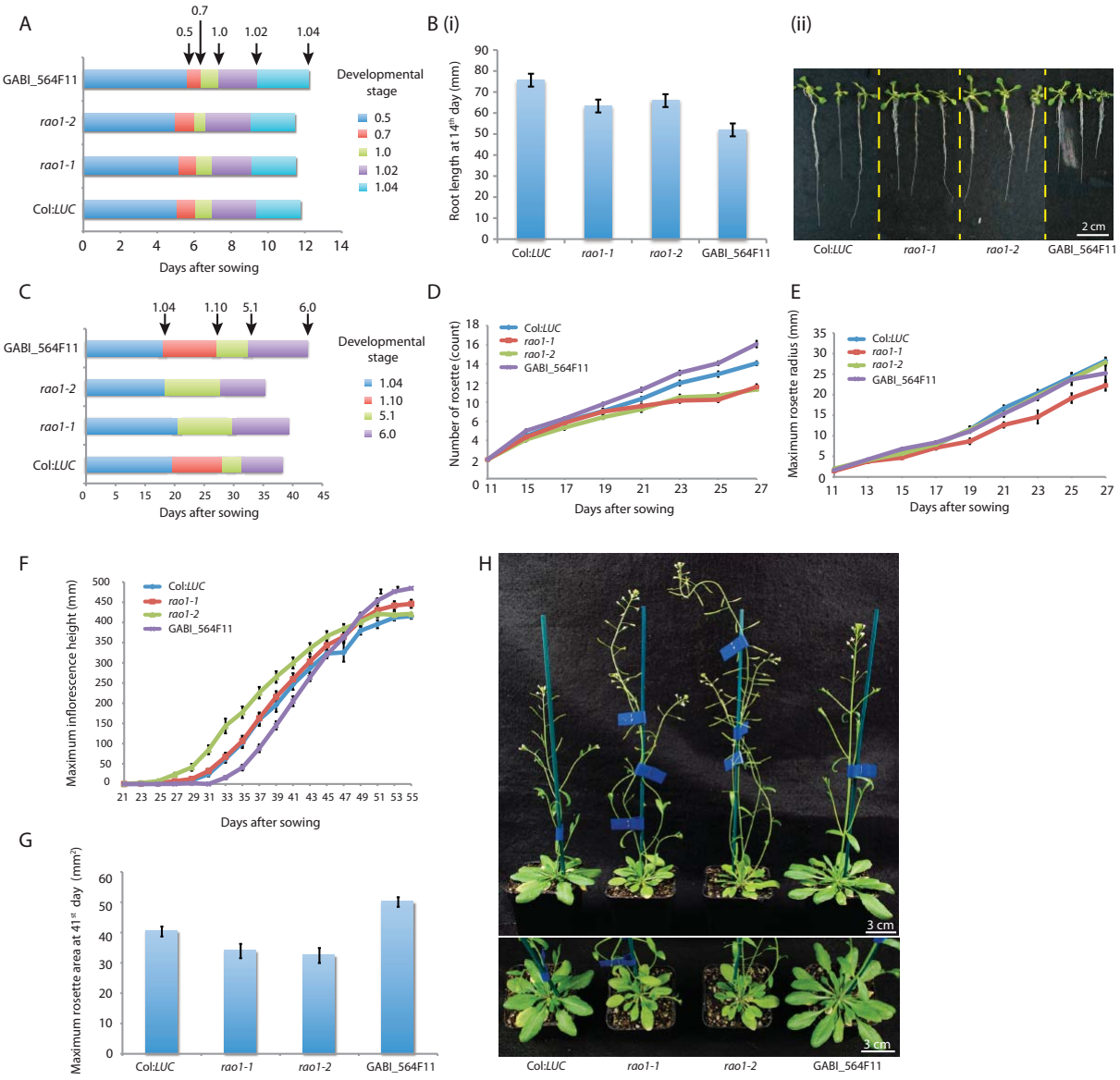

Supplementary Figure 9 **Phenotypic analysis of *rao1* mutants.** Seeds were sown on Gamborg's B5 agar plates (A-B) or on soil (C-H) and stratified for 36 h before moving to 16 h light/ 8 h dark long day conditions. At least 15 plants per genotype were used for analysis. (A) Plate-based developmental stage: 0.5 (first radicle emerged), 0.7 (cotyledon visible), 1.0 (cotyledon fully opened), 1.02 (two rosette leaves fully opened), 1.04 (four rosette leaves fully opened). (B) (i) Longest root length at 14th day and representative seedlings are shown in (ii). (C) Soil-based developmental stage: 1.04 (four rosette leaves >1mm in length), 1.10 (ten rosette leaves >1mm in length), 5.1 (first flower buds visible), 6.0 (first flower opened). (D-F) Representative growth parameters (G) Areas of the largest rosette leaves were measured at 41st day and a representative plant from each genotype are shown in (H).

Chapter 4

A Membrane-bound NAC Transcription Factor Controls Mitochondrial Retrograde and Reactive Oxygen Species Signalling in Arabidopsis

A membrane-bound NAC transcription factor controls mitochondrial retrograde and reactive oxygen species signalling in Arabidopsis

Sophia Ng[1‡], Aneta Ivanova[1‡], Owen Duncan[1], Simon Law[1], Olivier van Aken[1], Inge de Clercq[2], Yan Wang[1], Chris Carrie[1], Lin Xu[1], Hayden Walker[1], Frank Van Breusegem[2], James Whelan[1], Estelle Giraud[1*]

[1]Australian Research Council Centre of Excellence in Plant Energy Biology. University of Western Australia, 35 Stirling Highway, Crawley, Western Australia, 6009. Australia. [2]VIB Department of Plant Systems Biology, Ghent University. Department of Plant Biotechnology and Bioinformatics, Ghent University Technologiepark 927, 9052 Gent, Belgium.

Running Title: Mitochondrial retrograde regulation

* Author to whom all correspondence is to be addressed

Estelle Giraud

ARC Centre of Excellence in Plant Energy Biology

University of Western Australia

35 Stirling Highway, Crawley 6009 WA, Australia

Ph: +61-8-64881749

Email: estelle.giraud@uwa.edu.au

The author responsible for distribution of materials integral to the findings presented in this article in accordance with the policy described in the

Instructions for Authors (www.plantcell.org) is: Estelle Giraud (estelle.giraud@uwa.edu.au).

‡These authors contributed equally to this work

Calculated Length of Article: 15 pages

ABSTRACT

Plants require daily coordinated control of energy metabolism for optimal growth and survival, and therefore need to integrate cellular responses with both mitochondrial and plastid retrograde signalling. Using a forward genetic screen to characterise *Regulators of the Alternative Oxidase* (*RAO* mutants), we have identified RAO2/ANAC017 as a direct positive regulator of *AOX1a*. RAO2/ANAC017 is targeted to connections and junctions in the ER and F-actin via a C-terminal transmembrane domain and upon deletion of this domain, is exclusively located in the nucleus. Furthermore, genome wide analysis of the transcriptional network controlled by RAO2/ANAC017 under stress treatment revealed that RAO2/ANAC017 function was necessary for >85% of the changes observed as a primary response to cytosolic H_2O_2, indicating ANAC017 plays a central role or convergence point in these primary responses to H_2O_2. However, only ~40% of transcriptional changes observed in response to Antimycin A treatment required ANAC017, indicating potential redundancy in mitochondrial stress signals. Plants with mutated *rao2/anac017* were more stress sensitive, while a gain-of-function mutation resulted in plants that were more stress resistant and had lower cellular levels of H_2O_2 under untreated conditions. Thus, RAO2/ANAC017 acts as a convergence point for oxidative stress signalling, via both anterograde and retrograde pathways.

INTRODUCTION

Mitochondria and plastids (chloroplasts) are composed of ~1500 and ~3000 proteins respectively, however greater than 95% of organellar proteins are encoded by nuclear located genes, translated in cytosol and post translationally imported to organelles (Woodson and Chory, 2008). It has been shown that two-way communication pathways exist between the nucleus and mitochondria and chloroplasts, called anterograde and retrograde signaling pathways (Rhoads and Subbaiah, 2007; Woodson and Chory, 2008). Anterograde regulation refers to a top-down regulatory pathway, where signals have a direct impact on gene expression in the nucleus. Conversely, nuclear gene expression is also influenced by signals that originate from within the organelles, mitochondria or chloroplasts, and is referred to as retrograde regulation.

Several components involved in plastid retrograde signaling have been identified, with at least five different pathways, ROS, Redox signals, plastidial gene expression, pigment biosynthesis and specific signaling metabolites (Pfannschmidt, 2010). The most intensively studied retrograde signaling pathway is shown in the *genomes uncoupled (gun)* mutants that uncouple the expression of nuclear encoded chloroplastic proteins from the functional state of chloroplasts (Susek et al., 1993; Woodson and Chory, 2008; Woodson et al., 2011). A recently identified plastid-bound transcription factor PTM (plant homeodomain transcription factor (PHD)-type transcription factor with transmembrane domains), was also identified as the regulator for plastid retrograde signaling and acted downstream of GUNs (Sun et al., 2011). Additional plastid retrograde signals that have been identified more recently are 3'-phosphoadenosine 5'-phosphate (PAP) (Estavillo et al., 2011), β-cyclocitral

that is produced in plastids during high light stress (Ramel et al., 2012), and pathogen-associated molecular pathogen (PAMP) signals that are relayed via the chloroplasts through a Ca^{2+} mediated signal transduction pathway (Nomura et al., 2012).

At least some of the components involved in mitochondrial retrograde signaling pathways have been identified in yeast (Butow and Avadhani, 2004). Reactive oxygen species (ROS) have been implicated in mitochondrial retrograde signaling in both plants and animals (Murphy, 2009; Kim et al., 2010; Petrov and Van Breusegem, 2012), but the means by which a ROS signal can be transmitted to activate gene expression in the nucleus is still unknown, along with the fact that ROS is produced in a variety of locations in the cell (Moller and Sweetlove, 2010). In plants, several *mitochondrial retrograde regulation deficient* (*mrrd*) mutants have been isolated using the lack of response of *Alternative Oxidase1a* (*AOX1a*) to mitochondrial dysfunction as the gene model for mitochondrial retrograde regulation (Dojcinovic et al., 2005; Zarkovic et al., 2005). However, the identities of these *mrrd* mutants are yet to be characterised. The only identified component mediating mitochondrial retrograde response in plants is ABI4 (Giraud et al., 2009).

In this work, we employed a forward genetic approach using *AOX1a* as a gene model for mitochondrial retrograde regulation to identify *Regulators of AOX1a* (*RAO* mutants). Here, we report a membrane-bound NAC (NAM, ATAF1,2, and CUC2) transcription factor, RAO2/ANAC017, that is a transcriptional activator of *AOX1a* during mitochondrial dysfunction. Furthermore, we show that this transcription factor mediates H_2O_2 induced changes in transcript abundance, thus integrating anterograde and retrograde regulatory pathways.

RESULTS

RAO2 Encodes the NAC Domain Transcription Factor, ANAC017

To identify the molecular components necessary for mitochondrial retrograde signaling under stress in plant cells, a forward genetic screen was conducted using *AOX1a* as a model, stress responsive, nuclear encoded mitochondrial component to identify Regulators of Alternative Oxidase, RAO mutants. A construct with the *AOX1a* 2 kb upstream promoter region driving a firefly luciferase gene (*AOX1a-LUC*) was used as a reporter gene system and permanently transformed into *Arabidopsis thaliana* Columbia-0 (Col-0) to generate Col:*LUC* germ lines (Figure 1A). Antimycin A (AA), a chemical inhibitor of the mitochondrial cytochrome bc_1 (Rieske et al., 1967), was used to induce the up-regulation of *AOX1a* expression (Clifton et al., 2005) (Figure 1A). Two-week-old Col:*LUC* seedlings, when treated with 50 μM AA, show dramatically increased expression of *LUC* driven by the *AOX1a* promoter (Figure 1A). Col:*LUC* plants were subjected to ethyl methanesulfonate (EMS) mutagenesis, and two independent lines, *rao2-1* and *rao2-2*, were identified as loss-of-function alleles that showed little or no induction of AOX1a-LUC under AA treatment (Figure 1A).

To confirm that RAO2 is a necessary and specific component required for mitochondrial retrograde signaling, myxothiazol was used as an independent chemical agent to induce the expression of *AOX1a*. Myxothiazol specifically targets the cytochrome bc_1 complex in the mitochondrial respiratory chain; however, the mechanism of inhibition is different from AA (von Jagow et al., 1984). Consistent with the results from AA treatment, *AOX1a-LUC* was expressed in myxothiazol treated Col:*LUC* seedlings but not in the *rao2* lines

(Figure 1B) and the corresponding LUC expression under both treatments was quantified (Figure 1C). For both AA and myxothiazol, LUC was 5-fold less abundant (p<0.001, Student's t-test) in the *rao2* background compared to Col:*LUC* seedlings. A number of other treatments, including MFA (Dojcinovic et al., 2005; Zarkovic et al., 2005), and H_2O_2 displayed a significant reduction in the induction of LUC in the *rao2* background (Supplemental Figure 1). In contrast other more general cellular stresses such as ultra violet light (UV), 4°C cold, Abscisic acid (ABA) and Salicylic acid (SA) did not show compromised induction of LUC indicating that RAO2 is likely to mediate a specific mitochondrial and/or ROS (H_2O_2) dependent signaling pathway (Supplemental Figure 1).

A combination of classical positional cloning based techniques with next generation sequencing technology was utilized to identify the mutations in *rao2* mutants. Both *rao2-1* and *rao2-2* are recessive mutations and mapped to the same 2.47-Mb region on chromosome 1 between In/Ddel markers CER449719 and CER450671 (see Methods, Supplemental Table 1) and were therefore crossed to test whether these were allelic mutations within the same gene product. Plants from the first filial generation (F1) were unable to induce *AOX1a-LUC* expression in response to AA treatment (Figure 1D), confirming that *rao2-1* and *rao2-2* are in fact allelic mutations. To identify candidate point mutations within this 2.47-Mb region in the *rao2* mutant lines, whole genome next-generation re-sequencing was used (Supplemental Table 2). A candidate gene at the locus At1g34190, encoding a NAC domain transcription factor ANAC017, was identified with non-synonymous mutations in each of the mutant alleles (Supplemental Table 2, Figure 1F). Wild-type coding sequence for At1G34040, expressed under the control of the cauliflower mosaic virus (CaMV)

35S promoter, was transformed into *rao2-1* mutants and restored the ability of transgenic plants to induce *AOX1a-LUC* under AA treatment (Figure 1E), thus confirming that the *rao2* phenotype was the result of a specific mutation in ANAC017. Furthermore, point mutations in both *rao2-1* and *rao2-2* were confirmed by Sanger sequencing (Figure 1G). A single nucleotide polymorphism (SNP) in *rao2-1* introduced a stop codon at a tryptophan at amino acid position 99 (W99); while the SNP in *rao2-2* produced an amino acid change from a proline into a leucine at amino acid 180 (P180L, Figure 1G and H). The RAO2/ANAC017 protein is predicted to be a type II membrane protein with a single transmembrane (TM) motif at the C-terminal end and an N-terminus containing the NAC domain (PROSITE accession PS51005) (Figure 1G) (Kim et al., 2010). RAO2/ANAC017 belongs to NAC2 subfamily according to (Ooka et al., 2003) classification (Supplemental Figure 2). The point mutations in *rao2-1* and *rao2-2* are in highly conserved protein regions between members of the NAC2 sub-family (Figure 1H). The *rao2-1* allele harbors a mutation in the NAC domain while the *rao2-2* mutation lies near the boundary of the NAC domain (Figure 1G and H).

RAO2 is required for induction of AOX1a transcript and protein

To further confirm that any deficiency in mitochondrial retrograde signaling in the *rao2* mutant lines was as a result of specific inactivation of ANAC017, two T-DNA lines (SALK_022174 and SALK_044777) in the Col-0 background were also used in downstream analyses (Figure 2A, Supplemental Figure 3A). The two lines were screened and found to have T-DNA insertions in the second and fourth exons of the *ANAC017* coding sequence, respectively (Supplemental Figure 3B-D). One SALK line (SALK_022174, referred to as

anac017-1) contained the insertion in the same exon as the EMS mutants and was shown to be a true knock-out line, as the full length transcript could not be amplified in this background and the NAC domain was disrupted. Interestingly, the T-DNA insertion in the second line (SALK_044777, referred to as *anac017-2*) was in exon 4, just upstream of the predicted TM region (Figure 2A) but did not disrupt the N-terminal NAC domain at all. A truncated transcript could be amplified in this *anac017-2* background, missing the predicted TM domain.

AOX1a transcript and protein abundance were examined by QRT-PCR and Western blot analyses in Col:*LUC* and independent *rao2/anac017* mutant lines: *rao2-1* representing EMS mutation, the SALK T-DNA insertion line, *anac017-1* (SALK_022174) and the SALK T-DNA insertion line, *anac017-2* (SALK_044777), over a period of 6 h treatment with AA. After 3 h of AA treatment, greater than 40-fold significant induction (p<0.001, Student's *t*-test) of *AOX1a* transcript level was observed in Col:*LUC* as a primary response, and after 6 h of treatment this response had already decreased (Figure 2Bi). The magnitude of induction was significantly lower (p<0.001, Student's *t*-test) in *rao2-1* and *anac017-1,* with only 10 to 20-fold *AOX1a* induction (p<0.001, Student's *t*-test) (Figure 2Bi). This result was consistent with a higher level of the *LUC* transcript abundance in Col:*LUC* under AA treatment (12-fold induction, p<0.001, Student's *t*-test) compared to that of *rao2-1* (3-fold induction, p<0.001, Student's *t*-test) (Supplemental Figure 4). To confirm that the aberrations in transcriptional regulation of *AOX1a* were carried through at a protein level, Western blot analysis was carried out (Fig 2B iii). Consistent with the transcript analysis, AOX1a protein abundance was 4-fold higher (p<0.001, Student's *t*-test) in Col:*LUC* with AA treatment compared to *rao2-1* and *anac017-1* (Figure 2Biii). In the case of *anac017-2 AOX1a* transcript abundance was significantly

higher (p<0.01, Student's *t*-test) than Col:*LUC* under untreated conditions at all time points examined (Figure 2Bi). Thus, it appears that the *anac017-2* allele may produce a constitutively active functional protein that is able to induce *AOX1a* expression regardless of stress conditions and is likely to be a gain-of-function mutant. Notably induction of *AOX1a* in *anac017-2* was similar to both the *rao2-1* and ana0*17-1* mutants in that it was significantly reduced compared to Col-*LUC*.

Next, we examined the role of RAO2/ANAC017 in response to general cellular stresses. Excessive ROS are toxic to cells and it has been observed that *AOX1a* expression increases under conditions of oxidative stress (Vanlerberghe and McIntosh, 1997; Rhoads and Subbaiah, 2007; Millar et al., 2011). Seedlings were treated with 20 mM H_2O_2 for 6 h. 3 h after treatment a primary stress response was observed, with a greater than 6-fold *AOX1a* induction (*p*<0.001, Student's *t*-test) in Col:*LUC* plants (Figure 2Ci). H_2O_2 responsive induction of *AOX1a* was significantly reduced (*p*<0.001, Student's *t*-test) in *rao2-1* and *anac017-1* at both a transcript level and a protein level (Figure 2Ci and iii). In the case of *anac017-2,* as observed previously, the constitutive level of *AOX1a* was higher than in Col-*LUC,* however, in contrast to treatment with AA, treatment with H_2O_2 did induce *AOX1a* transcript. Two points to note are; i) induction with AA produced a greater induction in *AOX1a* than treatment with H_2O_2, in fact the response to AA in the *rao* mutant and T-DNA lines was still greater than the response in wild-type control, Col-*LUC*, to H_2O_2, and, ii) at 6 h the response was decreasing and was returning to untreated levels in Col-*LUC*, and also in mutants with H_2O_2 treatment. This is consistent with the LUC imaging results for the *rao* mutants, where imaging takes place 6 h after application of AA or H_2O_2. In the case of AA (and myxothiazol and MFA)

a large reduction in luminescence was still evident, but for H_2O_2 the difference after 6 h, while significant ($p<0.01$, Student's *t*-test), was smaller in magnitude (Supplemental Figure 1).

RAO2/ANAC017 binds to specific NAC binding sites in the AOX1a promoter

The identification of an annotated transcription factor (ANAC017) in this forward genetic screen for cellular components of mitochondrial retrograde signaling in plants prompts the obvious question; whether ANAC017 directly binds to the *AOX1a* promoter to influence stress responsive induction? Analysis of the *AOX1a* promoter sequence revealed three consensus NAC protein binding site sequences, (TG)CGTGT, identified in two independent studies (Tran et al., 2004; Olsen et al., 2005) (Figure 3A). NAC binding sites 1, 2 and 3 are at positions -311 bp, - 264 bp and -94 bp upstream from the transcriptional start site, respectively (Figure 3A). Transient biolistic transformation assays using GUS activity driven by the *AOX1a* promoter in Arabidopsis seedlings revealed that the *AOX1a* promoter activity increases significantly in response to AA treatment (Figure 3B). Mutation of any single NAC binding sites within the promoter showed limited or no significant changes for basal or induced promoter activity, however, when a combination of elements were deleted the basal promoter activity and stress inducibility were severely compromised ($p<0.01$, Student's *t*-test) (Figure 3B).

Further evidence of positive binding of RAO2/ANAC017 to the *AOX1a* promoter was detected by yeast-1-hybrid analyses, with RAO2/ANAC017 and *AOX1a* promoter fragments containing NAC binding sites 1, 2 and 3 (Figure 3C). Binding was greatly reduced, as evidenced by little or no yeast colony growth,

when NAC binding sites 2 and 3 were mutated, indicating that the binding of RAO2/ANC017 to binding site 2 and 3 was specific (Figure 3C). Finally, the binding of RAO2/ANC017 to the *AOX1a* promoter was also validated by electro mobility shift assays (EMSA). While NAC binding sites 1 and 3 did not show a specific interaction with ANAC017 protein (Figure 3D), a clear band shift of radiolabelled probes containing the NAC binding site 2 was detected when RAO2/ANAC017 protein was added (Figure 3D, NAC binding site 2), due to binding to the protein. Unlabeled NAC binding site 2 probes could effectively compete out binding (Figure 3D, NAC binding site 2) and mutation of the NAC binding site 2 resulted in a loss of that binding (Figure 3D, NAC binding site 2).

The positive, stress responsive control exerted by NAC binding site 2 within the *AOX1a* promoter was confirmed *in vivo* in Arabidopsis plants transformed with *AOX1a* promoter:*GUS* reporter constructs. The increase in GUS expression driven by the full length *AOX1a* promoter region in response to AA treatment was substantially reduced in transgenic plants carrying the promoter segment with the NAC binding site 2 mutated (Figure 3E). In conclusion, it is clear that at least one site in the *AOX1a* promoter, NAC binding site 2, is a canonical *cis*-acting regulatory element, necessary for the positive induction of the *AOX1a* promoter under AA treatment and that RAO2/ANAC017 was able to specifically bind to this NAC site 2 in the promoter.

RAO2/ANAC017 is co-localized to actin and endoplasmic reticulum and released to the nucleus upon removal of the C-terminal TM region

The sub-cellular localization of RAO2/ANAC017 was examined using green fluorescence protein (GFP) targeting assays. Full-length RAO2/ANAC017 fused to GFP was seen dispersed in the cytoplasm and formed a web-like

structure that did not co-localize with mitochondria (Figure 4A), unlike other transcription factors involved in plastid retrograde signaling that have been recently characterized to be bound within the organelle envelope (Sun et al., 2011). When the predicted TM region was deleted from the RAO2/ANAC017-GFP fusion, GFP fluorescence was only detected in the nucleus (Figure 4A ii). A GFP fusion containing only the predicted TM region of RAO2/ANAC017 displayed a similar pattern as the full-length construct (Figure 4A iii). Thus, it was concluded that the predicted TM region was responsible for the localisation of RAO2/ANAC017 outside the nucleus.

Furthermore, the full-length RAO2/ANAC017-GFP showed overlapping fluorescent signal with F-actin with two independent markers for actin. Firstly, with a rhodamine-labelled phalloidin control (Figure 4Bi) (Olyslaegers Verbelen 1988), and secondly, in co-transformations with an AtFimbrin-1-RFP control (Figure 4Bii) (Wang et al., 2004). Together these analyses confirm that RAO2/ANAC017 is co-localized with F-actin filaments within the cell. Endoplasmic reticulum (ER) is intimately connected with F-actin and forms a cellular transportation network (Boevink et al., 1998). Co-localisation with ER was also tested and revealed consistent overlapping fluorescent signal between the full-length RAO2/ANAC017-GFP and ER-RFP (Figure 4C). Thus, we concluded that RAO2/ANAC017 is targeted to connections and junctions in the ER and F-actin via a C-terminal TM domain and upon release of this domain is exclusively located in the nucleus.

To characterize the nature of RAO2/ANAC017 activation, a variety of treatments were carried out that have been previously used to inhibit the release of membrane bound transcription factors in plants (Seo et al., 2010a). Col:*LUC* plants were treated with a variety of inhibitors targeting various

proteases, MG132 (26S proteasome inhibitor), ALLN (calpain protease inhibitor), a protease inhibitor cocktail and 1,10-phenanthroline (a metalloprotease inhibitor), all failed to significantly reduce the induction of LUC activity in Col;*LUC* or inhibit the induction of *AOX1a* transcript abundance under AA treatment (Supplemental Figure 5). The ER stress response is characterized in plant and mammalian cells to be involved in protein release and modification events and therefore chemicals known to induce the ER stress response were also tested for the ability to activate the AA responsive induction of *AOX1a*. Tunicamycin, a mixture of homologous compounds that prevent the first committed step of N-linked glycosylation of proteins in the ER, causes extensive protein misfolding and induces a "slow motion" ER stress response (Li et al., 2011a). Treatment with tunicamycin resulted in normal *AOX1a* induction profiles in response to AA (Supplemental Figure 5C and D). However, interestingly, treatment with Dithiothreitol (DTT), that induces a "fast motion" ER stress response by inhibiting disulfide bond formation in proteins (Deng et al., 2011), resulted in no increase in LUC activity or *AOX1a* transcript abundance in response to mitochondrial stress (Supplemental Figure 5C and D). Finally, using a T-DNA mutant of the site 2-protease (S2-P), the latter previously shown to be required for the release of a variety of membrane tethered bZIP transcription factors (Seo et al., 2010a), the induction of *AOX1A* was not compromised in this mutant background (Supplemental Figure 5E).

Global transcriptional analysis reveals RAO2/ANAC017 as a high level primary response regulator in H_2O_2 mediated stress signaling

In order to investigate the extent of the transcriptional network regulated by this transcription factor under the two model stress treatments, i.e. AA and

H_2O_2, changes in the transcriptome were examined using microarray analysis. While AA acts as a inhibitor of mitochondrial electron transport, H_2O_2, in addition to being produced in mitochondria by manganese superoxide dismutase from the more reactive superoxide radical (O_2•−) (Murphy, 2009), can be produced by a variety of other cellular sources (Petrov and Van Breusegem, 2012). Analysis was carried out on Col:*LUC,* as a wild-type control, the *rao2-1* EMS mutant and the *anac017-1* T-DNA insertion knock-out line. Additionally, transcriptomic profiles were examined in *anac017-2*, that is predicted to be missing the TM region and thus likely to produce a truncated protein targeted to the nucleus based on the localization studies (Figure 2A, B and C).

For both AA stress treatment and H_2O_2 stress treatment, transcripts were catalogued into 1 of 4 gene list sets based on changes in transcript abundance in response to stress in wild-type versus the mutant lines (see Supplementary Figure 6 – AA and Supplementary Figure 7 – H_2O_2 for summary of classifications). For both treatments, genes classified as Group 1 did not change in transcript abundance in response to stress in any lines tested i.e. are constitutively expressed (7,767 genes for AA and 14,153 genes for H_2O_2). Group 2 consists of genes that are stress responsive in Col:*LUC* but changes in transcript abundance were not altered by *rao2-1* and *anac017-1* mutation, i.e. stress responsive genes that are regulated independently from RAO2/ANAC017 function (3297 genes for AA and 229 genes for H_2O_2) (Figure 5A and B). Genes from group 3 and 4 were stress responsive and this transcriptional response to stress was mediated either positively or negatively through ANAC017 functionality, respectively (Figure 5A and B, Supplemental Figure 6 and 7). These genes represented in Group 3 and Group 4 make up the

transcriptomic network regulated through ANAC017 as the primary stress response in plant cells in response to general oxidative stress and specific mitochondrial dysfunction (Supplemental Table 3).

To investigate the potential that signals induced via these two stress treatments may converge or overlap, the overlap in genes categorized into Groups 2, 3 and 4 were examined (Figure 5C). For Group 2 genes, as well as Group 3 and 4 genes, the overlap in these transcriptional responses for the two treatments was significantly less than would be expected by random chance, indicating that while there are some core transcripts regulated similarly in both treatments, signals mediating these responses are largely independent or integrate with other cellular signals (Figure 5C)

The proportions of the total stress responsive transcriptomic changes that are mediated through ANAC017 function were examined for the two stress treatments, compared to the percentage of stress response changes mediated independently of ANAC017 function. Strikingly, ANAC017 function is necessary and sufficient for the correct induction and repression of 87% of transcripts genome wide that are involved in a primary response to H_2O_2, and this cannot be compensated for by other transcription factors in plants lacking a functional ANAC017 (Figure 5D). Furthermore, this phenomenon was observed in the stress responses of two independent lines. The *rao2-1* EMS line and the *anac017-1* T-DNA knock-out line showed remarkable overlap in transcriptomic profiles in response to H_2O_2, with greater than 91% of transcripts (15,8550 out of 17,301) responding in a similar manner (Supplemental Figure 7). In contrast, only 40% of the AA response could be attributed to RAO2/ANAC017 function (Figure 5D), while the remaining 60% of AA responsive transcripts maintain the correct induction and repression in the absence of a functional ANAC017. This

indicates that AA treatment may recruit multiple signaling pathways from the mitochondria, utilizing numerous transcription factors or signal transduction mechanisms that allow redundancy and other factors to compensate for the absence of ANAC17 on a genomic scale. This redundancy may be provided by other NAC transcription factor family members (De Clercq et al., 2012).

ANAC017 is a high-level regulator mediating primary and specific response to stress via the induction of transcription factor cascades

Analysis of the 1116 genes positively regulated through the activity of RAO2/ANAC017 under AA treatment revealed 87 annotated as transcription factors (7.8% versus 4.9% of the whole genome annotated as transcription factors), and notably five other NAC transcription factors, *ANAC042, ANAC087, ANAC019, ANAC041, ANAC096* (arranged by order of fold-change in Col:*LUC*) were in this group (Supplemental Table 4). Notably, none of these NAC transcription factors are predicted to contain a TM region (Supplemental Figure 2). Notably, *BZIP60* is also within this list of stress responsive transcription factors that require ANAC017 functionality, which has defined roles in the first steps of ER-stress mediated release of other transcription factors in plant cells (Deng et al., 2011). Under H_2O_2 treatment, of the 837 genes that were defined as being positively regulated through the functionality of RAO2/ANAC017, 88 were annotated as transcription factors (10.5% versus 4.9% of the whole genome annotated as transcription factors), *ANAC019, ANAC042, ANAC102, ANAC055, ANAC087, ANAC046, ANAC003, ANAC032* were in this group, and again none are predicted to contain a TM region (Supplemental Table 4 and Supplemental Figure 2).

Furthermore, analysis of the second T-DNA insertion line, *anac017-2,* (Supplemental Figure 3), that likely contains a constitutively nuclear localized ANAC017 and has elevated levels of *AOX1a* transcript under untreated conditions, provided insight into the extent of secondary regulatory networks provided by the transcription factors that are directly regulated via ANAC017. Transcripts that are altered in abundance in this background are likely to represent components that are directly regulated via ANAC017 due to the constitutive nuclear localization in this line. Analysis of the 1000 bp promoter regions of the 533 transcripts with altered abundance in the *anac017-2* line under normal conditions show that greater than 65% contain a consensus NAC binding site in their promoters (350/533 genes, Supplemental Table 4). GO annotations for transcripts with altered abundance in this line are over-represented in components involved in responses to biotic and abiotic stress and are under-represented in the functional categories or cell organization, biogenesis, protein metabolism and development (Supplemental Figure 8, Supplementary Table 4). Additionally, 50 out of these 533 transcripts encode transcription factors, many of which with well established roles in the literature in regards to integrating stress and energy metabolism, and of these 50 transcription factors, 84% (42/50) contain one or more consensus NAC binding sites within their 1000bp promoter regions (Supplemental Table 4). Within this list of transcription factors, in order of magnitude of fold change, are *ANAC013*, *ANAC102, ANAC019, ANAC002/ATAF1* and *ANAC032*. Furthermore, all 5 of these NAC transcription factors contain one or more NAC consensus binding site within the promoter regions and are all likely to be implicated in regulating downstream secondary responses to cellular stress with metabolic signals and other stress signals (Supplementary Table 4, also see accompanying

manuscript). ANAC017 is significantly reduced in abundance in the *anac017-2* background; arguably as the result of secondary repression by the cell to dampen and regain control of wayward stress responses induced by the constitutive nuclear localization of ANAC017. Interestingly, ANAC002/ATAF1 is also significantly up-regulated in the *anac017-2* background under normal conditions. This transcription factor is a membrane bound transcription factor and has been linked with mediating and integrating cellular responses to abiotic and biotic stresses, ABA, drought and cellular ROS as a high level regulator (Wu et al., 2009). Together these analyses suggest that RAO2/ANAC017 is a high level regulator of NAC and other transcription factor families tightly coordinated with cellular stress responses.

In order to gain a better understanding of the RAO2/ANAC017 dependent and independent stress responsive changes, changes observed were compared to i) common changes that occur under oxidative stress as defined previously (Gadjev et al., 2006), and, ii) genes encoding mitochondrial proteins defined as stress responsive (Van Aken et al., 2009). In terms of stress responsive mitochondrial components RAO2/ANAC017 accounts for 11/26 and 10/26 of these changes under AA and H_2O_2 treatment (Supplemental Table 5). From 66 genes defined to change in the *flu* mutant, O_3 and methyl viologen (Gadjev et al., 2006), 34 of these transcripts were defined in this study as stress responsive and mediated via ANAC017 function (Supplemental Table 5). From these analyses it appears that RAO2/ANAC017 does not only account for a large proportion of the H_2O_2 driven changes in transcript abundance observed in this study, but can also be seen to account for ~50 % of the changes observed under various oxidative stress treatments from diverse cellular signals.

Physiological and phenotypic consequences of altered RAO2/ANAC017 expression

It has been previously shown that *aox1a* mutant plants are more sensitive to drought stress combined with moderate light treatment compared to wild-type and do not recover after re-watering (Giraud et al., 2008). As we have shown that RAO2/ANAC017 is a regulator of *AOX1a,* and is intimately linked with controlling stress responses genome wide to H_2O_2 in particular, the affect of this treatment on *rao2/anac017* mutants was also investigated. Exposure to moderate light (300 μE $m^{-2}s^{-1}$) during drought stress produced a notable difference in leaf color between Col-*LUC* and *rao2*, *anac017-1* and *aox1a* plants, in that wild-type remained largely green, in contrast to the other lines that were purple in color (Figure 6A top panel). Previously under similar conditions it was shown this was due to a 10-fold increase in anthocyanins in *aox1a* compared to wild-type plants (Giraud et al., 2008). Notably, *anaco17-2* appears to behave as wild-type, likely because of the constitutive nuclear localization of the ANAC17 in this line. The purple pigmentation resulting from increased anthocyanin content (Giraud et al., 2008) was much greater in *aox1a* and even greater in *rao2* and *anac017-1* plants. Both Col:*LUC* and *anac017-2* survived the stress treatment and recovered after being returned to normal conditions, while *rao2*, *anac017-1* and *aox1a* plants died (Figure 6A bottom panel). Analysis of cellular content of H_2O_2 by staining with 3,3'-diaminobenzidine (DAB) showed that there were no visible differences between non stressed leaves of Col:*LUC* and *rao2/anac017* mutants, however, for *anaco17-2* there were substantially lower levels of DAB precipitate indicating the response within these plants to a nuclear localized ANAC017 protein results in lower ROS production under normal conditions (Figure 6B left panel). No significant difference was observed

when visualizing superoxide levels by staining with nitroblue tetrazolium (NBT) (Figure 6B). Thus, dysfunction of RAO2/ANAC017 protein resulted in significantly reduced drought/moderate light stress tolerance possibly due to failed induction of AOX1a protein itself. In contrast, a gain of function allele, *anac017-2*, with elevated *AOX1a* transcript levels did not exhibit a stress phenotype and had less cellular H_2O_2 under normal conditions.

DISCUSSION

While the induction of *AOX* under a variety of treatments from several plant species has been documented (Millar et al., 2011), the results presented here identify a positive regulator required for mitochondrial retrograde signaling. The results presented support a role for RAO2/ANAC017 to directly bind the promoter region of *AOX1a* to regulate transcription, and also shed light on the mechanism of signal transduction from signals perceived in the cytosol that release ANAC017 from its bound state within the ER/F-actin to the nucleus to affect a response to stress. This dynamic sub-cellular localization provides a mechanism for the activation of RAO2/ANAC017 by mitochondrial generated ROS as follows; Actin, and F-Actin in particular, are well established to play a role in mitochondrial movement in several independent studies (Van Gestel et al., 2002; Sheahan et al., 2004; Wang et al., 2004; Sheahan et al., 2005; Boldogh and Pon, 2006; Logan, 2010), and also F-actin has been shown “to match precisely the architecture of the ER network” (Boevink et al., 1998). Thus, mitochondria and ER can be positioned together via interaction with F-actin. Intimate mitochondrial-ER interactions have been described in yeast and mammalian systems that play an important role in stress signaling (Pizzo and Pozzan, 2007; Kornmann and Walter, 2010). Thus, mitochondrial ROS

production, specifically H_2O_2, may directly signal RAO2/ANAC017 activation in the ER by close intimate contacts (this may also explain why ANAC017 activity seems so central to the transcriptomic response to H_2O_2). This signaling also means that ROS mediated mitochondrial signaling could be specific (Moller and Sweetlove, 2010). A recent study by Maruta et al., (2012) defined transcripts that respond specifically to plastid generated H_2O_2 signaling, interestingly there is little overlap between this list and the list of transcripts that respond to exogenous H_2O_2 application in the current study (only 15 transcripts show common responses out of greater than 1000 transcripts that are altered in abundance in the two studies) (Maruta et al., 2012). This would indicate that there is a distinct signal for plastid generated H_2O_2 separate from ANAC017 function or mitochondrial/cytosolic H_2O_2 production. It has been suggested that plastid generated H_2O_2 is involved with antagonistic signaling to balance pathways initiated via plastid generated superoxide and there appears to be little or no overlap with plastidial H_2O_2 production and the hallmarks of oxidative stress (Gadjev et al., 2006; Laloi et al., 2007; Maruta et al., 2012). Here, we have shown that ANAC017 is necessary for correct cellular responses to exogenous H_2O_2 signaling molecules, these stress responses are intimately linked with mitochondrial dysfunction and there is a significant overlap in these responses and those defined as hallmarks of general oxidative stress and superoxide stress (Supplemental Table 5). Thus, ANAC017 appears to induce a primary response to H_2O_2 at a point of convergence that is distinct from plastid specific H_2O_2. This also appears to be a primary response, due to the fact that it is most significantly compromised at the 3 h time point, by 6 h secondary transcriptional networks are induced to result in increased *AOX1a* transcript abundance (Figure 2). At 6 h and later, it is likely that downstream stress

responsive transcriptional networks are activated involving other transcription factors and further responses will need to be integrated with the specific metabolic needs of the cell (see accompanying manuscript (De Clercq et al., 2012).

The presence of a membrane tethered transcription factor immediately prompts the question of how it is released from the membrane under appropriate signals. Membrane tethered transcription factors are known in yeast and mammalian systems (Ye et al., 2000; Espenshade and Hughes 2007), S1P and S2P peptidases have been described that release the transcription factors upon stimulation (Seo et al., 2010a,b). Here, we show that the release of ANAC017 is not dependent on S2P function (Supplemental Figure 5). Interestingly, while there is very little overlap between the transcriptional responses mediated through ANAC017 activity in the current study and plastid generated H_2O_2 described above (Maruta et al., 2012), the top common transcript that responds to H_2O_2 in both these studies is a gene that encodes an S2P-like protease, At1g17870. This suggests that ANAC017 may play a role to activate the release of a variety of other membrane bound transcription factors integral to downstream secondary cellular responses to H_2O_2 production. As the addition of DTT suppresses the induction of *AOX1a* it suggests that the release of ANAC017 from the ER membrane is not dependent on an ER stress response, as has been described for other membrane bound transcription factors. The addition of DTT may suppresses the induction of *AOX1a* by simply acting to suppress H_2O_2 mediated signaling (Cvetkovska and Vanlerberghe, 2012), that is consistent with the finding in this study that ANAC017 accounts for >85% of the response to H_2O_2.

While the function of RAO2/ANAC017 is non-redundant in that induction of *AOX1a* was significantly reduced in its absence; the analysis of the promoter region suggests there is more than one binding site for RAO2/ANAC017 or other NAC transcription factors. Thus, it was the mutation of two or more NAC binding sites in combination that resulted in a decrease in *AOX1a* promoter activity. This suggests some synergy or possible redundancy exists between these sites, and that while the binding of RAO2/ANAC017 could only be detected for the predicted NAC binding site 2 in EMSA analyses; site 1 and 3 may also bind RAO2/ANAC017, as shown using the yeast one-hybrid assay and analysis of the *AOX1a* promoter activity. It is likely that the transcription factors induced by ANAC017 integrate with other secondary signals within the cell to mediate downstream responses; and this downstream control may even utilize the same NAC binding sites in the *AOX1a* promoter. For example, *ANAC013* is shown as the top transcription factor altered in abundance in the *anac017-2* mutant line, it contains a NAC binding site within the 1000 bp promoter and is likely to be involved with stress responsive induction in the *AOX1a* promoter via a so-called mitochondrial stress motif (MSM) (De Clercq et al., 2012). Notably, the NAC binding site 2 identified in the current study actually overlaps with this very MSM element identified to bind ANAC013. There are a number of other NAC transcription factors that bind the *AOX1a* promoter (see accompanying manuscript), and other factors that may activate *AOX1a* over longer time periods as part of secondary and tertiary signaling cascades, such as WRKY and other transcription factors (Dojcinovic et al., 2005; Giraud et al., 2009). Analysis of the list of genes that are regulated by RAO2/ANAC017 reveal that several transcription factors in the AP2 family, including DRE2B and RAP2 involved in resistance to abiotic stresses (Zhu, 2002; Mizoi et al., 2012),

and other NAC transcription factors, ATAF1/ANAC002 (Wu et al., 2009), ANAC042 (JUNGBRUNNEN1) (Wu et al., 2012), and ANAC019 (Bu et al., 2008). Many NAC transcription factors are known to play a role in mediating stress, development and growth responses (Chen et al., 2008; Nakashima et al., 2012), and NAC transcription factors represent one of the largest family of transcription factors in plants (Riechmann and Ratcliffe, 2000). However, no function has been previously ascribed to RAO2/ANAC017 in Arabidopsis.

Given the central role of ANAC017 in mediating ROS responses in the cell it is somewhat surprising that prior studies have not identified this factor. *RAO2/ANAC017* is not induced by stress or light treatment in Arabidopsis and the closest orthologous genes are not stress induced in *Oryza sativa* (Nuruzzaman et al., 2010), thus it could be over-looked in profiling experiments that look for stress responsive targets. Indeed, an analysis of ANAC017 alterations in transcript abundance across a number of aberrations, developmental and anatomical conditions in the public database Genevestigator (https://www.genevestigator.com/gv/) revealed that ANAC017 is constitutively expressed and only shows fold changes greater that 2.5 fold in 9 conditions out several hundred experimental conditions (Hruz et al., 2008) (Supplementary Figure 8B). Furthermore, inactivation of *RAO2/ANAC017* does not have a severely altered phenotype under normal/standard growth conditions, so it would be overlooked if directed screening was carried out. Thus, the forward screen carried out can identify important regulatory factors that would go unnoticed by other discovery based screening methods.

In conclusion, we have identified a biological role for ANAC017 as an integral cellular component in mitochondrial retrograde signaling and a high level transcriptional regulator that is necessary for H_2O_2 mediated primary

stress responses in plants. The location based regulation of ANAC017 functionality provides an elegant mechanism of signal transduction and integration within the plant cell under stress and together these results significantly contribute to our understanding of retrograde regulation pathways.

METHODS

Col:*LUC* Construction and Line Selection

The -1850 bp *AOX1a* promoter region upstream of the transcriptional start site, previously shown to be responsive to a variety of treatments that perturb mitochondrial function (Ho et al., 2008; Giraud et al., 2009), was translationally fused to a luciferase reporter gene in pCambia 1301 (http://www.cambia.org/daisy/cambia/585.html), using standard methods and transformed into *Arabidopsis thaliana,* Col-0 ecotype, to generate Col:*LUC* plants (Clough and Bent, 1998). A Col:*LUC* line with a single T-DNA insertion was identified by Southern blot analysis (Southern, 1975). Probe labelling and detection were carried out using Roche DIG High Prime DNA Labelling and Detection Starter Kit (Roche). GUS staining was carried out as previously described (Jefferson et al., 1987).

T-DNA insertion mutants

Two T-DNA insertion lines for *anac017* (SALK_022174 and *SALK_044777*) were obtained from the NASC (European Arabidopsis Stock Centre). T-DNA insertion homozygous lines were confirmed by PCR using the gene-specific primers (LP and RP) and T-DNA-specific primer (LB) (Supplemental Table 1). The location of the T-DNA insert was confirmed by sequencing. Additionally, knockout lines of the *Site 2 Protease*, *s2p* plants, in Arabidopsis encoded by

At4g20310 were obtained (NASC N444004) and *AOX1a* induction was measured in these lines in response to AA treatment (outlined below) by QRT-PCR.

Mutagenesis, Mutant Screen and Stress Treatments

Approximately 30,000 homozygous Col*:LUC* seeds were mutagenised for 16 h in 100 ml of 0.25% (*v/v*) EMS, then washed in several volumes of water over a period of 6 h. Seeds were sown on soil and grown in growth chambers at 22 °C, 16 h 120 µmol $m^{-2}s^{-1}$ light /8 h dark. M2 seeds from ~ 2,000 M1 plants were harvested and pooled in 20 individual families. Approximately 20,000 M2 plants, representing all 20 families were screened for altered *LUC* reporter gene expression Plants were grown for 14 days on Gamborg's B5 growth media (PhytoTechnology) with 3% (*w/v*) sucrose and 0.75% agar (*w/v*). Plants were sprayed with 50 µM AA, 50 µM myxothiazol, 25 mM Sodium Fluoroacetate (MFA), 200 µM ABA or 50 µM SA or treated for 18 h at 4^{o}C in the dark (cold treatment) or 30 min under UV light (280 – 100 nm), and after 6 h sprayed with 2.5 mM luciferin (GoldBio), and luminescence was measured using a NightOWL bioluminescence imaging system (Berthold). Quantification of LUC expression was performed by calculating the Integrated Light Intensity from 8-bit images using the Image Processing and Analysis tool in ImageJ (Collins, 2007). Measurements were taken from plants grown on a minimum of 3 independent plates. Averages and standard errors are shown. Protease inhibitor treatment was applied as follows: 14 day old plants were sprayed with water, 5 µg/ml Tunicamycin (Sigma) or 4 mM Dithiothreitol (DTT) (Sigma). Thirty min later plants were sprayed with AA and screened as described above or plant tissue collected 3 h after AA treatment for qRT-PCR.

Genetic Mapping and Gene Identification

rao2 mutants were crossed with Arabidopsis ecotype Landsberg *erecta* (L.*er*) transgenic plants that also contained a single T-DNA insert of the same *AOX1a:LUC* construct. Homozygous F2 *rao2* plants were selected according to their phenotype and DNA extracted. Linkage between Small Sequence Length Polymorphism (SSLP) markers (Bell and Ecker, 1994) across the genome and a mutation was established based on a low recombination frequency. Markers were selected from Cereon database - www.arabidopsis.org/Cereon/index.jsp (Supplementary Table 1). Full-length coding sequence of *ANAC017* was PCR amplified from Col-0 cDNA, cloning, transformation and selection of transformants were carried out using standard procedures (Clough and Bent, 1998; Harrison et al., 2006)Next Generation

Sequencing and Data Analysis 50 ng of genomic DNA isolated from pooled Arabidopsis seedlings for each line (Col:*LUC* (wild-type), *rao2-1* and *rao2-2* was isolated using DNeasy Plant Maxi kit (QIAGEN). Genomic DNA was used as input in library generation using Nextera DNA sample prep kits (EpiCentre). Library quality, sequencing with 2x50 bp paired-end read lengths on an Illumina HiSeq1000 and data processing are outlined in Supplemental Materials and Mathods.

Quantitative Reverse Transcriptase PCR (qRT-PCR)

Rosette leaf tissue from Col*:LUC*, *rao2-1, anac017-1* and *anac017-2* 14-day-old seedlings treated with 50 µM AA or 20 mM H_2O_2, as described above, were harvested in biological triplicate at 1 h, 3 h and 6 h after treatment. RNA

isolation, cDNA generation and QRT-PCR were performed as described previously (Giraud et al., 2008). For mock control, plants were treated with deionised water. Primers and assay details for *AOX1a* have been described previously (Giraud et al., 2008). *LUC* primers are listed in Supplemental Table 1.

Western Blots

Mitochondria were isolated from 14-day-old plants treated with 50 µM AA and 20 mM H_2O_2, as described above. Immunodetections were carried out as described previously (Wang et al. 2012) using antibodies to AOX (Elthon et al., 1989) and TOM40 (Carrie et al., 2009). To ensure linearity of detection three dilution of mitochondria were loaded. The intensity of cross reacting bands where quantitated at Quantity One software (Bio-Rad, Sydney). The pixel densities were expressed relative to Col-*LUC*, where the highest value adjusted to 100 (i.e. mitochondria isolated from Col-*LUC* treated with AA). Three biological replicates were performed average determined. The intensity of the cross reacting bands probed with the antibody to AOX was adjusted to the intensity of TOM40 that was used as a loading control.

Transient Transformation Constructs

A pLUS transformation vector containing 1850 bp upstream sequences of *AOX1a* promoter driving a beta-glucuronidase (GUS) gene, previously used in (Ho et al., 2008), was used a template for the mutagenesis of NAC binding sites using Quik®Change II XL Site-Directed Mutagenesis Kit (Stratagene) according to the manufacturer's instructions. Site-directed mutagenesis primers are listed in Supplemental Table 1.

Biolistic Transient Transformation

Col-0 suspension cell culture was grown on 1/2 MS growth medium (PhytoTechnology), supplemented with 3% (*w/v*) sucrose and 0.75% (*w/v*) agar, under continuous 120 µmol $m^{-2}s^{-1}$ light for 5 d before transformations. Transformation was performed with PDS-1000 system with the hepta adaptor according to the manufacturer's instructions (Bio-Rad), as described previously (Ho et al., 2008). Seedlings were sprayed with 50 µM AA or deionised water (mock) 2 h before and after the transformations. Tissue was collected 24 h after transformation. At least 3 independent transformations were carried out for each construct and 3 technical replicates were measured for each transformation. The promoter activities were measured and analyzed as described previously (Ho et al., 2008).

Yeast One-Hybrid Screen

The coding sequence of *RAO2/ANAC017* was cloned from Arabidopsis Col-0 cDNA into pDRIVE (Qiagen) using standard protocols. The PCR products were then subcloned into the pGADT7-rec2 prey vector (Clontech). The pGADT7-rec2-p53 prey vector in combination with p53HIS2 was used as a positive control as outlined in manufacturers' instructions (Clontech). Approximately 50 bp surrounding the putative NAC-binding sites were cloned into pHIS2 vector upstream of the *HIS3* promoter region and *HIS3* reporter gene. Yeast one-hybrid screens were performed in strain Y187 strain according to Clontech Matchmaker One Hybrid kit (Clontech). Transformed cells were grown on SD media –Leu/Trp to select for co-transformed cells and SD media –His/Leu/Trp containing 150 mM 3-amino-1,2,4-triazole (3-AT; Sigma-Aldrich).

Electromobility Shift Assays

30-40 bp oligonucleotide probes (Supplemental Table 1) with wild-type or deleted NAC binding sites were annealed by heating to 99 °C and cooled gradually. Annealed probes were radiolabelled using ^{32}P γ-ATP (Perkin Elmer) and polynucleotide kinase (Roche), and purified using Sephadex G-25 radiolabelled DNA Quick Spin columns (Roche). The full coding sequence of ANAC017 was cloned into GST-tag expression vector pDEST15 (Invitrogen) and transformed into Rosetta^{TM} 2(DE3) pLysS competent expression cells (Life technologies). For gel shift assays, 20 µL reactions were setup with 4 µL 5x binding buffer (100 mM HEPES pH 7.8, 0.5 M KCl, 5 mM $MgCl_2$, 2.5 mM DTT, 5 mM EDTA, 0.25 mg/mL poly dI-dC, 50% (*v/v*) glycerol), 1 fmol radiolabelled probe (500 fmol unlabelled probe for competitor reactions), 1.5 µg purified protein extract. Reactions were incubated for 20 min and separated on polyacrylamide gels (0.5x TBE, 2.5% glycerol, 6% acrylamide) for 2 h at 200V on a 16 x 20 cm^2 Bio-Rad Protean II gel system.

GFP Targeting Assay

The cDNAs of full-length ANAC017 (AA 1 to 557), ANAC017 minus the predicted transmembrane domain (AA 1 to 523) and the predicted isolated transmembrane of ANAC017 (AA 458 to 557) (see Figure 4) were cloned in frame with GFP using Gateway® cloning (Invitrogen), as previously described (Carrie et al., 2009). Constructs were biolistically transformed into both Arabidopsis cell suspension and onion epidermal cell (Carrie et al., 2007). In addition to the GFP constructs, a series of organelle markers were employed, including: an ER targeted RFP (Nelson et al., 2007), a mitochondrial targeted RFP (Carrie et al., 2007) and the isolated actin-binding domain of the ATFIM1

protein (At4g26700) fused to RFP. Additionally, actin was stained using the glycerol method for actin staining outlined in (Olyslaegers and Verbelen, 1998), with a rhodamine-labelled phalloidin conjugate (Invitrogen, Molecular Probes®). Visualisation of the fluorescent proteins was carried out using an Olympus BX61 fluorescence microscope (Olympus) with excitation wavelengths of 460/480 nm for GFP and 535/555 nm for RFP; while emission wavelengths were measured at 495-540 nm for GFP and 570-625 nm for RFP. Micrographs were captured and processed using Cell® imaging software as previously described (Carrie et al., 2007).

Global Transcript Analyses

Analysis of the global changes in transcript abundance in response AA treatment in the *rao2* mutant was carried out using Affymetrix ATH1 microarray gene chips. Arrays were performed using RNA isolated 3 h post treatment in biological triplicate from Col:*LUC*, *rao2-1, anac017-1* and *anac017-2.* 14-day-old seedlings were treated with 50 µM AA or 10 mM H_2O_2.

Accession Numbers

RAO2/ANAC017 (At1g34190) and *AOX1a* (At3g22370). All microarray data has been deposited at GEO (http://www.ncbi.nlm.nih.gov/geo) under the accession dataset (GSE41136).

Supplemental Data

Supplemental information includes 9 figures and 5 tables.

Supplemental Figure 1. Characterisation and quantification of *AOX1a* promoter inductions in *rao2-1* and *rao2-2* following different stress treatments.

Supplemental Figure 2 Phylogenetic analyses of NAC domain containing transcription factors closely related to AT1G34190, ANAC017**.**

Supplemental Figure 3. Confirmation of T-DNA insertion lines, *anac017-1* and *anac017-2*.

Supplemental Figure 4. *LUC* Transcript level in *rao2-1* under AA and H_2O_2 treatment.

Supplemental Figure 5. *AOX1a* induction under AA treatment in the presence of protease inhibitors.

Supplemental Figure 6. Overview of microarray analysis for Antimycin A

Supplemental Figure 7. Overview of microarray analysis for H_2O_2.

Supplemental Figure 8. ANAC017 is constitutively expressed and regulates stress responsive transcripts genome wide.

Supplemental Figure 9. Phenotypic analysis of *rao2* mutants.

Supplemental Table 1. List of primers.

Supplemental Table 2. Next-gen sequencing candidate SNP calls.

Supplemental Table 3. RAO2/ANAC017 regulated stress responsive transcripts based on microarray analyses.

Supplemental Table 4. Transcripts regulated by ANAC017 function that encode transcription factors**.**

Supplemental Table 5. Overlap between RAO2/ANAC017 regulated stress responsive transcript and hallmarks of oxidative stress.

Acknowledgements

This work was supported by an Australian Research Council Centre of Excellence Grant CEO561495.

AUTHOR CONTRIBUTIONS

JW and AI conceived and designed the screen. AI carried out the screen. AI, SN and EG carried out the genetic mapping, complementation, QRT-PCR transcript measurements and microarray analysis. SN carried out the SDM and biolistic transient transformation. OD and YW carried out biochemical analyses, SL, LX and CC carried out GFP localization, EG and HW carried out bioinformatic analyses of NGS data, OVA carried out yeast 1-hybrid and EMSA. EG, SN, AI, FvB, IdC and JW, designed and interpreted results with regards to integration with cellular stress and energy pathways. All authors contributed to writing the manuscript.

FIGURE LEGENDS

Figure 1. Identification of RAO2/ANAC017 as a regulator of AOX1a. (A) 14 day old seedlings (top panel) and luminescence of Col:*LUC* and *rao2* mutants after treatment with antimycin A (AA). Col:*LUC* plants generated from Columbia-0 transformed with a construct with a firefly luciferase reporter gene driven by the *ALTERNATIVE OXIDASE1A* promoter (*AOX1a-LUC*). Luciferase activity was then visualised in a NightOwl bioluminescence imager. (**B)** Luminescence of *rao2-1* and *rao2-2* after 6 h myxothiazol treatment. (**C)** Quantified luminesence of *rao2* mutants 6 h following AA or myxothiazol treatment. **(D)** Allelic test of *rao2-1* and *rao2-2*. F1 seedlings were the first generation from a cross between *rao2-1* and *rao2-2* mutants. **(E)** Complementation test of *rao2-1* transformed with full-length coding sequences of *ANAC017*. F2 generation of transformants (Complement) were able to induce LUC following AA treatment. **(F)** Next-generation sequence analysis identifying a candidate mutation in ANAC017 (At1g34190) **(G)** *ANAC017* gene model. ANAC017 contains a predicted NAC domain at its N-terminus and a predicted transmembrane (TM) domian at the C-terminus. Sanger sequencer analysis of *rao2-1* and *rao2-2* confirmed the point mutations that caused amino acid changes **(H)** Alignment of NAC proteins from rice (OANAC) and Arabidopsis (ANAC). Identical amino acids are coloured in black and amino acids that shared high similarity are coloured in grey. Asterisk indicates the position of the point mutation in *rao2* mutants.

Figure 2. Characterisation of *AOX1a* transcript and protein abundance in *rao2* and *anac017* T-DNA Insertion Lines. (A) A schematic gene model of

ANAC017. Numbers indicate the nucleotide position of the mutation or the T-DNA insertion. *rao2* mutants are marked in red asterisks and position of the T-DNA inserts (*anac017-1* and *anac017-2*) are indicated by inverted triangles. TSS, transcriptional start site; TM, transmembrane domain; NLS, putative nuclear localisation signal; NAC domain. **(B)** *AOX1a* transcript (i), Ubiquitin transcript (ii), and AOX1a protein (iii) abundance under antimycin A treatment. (i) Two-week-old seedlings were exposed to 50 µM of AA or deionised water (Mock, -AA) and were harvested at 1 h, 3 h and 6 h and transcript abundance analysed by QRT-PCR. (ii) *Ubiquitin* (*UBC*) was used as transcript abundance control. (iii) Protein abundance was quantified and AOX1a abundance was normalized against the corresponding TOM40-1 to give a loading corrected quantification. Relative protein abundance, below each blot, was expressed as a percentage of the highest value of the set, i.e. for AOX1a that is Col:*LUC* treated with AA set to 100**.** Apparent mol mass is indicated in kD. **(C)** As B except that induction was carried out with H_2O_2.

Figure 3. RAO2/ANAC017 binds to predicted NAC binding sites in the *AOX1a* Promoter. (A) A schematic diagram of *AOX1a* promoter region with NAC binding sites 1, 2 and 3. TSS, transcriptional start site. **(B)** Analysis of *AOX1a* promoter activity using GUS reporter assay. Wild-type plants (Col-0) were transiently transformed with constructs expressing wild-type *AOX1a* promoters fused with b-glucuronidase (GUS) or with constructs with NAC binding sites mutated in the *AOX1a* promoter. Asterisks indicates a significantly difference of GUS activity between wild-type promoter and mutated promoter constructs. Symbol # indicates significant induction of GUS activity between mock-treated (deionised water) control and antimycin A (AA) treatment. **(C)**

Yeast-one hybrid binding assay of RAO2/ANAC017 to *AOX1a* promoter. Bait vector contained a 50-bp region surrounding NAC binding sites. Prey vector contained the full-length coding sequence of *RAO2/ANAC017*. Serial dilutions of co-transformed yeast were spotted on synthetic dropout (SD) –Trp/Leu to select for co-transformants and SD-Trp/Leu/His to select for positive interactions. Numbers 1, 2 and 3 in bold represent predicted NAC binding site 1, 2 and 3 in *AOX1a* promoter. ∆NAC binding site are bait vector with NAC binding site deleted. The binding of p53 was used as positive (+) and negative (-) control according to manufacturer's instructions (Clontech). Trp, tryptophan; Leu, leucine; His, histidine. **(D)** Binding of RAO2/ANAC017 to NAC binding site 2 in the *AOX1a* promoter as determined by electromobility shift assay. **(E)** GUS histochemical staining of 13 day old transgenic Arabidopsis seedlings carrying either the wild-type *AOX1a* 1.85kb promoter driving GUS expression (top panel) or a construct with the NAC binding site 2 deleted (bottom panel) 6 h post Antimycin A treatment.

Figure 4. *In vivo* targeting of full-length and truncated forms of RAO2/ANAC017 linked to green fluorescence protein (A) Subcellular targeting of (i) Full-length RAO2/ANAC017, (ii) full-length RAO2/ANAC017 minus the predicted transmembrane (TM) region, and, (iii) the predicted TM region of RAO2/ANAC017 were tagged with green fluorescence protein (GFP) to assess targeting ability. These three constructs were transiently transformed into both Arabidopsis suspension cells and onion epidermal cells, in addition to a mitochondrial red fluorescence protein (Mito-RFP) control (see materials and methods). **(B)** Co-localization of RAO2/ANAC017 to actin filaments. Based on the localizations observed for the full-length construct, co-localization of

RAO2/ANAC017 was confirmed with (i), actin stained with rhodamine-labelled phalloidin control and (ii) AtFim1-RFP control. A magnified view of this co-localization has been provided. **(C)** Co-localization of RAO2/ANAC017 to endoplasmic reticulum (ER) with a ER-RFP control.

Figure 5. Characterization of the genome-wide transcriptional response to stress that is regulated through RAO2/ANAC017 and cannot be compensated for by other cellular components. Hierarchical cluster of gene set lists categorized as either positively or negatively regulated through ANAC017 activity under **(A)** Antimycin A (AA) or **(B)** H_2O_2 treatment, as described in Supplemental Figure 6-7. Blue color represent transcripts that are down-regulated in response to treatment and red/yellow color represented transcript that are up-regulated in response to treatment as shown by the color scale, log2 fold changes in untreated vs treated conditions. Fold changes in response to stress were calculated for Col:*LUC* (wild-type), *rao2-1* and *anac017*-1 T-DNA insertional knock-out lines. **(C)** Overlap in specific transcriptional responses for transcripts classified in each of the gene lists based on their regulation in regards to RAO2/ANAC017 under treatment. There was significantly less overlap than expected by random chance between the transcriptional responses for AA and H_2O_2 treatment. **(D)** Proportional breakdown of the degree that the response to AA or H_2O_2 is mediated through RAO2/ANAC017 function genome-wide.

Figure 6. Characterization of the physiological sensitivity to environmental stress and H_2O_2 in *rao2/anac017*. (A) Thirty-four-day old plants growth for 16 h at 120 µmol $m^{-2}s^{-1}$ light/ 8 h dark, 22 ºC were transferred

to 16 h at 300 µmol $m^{-2}s^{-1}$ light/ 8 h dark, 22 ºC without watering and response observed for 5 and 7 day, after which water was re-supplied at 120 µmol $m^{-2}s^{-1}$ light. **(B)** Thirty-four-day old plants growth for 16 h at 120 µmol $m^{-2}s^{-1}$ light/ 8 h dark, 22 ºC were stained for H_2O_2 (DAB - 3,3'-Diaminobenzidine) and superoxide radical $O_2^{\bullet -}$ (NBT - Nitroblue tetrazolium).

References

Bell, C.J., and Ecker, J.R. (1994). Assignment of 30 microsatellite loci to the linkage map of Arabidopsis. Genomics **19,** 137-144.

Boevink, P., Oparka, K., Santa Cruz, S., Martin, B., Betteridge, A., and Hawes, C. (1998). Stacks on tracks: the plant Golgi apparatus traffics on an actin/ER network. Plant J. **15,** 441-447.

Boldogh, I.R., and Pon, L.A. (2006). Interactions of mitochondria with the actin cytoskeleton. Biochim. Biophys. Acta **1763,** 450-462.

Bu, Q., Jiang, H., Li, C.B., Zhai, Q., Zhang, J., Wu, X., Sun, J., Xie, Q., and Li, C. (2008). Role of the Arabidopsis thaliana NAC transcription factors ANAC019 and ANAC055 in regulating jasmonic acid-signaled defense responses. Cell Res. **18,** 756-767.

Butow, R.A., and Avadhani, N.G. (2004). Mitochondrial signaling: the retrograde response. Mol. Cell **14,** 1-15.

Carrie, C., Murcha, M.W., Millar, A.H., Smith, S.M., and Whelan, J. (2007). Nine 3-ketoacyl-CoA thiolases (KATs) and acetoacetyl-CoA thiolases (ACATs) encoded by five genes in Arabidopsis thaliana are targeted either to peroxisomes or cytosol but not to mitochondria. Plant Mol. Biol. **63,** 97-108.

Carrie, C., Kuhn, K., Murcha, M.W., Duncan, O., Small, I.D., O'Toole, N., and Whelan, J. (2009). Approaches to defining dual-targeted proteins in Arabidopsis. Plant J. **57,** 1128-1139.

Chen, Y.N., Slabaugh, E., and Brandizzi, F. (2008). Membrane-tethered transcription factors in Arabidopsis thaliana: novel regulators in stress response and development. Curr. Opin. Plant Biol. **11,** 695-701.

Clifton, R., Lister, R., Parker, K.L., Sappl, P.G., Elhafez, D., Millar, A.H., Day, D.A., and Whelan, J. (2005). Stress-induced co-expression of alternative respiratory chain components in Arabidopsis thaliana. Plant Mol. Biol. **58,** 193-212.

Clough, S.J., and Bent, A.F. (1998). Floral dip: a simplified method for Agrobacterium-mediated transformation of Arabidopsis thaliana. Plant J. **16,** 735-743.

Collins, T.J. (2007). ImageJ for microscopy. Biotechniques **43,** 25-30.

Cvetkovska, M., and Vanlerberghe, G.C. (2012). Alternative oxidase modulates leaf mitochondrial concentrations of superoxide and nitric oxide. New Phytol. **195,** 32-39.

De Clercq, I., Vermeirssen, V., Van Aken, O., Vandepoele, K., Murcha, M.W., Law, S., Inzé, A., Ng, S., Ivanova, A., Rombout, D., van de Cotte, B., Japsers, P., Kangasjärvi,, J., Whalna, J., Van Breusegem, F. A membrane-bound NAC transcription factor is a regulator of mitochondrial retrograde regulation of the oxidative stress response in *Arabidopsis thaliana* (Submitted to Plant Cell as accompanying manuscript.

Deng, Y., Humbert, S., Liu, J.X., Srivastava, R., Rothstein, S.J., and Howell, S.H. (2011). Heat induces the splicing by IRE1 of a mRNA encoding a transcription factor involved in the unfolded protein response in Arabidopsis. Proc. Natl. Acad. Sci. U S A **108,** 7247-7252.

Dojcinovic, D., Krosting, J., Harris, A.J., Wagner, D.J., and Rhoads, D.M. (2005). Identification of a region of the Arabidopsis AtAOX1a promoter necessary for mitochondrial retrograde regulation of expression. Plant Mol. Biol. **58,** 159-175.

Elthon, T.E., Nickels, R.L., and McIntosh, L. (1989). Monoclonal antibodies to the alternative oxidase of higher plant mitochondria. Plant Physiol. **89,** 1311-1317.

E**spenshade, P.J., Hughes, A.L.** (2007). Regulation of Sterol Synthesis in Eukaryotes. Annu. Rev. Genet. **41,** 401-427.

Estavillo, G.M., Crisp, P.A., Pornsiriwong, W., Wirtz, M., Collinge, D., Carrie, C., Giraud, E., Whelan, J., David, P., Javot, H., Brearley, C., Hell, R., Marin, E., and Pogson, B.J. (2011). Evidence for a SAL1-PAP chloroplast retrograde pathway that functions in drought and high light signaling in Arabidopsis. Plant Cell **23,** 3992-4012.

Gadjev, I., Vanderauwera, S., Gechev, T.S., Laloi, C., Minkov, I.N., Shulaev, V., Apel, K., Inze, D., Mittler, R., and Van Breusegem, F. (2006). Transcriptomic footprints disclose specificity of reactive oxygen species signaling in Arabidopsis. Plant Physiol. **141,** 436-445.

Giraud, E., Van Aken, O., Ho, L.H., and Whelan, J. (2009). The transcription factor ABI4 is a regulator of mitochondrial retrograde expression of ALTERNATIVE OXIDASE1a. Plant Physiol. **150,** 1286-1296.

Giraud, E., Ho, L.H., Clifton, R., Carroll, A., Estavillo, G., Tan, Y.F., Howell, K.A., Ivanova, A., Pogson, B.J., Millar, A.H., and Whelan, J. (2008). The absence of ALTERNATIVE OXIDASE1a in Arabidopsis results in acute sensitivity to combined light and drought stress. Plant Physiol. **147,** 595-610.

Harrison, S.J., Mott, E.K., Parsley, K., Aspinall, S., Gray, J.C., and Cottage, A. (2006). A rapid and robust method of identifying transformed Arabidopsis thaliana seedlings following floral dip transformation. Plant Methods **2,** 19.

Ho, L.H., Giraud, E., Uggalla, V., Lister, R., Clifton, R., Glen, A., Thirkettle-Watts, D., Van Aken, O., and Whelan, J. (2008). Identification of regulatory pathways controlling gene expression of stress-responsive mitochondrial proteins in Arabidopsis. Plant Physiol. **147,** 1858-1873.

Hruz, T., Laule, O., Szabo, G., Wessendorp, F., Bleuler, S., Oertle, L., Widmayer, P., Gruissem, W., and Zimmermann, P. (2008). Genevestigator v3: a reference expression database for the meta-analysis of transcriptomes. Adv Bioinformatics **2008,** 420747.

Jefferson, R.A., Kavanagh, T.A., and Bevan, M.W. (1987). GUS fusions: beta-glucuronidase as a sensitive and versatile gene fusion marker in higher plants. EMBO J. **6,** 3901-3907.

Kim, S.G., Lee, S., Seo, P.J., Kim, S.K., Kim, J.K., and Park, C.M. (2010). Genome-scale screening and molecular characterization of membrane-bound transcription factors in Arabidopsis and rice. Genomics **95,** 56-65.

Kornmann, B., and Walter, P. (2010). ERMES-mediated ER-mitochondria contacts: molecular hubs for the regulation of mitochondrial biology. J. Cell Sci. **123,** 1389-1393.

Laloi, C., Stachowiak, M., Pers-Kamczyc, E., Warzych, E., Murgia, I., and Apel, K. (2007). Cross-talk between singlet oxygen- and hydrogen peroxide-dependent signaling of stress responses in Arabidopsis thaliana. Proc. Natl. Acad. Sci. U S A **104,** 672-677.

Li, B., Yi, P., Zhang, B., Xu, C., Liu, Q., Pi, Z., Xu, X., Chevet, E., and Liu, J. (2011a). Differences in endoplasmic reticulum stress signalling kinetics determine cell survival outcome through activation of MKP-1. Cell Signal. **23,** 35-45.

Logan, D.C. (2010). Mitochondrial fusion, division and positioning in plants. Biochem. Soc. trans. **38,** 789-795.

Maruta, T., Noshi, M., Tanouchi, A., Tamoi, M., Yabuta, Y., Yoshimura, K., Ishikawa, T., and Shigeoka, S. (2012). H2O2-triggered retrograde signaling from chloroplasts to nucleus plays specific role in response to stress. J. Biol. Chem. **287,** 11717-11729.

Millar, A.H., Whelan, J., Soole, K.L., and Day, D.A. (2011). Organization and regulation of mitochondrial respiration in plants. Annu. Rev. Plant Biol. **62,** 79-104.

Mizoi, J., Shinozaki, K., and Yamaguchi-Shinozaki, K. (2012). AP2/ERF family transcription factors in plant abiotic stress responses. Biochim. Biophys. Acta **1819,** 86-96.

Moller, I.M., and Sweetlove, L.J. (2010). ROS signalling--specificity is required. Trends Plant Sci. **15,** 370-374.

Murphy, M.P. (2009). How mitochondria produce reactive oxygen species. Biochem. J. **417,** 1-13.

Nakashima, K., Takasaki, H., Mizoi, J., Shinozaki, K., and Yamaguchi-Shinozaki, K. (2012). NAC transcription factors in plant abiotic stress responses. Biochim. Biophys. Acta **1819,** 97-103.**Nelson BK, Cai X, Nebenfuhr A. 2007.** A multicolored set of in vivo organelle markers for co-localization studies in Arabidopsis and other plants. Plant J. **51**(6): 1126-1136.

Nomura, H., Komori, T., Uemura, S., Kanda, Y., Shimotani, K., Nakai, K., Furuichi, T., Takebayashi, K., Sugimoto, T., Sano, S., Suwastika, I.N., Fukusaki, E., Yoshioka, H., Nakahira, Y., and Shiina, T. (2012).

Chloroplast-mediated activation of plant immune signalling in Arabidopsis. Nat. Commun. **3,** 926.

Nuruzzaman, M., Manimekalai, R., Sharoni, A.M., Satoh, K., Kondoh, H., Ooka, H., and Kikuchi, S. (2010). Genome-wide analysis of NAC transcription factor family in rice. Gene **465,** 30-44.

Olsen, A.N., Ernst, H.A., Leggio, L.L., and Skriver, K. (2005). NAC transcription factors: structurally distinct, functionally diverse. Trends Plant Sci. **10,** 79-87.

Olyslaegers, G., and Verbelen, J-P. (1998). Improved staining of F-actin and co-localization of mitochondria in plant cells. J. Microscopy **192,** 73-77.

Ooka, H., Satoh, K., Doi, K., Nagata, T., Otomo, Y., Murakami, K., Matsubara, K., Osato, N., Kawai, J., Carninci, P., Hayashizaki, Y., Suzuki, K., Kojima, K., Takahara, Y., Yamamoto, K., and Kikuchi, S. (2003). Comprehensive analysis of NAC family genes in Oryza sativa and Arabidopsis thaliana. DNA Res. **10,** 239-247.

Petrov, V.D., and Van Breusegem, F. (2012). Hydrogen peroxide-a central hub for information flow in plant cells. AoB plants **2012,** pls014.

Pfannschmidt, T. (2010). Plastidial retrograde signalling--a true "plastid factor" or just metabolite signatures? Trends Plant Sci. **15,** 427-435.

Pizzo, P., and Pozzan, T. (2007). Mitochondria-endoplasmic reticulum choreography: structure and signaling dynamics. Trends Cell Biol. **17,** 511-517.

Ramel, F., Birtic, S., Ginies, C., Soubigou-Taconnat, L., Triantaphylides, C., and Havaux, M. (2012). Carotenoid oxidation products are stress signals that mediate gene responses to singlet oxygen in plants. Proc. Natl. Acad. Sci. U S A **109,** 5535-5540.

Rhoads, D.M., and Subbaiah, C.C. (2007). Mitochondrial retrograde regulation in plants. Mitochondrion **7,** 177-194.

Riechmann, J.L., and Ratcliffe, O.J. (2000). A genomic perspective on plant transcription factors. Curr. Opin. Plant Biol. **3,** 423-434.

Rieske, J.S., Lipton, S.H., Baum, H., and Silman, H.I. (1967). Factors affecting the binding of antimycin A to complex 3 of the mitochondrial respiratory chain. J. Biol. Chem. **242,** 4888-4896.

Seo, P.J., Kim, M.J., Song, J.S., Kim, Y.S., Kim, H.J., and Park, C.M. (2010a). Proteolytic processing of an Arabidopsis membrane-bound NAC transcription factor is triggered by cold-induced changes in membrane fluidity. Biochemical J. **427,** 359-367.

Seo, P.J., Kim, M.J., Park, J.Y., Kim, S.Y., Jeon, J., Lee, Y.H., Kim, J., and Park, C.M. (2010b). Cold activation of a plasma membrane-tethered NAC transcription factor induces a pathogen resistance response in Arabidopsis. Plant J. **61,** 661-671.

Sheahan, M.B., Rose, R.J., and McCurdy, D.W. (2004). Organelle inheritance in plant cell division: the actin cytoskeleton is required for unbiased inheritance of chloroplasts, mitochondria and endoplasmic reticulum in dividing protoplasts. Plant J. **37,** 379-390.

Sheahan, M.B., McCurdy, D.W., and Rose, R.J. (2005). Mitochondria as a connected population: ensuring continuity of the mitochondrial genome during plant cell dedifferentiation through massive mitochondrial fusion. Plant J. **44,** 744-755.

Shen, H., Yin, Y., Chen., F., Xu, Y., and Dixon, R.A. (2009). A bioinformatic analysis of NAC genes for plant cell wall developement in relation to lignocellulosic bioenergy production. Bioenerg. Res. **2,** 217-232.

Southern, E.M. (1975). An improved method for transferring nucleotides from electrophoresis strips to thin layers of ion-exchange cellulose. Anal. Biochem. 62, 317-318

Sun, X., Feng, P., Xu, X., Guo, H., Ma, J., Chi, W., Lin, R., Lu, C., and Zhang, L. (2011). A chloroplast envelope-bound PHD transcription factor mediates chloroplast signals to the nucleus. Nat. Commun. **2,** 477.

Susek, R.E., Ausubel, F.M., and Chory, J. (1993). Signal transduction mutants of Arabidopsis uncouple nuclear CAB and RBCS gene expression from chloroplast development. Cell **74,** 787-799.

Tran, L.S., Nakashima, K., Sakuma, Y., Simpson, S.D., Fujita, Y., Maruyama, K., Fujita, M., Seki, M., Shinozaki, K., and Yamaguchi-Shinozaki, K. (2004). Isolation and functional analysis of Arabidopsis stress-inducible NAC transcription factors that bind to a drought-responsive cis-element in the early responsive to dehydration stress 1 promoter. Plant Cell **16,** 2481-2498.

Van Aken, O., Zhang, B., Carrie, C., Uggalla, V., Paynter, E., Giraud, E., and Whelan, J. (2009). Defining the mitochondrial stress response in Arabidopsis thaliana. Mol. Plant **2,** 1310-1324.

Van Gestel, K., Kohler, R.H., and Verbelen, J.P. (2002). Plant mitochondria move on F-actin, but their positioning in the cortical cytoplasm depends on both F-actin and microtubules. J. Exp. Bot. **53,** 659-667.

Vanlerberghe, G.C., and McIntosh, L. (1997). ALTERNATIVE OXIDASE: From Gene to Function. Annu. Rev. Plant Physiol. Plant Mol. Biol. **48,** 703-734.

von Jagow, G., Ljungdahl, P.O., Graf, P., Ohnishi, T., and Trumpower, B.L. (1984). An inhibitor of mitochondrial respiration which binds to

cytochrome b and displaces quinone from the iron-sulfur protein of the cytochrome bc1 complex. J. Biol. Chem. **259,** 6318-6326.

Wang, Y., Carrie, C., Giraud, E., Elhafez, D., Narsai, R., Duncan, O, Whelan, J., Murcha, M.W. (2012). Dual Location of the Mitochondrial Preprotein Transporters B14.7 and Tim23-2 in Complex I and the TIM17:23 Complex in Arabidopsis Links Mitochondrial Activity and Biogenesis. Plant Cell **24,** 2675-2695.

Wang, Y.S., Motes, C.M., Mohamalawari, D.R., and Blancaflor, E.B. (2004). Green fluorescent protein fusions to Arabidopsis fimbrin 1 for spatio-temporal imaging of F-actin dynamics in roots. Cell Motil. Cytoskeleton **59,** 79-93.

Woodson, J.D., and Chory, J. (2008). Coordination of gene expression between organellar and nuclear genomes. Nature reviews. Genetics **9,** 383-395.

Woodson, J.D., Perez-Ruiz, J.M., and Chory, J. (2011). Heme synthesis by plastid ferrochelatase I regulates nuclear gene expression in plants. Curr. Biol. **21,** 897-903.

Wu, A., Allu, A.D., Garapati, P., Siddiqui, H., Dortay, H., Zanor, M.I., Asensi-Fabado, M.A., Munne-Bosch, S., Antonio, C., Tohge, T., Fernie, A.R., Kaufmann, K., Xue, G.P., Mueller-Roeber, B., and Balazadeh, S. (2012). JUNGBRUNNEN1, a reactive oxygen species-responsive NAC transcription factor, regulates longevity in Arabidopsis. Plant Cell **24,** 482-506.

Wu, Y., Deng, Z., Lai, J., Zhang, Y., Yang, C., Yin, B., Zhao, Q., Zhang, L., Li, Y., and Xie, Q. (2009). Dual function of Arabidopsis ATAF1 in abiotic and biotic stress responses. Cell Res **19,** 1279-1290.

Ye, J., Rawson, R.B., Komuro, R., Chen, X., Dave, U.P., Prywes, R., Brown, M.S. Goldstein, J.L. (2000). ER stress induces cleavage of membrane-bound ATF6 by the same proteases that process SREBPs. Mol. Cell **6,** 1355-1364.

Zarkovic, J., Anderson, S.L., and Rhoads, D.M. (2005). A reporter gene system used to study developmental expression of alternative oxidase and isolate mitochondrial retrograde regulation mutants in Arabidopsis. Plant Mol. Biol. **57,** 871-888.

Zhu, J.K. (2002). Salt and drought stress signal transduction in plants. Annu. Rev. Plant Biol. **53,** 247-273.

Zhu, T., Nevo, E., Sun, D., and Peng, J. (2012). Phylogenetic analyses unravel the evolutionary history of NAC proteins in plants. Evolution **66,** 1833-1248.

Zmasek, C. M. and S. R. Eddy (2001). "ATV: display and manipulation of annotated phylogenetic trees." Bioinformatics **17**(4): 383-384.

Zmasek, C. M. and S. R. Eddy (2001). "A simple algorithm to infer gene duplication and speciation events on a gene tree." Bioinformatics **17**(9): 821-828.

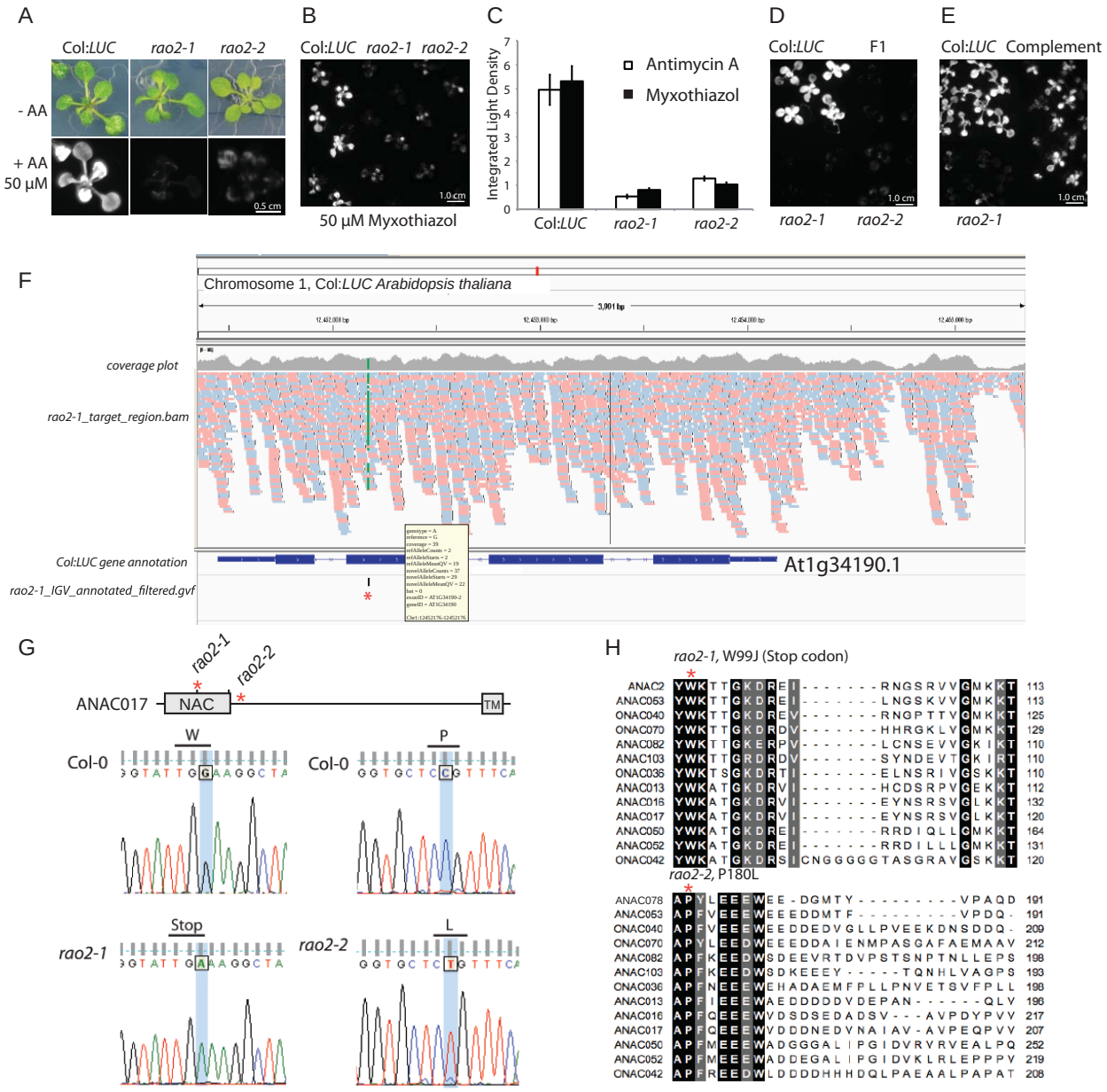

Figure 1. Identification of RAO2/ANAC017 as a regulator of AOX1a. (A) 14 day old seedlings (top panel) and luminescence of Col:*LUC* and *rao2* mutants after treatment with antimycin A (AA). Col:*LUC* plants generated from Columbia-0 transformed with a construct with a firefly luciferase reporter gene driven by the *ALTERNATIVE OXIDASE1A* promoter (*AOX1a-LUC*). Luciferase activity was then visualised in a NightOwl bioluminescence imager. **(B)** Luminescence of *rao2-1* and *rao2-2* after 6 h myxothiazol treatment. **(C)** Quantified luminescence of *rao2* mutants after 6 h AA and myxothiazol treatment. (**D)** Allelic test of *rao2-1* and *rao2-2*. F1 seedlings were the first generation from a cross between *rao2-1* and *rao2-2* mutants. **(E)** Complementation test of *rao2-1* transformed with full-length coding sequences of *ANAC017*. F2 generation of transformants (Complement) were able to induce LUC under AA treatment. (**F)** Next-generation sequence analysis identifying a candidate mutation in *ANAC017* (AT1G34190) **(G)** *ANAC017* gene model. ANAC017 contains a predicted NAC domain at its N-terminus and a transmembrane (TM) motif at the C-terminus. Sanger sequencer analysis of *rao2-1* and *rao2-2* confirmed the point mutations that caused amino acid changes **(H)** Alignment of NAC proteins from rice and Arabidopsis. Identical amino acids are coloured in black and amino acids that shared high similarity are coloured in grey. Asterisk indicates the point mutation in *rao2* mutants.

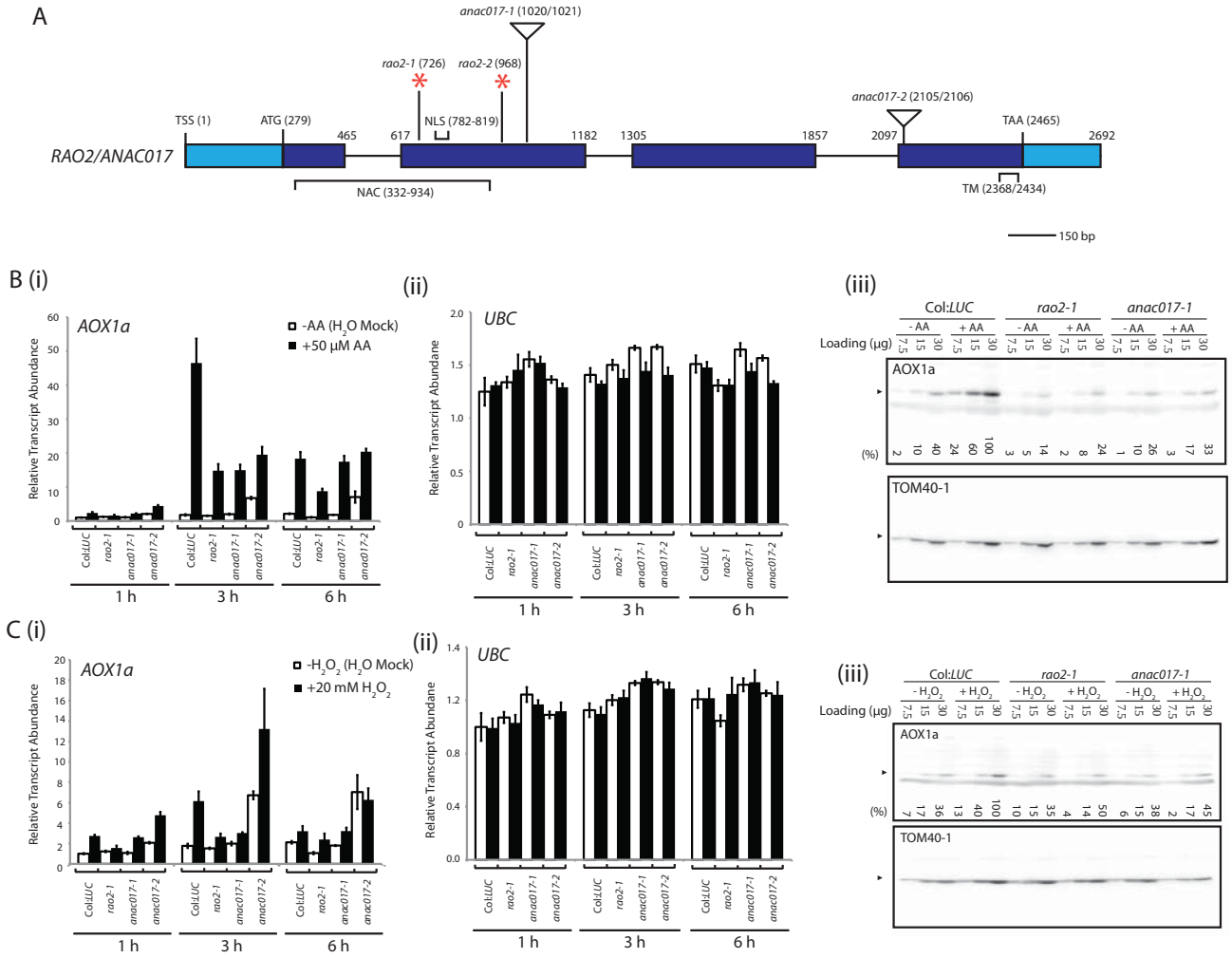

Figure 2. Characterisation of *AOX1a* transcript and protein abundance In *rao2* and *anac017* T-DNA Insertion Lines. **(A)** A schematic gene model of *ANAC017*. Numbers indicate the nucleotide position of the mutation or the T DNA insertion. *rao2* mutants are marked in red asterisks and T-DNA insertion lines (*anac017*) are indicated by inverted triangles. TSS, transcriptional start site; TM, transmembrane motif; NLS, putative nuclear localisation signal; NAC, NAM, ATAF1/2 and CUC2 domain. **(B)** *AOX1a* transcript (i), *Ubiquitin* transcript (ii), and AOX1a protein (iii) abundance under antimycin A treatment. (i) Two-week-old seedlings were exposed to 50 µM of AA or deionised water (Mock, -AA) and were harvested at 1 h, 3 h and 6 h and transcript abundance analysed by QRT-PCR. (ii) *Ubiquitin* (*UBC*) was used as transcript abundance control. (iii) Protein abundance was quantified and AOX1a values were normalized against the corresponding TOM40-1 to give a loading corrected quantification. Relative protein abundance, below each blot, was expressed as a percentage of the highest value of the set. **(C)** As B except that induction was carried out with H_2O_2.

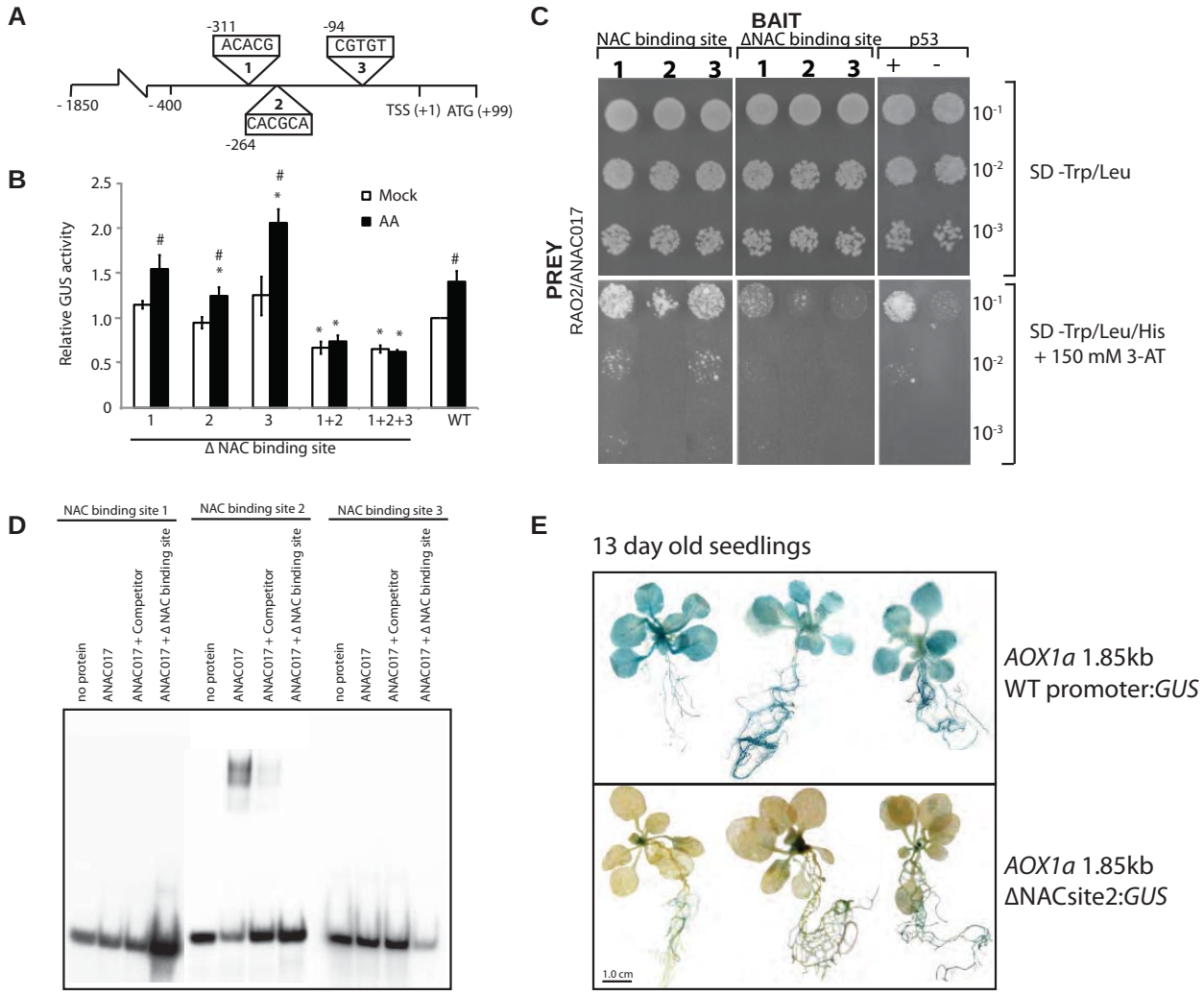

Figure 3. RAO2/ANAC017 binds to predicted NAC binding sites in the *AOX1a* Promoter. (A) A schematic diagram of *AOX1a* promoter region with NAC binding sites 1, 2 and 3. TSS, transcriptional start site. **(B)** Analysis of *AOX1a* promoter activity using GUS assay. Wild-type plants (Col-0) were transiently transformed with constructs expressing wild-type *AOX1a* promoters fused with *beta-glucuronidase (GUS)* or with constructs with NAC binding sites mutated in the *AOX1a* promoter. Asterisks indicates a significantly difference of GUS activity between wild-type promoter and mutated promoter constructs. Symbol # indicates significant induction of GUS activity between mock-treated (deionised water) control and antimycin A (AA) treatment. **(C)** Yeast-one hybrid binding assay of RAO2/ANAC017 to *AOX1a* promoter. Bait vector contained a 50-bp region surrounding NAC binding sites. Prey vector contained the full-length coding sequence of RAO2/ANAC017. Serial dilutions (10-2, 10-3) of co-transformed yeast were spotted on synthetic dropout (SD) –Trp/Leu to select for co-transformants and SD-Trp/Leu/His to select for interactions. Numbers 1, 2 and 3 in bold represent NAC binding site 1, 2 and 3 found in *AOX1a* promoter. ΔNAC binding site are bait vector with NAC binding site deleted. Binding of p53 to a sequence containing p53 or not containing p53 was used as positive (+) and negative (-) controls. Trp, tryptophan; Leu, leucine; His, histidine. **(D)** Binding of RAO2/ANAC017 to NAC binding site 2 in the *AOX1a* promoter as determined by electromobility shift assay. **(E)** GUS histochemical staining of 13 day old transgenic Arabidopsis seedlings carrying either the wild-type *AOX1a* 1.85kb promoter driving GUS expression (top panel) or a construct with NAC binding site 2 deleted (bottom panel) after treatment with 6 h Antimycin A

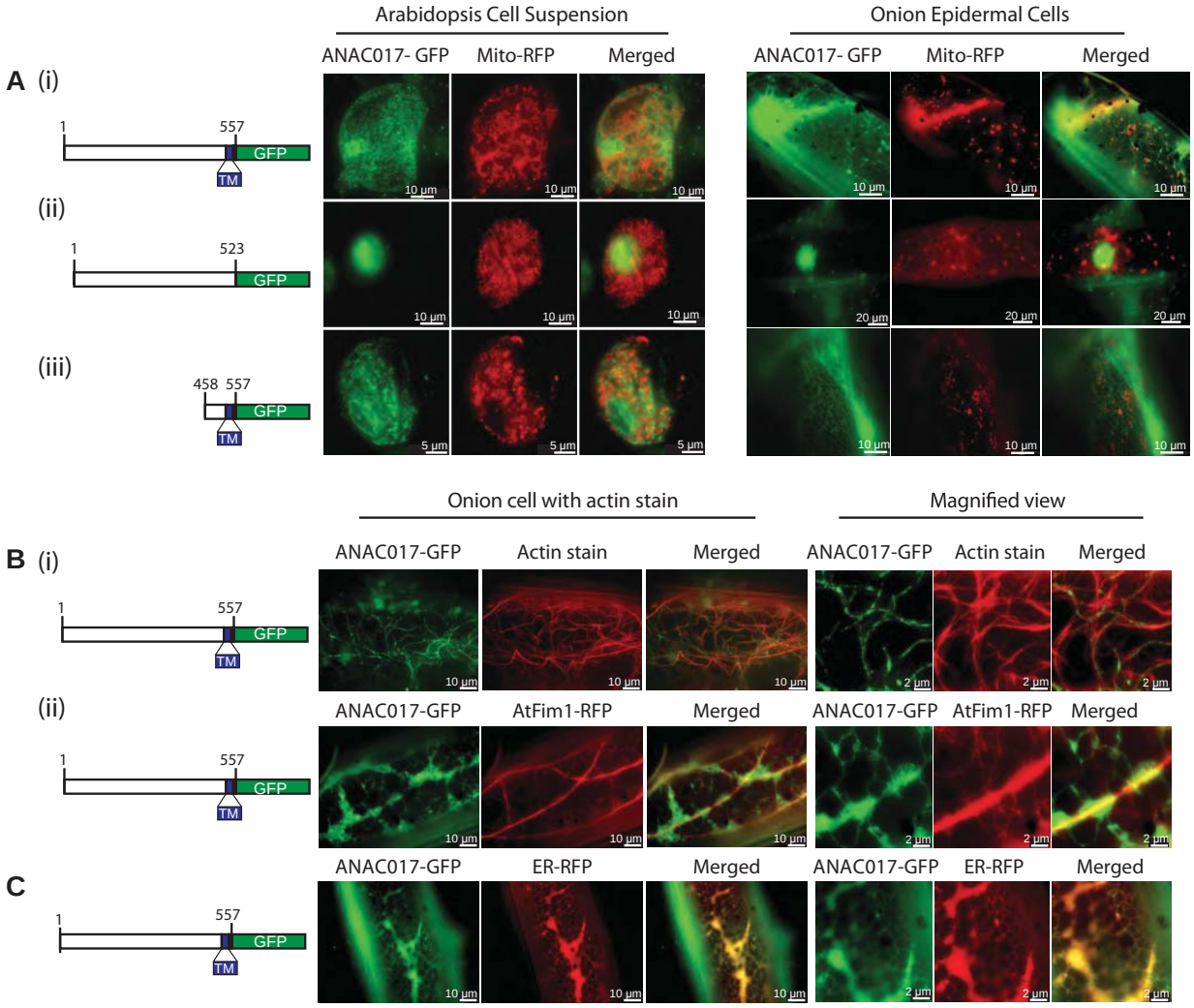

Figure 4. In vivo targeting of full-length and truncated forms of RAO2/ANAC017 linked to green fluorescence protein (A) Subcellular targeting of (i) Full-length RAO2/ANAC017, (ii) full-length RAO2/ANAC017 minus the predicted transmembrane (TM) region, and, (iii) the predicted TM region of RAO2/ANAC017 were tagged with green fluorescence protein (GFP) to assess targeting ability. These three constructs were transiently transformed into both Arabidopsis suspension cells and onion epidermal cells, in addition to a mitochondrial red fluorescence protein (Mito-RFP) control (see materials and methods). **(B)** Co-localization of RAO2/ANAC017 to actin filament. Based on the localizations observed for the full-length construct, co-localization of RAO2/ANAC017 was confirmed with (i), actin stained with rhodamine-labelled phalloidin control and (ii) AtFim1-RFP control. A magnified view of this co-localization has been provided. (**C)** Co-localization of RAO2/ANAC017 to endoplasmic reticulum (ER) using an ER-RFP control.

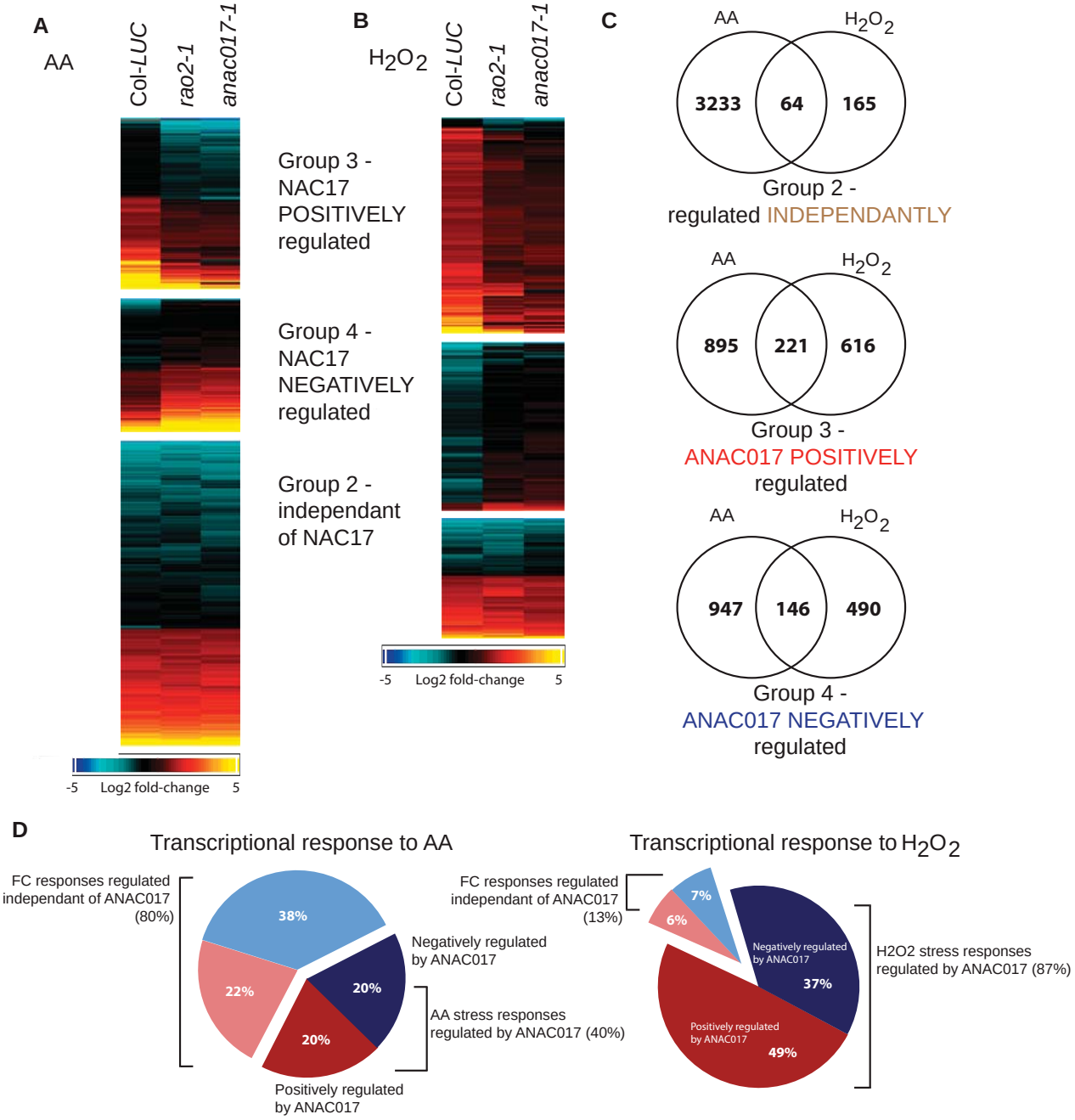

Figure 5. Characterization of the genome-wide transcriptional response to stress that is regulated through RAO2/ANAC017 and cannot be compensated for by other cellular components. Hierarchical cluster of gene set lists categorized as either positively or negatively regulated through ANAC017 activity under **(A)** Antimycin A (AA) or **(B)** H_2O_2 treatment, as described in Supplemental Figure 6-7. Blue color represent transcripts that are down-regulated in response to treatment and red/yellow color represented transcript that are up-regulated in response to treatment as shown by the color scale, log2 fold changes in untreated vs treated conditions. Fold changes in response to stress were calculated for Col:*LUC* (wild-type), *rao2-1* and *anac017-1* T-DNA insertional knock-out lines. **(C)** Overlap in specific transcriptional responses for transcripts classified in each of the gene lists based on their regulation in regards to RAO2/ANAC017 under treatment. There was significantly less overlap than expected by random chance between the transcriptional responses for AA and H_2O_2 treatment. **(D)** Proportional breakdown of the degree that the response to AA or H_2O_2 is mediated through RAO2/ANAC017 function genome-wide.

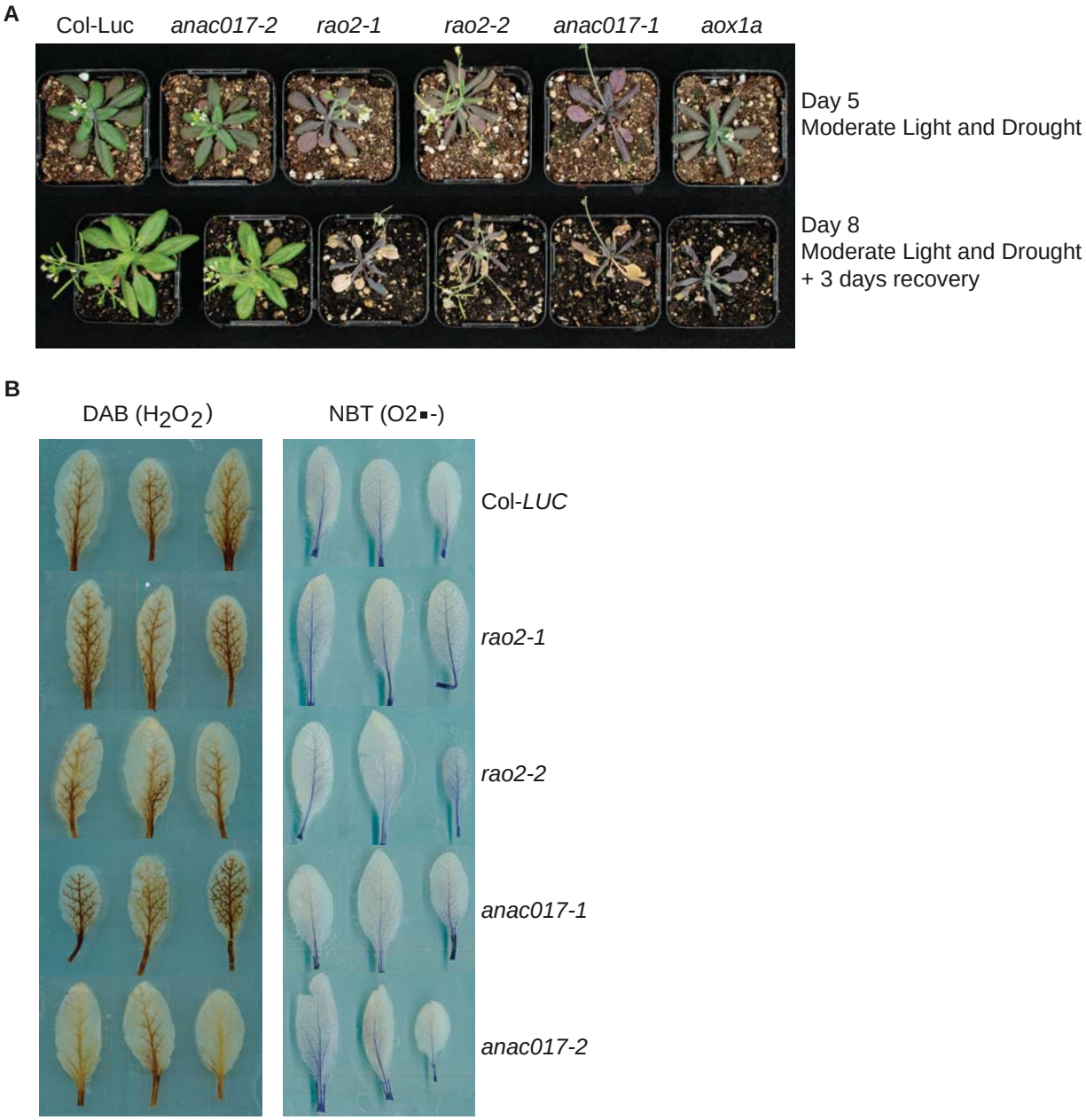

Figure 6. Characterization of the physiological sensitivity to environmental stress and H_2O_2 in plants with altered levels of functional RAO2/ANAC017. (A) Thirty-four-day old plants growth for 16 h at 120 µmol $m^{-2}s^{-1}$ light/ 8 h dark, 22 ºC were transferred to 16 h at 300 µmol $m^{-2}s^{-1}$ light/ 8 h dark, 22 ºC without watering and response observed for 5 and 7 days, after which water was re-supplied at 120 µmol $m^{-2}s^{-1}$ light. **(B)** Thirty-four-day old plants growth for 16 h at 120 µmol $m^{-2}s^{-1}$ light/ 8 h dark, 22 ºC were stained for H_2O_2 (DAB) and superoxide radical O2•– (NBT).

Supplemental Materials and Methods

Sequencing and Data Analysis

Library quality was checked using an Agilent bioanalyser and quantified using a Nanodrop (Thermo Scientific) and Qubit (Invitrogen) before Next-Generation Sequencing with 2x50 bp paired-end read lengths on an Illumina HiSeq1000. Primary data processing was performed by RTA (Real Time Analysis) software. BCL file (Base Call) conversion and de-multiplexing was performed by CASAVA V1.8.2 (Illumina). Alignments for Col*:LUC* read sequences were performed against TAIR9 reference genome (www.arabidopsis.org) and a FASTA reference genome sequence (Col*:LUC* reference) was generated for Col*:LUC* to ensure SNP calls present in the wild-type parental lineage could be excluded from *rao1* sequence data analysis. Read sequences for *rao1-1* and *rao1-2* re-sequencing were aligned to the Col*:LUC* reference genome sequence using CASAVA V1.8.2 and SNP calls generated using GATK software pipelines (www.broadinstitute.org/gsa/wiki/index.php/The_Genome_Analysis_Toolkit) and best practices (www.broadinstitute.org/gsa/wiki/index.php/Best_Practice_Variant_Detection_with_the_GATK_v3). All candidate SNP calls in the region of interest are shown in Supplemental Table 2 and were filtered to remove SNPs that occur in intergenic regions, SNPs that are not the result of EMS mutagenesis, heterozygous SNP calls and SNP calls with no corresponding SNP in allelic lines within common genes. Sorted .bam and .gvf files were visualised in IGV (http://www.broadinstitute.org/igv/) and Tablet (http://bioinf.scri.ac.uk/tablet/) viewers to identify candidate SNPs in the pre-defined genomic region of interest on chromosome 1.

Global Transcript Analyses

Amplified RNA generation, hybridisation, washing and scanning of gene chips were carried out according to manufacturer's instructions. Data quality was assessed using GCOS 1.4 prior to CEL files were exported into AVADIS Prophetic (version 4.3; Strand Genomics) and Partek Genomics Suite software, version 6.3, for further analysis. CEL files are available at GEO under the accession number GSE41136. MAS5 normalization algorithms were performed only to generate present/absent calls across the arrays. Probe sets that recorded absent calls in 2 or more of the 3 biological replicates for genotypes and treatment conditions for a particular analysis were removed. CEL files were also subjected to GC-content background Robust Multi-array Average normalization (GC-RMA) for computing fluorescence intensity values used in differential expression analyses. Correlation plots were examined between all arrays using the scatterplot function in the Partek Genomics Suite, and in all cases $r>0.98$ (data not shown). Analysis of differential expression was carried out using a regularized *t*-test based on a Bayesian statistical framework using the software program Cyber-T (Long et al., 2001) (http://cybert.microarray.ics.uci.edu/). Cyber-T employs a mixture model-based method described by (Allison et al., 2006) for the computation of the global false-positive and false-negative levels inherent in a DNA microarray experiment. To accurately control for FDR and minimize false positives within the differential expression analysis, posterior probability of differential expression PPDE(P) values and PPDE(>P) values were calculated, as a means to measure the true discovery rate (1 – FDR). Changes in transcript abundance

were considered significant with a PPDE(>P) > 0.95 and a fold change >1.5-fold. Details for the classification of transcripts into 1 of 4 gene lists based on the nature of the stress response in mutant backgrounds can be found in Supplemental Figure 6 and 7 for AA and H2O2, respectively. Hierarchical clusters were generated using Euclidean distance and average linkage measures in Partek Genomics suite V6.3. Overlaps in the transcript abundance responses for the different treatments were plotted on Venn diagrams to determine statistically significant over- or under-representation in the overlap, compared with that which is expected by random chance, using a Pearson's chi-squared test ($\chi 2$) for independence.

Allison, D.B., Cui, X., Page, G.P., and Sabripour, M. (2006). Microarray data analysis: from disarray to consolidation and consensus. Nature reviews. Genetics **7,** 55-65.

Long, A.D., Mangalam, H.J., Chan, B.Y., Tolleri, L., Hatfield, G.W., and Baldi, P. (2001). Improved statistical inference from DNA microarray data using analysis of variance and a Bayesian statistical framework. Analysis of global gene expression in Escherichia coli K12. J. Biol. Chem. **276,** 19937-19944.

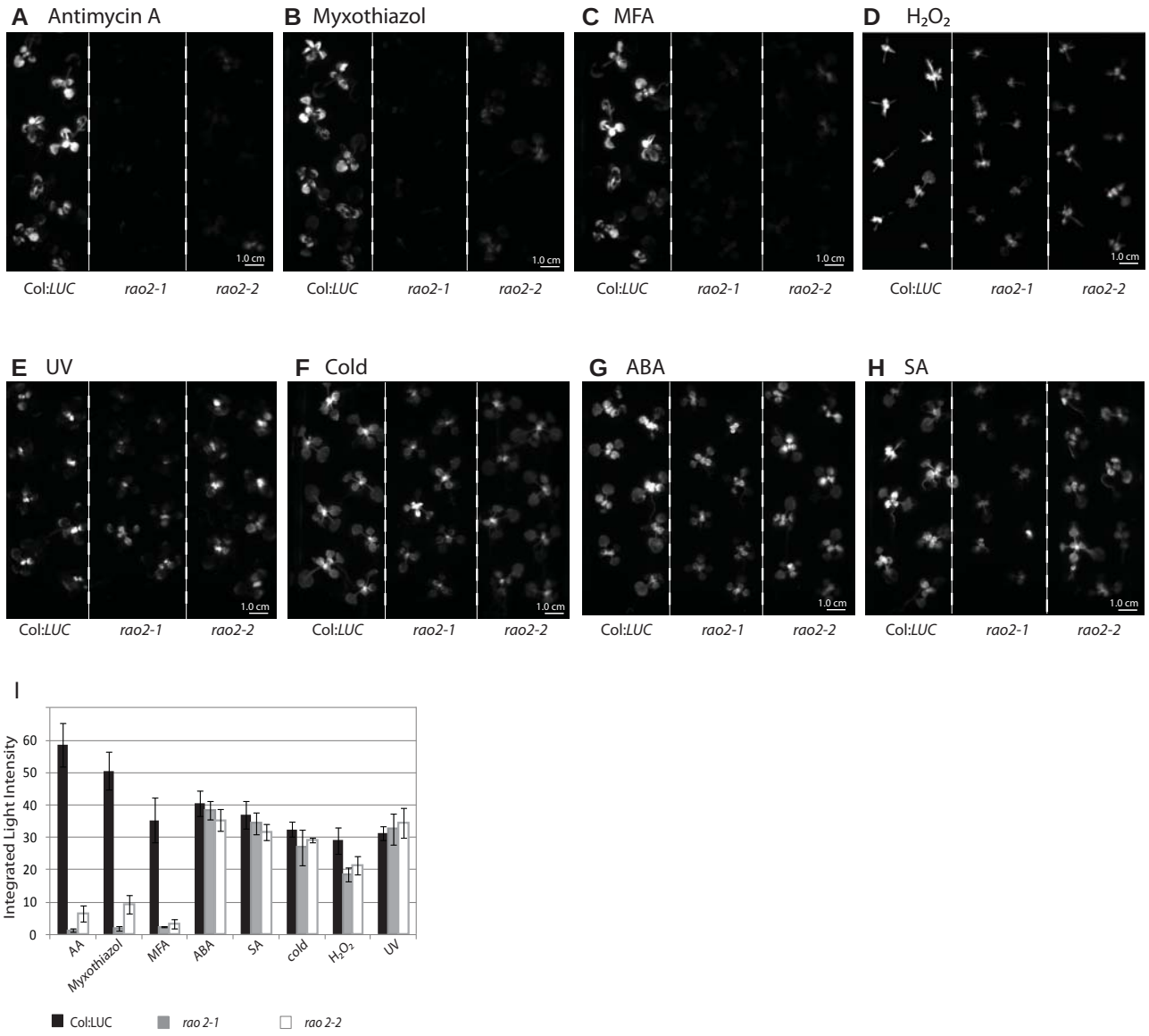

Supplemental Figure 1. Characterisation and quantification of *AOX1a* promoter inductions in *rao2-1* and *rao2-2* following different stress treatments. Col:*LUC*, *rao2-1* and *rao2-2* seedlings were treated with **(A)** 50 µM antimycin A (AA), **(B)** 50 µM myxothiazol, **(C)** 25 mM Monofluoracetate (MFA), **(D)** 20 mM H2O2, **(E)** 30 min ultraviolet (UV) light. **(F)** 16 h cold treatment (4°C). **(G)** 200 µM ABA. **(H)** 50 µM SA. *Luciferase* (*LUC*) reporter gene activity was visualised in a NightOwl bioluminescence imager after 6 h treatment unless otherwise stated. **(I)** Processed images were analysed for quantification of LUC expression using the Integrated Light Intensity from 8-bit images calculated in the Java software ImageJ. Error bars denote standard errors (n>8 measurements). (ABS - Abscisic Acid, SA - Salicylic Acid, MFA - Monoflouracetate).

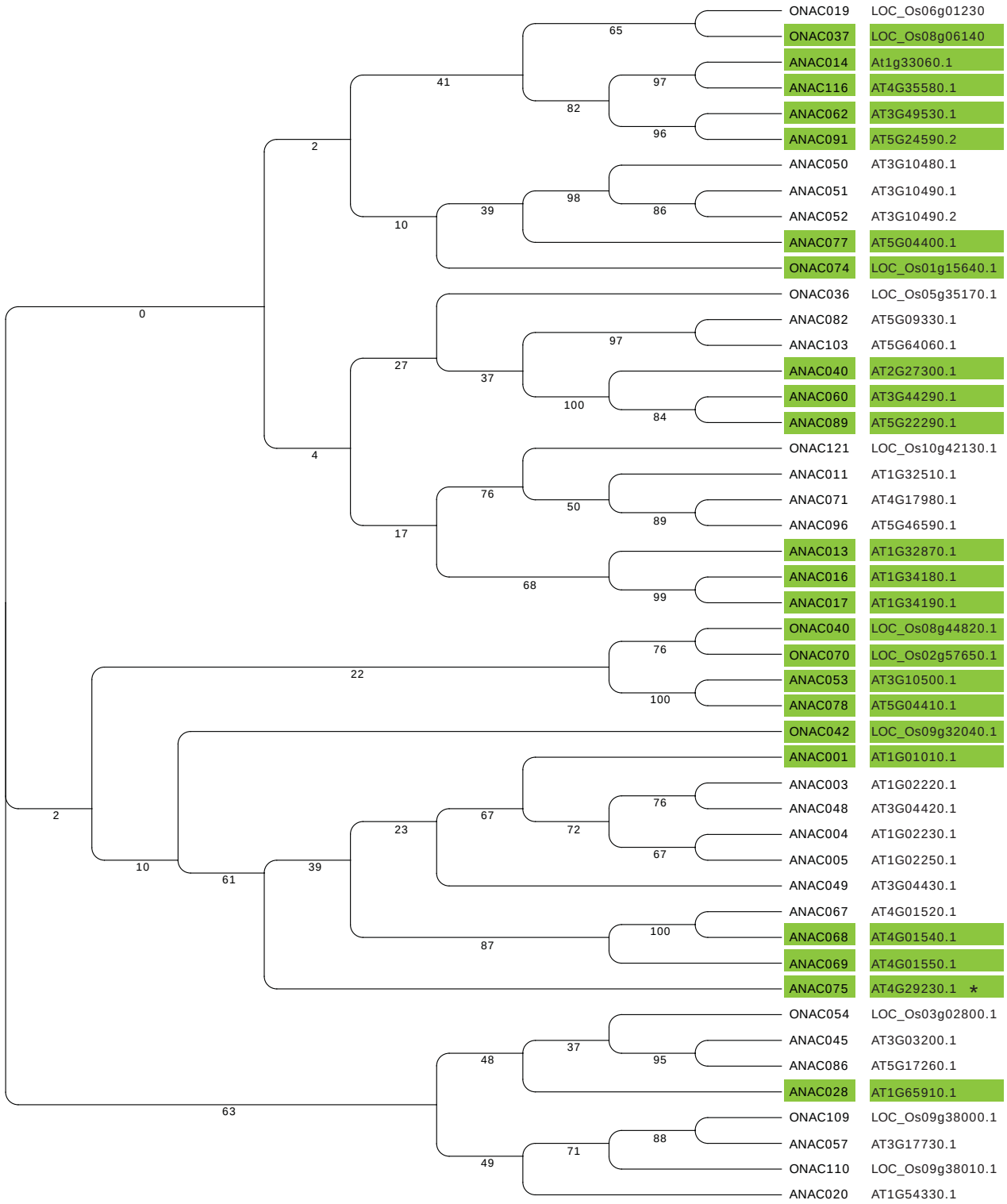

Supplemental Figure 2. Phylogenetic Tree of Arabidopsis and Rice NAC Domain Containing Proteins. Protein sequences of genes that belong to NAC-b group according to Shen, H. et al, (2009) were downloaded from TAIR (www.arabidopsis.org) or from Rice Genome Annotation project (http://rice.plantbiology.msu.edu/). Protein sequences were aligned and phylogenetic tree was drawn on the online version of MAFFT software (http://mafft.cbrc.jp/alignment/software/). Neighbour-Joining method (WAG model) was used and the tree was displayed using Archaeopteryx applet v0.955 (Zmasek and Eddy, 2001 a+b). Proteins with predicted transmembrane motif were highlighted in green. ANAC075 that does not belong to NAC-b group yet having a trasmembrane domain is indicated with an asterisk.

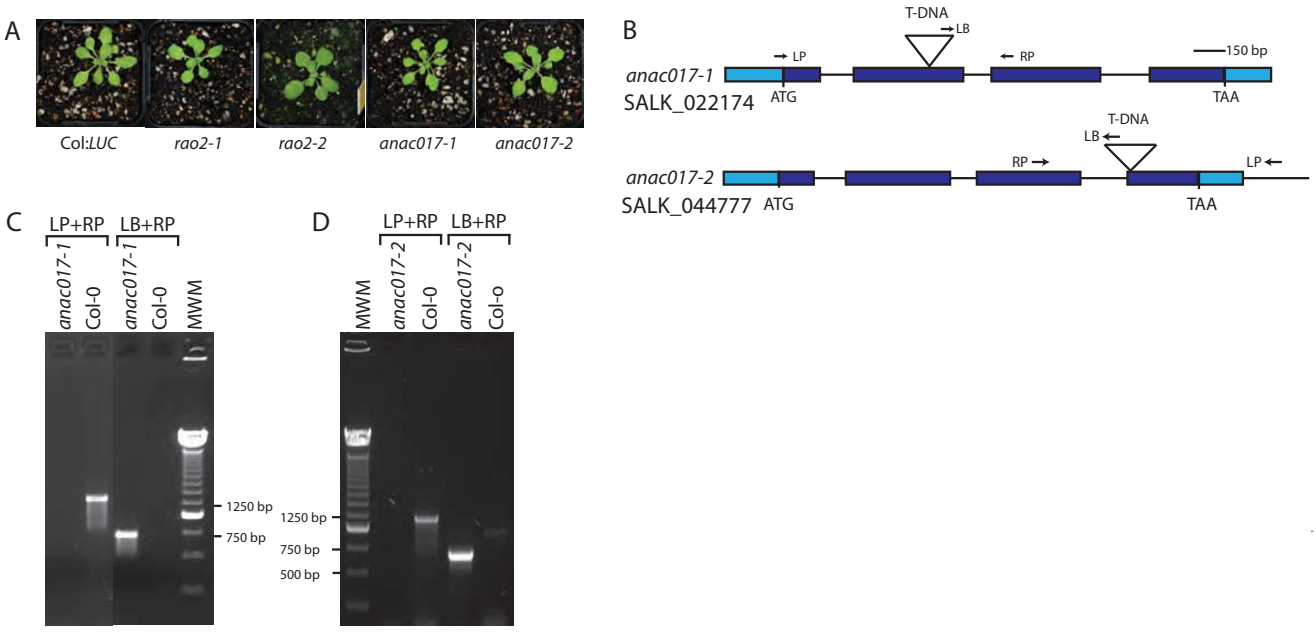

Supplemental Figure 3. Confirmation of T-DNA Insertion Lines, *anac017-1* and *anac017-2*. (A) Twenty-day-old seedlings grown under normal conditions. **(B)** Location of T-DNA inserts in *anac017-1* and *anac017-2* were confirmed through Sanger sequencing and a schematic diagram was shown. **(C)** and **(D)** Homozygous T-DNS knock-out lines were confirmed with PCR reactions using gene specific (LP+RP) and T-DNA specific (LB+RP) primers (Supplemental Table 1). MWM is a mol wt marker.

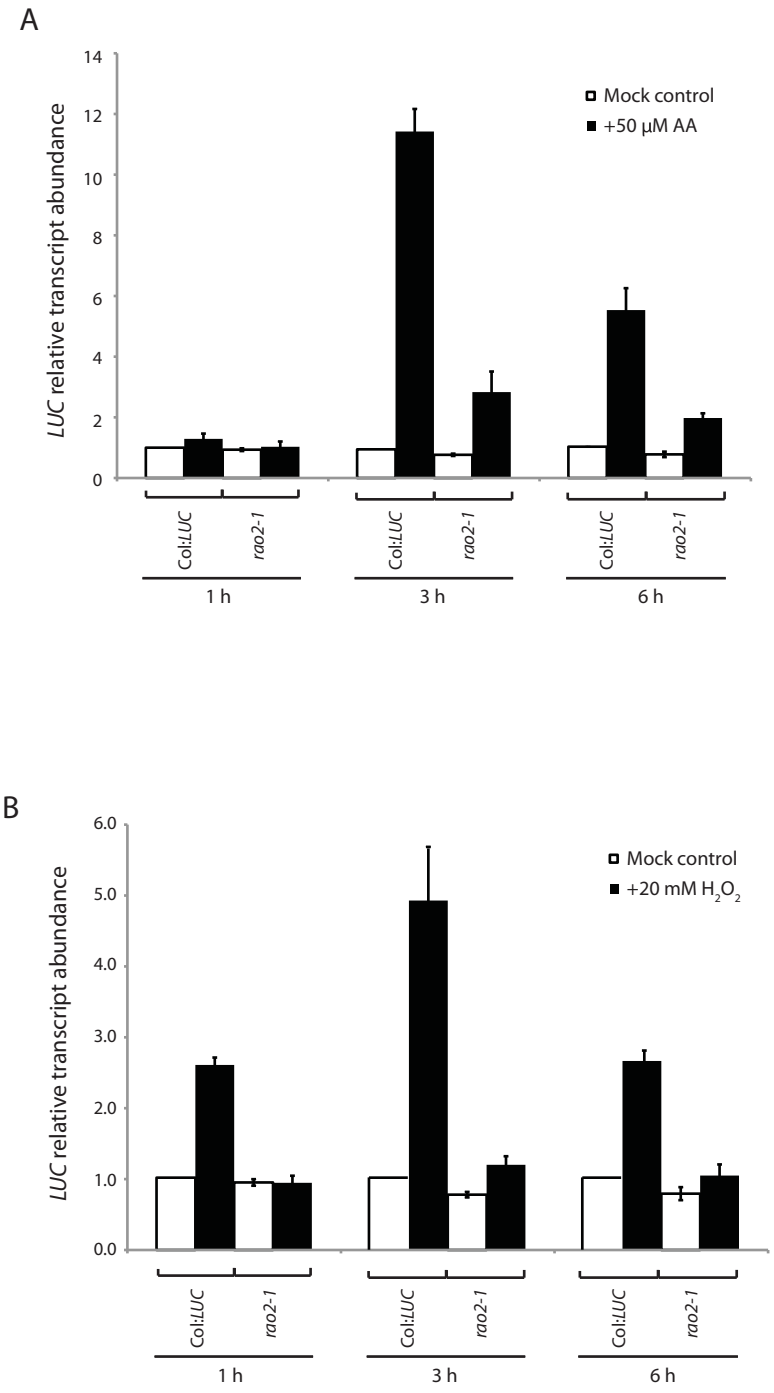

Supplemental Figure 4. *LUC* Transcript Level in *rao2-1* with AA and H2O2 Treatment. Col-*LUC* plants were treated for the time indicated and relative transcript level to Col:LUC, set to 1 at each time point. **(A)** AA treatment **(B)** H2O2 treatment

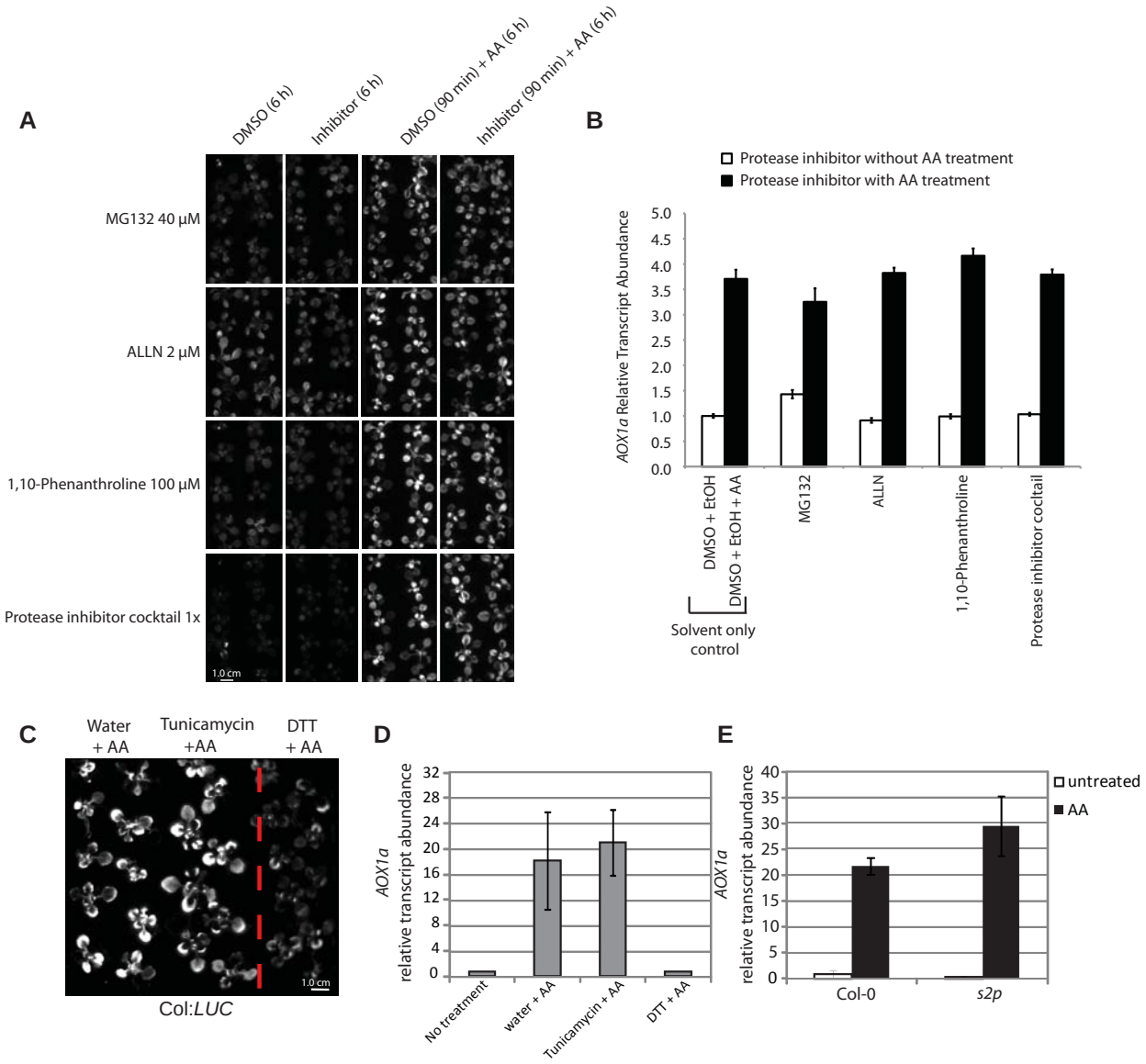

Supplemental Figure 5. The ability of various inhibitors to prevent the induction of *AOX1a* under AA treatment. **(A)** Two-week-old Col:*LUC* seedlings were exposed to protease inhibitors (MG132, ALLN, 1,10-phenanthroline or protease inhibitor cocktail [Sigma P9599]), or with DMSO only (mock control) for 90 min followed by 50 µM antimycin A (AA) for 6 h. Seedlings were then sprayed with luciferin and visualised under a bio-luminescence imager. All protease inhibitors were first dissolved in DMSO before diluted with de-ionised water for treatment. **(B)** Cell culture (Col-0) was first treated with protease inhibitors for 90 min followed by 3 h of AA or without AA before tissue sample was harvested for RNA isolation. All protease inhibitor was dissolved in DMSO while AA was dissolved in ethanol (EtOH). **(C)** NightOwl image of Col:*LUC* plants treated with water, 5 µg/ml Tunicamycin or 5 mM DTT for 30 min before AA application for 6 hr. **(D)** *AOX1a* transcript abundance fold change in Col-0 plants treated with water, 5 µg/m Tunicamycin or 5 mM Dithiothreitol (DTT) for 30 min before AA application for 3 h. **(E)** *AOX1a* transcript abundance fold change in Col-0 and *s2p* (S2 protease) mutant plants treated with AA for 3 h.

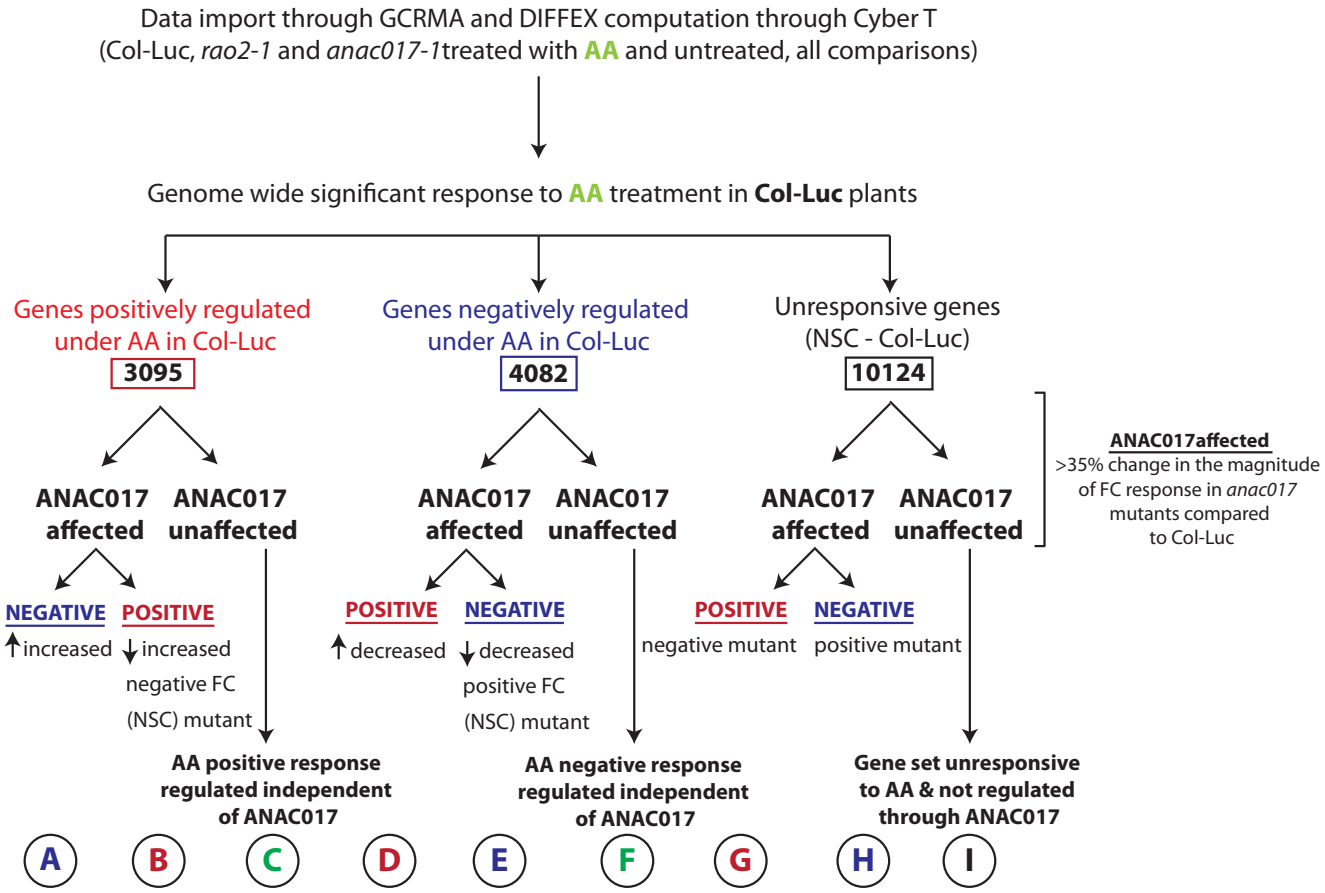

Gene lists defined

1) No significant changes = I
2) Response to AA regulated **independant of ANAC017** = C + F
3) Gene targets **positively** regulated through ANAC017 via retrograde signals = B + D + G
4) Gene targets **negatively** regulated through ANAC017 via retrograde signals = A + E + H

Analysis performed independently for *rao2-1* and *anac017-1*
Final gene lists contain only genes classified identically in both lines

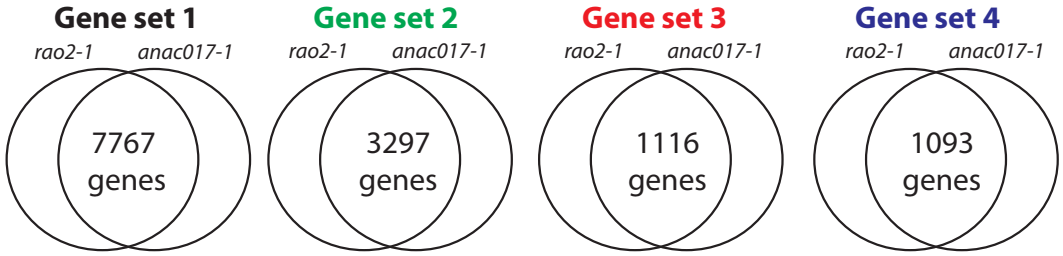

** 13, 273 out of 17, 301 (**>76 % genes, genome wide**) showed identical classification in Geneset lists in both rao2-1 and *anac017-1* microarray analysis for AA treatment.

Changes were considered significant if
Fold change >1.5 fold in magnitude
PPDE pvalue corection >0.95

Supplemental Figure 6. Overview of the logic and criteria for global transcript classification into one of four lists of genes depending on stress responses to Antimycin A and regulation through ANAC017.

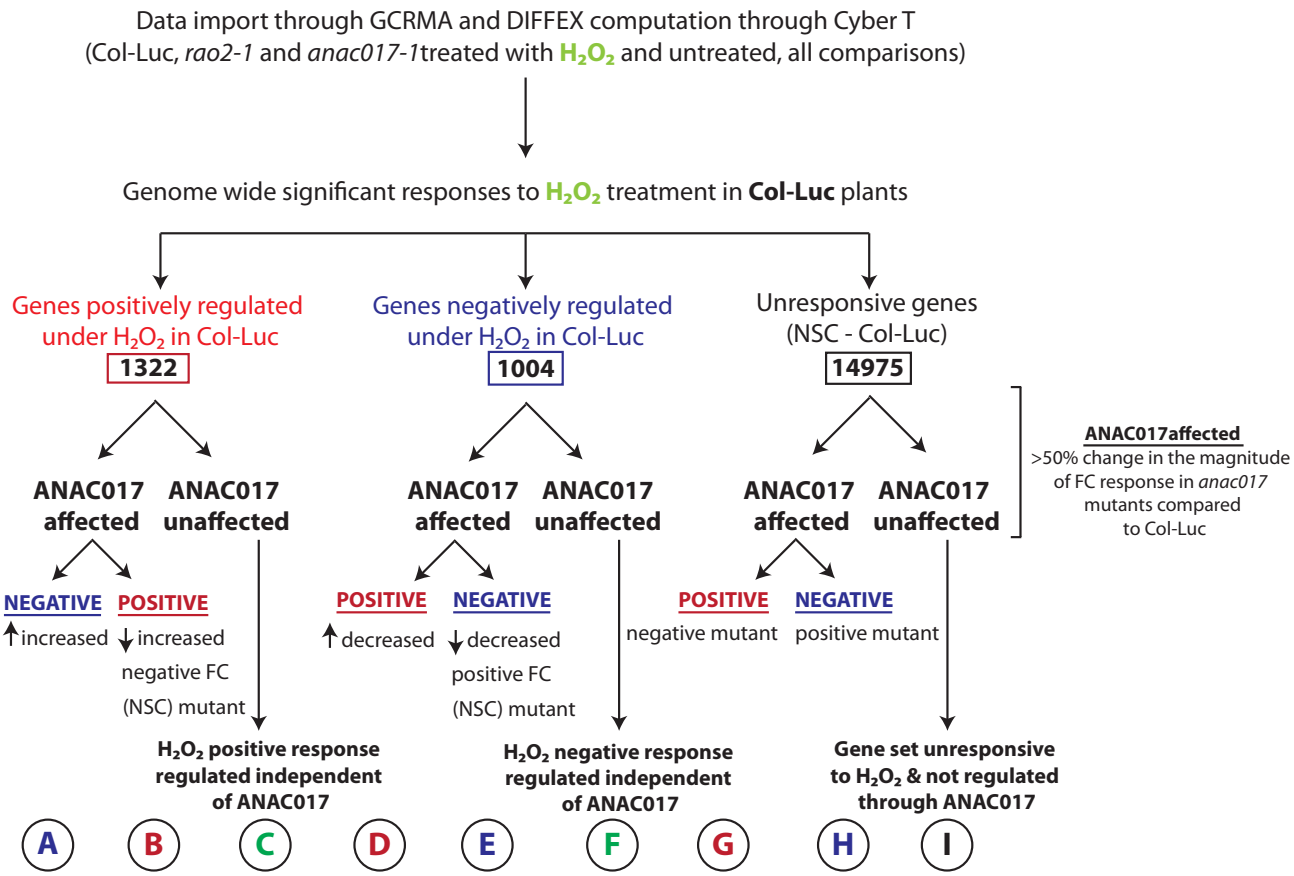

Gene lists defined

1) No significant changes = I
2) Response to H_2O_2 regulated **independant of ANAC017** = C + F
3) Gene targets **positively** regulated through ANAC017 via general stress signals = B + D + G
4) Gene targets **negatively** regulated through ANAC017 via general stress signals = A + E + H

Analysis performed independently for *rao2-1* and *anac017-1*
Final gene lists contain only genes classified identically in both lines

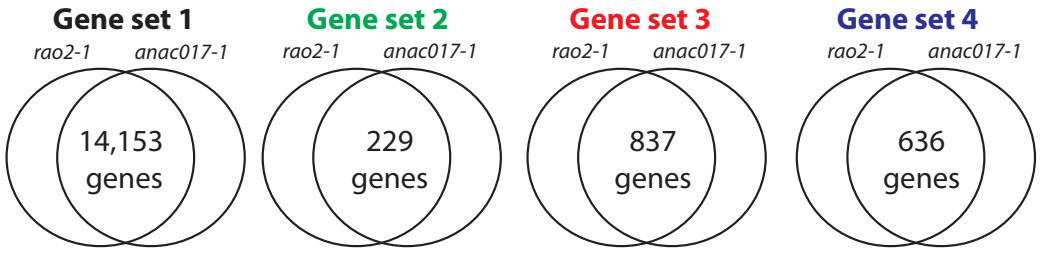

** 15, 8550 out of 17, 301 (**>91 % genes**, genome wide) showed identical classification in Geneset lists in both rao2-1 and *anac017-1* microarray analysis for H_2O_2 treatment.

Changes were considered significant if
Fold change >1.5 fold in magnitude
PPDE pvalue corection >0.95

Supplemental Figure 7. Overview of the logic and criteria for global transcript classification into one of four lists of genes depending on stress responses to H2O2 and regulation through ANAC017 function.

A

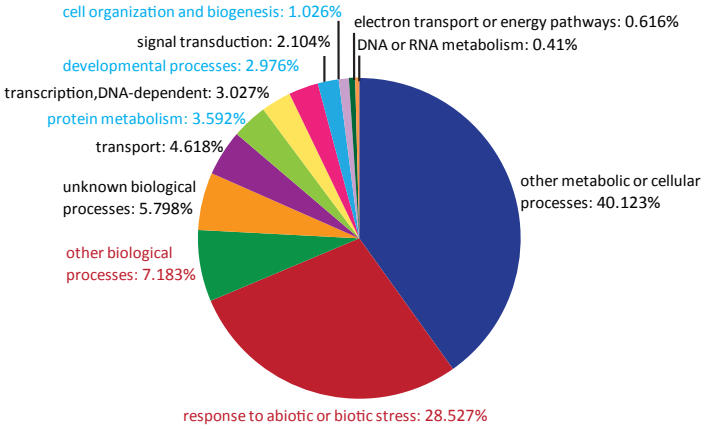

B

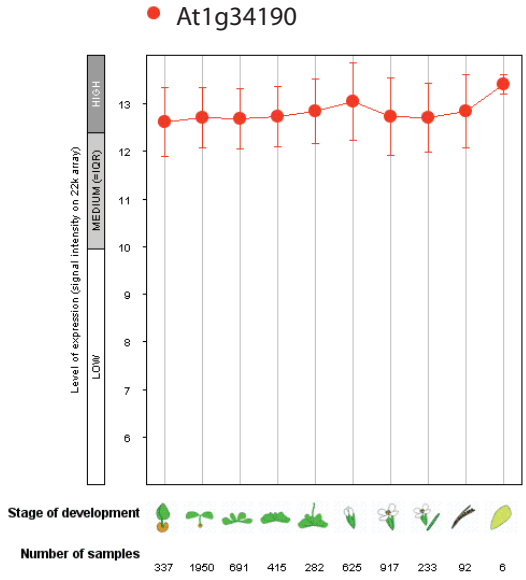

C

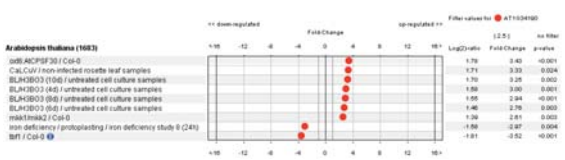

D

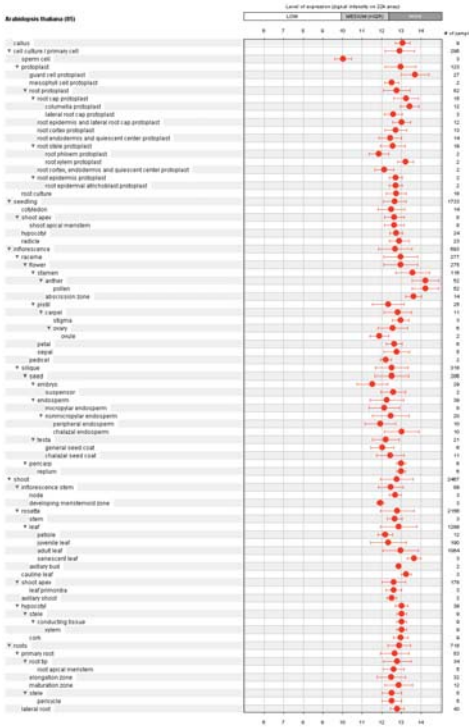

Supplemental Figure 8. ANAC017 is constitutively expressed and regulates stress responsive transcripts genome wide. (A) Functional categorization of transcripts that are significantly altered in abundance in *anac017-2* mutant plants under normal conditions compared to Col:*LUC* wild-type. Functional categories that are significantly over-represented compared to percentile distributions of the whole genome functional are shown in red and those that are significantly under-represented are shown in blue (Chi-squared, $p<0.001$). **(B-D)** Analysis of changes in transcript abundance levels for *ANAC017* over a range of **(B)** Developmental states **(C)** Chemical, environmental and genetic perturbations (Note that only those conditions that show a fold change over 2.5 fold are shown) and **(D)** Tissue types. All plots were generated in Genevestigator (https://www.genevestigator.com/gv/)

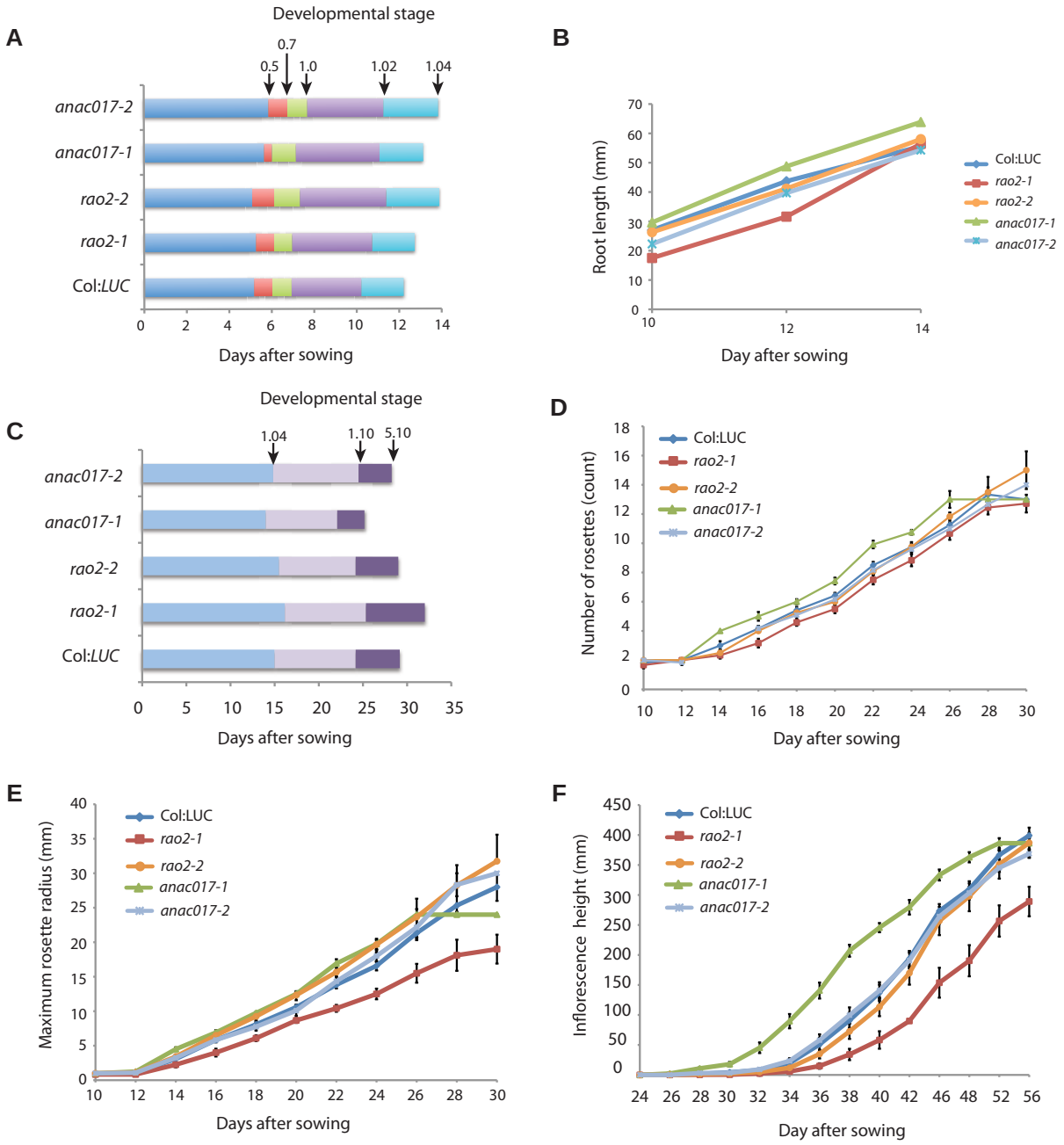

Supplemental Figure 9. Phenotypic analysis of *rao2* mutants. Seeds were sown on Gamborg's B5 agar plates **(A-B)** or on soil **(C-F)** and stratified for 36 h before moving to 16 h light/ 8 h dark long day conditions. Twelve plants per genotype were used for analysis. **(A)** Plate-based: 0.5 (first radical emerged), 0.7 (cotyledon visible), 1.0 (cotyledon fully opened), 1.02 (two rosette leaves fully opened), 1.04 (four rosette leaves fully opened). **(B)** Average root length at 10th, 12th and 14th day. **(C)** Soil-based: 1.04 (four rosette leaves >1mm in length), 1.10 (ten rosette leaves >1mm in length), 5.1 (first flower buds visible). **(D-F)** Representative growth parameters, number of rosettes, maximum rosette radius and plant height, according to Boyes et al., 2001.

Chapter 5 Discussion

The overall aim of the research described in this thesis was to uncover the molecular identity of components involved in the regulation of nuclear genes encoding mitochondrial proteins. Prior to the commencement of this thesis, little was known about these regulators, with only a handful being implicated, such as the transcription factor ABI4 regulating *AOX1a* in Arabidopsis (Giraud et al., 2009), the B3 domain transcription factors, ABI3, FUSCA3 and LEAFY COTYLEDON2, for the regulation of gene expression of *SUCCINATE DEHYDROGENASE2-3* (*SDH2-3*) during seed germination (Roschzttardtz et al., 2009) and the involvement of site II elements in the regulation of cytochrome *c* genes (Welchen and Gonzalez, 2005). While all the above examples represent advances in our understanding of the factors that regulate the expression of nuclear genes encoding mitochondrial proteins, they were isolated studies and do not give an overall picture of the gene regulation for mitochondrial proteins.

The research described in this thesis adds to this body of knowledge, and also try and gains an insight into how components that regulate genes encoding mitochondrial proteins may integrate mitochondrial functions with the multiple biochemical processes that take place in the rest of the cell. No study or thesis can elucidate this completely, but can only hope to make the picture somewhat clearer. The advances in various technologies, especially next-generation sequencing, facilitate approaches such as forward genetics, which in the past could take decades to complete. For example, the initial report of GUN mutants was in 1993 (Strand et al., 2003), yet the molecular identity of the components was only elucidated more than a decade later (Mochizuki et al., 2001). Likewise, *mrr* mutants have been described (Dojcinovic et al., 2005), but the molecular components remain uncharacterised due to the difficulty in

defining the mutations involved. Thus, in this thesis a variety of approaches were used, in an effort to define the components involved in regulating the expression of nuclear genes encoding mitochondrial components.

Mitochondrial gene expression is linked to the diurnal clock

While it has been long recognised that mitochondrial activity fluctuates between day and night periods (Millar et al., 2011), little was known if this difference in activity was reflected in the regulation of nuclear genes encoding mitochondrial proteins. Initial studies in our laboratory and in other laboratories suggested that site II elements played a role in regulating the expression of nuclear located genes encoding mitochondrial proteins (Welchen and Gonzalez, 2005, 2006; Ho et al., 2007; Ng, 2008). However, in our laboratory these results showed large variation and in the literature there was large differences in the degree to which site II elements were observed to regulate genes expression. Two observations were central to solving these dilemmas and establishing the role for site II elements in regulating nuclear located genes encoding mitochondrial proteins. Firstly, the site II sequence bears resemblance to elements that are involved in light regulation of several other genes (see Appendix I). Secondly, the publication of experiments that screened for binding partners for CIRCADIAN CLOCK ASSOCIATED 1 (CCA1), a central regulator of the diurnal clock, has identified transcription factor CCA1 HIKING EXPEDITION (CHE, also known as TCP11) as an interacting protein (Pruneda-Paz et al., 2009). TCP proteins are known binding factors for site II elements from a variety of studies (Li et al., 2005; Welchen and Gonzalez, 2005). By putting these observations together, it was determined that the regulation of

nuclear genes encoding mitochondrial proteins was via the binding of TCP transcription factors to site II elements in the promoter regions. The diurnal expression patterns of TCP transcription factors, their interaction with a variety of components involved in the diurnal clock [(Giraud et al., 2010) - Chapter 2] and the fact that they can act as repressors and activators provide a mechanism in which the expression of nuclear genes encoding mitochondrial proteins is affected by light.

In addition to the demonstration of the regulation of nuclear located genes was carried out by TCP transcription factors binding to site II elements, it was further concluded that this regulation at the transcriptional level did result in changes in mitochondrial protein abundance, where ~ 50 % of mitochondrial protein that were shown to differ in abundance during the diurnal cycle contained site II elements in their gene promoter regions (Lee et al., 2010). Importantly, this also revealed that the other 50 % of proteins that varied in abundance during the diurnal period could not be explained by site II element regulation, as they lacked these elements ((Giraud et al., 2010)- Chapter 2). This led to the conclusion that other mechanisms, as yet unknown, are also involved in the diurnal changes in mitochondrial protein abundances. Furthermore, while TCP transcription factors were characterised as regulators of nuclear genes encoding mitochondrial proteins, they were not sufficient to explain all of the gene expression patterns observed, thus additional factors are anticipated to be involved in the regulation of these genes.

Approaches to identify additional factors that are involved in regulating mitochondrial genes expression may come from findings that have been reported in the last 12 months. It has been shown that a disruption in complex I results in an up-regulation of mitochondrial protein import and vice versa,

therefore, an over-expression in mitochondrial translocase of inner membrane 23-2 (Tim23-2), a component of the mitochondrial protein import apparatus, results in a decrease in complex I (Wang et al., 2012b). More importantly, in regards to the gene regulation, the increase in Tim23-2, which resulted from a fortuitous insertion of a T-DNA in the promoter region of this gene, results in the up-regulation of transcript abundance for many mitochondrial components, including several components of the electron transport chain (Wang et al., 2012b). However as pointed out, these Tim23-2 over-expressing plants either lack or have significantly decreased amounts of complex I and hence growth was much slower (Wang et al., 2012b). Thus, a revertant screen on this Tim23-2 over-expressing line was carried out, i.e. to screen for restoration of plants with normal growth, would identify components required for the increased transcript abundance of many mitochondrial components. Another system that may be exploited to identify regulators of mitochondrial genes expression would be seed germination. During seed germination, a sequential expression of mitochondrial genes occurs. Firstly, components that are required for mitochondrial RNA and DNA metabolism followed by components involved in protein import and finally, proteins carrying out various metabolic functions (Howell et al., 2009; Narsai et al., 2011). The first peak in expression involved components required for the expression of mitochondrial encoded genes. This may provide a system to study factors controlling mitochondrial biogenesis, as this is the earliest event that can be detected associated with mitochondrial functions during germination. Thus, linking the promoters for a variety of these genes, of which their expression peaks early during germination, to a luciferase reporter gene followed by screening for altered expression, i.e. delayed expression, may identify regulators of mitochondrial genes expression.

A switch between growth and stress regulates expression of *AOX1a* in Arabidopsis

The second approach used in the studies outlined in this thesis was a forward genetic screen to identify regulators of *AOX1a*, a widely used model for mitochondrial retrograde regulation in plants (Rhoads and Subbaiah, 2007). This type of screen had been reported previously (Dojcinovic et al., 2005), so was not novel in approach, however, as no components were identified or characterised, it was felt that this was worth pursuing. The forward genetic screen generated in this project produced a variety of mutants, all of which could not be pursued in the course of this study, so two mutants (the CDKE;1 and ANAC017) were studied in detailed. Notably, mutants that had lost the ability to induce *AOX1a* are outlined in Chapters 3 and 4. Mutants that constitutively expressed *AOX1a* at high levels, and mutants that over-expressed *AOX1a* and did not turn it off were also characterised. However, the components responsible for the latter two groups await identification, but this do reveal that the regulation of *AOX1a* expression is complex and involved repressors, and once it is induced, there appears to be components that are involved in returning its expression to basal levels.

The first component identified to be required for the induction of *AOX1a* under AA treatment was CDKE;1, a previously identified component of the plant mediator complex (Gonzalez et al., 2007). While the mediator complex is not fully described, it plays a role in relaying the information from bound transcription factors to the RNA polymerase initiation complex, to determine the rate of transcript initiation, the rate limiting step of transcription. Identification of

CDKE;1 in this screen revealed that this was required for the activation of *AOX1a*. In an effort to gain more insight into how CDKE;1 might relay information about the functional state of mitochondria in order to initiate transcription, CDKE;1 was found to interact with KIN10, an orthologue to sucrose non-fermenting1 (SNF1) kinase subunit that was initially characterised in yeast and later was shown in plants to be a central integrator of stress and energy signalling (Baena-Gonzalez et al., 2007). Interaction with KIN10 was both shown at a molecular level, where both proteins interacted, and at the transcriptomic level with the transcript abundance of a variety of genes were affected, of which there was a large overlap between genes regulated via KIN10 and CDKE;1.

It is proposed that CDKE;1 acts downstream of KIN10, and it acts to relay information from KIN10 to alter transcriptional profiles of cells. This means that mitochondrial retrograde signalling is integrated with other signalling pathways at the level of KIN10. As KIN 10 integrates signals from the chloroplast, in particular sugar and stress signalling, it integrates mitochondrial retrograde signalling with energy signalling in the cell as a whole (Figure 5.1). This is consistent with what is observed for induction of *AOX1a* in Arabidopsis particularly, and in general with the induction of *AOX* in a variety of plant systems, where a variety of mutants or treatments that perturb chloroplast function lead to the induction of *AOX*. Furthermore, it has been previously shown that the transcription factors ABI4 acts as a repressor of *AOX1a* in Arabidopsis (Giraud et al., 2009). More recently, it has been demonstrated that the ABI4 transcription factor links redox, hormone and sugar signalling in Arabidopsis (Foyer et al., 2012). Thus, it is proposed that *AOX1a* is regulated

by a variety of signals that are integrated by KIN10 and ABI4. However, it is not known if ABI4 is regulated by KIN10 and/or CDKE;1.

The second factor characterised to regulate *AOX1a* is ANAC017, a membrane bound transcription factor that belongs to the NAM, ATAF1/2, CUC2 (NAC) family (Chapter 3). NAC transcription factors are characterised to regulate several stress responsive genes (Puranik et al., 2012). However, unlike many NAC transcription factors, ANAC017 is not itself responsive to stress. Rather, it appears to be expressed constitutively, and upon stimulation, it is released from the membrane to activate *AOX1a* and a variety of other genes (Chapter 4). From the analysis of the genes regulated by ANAC017, it is proposed that ANAC017 is involved in a primary stress response and also mediates responses to H_2O_2. ANAC017 is considered to mediate a primary stress response as it activates a variety of transcription factors that are associated with regulating stress responsive genes, thus, it represents a high level regulator to oxidative stress. Secondly, it appears to activate genes in response to H_2O_2, as > 80 % of the H_2O_2 responsive genes appeared to be regulated by ANAC017, while the overlap of responsive genes of the ROS generated from plastids was very little. Therefore, the specificity in ROS signalling may come from the type of ROS produced, with ANAC017 responsible for regulation of gene via H_2O_2.

There is still likely to be a variety of factors that regulate *AOX1a* that have yet to be characterised. However, the question remains if such studies are able to provide a larger picture of how genes encoding mitochondrial proteins are regulated. Overall, the regulation of genes encoding mitochondrial proteins by TCP transcription factors integrates mitochondrial function with growth and development, as shown in TCP transcription factors that are involved in

regulating ribosomal protein genes expression, growth and development (Cubas et al., 1999; Li et al., 2005). A large protein-protein interaction screen did suggest that CDKE;1 interacts with TCP19 (Arabidopsis Interactome Mapping Consortium, 2011; EMBL-EBI interaction accession number, EBI-4495320), although we have been unable to reproduce this interaction. However, if CDKE;1 does interact with TCP transcription factors, it readily presents a nice model to explain global regulation of genes encoding mitochondrial proteins. Essentially, genes encoding mitochondrial proteins are regulated in a coordinated manner with the diurnal clock (Lee et al., 2010), thus integrating chloroplast function and mitochondrial function, with signalling via KIN10 and CDKE;1 (Figure 5.1). In addition to TCP transcription factors, a variety of other transcription factors, many yet to be identified, will be involved in this regulatory loop. Under stress that perturbs mitochondrial or chloroplast function, there is a switch from growth to stress responses, again signalled via KIN10 and CDKE;1, except that a different series of transcription factors are activated. This model essentially states that there are two modes, growth verses a stress response, and plants do stop growing under stress. However, it should be noted that when in the stress mode, growth might slow in the short term, but it allows for survival, and studies on transgenic plants with *AOX* inactivated or over-expressed propose that AOX acts as a survival protein. Also of note is that when the cytochrome chain is blocked, AOX allows growth to proceed, albeit at a slower pace than when the cytochrome chain is fully operational (Liu and Butow, 2006). Thus, while there are conflicting signals promoting growth and stress response, both will be operational in plants under apparently “normal’ growth conditions. The integration of these pathways, via

the model and components elucidated in this study, allows plants to integrate these conflicting signals to optimise growth.

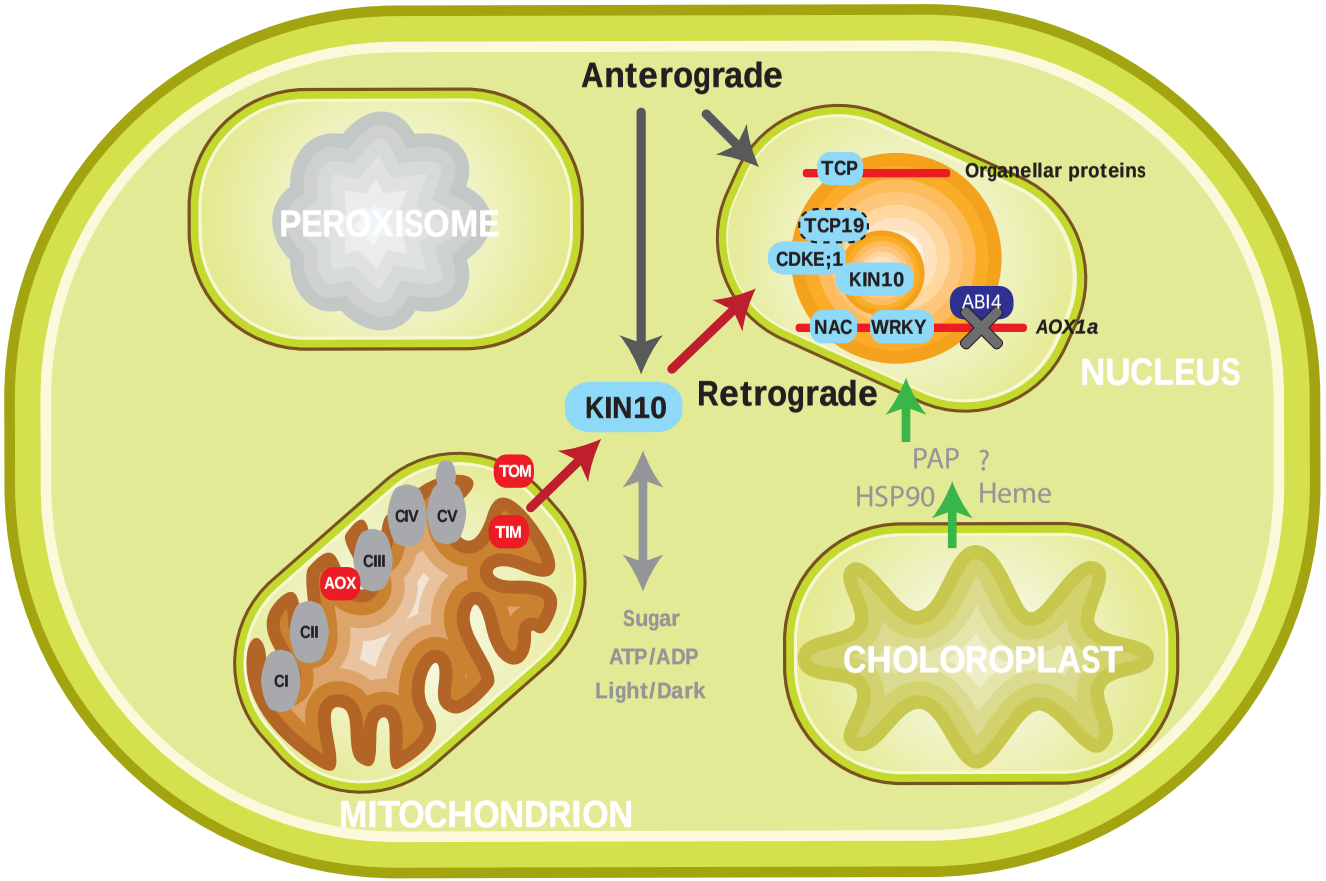

Figure 5.1 A schematic diagram of the signalling pathways between organelles and the nucleus. Red and green arrows indicate retrograde pathways from the mitochondrion and chloroplast respectively. Dark grey arrows indicate anterograde pathways. Interaction between TCP19 and CDKE;1 was reported in the literature however was not detected in this study, and is shown in dashed lines. ABI4 is a negative regulator of *AOX1a*. AOX, ALTERNATIVE OXIDASE; CI-CV, complex I to V of mitochondrial electron transport chain; TIM, TRANSLOCASE OF INNER MEMBRANE; TOM, TRANSLOCASE OF OUTER MEMBRANE; NAC, NAM, ATAF1/2, CUC2 transcription factor; ABI4, ABA-INSENSITIVE-4 transcription factor; CDKE;1, CYCLIN-DEPENDENT KINASE E;1; TCP, TEOSINTE-BRANCHED1, CYCLOIDEA, PCNA transcription factor; HSP90, HEAT SHOCK PROTEIN 90; PAP, 3′-Phosphoadenosine 5′-phosphate.

Chapter 6 References

Abascal, F., Posada, D., and Zardoya, R. (2012). The evolution of the mitochondrial genetic code in arthropods revisited. Mitochondrial DNA **23,** 84-91.

Allen, J.F. (1993). Control of gene expression by redox potential and the requirement for chloroplast and mitochondrial genomes. J. Theor. Biol. **165,** 609-631.

Alverson, A.J., Rice, D.W., Dickinson, S., Barry, K., and Palmer, J.D. (2011). Origins and recombination of the bacterial-sized multichromosomal mitochondrial genome of cucumber. Plant Cell **23,** 2499-2513.

Andersson, S.G., Zomorodipour, A., Andersson, J.O., Sicheritz-Ponten, T., Alsmark, U.C., Podowski, R.M., Naslund, A.K., Eriksson, A.S., Winkler, H.H., and Kurland, C.G. (1998). The genome sequence of *Rickettsia prowazekii* and the origin of mitochondria. Nature **396,** 133-140.

Andrews, T.J., Lorimer, G.H., and Tolbert, N.E. (1973). Ribulose diphosphate oxygenase. I. Synthesis of phosphoglycolate by fraction- 1 protein of leaves. J. Biol. Chem. **12,** 11-18.

Asin-Cayuela, J., and Gustafsson, C.M. (2007). Mitochondrial transcription and its regulation in mammalian cells. Trends Biochem. Sci. **32,** 111-117.

Baena-Gonzalez, E., Rolland, F., Thevelein, J.M., and Sheen, J. (2007). A central integrator of transcription networks in plant stress and energy signalling. Nature **448,** 938-942.

Balk, J., and Pilon, M. (2011). Ancient and essential: the assembly of iron-sulfur clusters in plants. Trends Plant. Sci. **16,** 218-226.

Beardslee, T.A., Roy-Chowdhury, S., Jaiswal, P., Buhot, L., Lerbs-Mache, S., Stern, D.B., and Allison, L.A. (2002). A nucleus-encoded maize protein with sigma factor activity accumulates in mitochondria and chloroplasts. Plant J. **31,** 199-209.

Bendich, A.J. (1987). Why do chloroplasts and mitochondria contain so many copies of their genome? Bioessays **6,** 279-282.

Bendich, A.J. (1993). Reaching for the ring: the study of mitochondrial genome structure. Curr. Genet. **24,** 279-290.

Biasutto, L., Szabo, I., and Zoratti, M. (2011). Mitochondrial effects of plant-made compounds. Antioxid. Redox Signal. **15,** 3039-3059.

Binder, S., and Brennicke, A. (2003). Gene expression in plant mitochondria: transcriptional and post-transcriptional control. Philos. Trans. R. Soc. Lond. B. Biol. Sci. **358,** 181-188; discussion 188-189.

Biswas, T.K., and Getz, G.S. (2002). Import of yeast mitochondrial transcription factor (Mtf1p) via a nonconventional pathway. J. Biol. Chem. **277,** 45704-45714.

Boldogh, I.R., and Pon, L.A. (2006). Interactions of mitochondria with the actin cytoskeleton. Biochim. Biophys. Acta. **1763,** 450-462.

Bolouri-Moghaddam, M.R., Le Roy, K., Xiang, L., Rolland, F., and Van den Ende, W. (2010). Sugar signalling and antioxidant network connections in plant cells. FEBS J. **277,** 2022-2037.

Bryan, A.C., Rodeheffer, M.S., Wearn, C.M., and Shadel, G.S. (2002). Sls1p is a membrane-bound regulator of transcription-coupled processes involved in *Saccharomyces cerevisiae* mitochondrial gene expression. Genetics **160,** 75-82.

Bych, K., Kerscher, S., Netz, D.J., Pierik, A.J., Zwicker, K., Huynen, M.A., Lill, R., Brandt, U., and Balk, J. (2008). The iron-sulphur protein Ind1 is required for effective complex I assembly. EMBO J. **27,** 1736-1746.

Caballero, A., Ugidos, A., Liu, B., Oling, D., Kvint, K., Hao, X., Mignat, C., Nachin, L., Molin, M., and Nystrom, T. (2011). Absence of mitochondrial translation control proteins extends life span by activating sirtuin-dependent silencing. Mol. Cell. **42,** 390-400.

Calegario, F.F., Cosso, R.G., Fagian, M.M., Almeida, F.V., Jardim, W.F., Jezek, P., Arruda, P., and Vercesi, A.E. (2003). Stimulation of potato tuber respiration by cold stress is associated with an increased capacity of both plant uncoupling mitochondrial protein (PUMP) and alternative oxidase. J. Bioenerg. Biomembr. **35,** 211-220.

Castandet, B., Choury, D., Begu, D., Jordana, X., and Araya, A. (2010). Intron RNA editing is essential for splicing in plant mitochondria. Nucleic. Acids. Res. **38,** 7112-7121.

Chase, C.D. (2007). Cytoplasmic male sterility: a window to the world of plant mitochondrial-nuclear interactions. Trends Genet. **23,** 81-90.

Chateigner-Boutin, A.L., and Small, I. (2011). Organellar RNA editing. Wiley Interdiscip. Rev. RNA **2,** 493-506.

Clifton, R., Millar, A.H., and Whelan, J. (2006). Alternative oxidases in Arabidopsis: a comparative analysis of differential expression in the gene family provides new insights into function of non-phosphorylating bypasses. Biochim. Biophys. Acta. **1757,** 730-741.

Clifton, R., Lister, R., Parker, K.L., Sappl, P.G., Elhafez, D., Millar, A.H., Day, D.A., and Whelan, J. (2005). Stress-induced co-expression of alternative respiratory chain components in *Arabidopsis thaliana*. Plant Mol. Biol. **58,** 193-212.

Cubas, P., Lauter, N., Doebley, J., and Coen, E. (1999). The TCP domain: a motif found in proteins regulating plant growth and development. Plant J. **18,** 215-222.

Cvetkovska, M., and Vanlerberghe, G.C. (2012a). Coordination of a mitochondrial superoxide burst during the hypersensitive response to bacterial pathogen in Nicotiana tabacum. Plant Cell. Environ. **35,** 1121-1136.

Cvetkovska, M., and Vanlerberghe, G.C. (2012b). Alternative oxidase modulates leaf mitochondrial concentrations of superoxide and nitric oxide. New Phytol. **195,** 32-39.

Daley, D.O., and Whelan, J. (2005). Why genes persist in organelle genomes. Genome Biol. **6,** 110.

Djajanegara, I., Finnegan, P.M., Mathieu, C., McCabe, T., Whelan, J., and Day, D.A. (2002). Regulation of alternative oxidase gene expression in soybean. Plant Mol. Biol. **50,** 735-742.

Dojcinovic, D., Krosting, J., Harris, A.J., Wagner, D.J., and Rhoads, D.M. (2005). Identification of a region of the Arabidopsis *AtAOX1a* promoter necessary for mitochondrial retrograde regulation of expression. Plant Mol. Biol. **58,** 159-175.

Duncan, O., Taylor, N.L., Carrie, C., Eubel, H., Kubiszewski-Jakubiak, S., Zhang, B., Narsai, R., Millar, A.H., and Whelan, J. (2011). Multiple lines of evidence localize signaling, morphology, and lipid biosynthesis machinery to the mitochondrial outer membrane of Arabidopsis. Plant Physiol. **157,** 1093-1113.

Estavillo, G.M., Crisp, P.A., Pornsiriwong, W., Wirtz, M., Collinge, D., Carrie, C., Giraud, E., Whelan, J., David, P., Javot, H., Brearley, C., Hell, R., Marin, E., and Pogson, B.J. (2011). Evidence for a SAL1-PAP chloroplast retrograde pathway that functions in drought and high light signaling in Arabidopsis. Plant Cell **23,** 3992-4012.

Fan, J., and Lee, R.W. (2002). Mitochondrial genome of the colorless green alga *Polytomella parva*: two linear DNA molecules with homologous inverted repeat termini. Mol. Biol. Evol. **19,** 999-1007.

Farre, E.M., and Weise, S.E. (2012). The interactions between the circadian clock and primary metabolism. Curr. Opin. Plant Biol. **15,** 293-300.

Ferreira Junior, J.R., Spirek, M., Liu, Z., and Butow, R.A. (2005). Interaction between Rtg2p and Mks1p in the regulation of the RTG pathway of *Saccharomyces cerevisiae*. Gene **354,** 2-8.

Fey, V., Wagner, R., Brautigam, K., Wirtz, M., Hell, R., Dietzmann, A., Leister, D., Oelmuller, R., and Pfannschmidt, T. (2005). Retrograde plastid redox signals in the expression of nuclear genes for chloroplast proteins of *Arabidopsis thaliana*. J. Biol. Chem. **280,** 5318-5328.

Fiorani, F., Umbach, A.L., and Siedow, J.N. (2005). The alternative oxidase of plant mitochondria is involved in the acclimation of shoot growth at low temperature. A study of Arabidopsis AOX1a transgenic plants. Plant Physiol. **139,** 1795-1805.

Foury, F., Roganti, T., Lecrenier, N., and Purnelle, B. (1998). The complete sequence of the mitochondrial genome of *Saccharomyces cerevisiae*. FEBS letters **440,** 325-331.

Foyer, C.H., Kerchev, P.I., and Hancock, R.D. (2012). The ABA-INSENSITIVE-4 (ABI4) transcription factor links redox, hormone and sugar signaling pathways. Plant Signal. Behav. **7,** 276-281.

Fransz, P., and de Jong, H. (2011). From nucleosome to chromosome: a dynamic organization of genetic information. Plant J. **66,** 4-17.

Fujiwara, M., Nagashima, A., Kanamaru, K., Tanaka, K., and Takahashi, H. (2000). Three new nuclear genes, sigD, sigE and sigF, encoding putative plastid RNA polymerase sigma factors in *Aarabidopsis thaliana*. FEBS letters **481,** 47-52.

Fuks, F. (2005). DNA methylation and histone modifications: teaming up to silence genes. Curr. Opin. Genet. Dev. **15,** 490-495.

Gabaldon, T., and Huynen, M.A. (2004). Shaping the mitochondrial proteome. Biochim. Biophys. Acta. **1659,** 212-220.

Gardner, M.J., Hall, N., Fung, E., White, O., Berriman, M., Hyman, R.W., Carlton, J.M., Pain, A., Nelson, K.E., Bowman, S., Paulsen, I.T., James, K., Eisen, J.A., Rutherford, K., Salzberg, S.L., Craig, A., Kyes, S., Chan, M.S., Nene, V., Shallom, S.J., Suh, B., Peterson, J., Angiuoli, S., Pertea, M., Allen, J., Selengut, J., Haft, D., Mather, M.W., Vaidya, A.B., Martin, D.M., Fairlamb, A.H., Fraunholz, M.J., Roos, D.S., Ralph, S.A., McFadden, G.I., Cummings, L.M., Subramanian, G.M., Mungall, C., Venter, J.C., Carucci, D.J., Hoffman, S.L., Newbold, C., Davis, R.W., Fraser, C.M., and Barrell, B. (2002). Genome sequence of the human malaria parasite *Plasmodium falciparum*. Nature **419,** 498-511.

Giege, P., Sweetlove, L.J., Cognat, V., and Leaver, C.J. (2005). Coordination of nuclear and mitochondrial genome expression during mitochondrial biogenesis in Arabidopsis. Plant Cell **17,** 1497-1512.

Giraud, E., Van Aken, O., Ho, L.H., and Whelan, J. (2009). The transcription factor ABI4 is a regulator of mitochondrial retrograde expression of *ALTERNATIVE OXIDASE1a*. Plant Physiol. **150,** 1286-1296.

Giraud, E., Ng, S., Carrie, C., Duncan, O., Low, J., Lee, C.P., Van Aken, O., Millar, A.H., Murcha, M., and Whelan, J. (2010). TCP transcription factors link the regulation of genes encoding mitochondrial proteins with the circadian clock in *Arabidopsis thaliana*. Plant Cell **22,** 3921-3934.

Giraud, E., Ho, L.H., Clifton, R., Carroll, A., Estavillo, G., Tan, Y.F., Howell, K.A., Ivanova, A., Pogson, B.J., Millar, A.H., and Whelan, J. (2008). The absence of ALTERNATIVE OXIDASE1a in Arabidopsis results in acute sensitivity to combined light and drought stress. Plant Physiol. **147,** 595-610.

Gonzalez, D., Bowen, A.J., Carroll, T.S., and Conlan, R.S. (2007). The transcription corepressor LEUNIG interacts with the histone deacetylase HDA19 and mediator components MED14 (SWP) and CDK8 (HEN3) to repress transcription. Mol. Cell Biol. **27,** 5306-5315.

Gray, M.W., Burger, G., and Lang, B.F. (1999). Mitochondrial evolution. Science **283,** 1476-1481.

Gray, M.W., Burger, G., and Lang, B.F. (2001). The origin and early evolution of mitochondria. Genome Biol. **2,** REVIEWS1018.

Greenleaf, A.L., Kelly, J.L., and Lehman, I.R. (1986). Yeast *RPO41* gene product is required for transcription and maintenance of the mitochondrial genome. Proc. Natl. Acad. Sci. U. S. A. **83,** 3391-3394.

Gupta, K.J., Shah, J.K., Brotman, Y., Jahnke, K., Willmitzer, L., Kaiser, W.M., Bauwe, H., and Igamberdiev, A.U. (2012). Inhibition of aconitase by nitric oxide leads to induction of the alternative oxidase and to a shift of metabolism towards biosynthesis of amino acids. J. Exp. Bot. **63,** 1773-1784.

Haas, R.H. (2010). Autism and mitochondrial disease. Dev. Disabil. Res. Rev. **16,** 144-153.

Hackenbrock, C.R. (1966). Ultrastructural bases for metabolically linked mechanical activity in mitochondria. I. Reversible ultrastructural changes with change in metabolic steady state in isolated liver mitochondria. J. Cell Biol. **30,** 269-297.

Harmer, S.L., Hogenesch, J.B., Straume, M., Chang, H.S., Han, B., Zhu, T., Wang, X., Kreps, J.A., and Kay, S.A. (2000). Orchestrated transcription of key pathways in Arabidopsis by the circadian clock. Science **290,** 2110-2113.

Heeren, G., Rinnerthaler, M., Laun, P., von Seyerl, P., Kossler, S., Klinger, H., Hager, M., Bogengruber, E., Jarolim, S., Simon-Nobbe, B., Schuller, C., Carmona-Gutierrez, D., Breitenbach-Koller, L., Muck, C., Jansen-Durr, P., Criollo, A., Kroemer, G., Madeo, F., and Breitenbach, M. (2009). The mitochondrial ribosomal protein of the large subunit, Afo1p, determines cellular longevity through mitochondrial back-signaling via TOR1. Aging (Albany NY) **1,** 622-636.

Herrmann, J.M., and Riemer, J. (2010). The intermembrane space of mitochondria. Antioxid. Redox Signal. **13,** 1341-1358.

Herrmann, J.M., Woellhaf, M.W., and Bonnefoy, N. (2012a). Control of protein synthesis in yeast mitochondria: The concept of translational activators. Biochim. Biophys. Acta., 286-294.

Herrmann, J.M., Longen, S., Weckbecker, D., and Depuydt, M. (2012b). Biogenesis of mitochondrial proteins. Adv. Exp. Med. Biol. **748,** 41-64.

Ho, L.H., Giraud, E., Lister, R., Thirkettle-Watts, D., Low, J., Clifton, R., Howell, K.A., Carrie, C., Donald, T., and Whelan, J. (2007). Characterization of the regulatory and expression context of an alternative oxidase gene provides insights into cyanide-insensitive respiration during growth and development. Plant Physiol. **143,** 1519-1533.

Howell, K.A., Narsai, R., Carroll, A., Ivanova, A., Lohse, M., Usadel, B., Millar, A.H., and Whelan, J. (2009). Mapping metabolic and transcript temporal switches during germination in rice highlights specific transcription factors and the role of RNA instability in the germination process. Plant Physiol. **149,** 961-980.

Ivanov, B., Kobayashi, Y., Bukhov, N.G., and Heber, U. (1998). Photosystem I-dependent cyclic electron flow in intact spinach chloroplasts: Occurrence, dependence on redox conditions and electron acceptors and inhibition by antimycin A. Photosynth. Res. **57,** 61-70.

Jazwinski, S.M. (2005a). The retrograde response links metabolism with stress responses, chromatin-dependent gene activation, and genome stability in yeast aging. Gene **354,** 22-27.

Jazwinski, S.M. (2005b). Rtg2 protein: at the nexus of yeast longevity and aging. FEMS Yeast Res. **5,** 1253-1259.

Jazwinski, S.M. (2012). The retrograde response and other pathways of interorganelle communication in yeast replicative aging. Subcell. Biochem. **57,** 79-100.

Karlberg, O., Canback, B., Kurland, C.G., and Andersson, S.G. (2000). The dual origin of the yeast mitochondrial proteome. Yeast **17,** 170-187.

Karpova, O.V., Kuzmin, E.V., Elthon, T.E., and Newton, K.J. (2002). Differential expression of alternative oxidase genes in maize mitochondrial mutants. Plant Cell **14,** 3271-3284.

Keeling, P.J., and Palmer, J.D. (2008). Horizontal gene transfer in eukaryotic evolution. Nat. Rev. Genet. **9,** 605-618.

Kindgren, P., Noren, L., Barajas Lopez Jde, D., Shaikhali, J., and Strand, A. (2012). Interplay between HEAT SHOCK PROTEIN 90 and HY5 Controls PhANG Expression in response to the GUN5 plastid signal. Mol. Plant **5,** 901-913.

Kindgren, P., Eriksson, M.J., Benedict, C., Mohapatra, A., Gough, S.P., Hansson, M., Kieselbach, T., and Strand, A. (2011). A novel proteomic approach reveals a role for Mg-protoporphyrin IX in response to oxidative stress. Physiol. Plant **141,** 310-320.

Klodmann, J., Senkler, M., Rode, C., and Braun, H.P. (2011). Defining the protein complex proteome of plant mitochondria. Plant Physiol. **157,** 587-598.

Knoop, V. (2004). The mitochondrial DNA of land plants: Peculiarities in phylogenetic perspective. Curr. Genet. **46,** 123-139.

Kobayashi, Y., Dokiya, Y., and Sugita, M. (2001). Dual targeting of phage-type RNA polymerase to both mitochondria and plastids is due to alternative translation initiation in single transcripts. Biochem. Biophys. Res. Commun. **289,** 1106-1113.

Koussevitzky, S., Nott, A., Mockler, T.C., Hong, F., Sachetto-Martins, G., Surpin, M., Lim, J., Mittler, R., and Chory, J. (2007). Signals from chloroplasts converge to regulate nuclear gene expression. Science **316,** 715-719.

Kuhn, K., Richter, U., Meyer, E.H., Delannoy, E., de Longevialle, A.F., O'Toole, N., Borner, T., Millar, A.H., Small, I.D., and Whelan, J. (2009). Phage-type RNA polymerase RPOTmp performs gene-specific transcription in mitochondria of *Arabidopsis thaliana*. Plant Cell **21,** 2762-2779.

Lang, B.F., Gray, M.W., and Burger, G. (1999). Mitochondrial genome evolution and the origin of eukaryotes. Annu. Rev. Genet. **33,** 351-397.

Larkin, R.M., Alonso, J.M., Ecker, J.R., and Chory, J. (2003). GUN4, a regulator of chlorophyll synthesis and intracellular signaling. Science **299,** 902-906.

Lee, C.P., Eubel, H., and Millar, A.H. (2010). Diurnal changes in mitochondrial function reveal daily optimization of light and dark respiratory metabolism in Arabidopsis. Mol. Cell Proteomics **9,** 2125-2139.

Li, C., Potuschak, T., Colon-Carmona, A., Gutierrez, R.A., and Doerner, P. (2005). Arabidopsis TCP20 links regulation of growth and cell division control pathways. Proc. Natl. Acad. Sci. U. S. A. **102,** 12978-12983.

Lipinski, K.A., Kaniak-Golik, A., and Golik, P. (2010). Maintenance and expression of the *S. cerevisiae* mitochondrial genome - from genetics to

evolution and systems biology. Biochim. Biophys. Acta. **1797,** 1086-1098.

Liu, X., Weaver, D., Shirihai, O., and Hajnoczky, G. (2009). Mitochondrial 'kiss-and-run': Interplay between mitochondrial motility and fusion-fission dynamics. EMBO J. **28,** 3074-3089.

Liu, Y., Fiskum, G., and Schubert, D. (2002). Generation of reactive oxygen species by the mitochondrial electron transport chain. J. Neurochem. **80,** 780-787.

Liu, Z., and Butow, R.A. (2006). Mitochondrial retrograde signaling. Annu. Rev. Genet. **40,** 159-185.

Logan, D.C., and Leaver, C.J. (2000). Mitochondria-targeted GFP highlights the heterogeneity of mitochondrial shape, size and movement within living plant cells. J. Exp. Bot. **51,** 865-871.

Mannella, C.A. (2006). Structure and dynamics of the mitochondrial inner membrane cristae. Biochim Biophys Acta **1763,** 542-548.

Mannella, C.A., Pfeiffer, D.R., Bradshaw, P.C., Moraru, II, Slepchenko, B., Loew, L.M., Hsieh, C.E., Buttle, K., and Marko, M. (2001). Topology of the mitochondrial inner membrane: dynamics and bioenergetic implications. IUBMB Life. **52,** 93-100.

McDonald, A.E., Vanlerberghe, G.C., and Staples, J.F. (2009). Alternative oxidase in animals: Unique characteristics and taxonomic distribution. J Exp. Biol. **212,** 2627-2634.

Mezghani, N., Mnif, M., Kacem, M., Mkaouar-Rebai, E., Hadj Salem, I., Kallel, N., Charfi, N., Abid, M., and Fakhfakh, F. (2011). A whole mitochondrial genome screening in a MELAS patient: A novel mitochondrial tRNA(Val) mutation. Biochem. Biophys. Res. Commun. **407,** 747-752.

Miceli, M.V., Jiang, J.C., Tiwari, A., Rodriguez-Quinones, J.F., and Jazwinski, S.M. (2012). Loss of mitochondrial membrane potential triggers the retrograde response extending yeast replicative lifespan. Front. Genet. **2,** 102.

Millar, A.H., Small, I.D., Day, D.A., and Whelan, J. (2008). Mitochondrial biogenesis and function in Arabidopsis. Arabidopsis Book **6,** e0111.

Millar, A.H., Whelan, J., Soole, K.L., and Day, D.A. (2011). Organization and regulation of mitochondrial respiration in plants. Annu. Rev. Plant Biol. **62,** 79-104.

Millerd, A., and Bonner, J. (1953). The biology of plant mitochondria. J. Histochem. Cytochem. **1,** 254-264.

Mochizuki, N., Brusslan, J.A., Larkin, R., Nagatani, A., and Chory, J. (2001). Arabidopsis genomes uncoupled 5 (GUN5) mutant reveals the involvement of Mg-chelatase H subunit in plastid-to-nucleus signal transduction. Proc. Natl. Acad. Sci. U. S. A. **98,** 2053-2058.

Mochizuki, N., Tanaka, R., Tanaka, A., Masuda, T., and Nagatani, A. (2008). The steady-state level of Mg-protoporphyrin IX is not a determinant of plastid-to-nucleus signaling in Arabidopsis. Proc. Natl. Acad. Sci. U. S. A. **105,** 15184-15189.

Moulin, M., McCormac, A.C., Terry, M.J., and Smith, A.G. (2008). Tetrapyrrole profiling in Arabidopsis seedlings reveals that retrograde plastid nuclear signaling is not due to Mg-protoporphyrin IX accumulation. Proc. Natl. Acad. Sci. U. S. A. **105,** 15178-15183.

Mower, J.P., Sloan, D.B., and Alverson, A.J. (2012). Plant mitochondrial genome diversity: The genomics revolution. In plant genome diversity. J.F. Wendel, J. Greilhuber, J. Dolezel, and I.J. Leitch, eds (Springer-Verlag Wien.

Murphy, M.P. (2009). How mitochondria produce reactive oxygen species. Biochem. J. **417,** 1-13.

Narsai, R., Law, S.R., Carrie, C., Xu, L., and Whelan, J. (2011). In-depth temporal transcriptome profiling reveals a crucial developmental switch with roles for RNA processing and organelle metabolism that are essential for germination in Arabidopsis. Plant Physiol. **157,** 1342-1362.

Neupert, W. (2012). SnapShot: Mitochondrial architecture. Cell **149,** 722-722 e721.

Newton, K.J., and Coe, E.H. (1986). Mitochondrial DNA changes in abnormal growth (nonchromosomal stripe) mutants of maize. Proc. Natl. Acad. Sci. U. S. A. **83,** 7363-7366.

Ng, S. (2008). The role of site II elements in coordinating the expression of nuclear genes encoding organellar proteins in *Arabidopsis thaliana*.

Honours thesis in School of Biomedical, Biomolecular and Chemical Sciences (Western Australia, Australia: University of Western Australia).

Pogson, B.J., Woo, N.S., Forster, B., and Small, I.D. (2008). Plastid signalling to the nucleus and beyond. Trends Plant Sci. **13,** 602-609.

Pruneda-Paz, J.L., Breton, G., Para, A., and Kay, S.A. (2009). A functional genomics approach reveals CHE as a component of the Arabidopsis circadian clock. Science **323,** 1481-1485.

Puranik, S., Sahu, P.P., Srivastava, P.S., and Prasad, M. (2012). NAC proteins: Regulation and role in stress tolerance. Trends Plant Sci. **17,** 369-381.

Rackham, O., Mercer, T.R., and Filipovska, A. (2012). The human mitochondrial transcriptome and the RNA-binding proteins that regulate its expression. Wiley Interdiscip. Rev. RNA.

Rasmusson, A.G., Soole, K.L., and Elthon, T.E. (2004). Alternative NAD(P)H dehydrogenases of plant mitochondria. Annu. Rev. Plant Biol. **55,** 23-39.

Rhoads, D.M., and Subbaiah, C.C. (2007). Mitochondrial retrograde regulation in plants. Mitochondrion **7,** 177-194.

Rieske, J.S., Baum, H., Stoner, C.D., and Lipton, S.H. (1967). On the antimycin-sensitive cleavage of complex III of the mitochondrial respiratory chain. J. Biol. Chem. **242,** 4854-4866.

Rodeheffer, M.S., Boone, B.E., Bryan, A.C., and Shadel, G.S. (2001). Nam1p, a protein involved in RNA processing and translation, is coupled to transcription through an interaction with yeast mitochondrial RNA polymerase. J. Biol. Chem. **276,** 8616-8622.

Roschzttardtz, H., Fuentes, I., Vasquez, M., Corvalan, C., Leon, G., Gomez, I., Araya, A., Holuigue, L., Vicente-Carbajosa, J., and Jordana, X. (2009). A nuclear gene encoding the iron-sulfur subunit of mitochondrial complex II is regulated by B3 domain transcription factors during seed development in Arabidopsis. Plant Physiol. **150,** 84-95.

Saisho, D., Nambara, E., Naito, S., Tsutsumi, N., Hirai, A., and Nakazono, M. (1997). Characterization of the gene family for alternative oxidase from *Arabidopsis thaliana*. Plant Mol. Biol. **35,** 585-596.

Sanchez, A., Shin, J., and Davis, S.J. (2011). Abiotic stress and the plant circadian clock. Plant Signal. Behav. **6,** 223-231.

Schwarzlander, M., Konig, A.C., Sweetlove, L.J., and Finkemeier, I. (2012). The impact of impaired mitochondrial function on retrograde signalling: a meta-analysis of transcriptomic responses. J Exp. Bot. **63,** 1735-1750.

Sherer, T.B., Betarbet, R., Stout, A.K., Lund, S., Baptista, M., Panov, A.V., Cookson, M.R., and Greenamyre, J.T. (2002). An in vitro model of Parkinson's disease: Linking mitochondrial impairment to altered alpha-synuclein metabolism and oxidative damage. J Neurosci. **22,** 7006-7015.

Strand, A., Asami, T., Alonso, J., Ecker, J.R., and Chory, J. (2003). Chloroplast to nucleus communication triggered by accumulation of Mg-protoporphyrinIX. Nature **421,** 79-83.

Sun, X., Feng, P., Xu, X., Guo, H., Ma, J., Chi, W., Lin, R., Lu, C., and Zhang, L. (2011). A chloroplast envelope-bound PHD transcription factor mediates chloroplast signals to the nucleus. Nat. Commun. **2,** 477.

Tanaka, K., Tozawa, Y., Mochizuki, N., Shinozaki, K., Nagatani, A., Wakasa, K., and Takahashi, H. (1997). Characterization of three cDNA species encoding plastid RNA polymerase sigma factors in *Arabidopsis thaliana*: evidence for the sigma factor heterogeneity in higher plant plastids. FEBS letters **413,** 309-313.

Temperley, R.J., Wydro, M., Lightowlers, R.N., and Chrzanowska-Lightowlers, Z.M. (2010). Human mitochondrial mRNAs-like members of all families, similar but different. Biochim. Biophys. Acta. **1797,** 1081-1085.

Turner, S.R., Hellens, R., Ireland, R., Ellis, N., and Rawsthorne, S. (1993). The organisation and expression of the genes encoding the mitochondrial glycine decarboxylase complex and serine hydroxymethyltransferase in pea (*Pisum sativum*). Mol. Gen. Genet. **236,** 402-408.

Unseld, M., Marienfeld, J.R., Brandt, P., and Brennicke, A. (1997). The mitochondrial genome of *Arabidopsis thaliana* contains 57 genes in 366,924 nucleotides. Nat. Genet. **15,** 57-61.

Valach, M., Pryszcz, L.P., Tomaska, L., Gacser, A., Gabaldon, T., and Nosek, J. (2012). Mitochondrial genome variability within the *Candida parapsilosis* species complex. Mitochondrion.

van der Giezen, M., and Tovar, J. (2005). Degenerate mitochondria. EMBO Rep. **6,** 525-530.

van Heusden, G.P., and Steensma, H.Y. (2001). 14-3-3 Proteins are essential for regulation of RTG3-dependent transcription in *Saccharomyces cerevisiae*. Yeast **18,** 1479-1491.

Vanlerberghe, G.C., and McLntosh, L. (1996). Signals regulating the expression of the nuclear gene encoding alternative oxidase of plant mitochondria. Plant Physiol. **111,** 589-595.

Vanlerberghe, G.C., and McIntosh, L. (1997). ALTERNATIVE OXIDASE: From gene to function. Annu. Rev. Plant Physiol. Plant Mol. Biol. **48,** 703-734.

von Heijne, G. (1986). Why mitochondria need a genome. FEBS letters **198,** 1-4.

von Jagow, G., Ljungdahl, P.O., Graf, P., Ohnishi, T., and Trumpower, B.L. (1984). An inhibitor of mitochondrial respiration which binds to cytochrome *b* and displaces quinone from the iron-sulfur protein of the cytochrome *bc1* complex. J. Biol. Chem. **259,** 6318-6326.

Walker, J.L., and Oliver, D.J. (1986). Glycine decarboxylase multienzyme complex. Purification and partial characterization from pea leaf mitochondria. J. Biol. Chem. **261,** 2214-2221.

Wallace, D.C., Singh, G., Lott, M.T., Hodge, J.A., Schurr, T.G., Lezza, A.M., Elsas, L.J., 2nd, and Nikoskelainen, E.K. (1988). Mitochondrial DNA mutation associated with Leber's hereditary optic neuropathy. Science **242,** 1427-1430.

Walters, R.G., and Horton, P. (1994). Acclimation of *Arabidopsis thaliana* to the light environment: Changes in composition of the photosynthetic apparatus. Planta **195,** 248-256.

Wang, J., Rajakulendran, N., Amirsadeghi, S., and Vanlerberghe, G.C. (2011). Impact of mitochondrial alternative oxidase expression on the response of *Nicotiana tabacum* to cold temperature. Physiol. Plant. **142,** 339-351.

Wang, S., Xiao, W., Shan, S., Jiang, C., Chen, M., Zhang, Y., Lu, S., Chen, J., Zhang, C., Chen, Q., and Long, M. (2012a). Multi-patterned dynamics of mitochondrial fission and fusion in a living cell. PLoS One **7,** e19879.

Wang, Y., Carrie, C., Giraud, E., Elhafez, D., Narsai, R., Duncan, O., Whelan, J., and Murcha, M.W. (2012b). Dual location of the

mitochondrial preprotein transporters B14.7 and Tim23-2 in complex I and the TIM17:23 complex in Arabidopsis links mitochondrial activity and biogenesis. Plant Cell **24,** 2675-2695.

Ward, B.L., Anderson, R.S., and Bendich, A.J. (1981). The mitochondrial genome is large and variable in a family of plants (cucurbitaceae). Cell **25,** 793-803.

Welchen, E., and Gonzalez, D.H. (2005). Differential expression of the Arabidopsis cytochrome *c* genes *Cytc-1* and *Cytc-2*. Evidence for the involvement of TCP-domain protein-binding elements in anther- and meristem-specific expression of the *Cytc-1* gene. Plant Physiol. **139,** 88-100.

Welchen, E., and Gonzalez, D.H. (2006). Overrepresentation of elements recognized by TCP-domain transcription factors in the upstream regions of nuclear genes encoding components of the mitochondrial oxidative phosphorylation machinery. Plant Physiol. **141,** 540-545.

Wenz, T., Luca, C., Torraco, A., and Moraes, C.T. (2009). mTERF2 regulates oxidative phosphorylation by modulating mtDNA transcription. Cell Metab. **9,** 499-511.

Wolfe, K.H., Li, W.H., and Sharp, P.M. (1987). Rates of nucleotide substitution vary greatly among plant mitochondrial, chloroplast, and nuclear DNAs. Proc. Natl. Acad. Sci. U. S. A. **84,** 9054-9058.

Woodson, J.D., Perez-Ruiz, J.M., and Chory, J. (2011). Heme synthesis by plastid ferrochelatase I regulates nuclear gene expression in plants. Curr. Biol. **21,** 897-903.

Yoshida, K., Terashima, I., and Noguchi, K. (2007). Up-regulation of mitochondrial alternative oxidase concomitant with chloroplast over-reduction by excess light. Plant. Cell Physiol. **48,** 606-614.

Appendix

Appendix I. Summary of Site II alias cis-acting regulatory elements previously defined in the literature as involved in circadian or diurnal regulation of gene expression. The name of each *cis*-acting regulatory element as outlined in the literature, the consensus DNA sequence and appropriate references are listed.

Element	Sequence	Function	Reference
Site II	TGGGC(C/T)	Extensive involvement in control of mitochondrial metabolism, develop mental processes and ribosomal protein expression	extensive (1997-current) - see introduction
RE1	TGGGC	Characterised in Arabidopsis PhyA promoter as part of a negative feedback loop	Bruce et al (1991)
SORLIP2	GGGCC	overrepresented in phyA responsive gene in Arabidopsis and top element represented in diurnal gene expression analysis in soybean	Hudson and Quail (2003)
Protein Box Element	ATGGGCC	Key element overrepresented in diurnal regulated genes to confer midnight phased expression	Michael et al (2008)
SBX Element	AAGCCC	also known as the maise sbe1 motif or starch box - related to starch metabolism	Michael et al (2008)
Telo Box	AAACCCT	Over-represented along with SBX and Protein Box element in genes phased to midnight phased expression, extensive site II litterature confirms that Site II elements are functional partners with Telo Boxes	extensive (1997-current), Michael et al (2008)